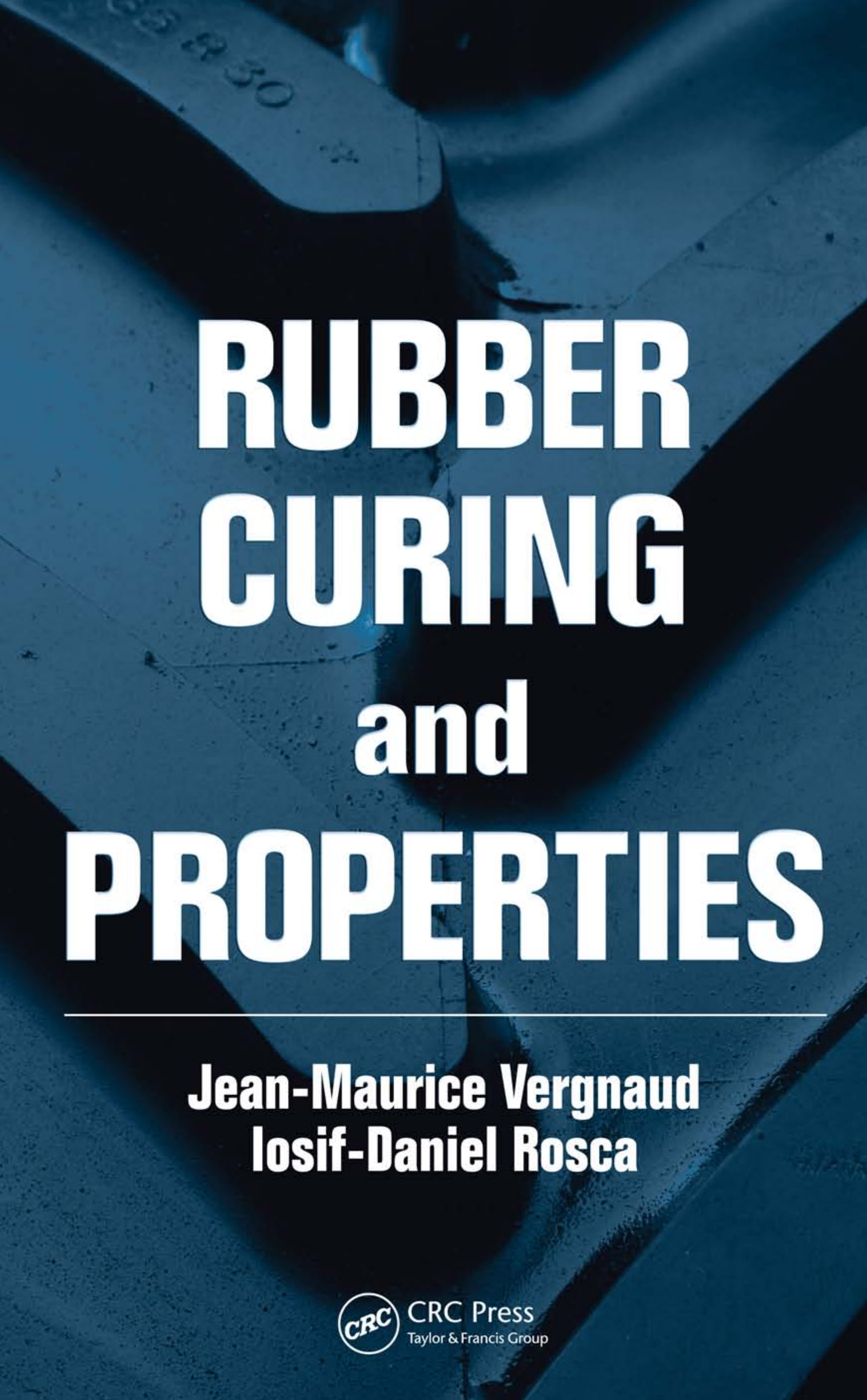

RUBBER CURING and PROPERTIES

Jean-Maurice Vergnaud
Iosif-Daniel Rosca

CRC Press
Taylor & Francis Group

RUBBER
CURING
and
PROPERTIES

RUBBER CURING and PROPERTIES

Jean-Maurice Vergnaud
Iosif-Daniel Rosca

CRC Press
Taylor & Francis Group
Boca Raton London New York

CRC Press is an imprint of the
Taylor & Francis Group, an **informa** business

CRC Press
Taylor & Francis Group
6000 Broken Sound Parkway NW, Suite 300
Boca Raton, FL 33487-2742

© 2009 by Taylor & Francis Group, LLC
CRC Press is an imprint of Taylor & Francis Group, an Informa business

No claim to original U.S. Government works
Printed in the United States of America on acid-free paper
10 9 8 7 6 5 4 3 2 1

International Standard Book Number-13: 978-1-4200-8522-8 (Hardcover)

This book contains information obtained from authentic and highly regarded sources. Reasonabl efforts have been made to publish reliable data and information, but the author and publisher cannot assume responsibility for the validity of all materials or the consequences of their use. Th authors and publishers have attempted to trace the copyright holders of all material reproduce in this publication and apologize to copyright holders if permission to publish in this form has no been obtained. If any copyright material has not been acknowledged please write and let us know s we may rectify in any future reprint.

Except as permitted under U.S. Copyright Law, no part of this book may be reprinted, reproduced transmitted, or utilized in any form by any electronic, mechanical, or other means, now known o hereafter invented, including photocopying, microfilming, and recording, or in any informatio storage or retrieval system, without written permission from the publishers.

For permission to photocopy or use material electronically from this work, please access www.copyright.com (http://www.copyright.com/) or contact the Copyright Clearance Center, Inc. (CCC), 22 Rosewood Drive, Danvers, MA 01923, 978-750-8400. CCC is a not-for-profit organization that provides licenses and registration for a variety of users. For organizations that have been granted photocopy license by the CCC, a separate system of payment has been arranged.

Trademark Notice: Product or corporate names may be trademarks or registered trademarks, an are used only for identification and explanation without intent to infringe.

Library of Congress Cataloging-in-Publication Data

Vergnaud, J. M.
Rubber curing and properties / Jean-Maurice Vergnaud and Iosif-Daniel Rosca.
p. cm.
Includes bibliographical references and index.
ISBN 978-1-4200-8522-8 (alk. paper)
1. Rubber. I. Rosca, Iosif-Daniel. II. Title.

TS1891.V47 2008
678'.2--dc22 2008030736

Visit the Taylor & Francis Web site at
http://www.taylorandfrancis.com

and the CRC Press Web site at
http://www.crcpress.com

Contents

Chapter 1

Chapter 2

Chapter 3

Chapter 4

Chapter 5

Chapter 6

Chapter 7

Chapter 8

Chapter 9

Preface

Rubbers are widely used in various applications, from tires to flexible tubings or absorbing systems, to mention just a few applications. They are favored when, in sharp contrast to other engineering materials, their relatively stronger attributes are needed and, at the same time, their highly deformable characteristics are desirable. Exhibiting almost complete recovery, they are virtually incompressible with a bulk modulus some thousand times greater than its shear or than Young's modulus. Moreover, rubbers are to some large extent impermeable to liquids and, especially, to gases. Both these qualities are of considerable value for tires in their utility on cars, planes, or bicycles. Thus, to sum up the importance of rubber in our life, it is virtually irreplaceable. It was said in 1941, when the United States decided to get involved in the Second World War, that no war could be started when no rubber is available in a country.

But the physical properties of a rubber material are not only innate; they largely depend on the state of cure of the final compound, as well as on the nature of the initial fresh rubber selected for the cure, this uncured rubber being either natural or synthetic. Following the process of cure, the compound, made of uncured rubber and of curing agents as well as of additives, is heated in a mold up to a temperature at which the reaction starts, the shape of the final material being given by the mold. During the cure, an irreversible reaction takes place, leading to a three-dimensional molecular network, and the plastic material is converted into an elastic one.

Thus, good knowledge of the process of cure is of high concern, for three reasons at least: the quality of the final product depends on the value of the state of cure as well as of its homogeneity through the material; moreover, it cannot be recycled if it is badly cured; and, for economical reasons, in addition, it is necessary to reduce the cure–time cycle.

Coming back to the process of cure, it consists essentially of two stages—that is, the heat transfer by conduction through the rubber mass as well as at the mold–rubber interface, and the cure reaction which starts at a temperature around 120–150°C, depending on the nature of the material. When the mold temperature is too low, the reaction is not achieved properly, and the final material, generally visco-elastic, has little interest for industrial application. Conversely, when the temperature is too high, the final material is burnt and breaking, without any quality of elasticity. Moreover, there is a narrow temperature window through which the reaction should be conducted. Thus, considerable importance needs to be given to obtaining a good understanding not only of the thermal properties of the rubber material during the heating stage and the cure process in the mold, but also on the values of the parameters necessary to express the kinetics of the cure reaction. By simplifying the principle of the cure reaction, which is essentially highly complex, and taking it as an nth order reaction, only four kinetic parameters should be considered: the enthalpy of cure, which represents the heat evolved during the whole reaction; the two terms that enable the measurement of the temperature sensitivity of the reaction, i.e., the energy of activation and the rate constant that counterbalances the effect of the energy of reaction; and the amount of rubber remaining uncured, which is to the nth power, n being the order given to the overall reaction. And thus, in time, various techniques have been developed and used so as to determine the kinetics of the cure reaction from which are calculated the main kinetic parameters.

The importance given to the kinetics of cure is so great that various techniques have been tested or even created for determining the parameters of the kinetics of cure, the cure being considered on the whole as conforming to the Arrhenius's expression.

The first was calorimetry, conducted either under isothermal conditions or in a scanning mode with a constant heating rate. However, though this technique may be very well adapted to the cure of thermosetting resins, which develop a large enthalpy, it is not the perfect one in the present case, because of the rather low value of the cure enthalpy of rubbers, which does not exceed 8 Joules/gram rubber per 1% sulfur. Isothermal calorimetry has been used by assuming that the rate of cure varies with temperature according to an Arrhenius equation. The differential scanning calorimetry (DSC) technique has been employed for defining the temperature at which the reaction starts. The cure enthalpy has been obtained from DSC experiments. A question arose in the mid-eighties as to which could be the best calorimetry technique, the isothermal or the DSC. And finally in-depth studies on the process of heat transfer through the sample showed that in isothermal calorimetry, the operation is not as simple as it first looks; the sample initially at room temperature is dropped into the calorimeter, which is kept at the selected temperature, and the strong heating stage may hide the first part of the reaction, considerably reinforced by the fact that a temperature window of about 30 K is found over which meaningful data can be obtained. Finally, it has been proved that calorimetry in scanning mode is the best technique for evaluating not only the cure enthalpy, for thermosetting resins at least, but also for determining the kinetics of heat evolved from the overall cure reaction.

Another technique, interesting but highly time-consuming, was based on the measurement of the swelling of the rubber samples taken at various stages during the cure. In the late seventies, this method was used not exactly for measuring the kinetics of the cure reaction but especially for evaluating the state of cure for a given rubber-curing agent couple. Thin rubber sheets (0.5 mm) were heated isothermally within a range of time and temperature, and the state of cure was evaluated by measuring swelling in toluene of these final samples; afterward, using the data obtained, the degree of cure profiles in thicker blocks (25 mm) were calculated and compared with the profiles experimentally determined.

Other studies have been carried out by considering the heat transfer by conduction through the rubber, as well as the heat generated by the overall cure reaction. The state of cure at any time t is thus defined as the heat evolved up to time t as a fraction of the total heat evolved from the cure reaction. In a particular method, the state of cure was calculated from the temperature history at any place in the rubber by introducing a rate of reference at 149°C and a temperature coefficient of cure, assuming that the rate of cure increases by a factor of 1.85/10°C. In another study, the profiles of temperature developed through the rubber were calculated assuming that the rate of cure doubles for each 10°C increase in temperature around the temperature reference of 150°C. This reference temperature method avoids the use of the order of the reaction, but necessitates a full study of the material at this reference temperature. As the problem of heat transfer by conduction with internal heat generated by the cure reaction cannot be mathematically resolved, numerical models have been built by taking all the known facts into account, for various shapes of the material, either in the cylindrical sample in the calorimeter or more simply in the sheet located in the slabs of the heated mold.

Other methods widely used for the cure of rubbers consist of heating the sample and monitoring the viscosity or torque of the rubber during the cure. The Money viscosimeter, the Wallace–Shawbury curometer, the oscillating disc rheometer (ODR), and the moving die rheometer (MDR) have been developed and marketed, the MDR being introduced in 1985.

All these setups work under isothermal conditions. In the MDR, a thin sheet (around 2 mm) is placed between the two dies kept at the desired temperature; the lower disc oscillates and a reaction torque/pressure transducer is positioned above the upper die. It has been found that the MDR gives shorter times of cure than the ODR because of better heat transfer and higher torque values owing to the die design. The MDR is run at three temperatures to allow evaluation of the kinetic parameters of the cure reaction. Thus, the activation energy and the preexponential factor can be calculated from the fractional modulus time values obtained with this apparatus. The modulus value is assumed to vary with time following first-order kinetics, and the rate constant varies with temperature according to the Arrhenius equation.

The process of curing rubber taking place in the MDR is similar to that in a mold: heat transfer by conduction through the rubber with a coefficient of heat transfer at the die–rubber interface, followed by the cure reaction. Thus, with the MDR run under isothermal conditions, when the sample initially at room temperature is introduced between the heated dies, considerable heat transfer occurs through the rubber with a corresponding decrease in temperature at the die surface. As a result, steep gradients of temperature develop through the thickness of the rubber sample. The cure reaction starts at a given temperature and gradients of state of cure are expanded with a higher value on the surface in contact with the dies. After a time, the profiles of the state of cure become more and more uniform.

Then, three parameters become of great interest, regardless of the nature of the rubber and curing agent: the temperature of the dies, the thickness of the sample, and the quality of the contact between the rubber and the dies. It is not easy to place correctly the rubber sample between the dies when they are heated. And, moreover, another drawback brought by the isothermal conditions necessitates the right selection of three temperatures within a narrow temperature window. This is the reason why attempts have been made recently to upgrade this MDR technique by using it in scanning mode in various ways. Thus, instead of having to make three measurements with different samples at the selected temperatures, only one experiment is necessary. First, the scanning mode with a constant rate has to be considered from the beginning to the end of the process. In order to improve this process and to reduce the time of the experiment, a change in the rate of heating has been introduced, with a high rate at the beginning, followed by a lower rate as soon as the cure reaction takes place. Moreover, the effect of parameters of interest has been deeply studied, such as the heating rate and the quality of the contact between the rubber and the die. Finally, it has been found that the linear increase of temperature with time is perhaps not the best way of heating the apparatus, as a square root of time–temperature programming was proved to be shorter in time for the MDR used for the cure of rubber.

Another problem should be considered in detail with the process of curing the rubbers in the mold; this occurs when the cure reaction takes place, and is associated with the heating stage.

Thus, from the measurements providing the values of the kinetic parameters of the cure reaction, it is possible to evaluate the progress in the cure of a piece of rubber by using also the thermal parameters of the rubber and of the mold. In spite of the low value of the heat generated by the cure reaction, the profiles of temperature and of the state of cure developed through the sample at various times are obtained either by experiments or by calculation. Calculation is made by considering the heat transfer by conduction not only through the rubber but also through the mold, as the mathematical treatment is not possible in this case; numerical models, taking all known facts into account, have been built and successfully tested. Different topics concerned with the cure of rubbers and their properties, such as the process of cure and the methods of evaluating it through modeling, the correlation between the state of cure of the rubbers, and either their mechanical properties or their resistance to liquids, have thus been established.

Testing of rubber materials involves exposure to various types of environmental factors. One of the most important problems for rubbers is their resistance to liquids. The tests in which rubbers are in contact with liquids are often called “swelling tests,” because of the resulting change in volume of the test piece, or also “oil aging tests” because mineral oils are the liquids most specified. These tests generally consist of measuring the total uptake of toluene by a rubber after immersion in the liquid. Another way was explored by studying the process of absorption or desorption of the liquid previously absorbed, which are both controlled by diffusion through the rubber with a change in dimensions leading to typical boundary conditions. As the problem cannot be resolved by mathematical treatment, various numerical models have been built and tested, so as to take into account not only the diffusion with a concentration-dependent diffusivity and the change in dimensions but also the anisotropic swelling. The way of evaluating the concentration-dependency of the diffusivity, already successfully traced by using other polymers, has been used for these problems involving rubber.

Because of their typical properties in terms of mechanics, measuring the mechanical properties of rubber is of great concern. These are determined not only under static conditions but also under dynamic conditions, with the in-phase and out-of-phase modulus.

The main objectives of this book are varied. The first consists of giving, in Chapter 1, a bird’s eye view of the history of the cure process by recalling a few previous experiments and calculations of interest, which should be considered as decisive hallmarks in the developing of rubber curing processes.

In the second chapter, all the problems set by the process of heat transfer are considered, with convection at the solid–fluid interface, and with conduction through a solid, which can be the rubber or the mold. The situation of heated rubber after the extraction out of the mold requires an application of the heat process connecting the convection and the conduction.

In the third chapter, the methods used for evaluating the kinetics of the cure of rubbers are described and studied on the basis of either the heat evolved from the cure reaction (calorimetry) or the change in the mechanical properties during the cure (rheometers). Theoretical studies are made so as to improve either the isothermal MDR, or even the MDR in scanning mode, by considering different temperature–time relationships.

In Chapter 4, applying the information given in the two previous chapters is discussed in detail for the cure of rubber sheets in molds. Monodirectional heat transfer is thus considered, but the case of three-directional heating systems is also examined. The effect of various parameters such as the values of the kinetic data (rate constant, energy of activation, enthalpy of reaction, and order of the overall reaction); the thermal transfer data of the rubber; the characteristics of the mold; and finally the relation between the rubber and the mold are included. The important area of multilayer rubbers of various types has also been considered by combining the effects of diffusion of the active agents between these layers during the cure with the heat transfer and then the cure of the system. Thus, it is shown that this diffusion enables a final rubber system for which the properties vary continuously through their thickness, leading to high adhesion between these layers. The postcure of the already-cured rubbers that may take place when they are extracted out of the mold is also examined.

In Chapter 5 the principle of the injection molding principle is described, with its obvious advantage in reducing the time of the cure; the temperature at which the rubber can be injected without detriment to the mold filling is also evaluated. The important problems set up by the plasticity and by the scorch—that is, the onset of vulcanization—are probed in depth. If the isothermal MDR technique is able to give a rough idea of the scorch time, it is shown that the MDR run in scanning mode—that is, the apparatus commercially called the rubber process analyzer (RPA)—is capable of providing two characteristics of the scorch, the time and temperature.

An attempt is made in Chapter 6 to relate the mechanical property of the rubber under dynamic conditions to the state of cure. The mechanical properties of the unvulcanized rubber are also evaluated, with plasticity versus temperature and the scorch. The mechanical properties of the vulcanized rubber are then considered, in static and dynamic modes.

In Chapter 7, in-depth studies are made on the resistance of rubbers to liquids, which is expressed by the amount of the liquid absorbed or, much better, by the kinetics of absorption. The process of liquid absorption in the rubber material, as well as of that of desorption of the liquid previously absorbed, are studied. These processes are driven by transient diffusion, which is examined in terms of rubber. As rubber may absorb a large quantity of liquid, a swelling takes place; thus, the diffusivity is not only concentration-dependent, but also the boundary is moving with the amount of the liquid absorbed. On the other hand, it will be seen that the processes of diffusion and cure can occur simultaneously, because a diffusion of the active agent is proved to take place through the interface between two rubber layers with different percentages of sulfur when they are cured together.

Chapter 8 is devoted to the on-going problems of recycling scrap rubber tire, in spite of the fact that this subject is somewhat beyond the scope of this book. Various solutions are regarded in succession, including burning, using pyrolysis in order to get some residues of interest, and using solvent as an agent of devulcanization. Finally, by considering scrap rubbers as new raw materials, the method based on vulcanizing the compound obtained after addition of curing agents to the scrap rubber, either in its pure state or in addition to fresh rubber, is especially studied.

Our book presents its main findings in terms of equations and figures. In all cases, the theoretical treatment is offered in a didactic manner, so that readers who are not fully familiar with the terms can, nevertheless, easily understand the developments in this field. The assumptions for which the calculations are made, and the solutions obtained, are clearly presented. It is true that the problems of heat transfer by conduction, as well as those of diffusion of liquid through a rubber, are not easy to understand. This is the reason why the solutions of the differential equations with partial derivatives that express these transfers are explained in detail. On the other hand, in order to facilitate the reader's understanding of the results, the figures are drawn by using dimensionless numbers as coordinates as often as possible; as a result, master curves are obtained that are of value in various applications.

Thus, by introducing the typical values of a problem, readers can obtain the result of the actual problem put before them.

The data published by various authors are given, so as to help readers in making their own calculations. They include the values that deal with heat transfer and the kinetics of the cure reaction, and cover the diffusion of liquids through rubber. In each case, references are given.

Finally, it should be added that various books of interest have already been published on rubber in domains other than the one considered in the present book: the process of cure and properties of the vulcanizates as a function of the state of cure. They are cited as much as possible. Among them, *Physical Testing of Rubbers* [1] is worth noting, and various notations are drawn from this book, especially in Chapters 2, 3, 4, 6, and 7. Let us remark that at the time the fourth edition of Brown's book had just been launched on the market; the objective of the present book on the cure of rubbers, however, being different from that of Roger Brown's, this first edition only has been considered. On the other hand, *The Analysis of Rubber and Rubber-like Materials* [2] is of interest as far as the chemistry of rubbers is concerned. Three other books are cited, as they contain at least one chapter devoted either to the cure of rubber [3] or to the stage of absorption of liquid [4], and to the subsequent stage of drying rubber containing a liquid [5]. One of the most specialized books on carbon black is also cited in Chapter 8, which is concerned with reclaiming scrap rubber [6]. But in all cases, the theory of the cure process has been developed and updated, and the results especially applied to rubber materials in the present book.

REFERENCES

1. R.P. Brown, *Physical Testing of Rubbers*, Applied Science Publisher, London, 1979, 1st edition. (The 4th edition has recently been published.)
2. W.C. Wake, *The Analysis of Rubber and Rubber-like Materials*, Mac Laren & sons, London, 1968.
3. J.M. Vergnaud and J. Bouzon, *Cure of Thermosetting Resins*, Springer-Verlag, London, 1992.
4. J.M. Vergnaud, *Liquid Transport Processes in Polymeric Materials,* Prentice Hall, Englewood Cliffs, NJ, 1991.
5. J.M. Vergnaud, *Drying of Polymeric and Solid Materials*, Springer-Verlag, London, 1992.
6. J.B. Donnet, R.C. Bansal, and M.J. Wang, *Carbon Black: Science and Technology*, 2nd ed., Marcel Dekker, New York, 1993.

About the Authors

Jean-Maurice Vergnaud is a professor at the University of Saint-Etienne, France, retired from teaching but not from research. He has earned several awards, either in industry or at university: the Prize of the French Chemical Industry (new methods in gas chromatography) in 1966; Silver Medal from the French Academy of Sciences (molecular sieves) in 1976; the George Stafford Whitby Award from the American Chemical Society, Rubber division in 1998; and the Gold Medal from the French Society for encouraging progress in 2007. He is the author of 450 papers and 300 communications, 30 plenary lectures, and has been speaker at 10 sessions of the prestigious Gordon Research conferences. He is the author of eight books published by international publishing companies, and belongs to the editorial boards of five international journals.

Iosif-Daniel Rosca, Associate Professor at the University of Bucharest, Romania, is currently a researcher at Concordia University, Montreal. He is co-author of two books with Jean-Maurice Vergnaud. He specializes in chemical engineering, with emphasis on studies regarding mass transfer controlled by diffusion and heat transfer with cure reaction.

1 Bird's Eye View of the Cure Process

First Attempts

It is well known that the cure reaction is complex, with initiation reactions starting first, followed by propagation reactions, and ending in termination reactions. In the early days of the rubber industry, there were various rule-of-thumb techniques for estimating the state of cure and the cure time evolved. They worked rather well for many purposes, although there were problems in some areas such as the curing of large articles. Since then, new polymers and new curing systems have been introduced, and thus today rubber is being used in more demanding applications. Moreover, in order to increase productivity, higher curing temperatures have been employed and more efficient curing systems have been developed. All these factors mean that more exact calculations have been, and still are, desirable, and more accurate experimental data are required.

Attempts in various directions were made in the early 1970s to obtain a better understanding of the process of cure with heat transfer. The objective of this first chapter is to give an overview of some studies of interest.

1.1 METHOD BASED ON THE CAPACITY OF LIQUID ABSORPTION

1.1.1 Principle of the Method

The basis of the method described by Hands and Horsfall [1] consists of calculating the temperature distribution as a function of time first, then evaluating the distribution of the cure. Taking a temperature profile, a technique is described enabling the evaluation of the state of cure. When the form of the relationship between cure and temperature history is known, the basic cure parameters can be obtained from experiments in which temperature varies with time. When the relationship is not known, it is preferable to conduct experiments at various fixed temperatures in order to separate the dependence on time and temperature. An apparatus was built for measuring cure as a function of time at a constant temperature. The data obtained from this isothermal apparatus and a new mathematical model of cure was used to predict the cure distribution obtained in nonisothermal experiments.

1.1.2 Experimental

The sample, 20 mm in diameter and 0.5 mm thick, is placed between press platens heated at the selected temperature for over 1 second; it is then quickly removed, quench-cooled in water, and the degree of cure measured. This operation is repeated

TABLE 1.1
Composition of the Rubber Samples

Rubber A		Rubber B	
RSS1	100	RSS1	100
HAF black	50	HAF black	50
Stearic acid	1	Stearic acid	1
Zinc oxide	5	Zinc oxide	5
Amine	1	Amine	1
Dutrex 729	5	Dutrex 729	5
MBT	0.7	CBS	1
Sulfur	3	Sulfur	1
		Sulfasan R	1

at various times to build up a complete cure curve at the same temperature. It can also be done at various other temperatures.

The degree of cure is determined by swelling each sample in toluene, using two possible methods. One is by measuring the increase in weight resulting from the toluene absorbed, and the other by evaluating the change in dimensions by using a traveling microscope. A correction was made for any weight loss that might occur during swelling.

Measurements were taken on two natural rubber compounds: rubber A with a very short scorch time, and rubber B with a very long one. For both rubbers, experiments were conducted at 120°C, 140°C, 160°C, 180°C, and 200°C. A Monsanto rheometer and a Wallace–Shawbury curometer were used, as well as isothermal apparatuses (see Table 1.1).

1.1.3 EXPERIMENTAL RESULTS AND DISCUSSION

Three cure curves at 200°C for the A rubber are shown in Figure 1.1. From these it can be seen that the rheometer gives longer times than the curometer, and both give longer cure times than the isothermal apparatus. According to Hands and Horsfall [1], there are probable reasons for this increase in the apparent cure time. In the first place, heat is lost continuously by conduction from the paddle rotor during the measurement. Hence, the center is always cooler than the platens, and the average temperature is less than the set temperature. Secondly, the curometer samples take longer to heat up because they are thicker than the samples used in the isothermal apparatus. The heating-up time becomes more important as the temperature is increased; at 200°C, for example, the time taken for the rheometer sample to heat up is longer than the isothermal cure time. These differences are greater in the rheometer than in the curometer because the rheometer has a bigger heat sink and uses thicker samples.

In terms of a provisory conclusion, it takes a few weeks to determine a complete family of cure–time curves using the isothermal apparatus because each point has to be obtained separately [1]. Another disadvantage with the method is that the scatter in the data is too high, especially at low levels of cure. There is obviously a need for a faster and better technique.

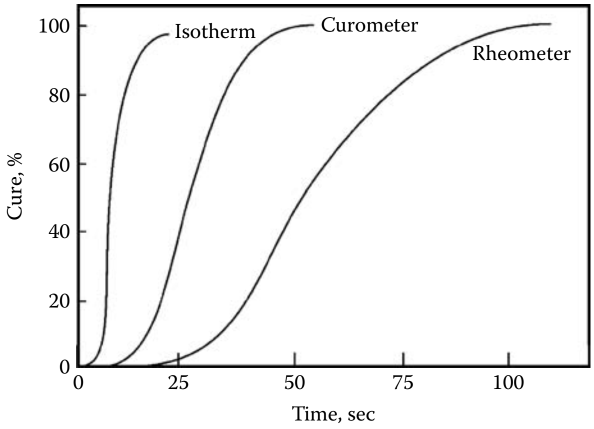

FIGURE 1.1 Comparison of isothermal, curometer, and rheometer results obtained at 200°C [1] for the same rubber compound. (With permission of the editor Hütthig Verlag. Figure 2. A new method for simulating industrial cure processes. *Kautschuk Gummi Kunststoffe*, D. Hands and F. Horsfall (1980) 33, 440.)

1.1.4 CALCULATION OF THE STATE OF CURE

The rate of cure is a function of the temperature θ and the level of cure c according to [1]:

$$\frac{dc}{dt} = f(\theta, c) \tag{1.1}$$

The cure level can be obtained from Equation 1.1 by substituting θ as a function of time t and integrating it.

Under isothermal conditions, according to standard rate kinetics, the rate of cure is:

$$\frac{dc}{dt} = k(\theta)(c_\infty - c)^n \tag{1.2}$$

where c_∞ is the final level of cure, n is the order of the reaction, and $k(\theta)$ is an Arrhenius equation. The difficulty with this approach is that Equation 1.2 is not able to represent the family cure–time curves, which are S-shaped, as drawn in Figure 1.1.

Thus, the problem that worried the researchers [1] was that neither of the expressions obtained by integrating Equation 1.2 by taking the order n equal to 1 or 2, bears any resemblance to an S-shaped curve. For these investigators, it is taken for granted that the heat transfer is accomplished quite instantaneously but, in fact, in spite of the thin thickness of the sample (0.5 mm), it takes some time for the heat transfer to be achieved.

According to Hands and Horsfall [1] the usual way around this difficulty is to work in terms of an equivalent cure time t_{eq} at an arbitrary reference temperature θ_0. If there is an increase in cure dc at a cure level c at the reference temperature, but taking place in a different time, dt_{eq}, Equation 1.2 becomes:

$$\frac{dc}{dt_{eq}} = k(\theta_0)(c_\infty - c)^n \tag{1.3}$$

Dividing Equation 1.2 by 1.3 gives:

$$\frac{dt_{eq}}{dt} = \frac{k(\theta)}{k(\theta_0)} \tag{1.4}$$

Thus, by working in terms of equivalent time instead of cure, the dependence of $\frac{dc}{dt}$ on c is eliminated. For a nonisothermal experiment, Equation 1.4 can be integrated:

$$t_{eq} = \int \frac{k(\theta)}{k(\theta_0)} dt \tag{1.5}$$

Another approach due to Claxton and Liska [2] is to assume a first-order reaction preceded by a temperature-dependent scorch period.

1.1.5 TEMPERATURE DEPENDENCE AND REFERENCE TEMPERATURE

Two methods have been discussed in the literature for relating the effect of temperature to cure rate: temperature coefficient and activation energy. The temperature coefficient method was usually used at that time, but most workers suggested that the activation energy approach is more fundamental [2].

The temperature coefficient of cure is defined as the ratio of the cure times for a 10°C change in the cure temperature. It appears in the equation:

$$t = \frac{B}{k(\theta)} = t_0 \cdot TC^{(\theta-\theta_0)/10} \tag{1.6}$$

where TC is the temperature coefficient, t is the cure time at a temperature θ, t_0 is the cure time at a standard temperature θ_0, and B depends on the cure and the order of reaction. Optimum cure for the compound is chosen with reference to the cure–time curves from a cure meter. The precise definition of optimum cure depends on the type of compound and on the end use, but usually 90% of the maximum level is used. The temperature coefficient can be obtained from the slope of a graph of log (cure time) against temperature.

For calculation purposes the temperature coefficient is usually assumed to be constant, and the isothermal results show that this assumption is correct for the two compounds examined in this study. Both compounds have the same temperature coefficient of 1.9, although they have very different scorch times. However, if the temperature coefficient is calculated from the rheometer results, it appears to be temperature-dependent and decreases in value by about 50% over the temperature range from 120 to 200°C.

An alternative approach is to assume that the temperature dependence can be represented by an Arrhenius equation from which the activation energy E is calculated:

$$t = \frac{B}{k(\theta)} = A \cdot \exp\left(\frac{E}{R(\theta + 273)}\right) \tag{1.7}$$

where t is the cure time at the temperature θ expressed in Celsius.

1.1.6 NEW MODEL BUILT BY HANDS AND HORSFALL [1]

In the case where two materials have different scorch times but the same 90% crosslink cure time, it is obvious that the cure reaction is proceeding faster in the latter stages for the material with the longer scorch time. A calculation based on a single point from the cure–time curve will give the same answer for both samples, although in practice they have different cure distributions. To make accurate calculations the whole of the cure–time curve must be used, and this is the basis of this new model.

The isothermal S-shaped cure–time curves are represented by two exponentials joined together at $c = c_m$, the rate of cure being continuous across the junction.

The model was fitted to each set of experimental data points to obtain the gradient at the junction point.

There is an apparent degree of cure for the unvulcanized black loaded rubber c_0, and this point is the most difficult to obtain experimentally.

1.1.7 VERIFICATION OF THE METHOD ON THICK RUBBER SAMPLES

Blocks of rubber 150 mm in diameter and 25 mm thick were compression molded at temperatures from 120 to 180°C for different lengths of time, and quenched in cold water. To obtain the cure distribution through the thickness of the slab obtained under the conditions of temperature and time, a cylindrical plug 20 mm in diameter was taken from the center of each block when cold, and this plug was mounted on a lathe and cut into sections 1 mm thick. These sections were swollen in toluene in order to determine the degree of cure.

The temperature history at equally spaced points through the thickness of the rubber sample was calculated, giving the temperature profiles obtained at a time when the sample is heated in the mold at a constant temperature. The degree of cure was then evaluated from this temperature–time history.

A rather good agreement was obtained between the calculated and experimental data, as shown in Figure 1.2, showing the cure distribution in a 25-mm-thick slab of rubber heated in a press at 160°C for 900 seconds.

1.1.8 CONCLUSIONS ON THIS METHOD

The following conclusions can be drawn from this method:

i. It is certain that this method was new at that time, in the late 1970s. Moreover, its principle is based on an interesting property of rubber, the swelling of the cured material.

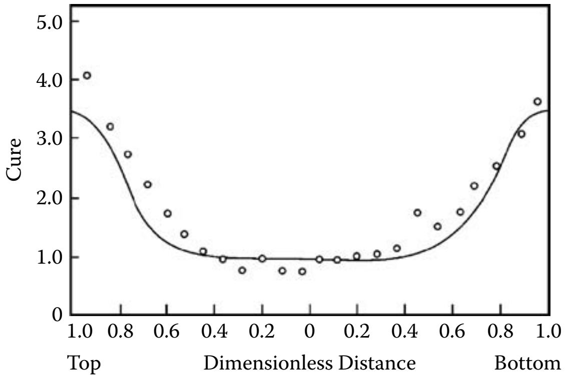

FIGURE 1.2 Cure distribution in a 25-mm-thick slab of A rubber heated in a press at 160°C for 900 s. The line was calculated from the model and the points are experimental. (With permission of the editor, Hütthig Verlag. Figure 10. A new Method for Simulating Industrial Cure Processes. *Kautschuk Gummi Kunststoffe*, D. Hands and F. Horsfall (1980) 33, 440.)

ii. It is a given that this method is highly time-consuming as frankly said many times [1]; in short, a few weeks were necessary to determine the cure and thermal parameters of a rubber compound.
iii. This is a discontinuous method necessitating the preparation of a great number of samples, cured at various values of temperature and time so as to be able to obtain a law expressed in terms of temperature and time.
iv. The principle of the reference temperature or of the reference time was used many times by various authors, and considered as the basis of their method.
v. A modern method of calculation was used at that time, in spite of the fact that an analytical solution exists for the profile of temperature developed through the thickness of the sample when heated in the mold.
vi. The enthalpy of the cure reaction, which is slightly exothermic, is not taken into account.
vii. Perhaps the more important drawback of this method is the fact that for a 0.5-mm-thick sample, the temperature through its thickness should instantaneously reach that of the heated slabs of the press. This assumption is not exactly true, as shown in Figure 1.6 with the curve expressing the increase in the state of cure at the mid-plane of the rubber sheet as a function of time. Thus, the S shape for the curve representing the cure (or rather the mean cure) versus time (Figure 1.1) is logical. Moreover, the scorch time [2,3], which is the time necessary for the onset of vulcanization to take place, will perhaps need another explanation.
viii. A striking result is shown in Figure 1.1 where the time of the cure process largely depends on the apparatus. There is already one reason, based on the heat transfer; as the time of heat conduction varies with the square of the thickness of the material, this time difference lets us suggest that the thickness of the rubber sample is quite different for these experiments, without speaking

of the quality of the contact between the rubber and the heated mold. This fact is considered in depth in Chapter 2 for heat transfer without cure reaction and in Chapter 4 for heat transfer associated with the cure reaction.

1.2 NUMERICAL EVALUATION OF THE STATE OF CURE

1.2.1 Principle of the Method

As noted by Prentice and Williams [4], an effective method of calculating the time-dependent temperature distribution in a vulcanizing article is actively sought in the rubber industry. Given the temperature history, one can readily optimize the cure cycle and thus reduce capital and energy requirements. Until the early 1970s, the state of cure (SOC) could only be crudely estimated for defined simple geometries from nomograms. A few years later, analogous methods were applied to this problem.

A digital method for calculating SOC in a vulcanizing tire was outlined [5]. A similar approach is used in this study, but the previous model has been extended to the following: the thermal conductivity varies with temperature; heat is conducted through materials with disparate properties; chemically generated heat production which is a function of temperature and SOC; and time-varying boundary conditions, as is typical of real-cure cycles.

1.2.2 Theoretical

The differential equation governing transient one-dimensional heat conduction, with application to rubber technology is:

$$\rho C\frac{\partial T}{\partial t}=\frac{\partial}{\partial x}\left[\lambda\frac{\partial T}{\partial x}\right]+Q \tag{1.8}$$

where Q is the heat source term due to the vulcanization reaction. The thermal conductivity λ, as well as the density ρ and the heat capacity C of the rubber, may vary with temperature.

From the temperature history, the SOC can be calculated at any location by:

$$\mathrm{SOC}=\int_0^t r\cdot dt \tag{1.9}$$

where $r(T)$, in "equivalent minutes"/minute, expresses the instantaneous rate of vulcanization at that point, referred to the rate of a reference temperature. The temperature coefficient of vulcanization is chosen to be 1.85, meaning that the reaction rate increases by a factor of 1.85 per 10°C, and the reference temperature is taken as 149°C. Thus, Equation 1.9 becomes:

$$\mathrm{SOC}=\int_0^t 1.85^{\frac{T-149}{10}}dt \tag{1.10}$$

With this definition, a minimum of 8 equivalent minutes (SOC = 8 equivalent minutes) is required to effect a soft cure. The optimal properties are developed in 15 to 35 equivalent minutes, and some deterioration occurs after 50 equivalent minutes.

By assuming that the rate of heat generation by the vulcanization reaction is proportional to the rate of disappearance of free sulfur over the 50 equivalent minutes period, it means that during the entire vulcanization period, a first-order expression (the rate being proportional to remaining sulfur) describes the reaction rate over the range of interest.

Realistic boundary conditions are used either during the cure or after cure. Especially during the cooling period of the rubber, the coefficient of convection at the surface of the rubber h_{conv} is calculated for natural convection to vertical surfaces, leading to:

$$h_{conv} = \text{constant.}(T_{sur} - T_{air})^{0.25} \tag{1.11}$$

and the boundary equation between the vulcanized rubber and air becomes:

$$-\lambda \frac{\partial T}{\partial x} = h_{conv}(T_{sur} - T_{air}) \tag{1.12}$$

Calculation was made by using a finite difference method in an explicit form.

1.2.3 Results

A compete temperature history was obtained either from experiment or calculation. Moreover, the values of the state of cure SOC, as defined by Equation 1.10, are evaluated at each location.

1.3 HEAT CONDUCTION AND VULCANIZATION IN MOLDS

1.3.1 Principle of the Method

The purpose of the work done in Reference [6] was to model the curing processes occurring during molding of rubber compounds and to experimentally determine the thermal and vulcanization rate characteristics of compounds. Thus, the curing process is considered, and, in particular, instead of the model heat conduction in molds; present measurements of thermal conductivity using a new experimental apparatus; present experimental studies of vulcanization rates and heat generation using differential scanning calorimetry; and present calculations based on models and experimental data.

1.3.2 Theoretical

The rate of cure of a rubber compound in a mold is governed by the kinetic relation:

$$\frac{d\mu}{dt} = r(T, t, C_s, C_a) \tag{1.13}$$

expressing the rate of the increase in crosslinking density as a function of all the parameters, the temperature T, time t, concentrations of curatives C_s, and of accelerators C_a.

The general equation representing the energy balance has the usual form:

$$\rho c \frac{\partial T}{\partial t} = \lambda \frac{\partial^2 T}{\partial x^2} + r\Delta H \tag{1.14}$$

where the enthalpy of cure ΔH is seen, as well as its rate $r\Delta H$.

Dimensionless numbers are introduced, with the Damkohler and Fourier numbers, by using the thickness of the sample, a characteristic time t_{ch}, and the temperature difference T_{ch}, which are considered as being characteristics of the process.

Applications to curing at various sulfur levels were made, and two solutions to the heat conduction Equation 1.14, which contains heat generation induced by vulcanization kinetics, were critically studied:

i. By assuming, first, that $r\Delta H$ is constant, an analytical solution is obtained that has certain striking characteristics: the magnitude of the steady-state temperature rise increases not only with $r\Delta H$ but also with the square of the slab thickness, and thicker slabs increase in temperature more slowly as governed by the Fourier number.
ii. By assuming next that the rate of heat generated by the cure reaction $r\Delta H$ depends upon time and temperature. Calorimetric data obtained in scanning mode are used for evaluating the kinetics of the heat evolved by the cure reaction. Thus, the $r\Delta H$ calorimetric data were divided into sections (Figure 1.3):

Section 1, before the reaction starts with $r\Delta H = 0$; (1.15)

Section 2, where the temperature increases up to the peak with $r\Delta H = f(t, T)$;

Section 3, where temperature decreases down with $r\Delta H = E(t, T)$.

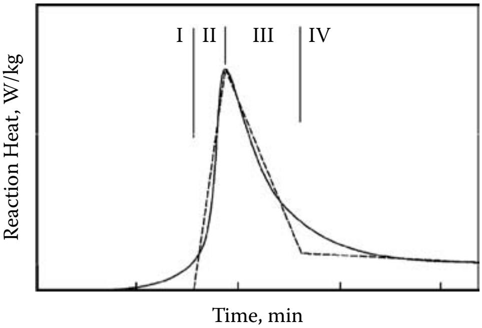

FIGURE 1.3 Four zones are divided to describe the reaction history during curing, obtained with a calorimeter in scanning mode. (With permission from *Rubber Chemistry and Technology,* copyright 1987, 60, 140, Figure 10. An experimental and theoretical study of heat conduction and vulcanization of rubber compounds in molds. D. Kong et al., Rubber Division, ACS.)

The second zone of Equation 1.15 was approximately represented by a series of three subzones, in each of which the time dependence is expressed in linear manner at the reference temperature T_r:

$$r\Delta H = (a_j t + b_j) \tag{1.16}$$

Values of a_j and b_j were evaluated for different recipes, together with the values of the temperatures corresponding to the beginning of Zones II and Zone III in Figure 1.3.

For the activation energy, the compounders' rule of a doubling of cure rate was chosen, and thus $r\Delta H$ for each 10°C increase in temperature. It is obtained from:

$$\exp\left[-\frac{E}{R(T_r+10)}\right] = 2\cdot\exp\left[-\frac{E}{RT_r}\right] \tag{1.17}$$

1.3.3 THEORETICAL AND EXPERIMENTAL RESULTS

Various results of interest are worth noting:

i. The calculation for the temperature was made by using the Crank–Nicholson finite-difference implicit method. Thus, the temperature profiles developed at the mid-plane of slabs of various sizes are obtained, showing that these curves pass through a maximum. The value of this maximum temperature increases with the percentage of sulfur.
ii. In the same way, the profiles of temperature developed through the thickness of the slab are calculated.
iii. In terms of boundary conditions, it should be noted that the temperature of the rubber is assumed to be instantaneously equal to the temperature of the mold surface with which it is in contact. If it is true, after a while when equilibrium is reached, for short times the equality of heat flux on both surfaces at the rubber–mold interface should stand as follows:

$$\lambda_m\left(\frac{\partial T}{\partial x}\right)_m = \lambda_r\left(\frac{\partial T}{\partial x}\right)_r \tag{1.18}$$

This equality in the flux at the beginning of the process leads to lower cure at short times. And more, it depends on the characteristics of the mold, i.e., thickness and heat diffusivity.

iv. If the values of the cure enthalpy are pretty well given for several varieties of rubber compounds, the values of the energy of activation are not shown.
v. An interesting apparatus was built and successfully tested for measuring the thermal conductivity of various rubbers with or without fillers.
vi. The effect of the percent sulfur and other curing additives was precisely shown by using calorimetry run in scanning mode.
vii. The exotherm obtained in scanning mode is divided into three parts, the separation between two of them being at the peak for evaluating the temperature dependence of the rate of cure, with the energy of activation (Figure 1.3).

viii. Moreover, the unit used on the ordinate of these exotherms obtained by DSC is the reaction heat, expressed in terms of *W* per kg rubber. In fact, as it is shown in Chapter 2 and more precisely evaluated in the following Chapters 3 and 4, the process of heat transfer at the rubber–calorimeter interface is more complex, leading to different conclusions.

1.3.4 Remarks on the Calorimetry Studies

From the recent knowledge, the following stages should be considered:

1. Either in isothermal or in scanning calorimetry, the temperature of the rubber increases.
2. Heat evolves from the exothermic curing reaction as soon as the temperature is high enough; this heat is responsible for another increase in temperature of the rubber.
3. A heat flux is thus emitted from the rubber surface to the surface of the calorimeter, according to Equation 1.18. Finally, the unit should be W/cm^2 for the given characteristics of the rubber sample in the calorimeter. This heat flux increases up to a maximum value associated with the top of the peak, and then decreases down to the base line.
4. The cure enthalpy is obtained from the area under the curve expressing the variation of the heat flux as a function of either time with isothermal calorimetry or temperature in scanning calorimetry. The integration of the heat flux given in Equation 1.18 leads to:

$$\int_{t_0}^{t_f} \lambda \cdot \frac{\partial T}{\partial x} \cdot dt = [Heat] \cdot [Length]^{-2}$$

   which is the amount of heat evolved from the reaction per unit area. Thus, the cure enthalpy is obtained for the area of the rubber in contact with the calorimeter sensor. Of course, calibration is necessary for the value of this enthalpy by using a material whose thermal property is known, for example, melting enthalpy, this material being placed under the same conditions as the rubber sample (e.g., same sample holder).

An identical result is obtained with calorimetry driven in scanning mode, the integration of the heat flux being made with respect to temperature.

1.4 EVALUATION OF TEMPERATURE AND EXTENT OF CURE DURING THE PROCESS

1.4.1 Scheme of the Method [7]

Heat involved in vulcanization of rubber containing a few parts of sulfur is small, but because rubber exhibits low thermal conductivity, the temperature and rate of reaction can vary within the curing mass, particularly for thick rubber slabs.

During the heating period, heat transfer plays a particular role, because the rate of reaction increases with a small increase in temperature. Therefore, the extent of cure reaction is a function of time and position as determined by the balance of internal heat generation from the curing reaction, conduction, and heat exchange with the mold. The vulcanization of unsaturated elastomers is a highly complex chemical process involving numerous simultaneous and consecutive reactions. Although vulcanization is a complex series of reactions, the overall result can be represented by a heat of reaction and a single activation energy with an Arrhenius equation.

The main assumption is that the partial enthalpy evolved up to time *t*, as a fraction of the total enthalpy evolved, represents the conversion up to time *t* [8].

1.4.2 Theoretical

The overall rate of cure is expressed in terms of heat evolved from this reaction:

$$\frac{dq}{dt} = k \cdot (q_\infty - q_t)^n \tag{1.19}$$

where q_∞ is the overall heat of reaction and q_t is the heat of reaction up to time *t*. The rate constant *k* is assumed to have the usual Arrhenius form, with the activation energy *E*.

For a plane sheet of rubber of thickness *L* and thermal conductivity λ, whose surfaces $x = 0$ and $x = L$ are in contact with the mold kept at the temperature T_m, the heat flow is unidirectional, and the general differential equation for transient conduction of heat is:

$$\rho C \frac{\partial T}{\partial t} = \lambda \frac{\partial^2 T}{\partial x^2} + \frac{dq_t}{dt} \tag{1.20}$$

The problem was solved by using a numerical method based mainly on the Dusinberre generalization of the increment method [9] applied to one-dimensional transient conduction. In fact, the heat transfer coefficient at the steel–rubber interface is very large, the surface rubber temperature changed very quickly, and consequently the initial temperature was taken as the arithmetic mean of the original surface temperatures of the mold and rubber.

1.4.3 Kinetic Study Using Isothermal Calorimetry [8]

Isothermal exotherms were obtained in isothermal calorimetry at 160, 165, and 170°C, successively. The increase in heat follows the first-order law with respect to time because plots of log (heat rate) against log $(q_\infty - q_t)$ are linear for the three temperatures, with a slope equal to 1; the temperature coefficients *k* were determined by measuring the ordinate intercept in these curves at the three temperatures. The energy of activation *E* was found from the slope of log *k* versus 1/*T* plots. The value

TABLE 1.2
Cure Kinetics and Heat Transfer data

Order $n = 1$	$q_\infty = 75.8$ J/g	$k_0 = 3 \cdot 10^9$/s	$E = 106$ kJ/mol
$\dfrac{\lambda}{\rho C} = 3.1 \cdot 10^{-3}$ cm^2/s	$\rho C = 1.47$ J/cm^3 deg		

of the activation energy was of the order of magnitude with corresponding values reported for natural rubber [10]. The enthalpies q_∞ and q_t were determined by measuring the area under each exotherm. It was recalled that the decrease of free sulfur was found to follow a first-order law with respect to time, for natural rubber and for SBR with sulfamide accelerators [10].

1.4.4 Results and Applications

Kinetic parameters of cure and thermal characteristics of the rubber are shown in Table 1.2.

The compound was made of scrap rubber from truck tires, essentially natural rubber, and sulfur. This compound is poor and vulcanization necessitates rather high pressure so as to compact the mixture. Nevertheless the final materials exhibit rather good mechanical properties measured either under static or dynamic conditions, as well as interesting qualities for absorption of impact noises [11].

Various results have been obtained either from experiments or calculation [7], and the following curves are drawn:

- Figure 1.4 showing the mid-plane temperature of a 1-cm-thick rubber sheet as a function of time at 180°C without and with 2% sulfur.
- Figure 1.5 showing the temperature profiles developed through the thickness of the rubber sheet at different times as they are calculated with two sheets of thickness 1 and 2 cm, respectively, at the cure temperature of 180°C, with 2% sulfur.
- Figure 1.6 showing the increase in the state of cure with time, as calculated at the mid-plane of rubber sheets of various thicknesses ranging from 0.5 to 5 cm, at 180°C, with 2% sulfur.

1.4.5 Conclusions

Various conclusions can be drawn from these results:

i. Rather good agreement is obtained between experimental and calculated, as shown in Figure 1.4, when the thickness is 1 cm.
ii. The effect of the internal heat generated by the cure reaction appears in Figures 1.4 and 1.5.

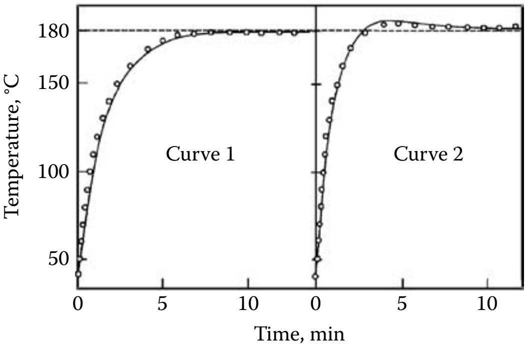

FIGURE 1.4 Mid-plane temperature with a 1-cm-thick rubber sheet as a function of time at 180°C. Left: 0% sulfur; right: 2% sulfur. Full line: calculated; plot: experimental. (With permission from *Rubber Chemistry and Technology*, copyright 1983, 56, 689, Figure 2. Calculation of the temperature and extent of reaction during the vulcanization of powdered rubber. A. Accetta and J. M. Vergnaud, Rubber Division, ACS.)

iii. Results of interest can be obtained by calculation, either for the profiles of temperature or, much better, for the state of cure.

iv. Let us notice the S-shaped curves obtained for the state of cure at the mid-plane in Figure 1.6. This is the answer to the question set by Hands and Horsfall [1] with Figure 1.1. In fact, as shown in this figure, it takes some time for the heat transfer to be achieved through the thickness of the rubber sheets. The obvious statement holds: the thicker the rubber sheet, the longer the sheet needs to be completely heated and cured.

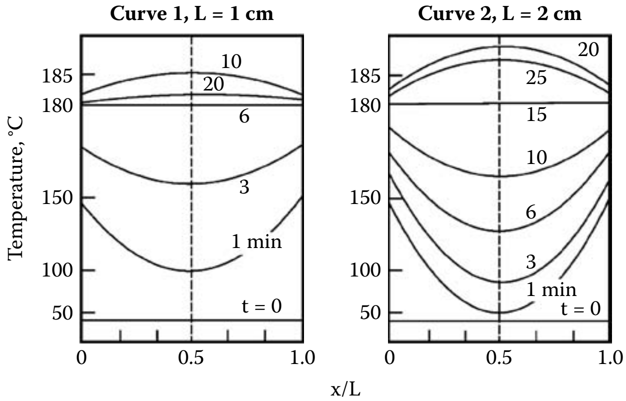

FIGURE 1.5 Temperature profiles developed through the thickness of rubber sheet cured at 180°C with 2% sulfur. Left: 1 cm thick; right: 2 cm thick. (With permission from *Rubber Chemistry and Technology,* copyright 1983, 56, 689, Figure 3. Calculation of the temperature and extent of reaction during the vulcanization of powdered rubber. A. Accetta and J. M. Vergnaud, Rubber Division, ACS.)

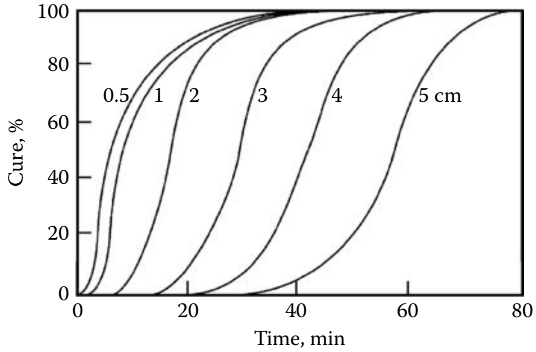

FIGURE 1.6 Extent of reaction as a function of time at the mid-plane of sheets of various thicknesses. Temperature of 180°C and 2% sulfur. (With permission from *Rubber Chemistry and Technology*, copyright 1983, 56, 689, Figure 6. Calculation of the temperature and extent of reaction during the vulcanization of powdered rubber. A. Accetta and J. M. Vergnaud, Rubber Division, ACS.)

v. It should be said that the state of cure at time *t* is expressed in this paper by the heat evolved at time *t* from the cure reaction as a fraction of the total heat evolved.

vi. The mathematical analysis is correct but the numerical treatment is poor, based on an explicit method with finite differences. The assumption used for the heat transfer at the rubber–mold interface is better than taking an infinite heat transfer at this interface, which leads to the fact that the temperature on the surface of the rubber reaches instantaneously that of the mold surface. Nevertheless, the best assumption is obtained with the equality of the heat flux through the mold–rubber interface, expressed by Equation 1.18.

vii. It is very difficult to intimately mix two powders, and this problem appears with the powders of rubber and sulfur. This difficulty has been overcome by using as vulcanizing agent the highly viscous compound made of an ultra-fine sulfur powder impregnated with a small amount of oil. Hence, this viscous system makes mixing with rubber powder easy, avoiding the electrostatic effects provoked by dry powders. The oil is absorbed by the rubber, letting the ultra-fine particles of sulfur adhere uniformly on the surface of the rubber powder.

1.5 EXPRESSION OF THE CURE REACTION

If it is easier to consider the cure reaction as a simple and unique reaction where the concentration of the remaining sulfur, or vulcanizing agent, appears, as described by a first-order reaction; in fact, the cure reaction is a complex one in terms of kinetics.

Thus, a bird's eye view of the actual kinetics could be informative, if it is not totally useful for the purposed calculation of rubbers sheets or blocks cured in a mold.

1.5.1 S-Shaped SOC–Time Curves and Scorch Period at the Beginning of the Cure

As already said, the SOC–time curves exhibiting an S-shaped form have found several explanations: The one [1,3] where this shape results from the presence at the very beginning of the process of a temperature-dependent period, called the scorch period, along which the cure reaction is very low, is followed by a sudden increase in the cure rate at the end of this scorch period. The other is obtained by considering either the stage of heating process or the stage of the cure reaction. The fact that it takes some time for heat to be transferred through the rubber mass is responsible for a lag time over which the cure reaction is very low.

Whatever the reason, it will be assumed that the cure reaction obeys a first-order reaction, as said by various authors. And, thus, a reference temperature with reference time will not be necessary or even useful. However, it is useful to know the time at which the cure reaction starts for a rubber sheet. The Mooney viscometer is pretty well described in Reference [3].

Parallel plate compression plastimeters have been quite widely used for measuring rate of cure, and in the past, methods have been standardized. The test pieces are heated for various times and then tested in the plastimeter. The change in plasticity, or recovery of some combination of these, is then plotted against time of heating to give a “scorch curve.” The Mooney viscometer offers a more convenient way of measuring scorch time and even rate of cure, and a standard method is given in ISO 667. This is essentially the method of ISO 289, continued until the viscosity reaches 40 Mooney units above its minimum value. Laboratory measurements of curing characteristics have been somewhat revolutionized by the introduction of so-called curemeters, which are now almost universally used for the routine control of fully compounded rubbers.

1.5.2 CURE REACTION DEFINED BY A COMPLEX REACTION SYSTEM

The cure reaction is obviously highly complex, and expressing such a system of reactions in a simple first-order reaction with an activation energy results from a strong assumption. As the problem is vast, only two studies are considered; the one concerned with the sulfur vulcanization process, and the other more specifically based on the explanation of the scorch delay kinetics.

i. The cure of elastomers is a process whereby chemical crosslinks are introduced between the elastomer chains, resulting in the formation of a three-dimensional network [12]. Numerous chemical agents or curatives are capable of reacting with unsaturated elastomers. However, sulfur, the first discovered curative, remains the most used in commercial applications. Sulfur was initially used alone to produce the so-called hard rubbers, but in modern usage in elastomeric products, cure systems based on sulfur generally include organic accelerators, an activator (zinc oxide), a fatty acid and, on occasion, a retarder. Several excellent texts are available [13–16]. Overall, the chemistry accompanying sulfur vulcanization is extremely complex and although several techniques have been developed to monitor the process and to analyze the products formed, most are time-consuming and tedious. According to a study made on the chemistry of sulfides, and written for a thiazole-type accelerator system [12], the reaction of the sulfurating agent with the rubber molecule can be schematized as follows:

- Vulcanizing ingredients {(accelerator + sulfur, sulfur donor) + activators}} gives:
- Active sulfurating agent, which acts upon rubber to give:
- Rubber-bound intermediate compounds $R - S_y - X$, giving in turn:
- Initial polysulfide crosslinks: $R - S_x - R$, followed by:
- Network maturing reactions, including: crosslink shortening with additional crosslinking, crosslink destruction, main-chain modification (dehydrogenation and cyclic sulfide formation), S–S bond interchange, leading to:
- Final vulcanizate network.

ii. Another study of interest is concerned with the long scorch delay period [17].

In order to explain the rather long delay period frequently encountered in accelerated sulfur vulcanization, especially wherein thiazole sulfonamides or other scorch delay accelerators are used, the following scheme has been proposed:

$$A \xrightarrow[k_1]{} B \xrightarrow[k_2]{} B' \xrightarrow[k_3]{} \alpha Vu \quad \text{and} \quad A + B' \xrightarrow[k_4]{} \beta B$$

where A is the accelerator, or the reaction products (with sulfur, Z_n^{++}); B is a precursor to crosslinks, probably polymeric: B' is an activated form of B; Vu is a crosslink; α and β adjust stoichiometry; and k_1 to k_4 are rate constants.

If the reaction through k_4 is much faster than through k_3, very little crosslink formation can occur until A is essentially depleted. Both the reaction through k_3 and that through k_4 are assumed to be much faster that the reaction through k_2; hence, after the delay required for the depletion of A, crosslink formation will proceed in a first-order fashion. As said by Coran [17], the proposed scheme for scorch delay vulcanization was largely substantiated by experimental observations.

1.6 GENERAL CONCLUSIONS

Improving on existing work is certainly easier than conducting the original study. It should be said that very often there is at least one good, and sometimes great, idea, in any research paper. Moreover, nobody can be perfect in all domains, and the problems concerned with the cure of rubbers are of all sorts, as already shown in this chapter. Thus, the following facts could be pointed out:

In the first case [1], the heat transfer process through a solid, and especially for a rubber which has a low heat diffusivity and conductivity, takes some time; even for a thin rubber sheet, this transfer cannot be so short that this time is neglected. The large difference in time for the rubber cure with the three techniques employed

(Figure 1.1) is due to the difference in the thickness used, as well as the quality of the contact between the rubber sample and the heating metal system.

In the third case [6], the process is rather complex in the calorimeter. Not only the heat brought by the apparatus run in scanning mode (DSC) is responsible for heating the rubber sample up to a temperature at which the cure takes place, but in turn, the exothermic cure reaction developed through the rubber sample is responsible for an increase in temperature through the rubber, which allows the production of a heat flux at the rubber–calorimeter interface. And this heat flux is monitored as a function of time in isothermal calorimetry (DC) or of temperature in calorimetry run in scanning mode (DSC). It is true that no value possibly given to the order of the overall cure reaction can be responsible for a "peak of heat" in the calorimeter. But it is also true that in the calorimeter the heat flux is registered but not the heat generated by the cure reaction [6]. As already said (Section 1.3.4) in this chapter, the cure enthalpy is obtained by integrating the heat flux emitted as a function of either the time in DC or the temperature in DSC.

In various papers of great interest [4,6], a reference temperature has been selected, around 150°C, for which an increase in temperature by 10°C from this reference allows an increase in the rate of cure by around 2. By making this choice, the order of the overall cure reaction may be neglected. Is it not better to develop a method able to obtain the energy of activation, as well as the order of this overall cure reaction?

REFERENCES

1. Hands D. and F. Horsfall. 1980. A new method for simulating industrial cure processes. *Kautschuk Gummi Kunststoffe* 33: 440–46.
2. Claxton W.E. and J.W. Liska. 1963. Calculation of state of cure in rubber under variable time-temperature conditions. *Rubber Age* 95: 237–43.
3. Brown, R.P. 1979. *Physical Testing of Rubbers*, Applied Science Publishers, 93.
4. Prentice G.A. and M.C. Williams. 1980. Numerical evaluation of the state of cure in a vulcanizing article. *Rubber Chem. Technol.* 53: 1023–31.
5. Ambelang J.C. and G.A. Prentice. 1972. Digital method of calculating the flow of heat through a tire during vulcanization. *Rubber Chem. Technol.* 45: 1195–1201.
6. Kong D., J.L. White, F.C. Weissert, and N. Nakajima. 1987. An experimental and theoretical study of heat conduction and vulcanization of rubber compounds in molds. *Rubber Chem. Technol.* 60: 140–58.
7. Accetta A. and J.M. Vergnaud. 1983. Calculation of the temperature and extent of reaction during the vulcanization of powdered rubber. *Rubber Chem. Technol.* 56: 689–02.
8. Accetta A., P. Le Parlouer, and J.M. Vergnaud. 1982. Kinetic parameters of the overall reaction of scrap rubber vulcanization by 2% sulfur. *Thermochim. Acta* 59:149–56.
9. Mac Adams W. 1954. *Heat Transmission*, McGraw Hill Series in Chemical Engineering. Tokyo. 44.
10. Bhatnagar S.K. and S. Banergie.1968. Kinetics of accelerated vulcanizates. Sulphur vulcanization accelerated with 2-mercatobenzothiazole and its Zn salts in presence of ZnO and stearic acid. *Angewandte Makromol. Chemie*. 3(1):177–121.
11. Accetta A. and J.M. Vergnaud. 1982. Rubber recycling. Upgrading of scrap rubber powder by vulcanization. II. *Rubber Chem. Technol.* 55: 961–66.

12. Brazier D.W. 1981. *Development in Polymer Degradation*. N. Grassie, Ed., Applied Science Publishers, London, tome 3. Chapter 2, 27.
13. Bateman L., C.G. Moore, P. Porter, and B. Sardle. 1963. *In the Chemistry and Physics of Rubber-Like Substances*. L. Bateman, Ed., Mac Laren and Sons, London. Chapter 15.
14. Hofman W. 1967. *Vulcanization and Vulcanizing Agents*. Mac Laren and Sons.
15. Coran A.Y. 1978. *Science and Technology of Rubber*. F.R. Eirich, Ed., Academic Press, New York.
16. Brydson J.A. 1978. *Rubber Chemistry*. Applied Science Publishers Ltd., London.
17. Coran A.Y. 1964. Vulcanization. Part VI. A model and treatment for scorch delay kinetics. *Rubber Chem. Technol.* 37: 689–97.

NOMENCLATURE

c, c_∞	concentration at time t, maximal concentration
C	heat capacity
ΔH	enthalpy of cure, in Equations 1.14–1.16
E	activation energy of the cure reaction
h	coefficient of heat convection at the rubber surface
k	constant rate of the cure reaction (/s)
λ, λ_r, λ_m	thermal conductivity, of the rubber, of the mold, respectively.
μ	used for the concentration in Equation 1.13
n	order of the cure reaction
Q	enthalpy of the cure reaction, in Equation 1.8.
q	heat evolved from the cure reaction, in Equation 1.19.
ρ	density of the rubber
$r(T)$	rate of vulcanization in Equation 1.9 (equivalent minutes/minutes)
R	ideal gas constant
SOC	state of cure
t, t_{eq}	time, equivalent time in Equation 1.3
θ	temperature in Equations 1.1–1.7
T, T_{sur}, T_{air}	temperature, on the rubber surface, in the surrounding air (Equation 1.11)
x	abscissa defining the position

2 General Study on Heat Transfer

The laws of heat transmission are of controlling importance in the design of equipment and the operation of many diverse instruments in many different industries. This applies particularly to the rubber industry.

2.1 VARIOUS MEANS OF HEAT TRANSFER

When different parts of a body are at different temperatures, heat flows from the hotter parts to the cooler. There are three distinct ways by which this transference of heat takes place: (i) conduction, in which the heat passes through the substance of the body itself, (ii) convection, in which heat is transferred by relative motion of portions of the heated body, and (iii) radiation, in which heat is transferred directly between distant portions of the body by electromagnetic radiation.

2.1.1 Heat Conduction

Conduction in a homogeneous opaque solid is the transfer of heat from one particle to another, under the influence of a temperature gradient, without appreciable displacement of the particles. Conduction involves the transfer of kinetic energy from one molecule to an adjacent molecule; it is the only mechanism of heat flow in an opaque solid. With gases and liquids, conduction may be supplemented by convection and radiation; within a fluid (motionless or in streamline motion), heat is transferred by conduction at right angles to the direction of fluid flow. Thus, heat is transferred by conduction either through the rubber materials or through the mold.

2.1.2 Heat Convection

Convection involves the transfer of heat by mixing one parcel of fluid with another. The motion of the fluid may be entirely the result of differences of density caused by temperature differences, as in natural convection, or it may be produced by mechanical means, as in forced convection. Energy is also transferred simultaneously by molecular conduction and, in transparent media, by radiation.

In summary, there is a natural (or free) convection between a rubber or a mold and a motionless fluid, either in liquid or in gaseous state.

2.1.3 HEAT RADIATION

A hot body emits radiant energy in all directions. When this energy strikes another body, part may be reflected, and another part may be transmitted through the body. In any case, the surface on an opaque solid is directly heated by the radiation.

2.2 HEAT CONDUCTION

2.2.1 PRINCIPLE OF HEAT CONDUCTION

The law for unidirectional conduction of heat was established in 1822 by Fourier [1].

It states that the instantaneous rate of heat flow $\frac{dQ}{dt}$ is equal to the product of three factors: the area A taken at right angles to the direction of heat flow; the temperature gradient $\frac{dT}{dx}$, which represents the change in temperature with respect to the length of path dx; and the factor of proportionality λ, called thermal conductivity, which is a physical property of the material.

Mathematically, Fourier's law is written as follows:

$$\frac{dQ}{dt} = -A.\lambda.\frac{dT}{dx} \tag{2.1}$$

This equation is of value and great importance under stationary conditions, when the temperature does not vary with time

On the contrary, in transient conditions, when the temperature and its gradient vary with space and time, Fourier's law should be written with partial derivatives:

$$F_{x,t} = -\frac{1}{A}\frac{dQ}{dt} = -\lambda \cdot \frac{\partial T}{\partial x} \tag{2.2}$$

where $F_{x,t}$ is the rate of heat transfer per unit area of section at position x and time t.

The negative sign arises because the heat flux occurs in the direction opposite to that of increasing temperature.

When Q is expressed in calories and T in degrees Celsius, the dimensional dimension of the thermal conductivity λ is cal/(cm.s.deg.), equal to 4.18 J/(cm.s.deg.) or 418 W/(m.deg.).

2.2.2 DIFFERENTIAL EQUATION OF HEAT CONDUCTION

The differential equation of heat conduction through a thin sheet of thickness dx is established as follows:

Consider the element of volume $A.dx$ (Figure 2.1), where dx is very small, and whose sides of area A are perpendicular to the axis of the heat flux. The rate of change of heat in the element of volume $A.dx$ is calculated by considering the rates of heat transfer through the area A of the plane x, leaving the same area of the plane $x + dx$ during the short time dt, the increments of time dt and of space dx being as small as possible:

$$A \cdot (F_x - F_{x+dx}) = -A \cdot \frac{\partial F}{\partial x} dx \tag{2.3}$$

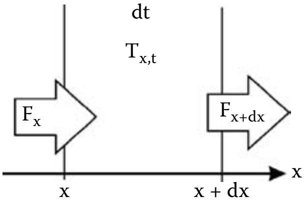

FIGURE 2.1 Scheme of the heat transferred by conduction through a sheet of thickness *dx* during time *dt*, while the temperature is a function of position *x* and time *t*, and F_x is the heat flux at position *x* and time *t*.

The rate at which the amount of heat changes in the volume *A.dx* is also:

$$A\cdot\rho\cdot C\cdot\frac{\partial T}{\partial t}\cdot dx \tag{2.4}$$

From the equality of these two expressions of the rate of heat, by recalling the value of the flux defined in Equation 2.2, by simplifying by the volume *A.dx*, it becomes:

$$\rho\cdot C\cdot\frac{\partial T}{\partial t}=\frac{\partial}{\partial x}\left[\lambda\cdot\frac{\partial T}{\partial x}\right] \tag{2.5}$$

This equation is fundamental for the monodirectional of heat transfer.

When the thermal conductivity is constant, this equation simplifies as follows:

$$\rho\cdot C\cdot\frac{\partial T}{\partial t}=\lambda\cdot\frac{\partial^2 T}{\partial x^2} \tag{2.6}$$

It can also been written, by considering the thermal diffusivity α defined by:

$$\alpha=\frac{\lambda}{\rho\cdot C} \tag{2.7}$$

which leads to the simple form of interest when the parameters ρ and C are constant:

$$\frac{\partial T}{\partial t}=\alpha\cdot\frac{\partial^2 T}{\partial x^2} \tag{2.8}$$

The parameters characterizing the solid through which heat is transferred are as follows:

The thermal conductivity λ, the density ρ, the heat capacity C, and the heat diffusivity α.

Following is the case of a solid with heat transfer through two directions perpendicular to each other:

When there are two axes of heat transfer, *x* and *y*, with the two values of the thermal conductivity dependent on the axis, the differential equation of heat conduction:

$$\rho\cdot C\cdot\frac{\partial T}{\partial t}=\frac{\partial}{\partial x}\left[\lambda_x\cdot\frac{\partial T}{\partial x}\right]+\frac{\partial}{\partial y}\left[\lambda_y\cdot\frac{\partial T}{\partial y}\right] \tag{2.9}$$

When the values of the thermal conductivity are the same, whatever the axis, it becomes:

$$\rho \cdot C \cdot \frac{\partial T}{\partial t} = \lambda \cdot \left[\frac{\partial^2 T}{\partial x^2} + \frac{\partial^2 T}{\partial y^2} \right] \tag{2.10}$$

In the case of a solid with heat transfer through three directions perpendicular to one another: The equation is general when the three axes are perpendicular to one another:

$$\rho \cdot C \cdot \frac{\partial T}{\partial t} = \frac{\partial}{\partial x} \left[\lambda_x \cdot \frac{\partial T}{\partial x} \right] + \frac{\partial}{\partial y} \left[\lambda_y \cdot \frac{\partial T}{\partial y} \right] + \frac{\partial}{\partial z} \left[\lambda_z \cdot \frac{\partial T}{\partial z} \right] \tag{2.11}$$

which is simplified, when the solid has the same thermal conductivity, whatever the axis:

$$\rho \cdot C \cdot \frac{\partial T}{\partial t} = \lambda \cdot \left[\frac{\partial^2 T}{\partial x^2} + \frac{\partial^2 T}{\partial y^2} + \frac{\partial^2 T}{\partial z^2} \right] \tag{2.12}$$

2.2.3 GENERAL SOLUTION OF HEAT CONDUCTION (SEPARATION OF VARIABLES)

Assuming that the variables are separable is the basic method of obtaining a solution of the partial differential equation. For the equation of heat conduction:

$$\frac{\partial T}{\partial t} = \alpha \cdot \frac{\partial^2 T}{\partial x^2} \tag{2.8}$$

an attempt to find a solution is made by putting the temperature function of space and time:

$$T_{x,t} = T_x \cdot T_t \tag{2.13}$$

where T_x and T_t are functions of space x and time t, respectively.

Substitution in Equation 2.8 gives

$$T_x \frac{dT_t}{dt} = \alpha \cdot T_t \frac{d^2 T_x}{dx^2} \tag{2.14}$$

which is rewritten as follows after the separation of the variable:

$$\frac{1}{T_t} \frac{dT_t}{dt} = \frac{\alpha}{T_x} \frac{d^2 T_x}{dx^2} \tag{2.15}$$

The left-hand side depends on time t only, while the right-hand side depends on space x only. The two members are thus equal to the same constant, which is conveniently taken as $-\omega^2 \alpha$.

Therefore, the two ordinary differential equations result in:

$$\frac{1}{T_t} \frac{dT_t}{dt} = -\omega^2 \alpha \tag{2.16}$$

$$\frac{1}{T_x} \frac{d^2 T_x}{dx^2} = -\omega^2 \tag{2.17}$$

The solution of these equations being:

$$T_t = \exp(-\omega^2\alpha \cdot t) \tag{2.18}$$

$$T_x = A \cdot \sin \omega x + B \cdot \cos \omega x \qquad \text{if } \omega \neq 0 \text{ (transient state)} \tag{2.19}$$

$$T_x = ax + b \qquad \text{if } \omega = 0 \text{ (steady state)} \tag{2.20}$$

A particular solution of Equation 2.8 is in the form:

$$T_{x,t} = [A \cdot \sin \omega x + B \cdot \cos \omega x] \cdot \exp(-\omega^2\alpha \cdot t) \tag{2.21}$$

And the most general solution of Equation 2.8 is obtained by summing solutions of the type given by Equation 2.21 and a linear function $ax + b$:

$$T_{x,t} = a \cdot x + b + \sum_{n=0}^{\infty} [A_n \cdot \sin \omega_n x + B_n \cdot \cos \omega_n x] \cdot \exp\left(-\omega_n^2\alpha \cdot t\right) \tag{2.22}$$

The values of parameters a, b, A_n, B_n, and ω_n have to be determined for each particular problem, by considering that the general solution 2.22 must satisfy the initial and boundary conditions of the problem.

2.2.4 INITIAL AND BOUNDARY CONDITIONS

2.2.4.1 Initial Conditions

The temperature throughout the solid must be known at the instant taken at the outset: $t = 0$. This initial condition of temperature is expressed as follows:

$$t = 0 \qquad T = f(x,y,z) \text{ within the solid.} \tag{2.23}$$

Generally, the temperature is uniform throughout the solid at the beginning of the process of heating. Just after cure, at time t_f, a nonuniform profile of temperature is often obtained through the rubber mass; in this case, the initial profile for the second stage at the new time $t = 0$, that is, the cooling period, is obtained by taking that final profile for the initial condition.

2.2.4.2 Boundary Conditions

Various surface conditions may arise, depending on the nature of the atmosphere surrounding the heated material, rubber, or mold.

2.2.4.2.1 No Heat Flux at the Surface

This case is very extreme from a practical point of view, as perfect insulators do not exist. Nevertheless, from a theoretical point of view, the problem can be considered as it leads generally to easier solutions. It is written as follows:

$$t > 0 \qquad \frac{\partial T}{\partial x} = 0 \quad \text{surface} \tag{2.24}$$

2.2.4.2.2 Constant Temperature at the Surface

This is the other extreme case, after the previous one obtained without heat transfer. Even though it is often used for the mathematical treatment leading to simple equations, it is practically unrealistic. Theoretically speaking, this condition needs such a perfect contact with the heating source that an infinite coefficient of heat transfer should be at the interface. It is written as

$$t > 0 \quad T_s = \text{constant surface} \tag{2.25}$$

2.2.4.2.3 Heat Flux at the Surface of Separation of Two Different Solid Materials

The heat flux has the same value on both sides of the interface. This is the typical condition for the rubber–mold interface. The following equality is obtained by considering the heat flux taking place in the materials in contact, this heat flux being defined by Equation 2.2:

$$t > 0 \quad \lambda_1 \frac{\partial T_1}{\partial x} = \lambda_2 \frac{\partial T_2}{\partial x} \quad \text{both sides at the interface} \tag{2.26}$$

Of course, in this case, it is implied that when the surface of the rubber is heated, the mold surface is somewhat cooled, at least over a given time which depends on the reactivity of the heating system of the mold.

2.2.4.2.4 Heat Transfer between a Solid and a Fluid

When a fluid (liquid or gas) of large volume at temperature T_{est} is in contact with the solid (rubber or mold), the heat transfer is achieved by convection in the fluid. The convection is forced when the fluid is stirred, and it is natural or free when the fluid is motionless.

The rate of transfer of heat through the surface of the solid is proportional to the temperature difference between the solid and the surrounding atmosphere (T_s–T_{ext}), the coefficient of proportionality being the coefficient of surface heat transfer *h*. The following equation relates the equality of the flux of heat at the surface of the solid and in the surrounding atmosphere.

$$t > 0 \quad -\lambda \cdot \left[\frac{\partial T}{\partial x}\right]_s = h \cdot (T_s - T_{ext}) \tag{2.27}$$

The value of the coefficient of convection h depends on the nature of the convection.

2.3 HEAT CONVECTION [2–4]

As already said, heat is transferred by convection through a fluid (liquid or gas). This case also intervenes at the interface of a solid and a fluid, and Equation 2.27 holds.

Heat convection in a fluid acting in a more efficient way than heat conduction through a solid may be considered uniform through the volume of the fluid or at a given thickness within the solid. The two cases of convection—for example, forced convection when the fluid is stirred, and free convection when the fluid is motionless—are considered successively; thus, the coefficient of heat transfer at the solid–fluid interface will be evaluated.

2.3.1 FORCED HEAT CONVECTION

In this case, the value of the coefficient of convection is rather high, and Equation 2.27 holds for calculation.

Various studies have been undertaken to resolve experimentally the problem of a fluid circulating in a tube [2]. The other problem of heat convection between the external surface of a cylinder and the fluid is quite different. The method to be followed is based on the relationship between two dimensionless numbers, the Nüsselt (Nu) number and the Reynold (Re) number.

$$Nu = a \cdot (\mathrm{Re})^n \tag{2.28}$$

where the Nüsselt and the Reynold numbers are given by:

$$Nu = \frac{h \cdot L}{\lambda} \tag{2.29}$$

$$\mathrm{Re} = \frac{L \cdot u \cdot \rho}{\mu} \tag{2.30}$$

where L represents the main dimension of the system—for example, the diameter of a tube—u is the linear velocity of the gas, a is a constant depending on the operational conditions, ρ and μ are the density and the viscosity of the gas, respectively.

Some values of the coefficient a and n are shown, as a function of the values of Re [3]

$1 < \mathrm{Re} < 4$	$n = 0.33$	$a = 0.89$
$4 < \mathrm{Re} < 40$	$n = 0.38$	$a = 0.82$
$40 < \mathrm{Re} < 4000$	$n = 0.47$	$a = 0.61$

2.3.2 NATURAL (FREE) HEAT CONVECTION

When the gas is motionless, the free convection is described by three dimensionless numbers: the Nüsselt number, the Grashof (Gr) number, and the Prandtl (Pr) number:

$$\mathrm{Gr} = \frac{\beta \cdot g \cdot \rho^2 \cdot L^3}{\mu^2} \Delta T \tag{2.31}$$

$$\mathrm{Pr} = \frac{\mu \cdot C}{\lambda} \tag{2.32}$$

where g is the acceleration due to the gravity, β and ρ are the cubic expansion and the density of the gas, respectively, C is the specific heat of the gas, and L is the representative dimension of the system—for example, plane height or cylinder diameter, with $\Delta T = T_s - T_{ext}$.

The Nüsselt number is expressed in terms of the other two dimensionless numbers:

$$\mathrm{Nu} = a \cdot (Gr \cdot \mathrm{Pr})^n \tag{2.33}$$

A few values of a and n shown in this equation depend on the nature of the convection:

In the laminar state, when $10^4 < Gr \cdot \Pr < 10^9$	$n = 0.25$
In the turbulent state, when $Gr \cdot \Pr > 10^9$	$n = 0.33$

A few values of the coefficients a and n are given, depending on the shape of the solid:

Vertical plane or cylinder	laminar: $a = 0.56$	turbulent: $a = 0.12$
Horizontal cylinder	laminar: $a = 0.47$	turbulent: $a = 0.10$
Horizontal plane facing upward	laminar: $a = 0.54$	turbulent: $a = 0.14$
Horizontal plane facing downward	laminar: $a = 0.24$	turbulent: $a = 0.14$

2.4 SOLUTIONS OF THE EQUATIONS OF HEAT TRANSFER

Various solutions are obtained according to the assumptions made for the initial and boundary conditions. A few of them are presented, and calculation is made for the more simple system, even if it is not realistic and should be used with great care—for example, when the temperature is uniform initially, and the temperatures are kept constant on the surfaces. The two other cases considered are (i) when a finite coefficient of heat transfer is at the surfaces of the solid, and (ii) when the rubber is heated by the mold on both surfaces.

2.4.1 Sheet Heated on Both Sides with Infinite Heat Transfer at the Interface

The sheet of thickness 2 L, in the region $-L < x < +L$ is initially at the uniform initial temperature T_{in} and the two surfaces in contact with the mold are maintained at the constant temperature of the mold: $T_{mould} = T_\infty$.

Let us note that the thickness taken as 2 L is of interest, for the symmetry.

The initial and boundary conditions shown in Figure 2.2 are:

$$t = 0 \qquad -L < x < +L \qquad T = T_{in} \qquad \text{sheet} \tag{2.34}$$

$$t > 0 \qquad x = +L \text{ and } x = -L \qquad T = T_{mould} = T_\infty \qquad \text{rubber sides} \tag{2.35}$$

The mid-plane of the sheet, at $x = 0$, being a plane of symmetry, there is also:

$$t > 0 \qquad x = 0 \qquad \frac{\partial T}{\partial x} = 0 \qquad \text{mid-plane} \tag{2.36}$$

The general solution of this problem is expressed by the Equation 2.22 in which the constants are to be determined from the initial and boundary conditions.

$$T_{x,t} = a \cdot x + b + \sum_{n=0}^{\infty} [A_n \cdot \sin \omega_n x + B_n \cdot \cos \omega_n x] \cdot \exp\left(-\omega_n^2 \alpha \cdot t\right) \tag{2.22}$$

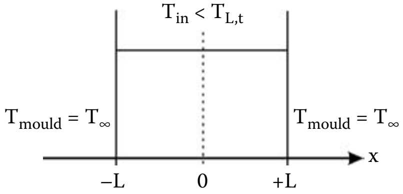

FIGURE 2.2 Scheme of heat transferred by conduction through a sheet of thickness $2L$ ($-L < x < L$) initially at uniform temperature with constant temperature on both sides $T_{L,t} = T_{mould} = T_\infty$.

At infinite time, $T_{x,t} = T_{mould} = T_\infty$, leading to:

$$a = 0 \quad \text{and} \quad b = T_{mould} = T_\infty \tag{2.37}$$

Consideration of this result yields for the general equation 2.22:

$$T_{x,t} - T_\infty = \sum_{n=0}^{\infty} [A_n . \sin \omega_n x + B_n \cdot \cos \omega_n x] \cdot \exp\left(-\omega_n^2 \alpha \cdot t\right) \tag{2.38}$$

The condition at the mid-plane

$$\frac{\partial T_{x,t}}{\partial x} = \frac{\partial T_{0,t}}{\partial x} = 0 \tag{2.36}$$

necessitates that the terms in the derived Equation 2.38 cosines are equal to 0, and $A_n = 0$.

The boundary condition 2.35—for example, $x = L$ and $T_{L,t} = T_{mould} = T_\infty$, for $t > 0$—is fulfilled when:

$$\cos \omega_n L = \cos(2n+1)\frac{\pi}{2} \quad \text{and} \quad \omega_n = \frac{(2n+1)\pi}{2L} \tag{2.37}$$

The initial condition 2.34 leads to:

$$T_{in} - T_\infty = \sum_{n=0}^{\infty} B_n \cdot \cos \frac{(2n+1)\pi x}{2L} \tag{2.38}$$

The coefficient B_n is obtained by multiplying both sides of Equation 2.38 by $\cos \frac{(2n+1)\pi x}{2L} dx$, and integrating between $-L$ and $+L$. Then it becomes:

$$(T_{in} - T_\infty) \cdot \int_{-L}^{+L} \cos \frac{(2n+1)\pi x}{2L} dx = B_n \cdot \int_{-L}^{+L} \cos^2 \frac{(2n+1)\pi x}{2L} dx \cdots +$$

$$B_p \cdot \int_{-L}^{+L} \cos \frac{(2n+1)\pi x}{2L} \cos \frac{(2p+1)\pi x}{2L} dx \cdots \tag{2.39}$$

By applying $\cos n \cdot \cos p = \frac{1}{2}[\cos(n+p) + \cos(n-p)]$ and $\cos^2 n = \frac{1}{2}[1 + \cos 2n]$ to Equation 2.39, all the terms in B_p where p is different from n are equal to 0, and the first term in the right side is equal to $B_n L$.

As the integral in the left-hand side of Equation 2.39 is:

$$\frac{4L}{(2n+1)\pi}\sin\frac{(2n+1)\pi}{2} = \frac{4L}{(2n+1)\pi}(-1)^n$$

the coefficient B_n becomes:

$$B_n = \frac{4L}{(2n+1)\pi}(-1)^n \tag{2.40}$$

Finally, the profile of temperature developed through the rubber sheet of thickness $2L$, with $-L < x < +L$, is expressed in terms of space x and time t by the following series:

$$\frac{T_{x,t} - T_\infty}{T_{in} - T_\infty} = \frac{4}{\pi} \cdot \sum_{n=0}^{\infty} \frac{(-1)^n}{2n+1} \cdot \cos\frac{(2n+1)\pi x}{2L} \cdot \exp\left[-\frac{(2n+1)^2 \pi^2}{4L^2}\alpha \cdot t\right] \tag{2.41}$$

The amount of heat entering the rubber sheet at time t, Q_t, is obtained by integrating the heat flux through the surface (unit area) with respect to time:

$$Q_t = 2\lambda \cdot \int_0^t \left[\frac{\partial T}{\partial x}\right]_L dt \quad \text{for } x = +L \text{ or } x = -L \tag{2.42}$$

As the gradient of temperature, for $x = +L$ or $x = -L$, becomes equal to:

$$\left[\frac{\partial T}{\partial x}\right]_L = \frac{2(T_{in} - T_\infty)}{L} \sum_{n=0}^{\infty} \exp\left[\frac{(2n+1)^2 \pi^2}{4L^2}\alpha \cdot t\right]$$

Because $(-1)^n \cdot \sin\frac{(2n+1)\pi}{2} = (-1)^{2n} = 1$ the amount of heat transferred into the rubber sheet at time t, Q_t, is expressed by:

$$Q_t = \frac{4\alpha(T_{in} - T_\infty)}{L} \int_0^t \exp\left[-\frac{(2n+1)^2 \pi^2}{4L^2}\alpha \cdot t\right] \cdot dt \tag{2.43}$$

As the series $\sum_{n=0}^{\infty} \frac{1}{(2n+1)^2} = \frac{\pi^2}{8}$, and the amount of heat that has entered the sheet after infinite time, $Q_\infty = 2(T_\infty - T_{in})L$, the kinetics of heat entering in the rubber sheet of thickness $2L$ is given by the relationship:

$$\frac{Q_t}{Q_\infty} = 1 - \frac{8}{\pi^2} \sum_{n=0}^{\infty} \frac{1}{(2n+1)^2} \cdot \exp\left[-\frac{(2n+1)^2 \pi^2}{4L^2}\alpha \cdot t\right] \tag{2.44}$$

2.4.2 HEAT TRANSFER THROUGH A RUBBER SHEET IMMERSED IN A LARGE VOLUME OF FLUID

This case is practically obtained when a rubber sheet is cooled down in a stirred fluid (gas or liquid), after extraction from the mold (Figure 2.3).

The equations that stand for this problem are:

$$\frac{\partial T}{\partial t} = \alpha \cdot \frac{\partial^2 T}{\partial x^2} \tag{2.8}$$

$$t > 0 \quad -\lambda \cdot \left[\frac{\partial T}{\partial x} \right]_s = h \cdot (T_s - T_{ext} \tag{2.27}$$

The solution for the profile of temperature developed through the thickness of the rubber sheet of thickness $2L$ is, with a constant surface heat convection h:

$$\frac{T_{x,t} - T_{sur}}{T_{in} - T_{sur}} = \sum_{n=1}^{\infty} \frac{2R \cdot \cos \beta_n \frac{x}{L}}{\cos \beta_n \cdot (\beta_n^2 + R^2 + R)} \exp\left[-\beta_n^2 \frac{\alpha \cdot t}{L^2} \right] \tag{2.45}$$

where the dimensionless number R is given as follows:

$$R = \frac{h \cdot L}{\lambda} \tag{2.46}$$

and the β_ns are the positive roots of:

$$\beta \cdot \tan \beta = R \tag{2.47}$$

The amount of heat exchanged between the rubber sheet of thickness $2L$ and the fluid of infinite volume is expressed by the series:

$$\frac{Q_\infty - Q_t}{Q_\infty} = \sum_{n=1}^{\infty} \frac{2R^2 \cdot \exp\left[-\beta_n^2 \frac{\alpha \cdot t}{L^2} \right]}{\beta_n^2 (\beta_n^2 + R^2 + R)} \tag{2.48}$$

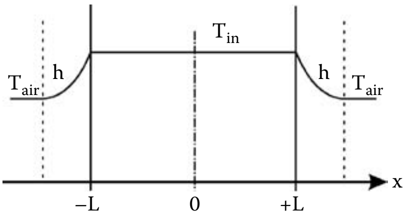

FIGURE 2.3 Scheme of heat transferred by conduction through the rubber sheet of thickness $2L$ ($-L < x < L$) and by convection on both sides, with the coefficient of convection h.

2.5 THERMAL PROPERTIES OF RUBBERS

Values of thermal conductivity and thermal diffusivity are needed for heat-flow calculations, for the determination of structure–property relationships, and for material selection and comparison. Heating and cooling are essential processes in the forming of most rubber articles. In the curing there are two main requirements: the heating and cooling cycle must be kept as short as possible for efficiency, and the temperature gradients in the articles must be minimized for uniformity in the finished products. To evaluate the best compromise, the temperature distribution in the article during heating must be calculated, and this depends on the knowledge of the appropriated thermal properties at the relevant temperature.

Most of the available thermal property values are each measured at only one temperature, which is much lower than the usual processing temperature. But the diffusivity and conductivity of black-loaded natural rubber compounds decrease with increasing temperature. The decrease, over the temperature range from ambient to 200°C, can be as much as 45% [5]. This large temperature dependence should obviously be taken into account in heat-flow calculations at processing temperatures.

In the last few years, the value of an analytical approach to heat transfer problems has been increasingly realized and considerable effort has been devoted to developing techniques and convenient methods of calculation. However, the measurement of thermal properties has remained a very specialized subject, there is little evidence of standard procedures and the tests are carried out in relatively few laboratories [6–9].

2.5.1 SPECIFIC HEAT [9]

As shown already, specific heat is the quantity of heat required to raise the unit mass of the material through 1°C, that is, the heat capacity of unit mass. There is the specific heat at constant volume which is virtually impossible to measure, and the specific heat at constant pressure, which is the quantity normally measured. The difference between the two specific heats is usually small enough to be ignored. In fact, the heat capacity at constant volume per unit volume is given by $\rho \cdot C$, so that it is found:

$$\rho \cdot C = \left[\frac{\partial Q}{\partial T} \right]_v \tag{2.49}$$

where Q is the internal energy per unit volume.

Specific heat is measured by supplying heat to a calorimeter containing the test piece and measuring the resulting temperature rise. An adiabatic calorimeter is one in which no exchange of heat between the calorimeter and its surroundings is allowed, and this is achieved by surrounding the calorimeter with a jacket that is heated to follow the temperature change of the calorimeter itself. A variation that results in a more simple apparatus is the drop calorimeter. The test piece is heated externally, then dropped into the calorimeter and the resultant change in temperature monitored.

Except where the very highest precision is required when an adiabatic calorimeter would be used, specific heat can be measured using differential scanning calorimetry

(DSC). Heat losses to the surrounding medium are allowed, but assumed to be dependent on temperature only. The heat input and temperature rise for the material under test are compared with those for a standard material of known specific heat.

2.5.2 THERMAL CONDUCTIVITY [9]

Thermal conductivity, as already stated, is the quantity of heat passing per unit time normally through unit area of a material of unit thickness for unit temperature difference between the faces.

In the steady state, when the temperature at any point is constant with time, this parameter controls heat transfer as follows:

$$Q = -\lambda \cdot A \cdot \frac{dT}{dx} \cdot dt \tag{2.50}$$

The methods of measurements are divided into steady-state methods and transient methods. Steady state methods are most widely used, but they are very time consuming and involve expensive apparatus; nonsteady state methods have been largely developed. There are standard methods for materials in BS 874 [10]. A heated disc method, as given in BS 874. Clause 4.2.3, is satisfactory for many purposes, but for lowest conductivity materials, a guarded hot plate gives more precise results (BS 874 Clause 4.2.1 [11]; ASTM C177 [12]). A comprehensive account of thermal transport properties of rubbers was given by Hands [5] including theory and a review of methods with discussion of the sources of errors. A method of measuring thermal conductivity [13] is of particular importance because, apart from eliminating heat losses from exposed edges of the test piece by enclosing the heat source and test pieces inside the heat sink, the apparatus allows measurements to be made through the solid phase, which is of great value when studying rubbers at the processing temperature.

The thermal conductivity of solid rubbers is of the order of 0.1–0.2 W/m. deg, which is in the region of fairly low value where experimental errors due to heat loss are the greatest.

2.5.3 THERMAL DIFFUSIVITY [9]

Thermal diffusivity is the parameter that determines the temperature distribution through a material in transient conditions, that is, when the material is being heated or cooled. As shown in Equation 2.7, it is a function of the thermal conductivity, specific heat, and density:

$$\alpha = \frac{\lambda}{\rho \cdot C} \tag{2.7}$$

By combining the Equation 2.2 with Equation 2.50, the heat flux can be rewritten:

$$J_x = -\alpha \cdot \frac{\partial Q}{\partial x} \tag{2.51}$$

Thus, thermal diffusivity α is the parameter relating energy flux to energy gradient, whereas thermal conductivity relates the energy flux to the temperature gradient.

Thermal diffusivity is of little interest in many insulation applications where steady-state conditions exist, such as civil engineering. However, in rubber processing, when temperatures are changing rapidly, it is of more interest than thermal conductivity, as shown in the Equations 2.45 and 2.48 established as a general case, or even as a particular case with the Equations 2.41 and 2.44.

Thermal diffusivity is actually easier to measure experimentally than thermal conductivity, because it is only necessary to measure the change in temperature with time at three collinear points in the rubber material taken in the direction of the heat flow. The mathematical treatment required for such calculation is obtained using Equations 2.41 or 2.45, expressing the profile of the temperature developed through the material with time. Quenching methods, when the solid rubber (sheet or cylinder) initially at a uniform temperature is immersed in a temperature-controlled bath kept at a different temperature [5], are the best. Calculation is based on the rapid convergence of the series solutions. For example, after about 10% of the time for the center temperature to reach 99% of the surface temperature has elapsed, the second term in the series is about 0.5% of the first term. Thus, after a certain time, only the first term is relevant, leading to simplified Equations 2.45 and 2.41 [5]. Using an infinite value of the surface heat coefficient h in Equation 2.41 leads to huge errors for α.

Methods of measurements have been reviewed in considerable detail, and the RAPRA apparatus has been described [5,14].

2.5.4 SURFACE HEAT TRANSFER COEFFICIENT

The surface heat transfer coefficient is the quantity of heat flow per unit time normal on the surface across unit area at the interface between two materials with unit temperature difference across the interface. Obviously, it depends on the nature of this interface, and especially on the nature of the material that is in contact with the rubber.

When a fluid surrounds the rubber piece, the effect of the coefficient h defined in Equation 2.29 is inversely proportional to the thickness of the rubber.

When the rubber is surrounded with a mold with a good contact, Equation 2.26 holds, as it expresses that the values of the heat flux on both sides of the interface are equal.

As said already in Part 2.3, considerable work has been done on the subject of heat transfer through a solid and a fluid, especially for evaluation of heat transfer systems [2], and various dimensionless numbers have been established, whatever the nature of the fluid motion. In any case, either with a motionless or a stirred fluid, the Nüsselt number expressed in Equation 2.29, appears as the most important parameter.

Perfect insulation, expressed by Equation 2.24, does not exist in practice. The only solution is to maintain the same temperature on both sides of the interface; this solution was applied in measuring the thermal conductivity in order to avoid the heat loss from the apparatus.

2.5.5 CONCLUSIONS ON GUM RUBBERS

Thermal transport properties of rubber depend not only on the temperature but also on the type of rubber and the type and quantity of filler. It is generally thought that they are not greatly affected by vulcanization [5].

The effect of temperature on the thermal conductivity of rubber is similar to that for amorphous plastics. Below the glass transition temperature T_g, the conductivity increases with increasing temperature, and above T_g it decreases. At around room temperature, the thermal conductivity becomes nearly temperature independent. However, the conductivity of some rubbers, for example butyl, increases with temperature from room temperature.

The addition of carbon black to natural rubber increases the conductivity at room temperature, and this conductivity decreases with increasing temperature in all cases. The diffusivity for the same material passes through a minimum at about 90°C. Because specific heat exhibits a small increase with temperature over this temperature range, the increase in diffusivity reflects the decrease in density with rising temperature.

Carbon, whether in amorphous or graphitic form, has a much higher conductivity and diffusivity than rubber, and the addition of carbon black to a rubber almost invariably increases the values of the thermal transport properties at room temperature. However, at higher temperatures, values for the gum in some cases exceed those of the filled compounds. Unlike the heat capacity, the resultant conductivity and diffusivity of a filled material cannot be calculated on a simple volume additivity basis.

The addition of a plasticizer to a polymer lowers the glass transition temperature and also extends the transition temperature range. Above T_g of the unplasticized material, the conductivity decreases with increasing plasticizer concentration, because of the increasing free volume. On the other hand, below T_g of the plasticized material, the conductivity increases with increasing plasticizer concentration.

A sample variability exists for the thermal properties, especially for rubber filled with carbon filler, while such a variation is not seen with gum natural rubber [5].

As a conclusion, it seems difficult to give some values of the thermal parameters of rubbers in one or several tables, as the rubber compounds are so different from one to another. And generally, people working on a rubber compound have to determine themselves the thermal properties of their material. Nevertheless, in our calculations for the profiles of temperature or of state of cure developed through the thickness of the sample during the cure, the values taken for these thermal properties will be given beforehand.

2.6 HEATING OR COOLING STAGES WITHOUT CURE REACTION

The cooling period is of practical importance for the vulcanized compound, when this material has been extracted from the mold and let cool in the surrounding atmosphere. On the other hand, the effect of the assumptions made on the heating process in the mold will be tested when there is no curing agent in the rubber. The effect of these assumptions will be considered in Chapter 4. These calculations could also be considered on rubbers perfectly cured, reheated in the mold after cooling to room temperature.

2.6.1 Cooling Stage of a Perfectly Cured Rubber Sheet in Motionless Fluid

2.6.1.1 Case of Motionless Air at Room Temperature in Laminar Mode

This is the case of a square rubber of side 12 cm and 1 cm thick initially at 160°C immersed in motionless air at 20°C, in a vertical position.

There is a free convection, and following Section 2.3.2, we have to evaluate the Nüsselt number through the Grashof and Prandtl numbers. There is the following:

$$\mathrm{Gr} = 2.5 \cdot 10^5 \cdot \Delta T_{interface} \quad \text{and} \quad Pr = 0.71$$

$$\mathrm{Gr.Pr} = 1.75 \cdot 10^5 \cdot \Delta T_{inter} < 10^9 \text{ for the value of } \Delta T_{inter}\text{, then laminar flow}$$

$$\mathrm{Nu} = 0.47 \cdot (Gr \cdot \mathrm{Pr})^{0.25} = 9.6 \cdot \Delta T^{0.25}$$

$$\text{As } \lambda_{air} = 2.7 \cdot 10^{-2}\, W/m \cdot \deg \quad \text{then } h = 2.2 \cdot \Delta T^{0.25}_{inter} \ \ \mathrm{W/m^2} \cdot \deg$$

Thus, the boundary condition 2.27 at the rubber–air interface becomes:

$$-\lambda \cdot \frac{\partial T}{\partial x} = 2.2 \cdot (T_{rs} - T_{air})^{1.25} \tag{2.27$'$}$$

The equations of heat transfer in the rubber thickness and next to the surface are:

$$\frac{T_{x,t} - T_{sur}}{T_{in} - T_{sur}} = \sum_{n=1}^{\infty} \frac{2R \cdot \cos\beta_n \frac{x}{L}}{\cos\beta_n \cdot (\beta_n^2 + R^2 + R)} \exp\left[-\beta_n^2 \frac{\alpha \cdot t}{L^2}\right] \tag{2.45}$$

$$\frac{Q_\infty - Q_t}{Q_\infty} = \sum_{n=1}^{\infty} \frac{2R^2 \cdot \exp\left[-\beta_n^2 \frac{\alpha \cdot t}{L^2}\right]}{\beta_n^2(\beta_n^2 + R^2 + R)} \tag{2.48}$$

where the dimensionless number R is given as follows:

$$R = \frac{h \cdot L}{\lambda} = \mathrm{Nu} = 0.47 \cdot (Gr \cdot \mathrm{Pr})^{0.25} = 9.6 \cdot \Delta T^{0.25} \tag{2.46}$$

and the β_ns are the positive roots of:

$$\beta \cdot \tan\beta = R \tag{2.47}$$

As the difference of the temperature at the rubber–air interface decreases continuously, it is difficult to use this method of calculation. And the solution of the problem is obtained by a numerical treatment with finite differences.

The profiles of temperature developed through the thickness of rubber sheets heated at 160°C immersed in motionless air at 20°C are shown when the thickness is 1 cm (Figure 2.4) and 2 cm (Figure 2.5), as they are calculated numerically. Only half the thickness is drawn, because of the symmetry. Thus, it takes some time for the rubber sheets to cool down, the time being obviously longer for the thicker sheet.

2.6.1.2 Case of Motionless Air at Room Temperature in Turbulent Mode

Two square rubbers of side 120 cm initially at 160°C are immersed in motionless air at 20°C, in a vertical position, with a thickness of 1 cm (Figure 2.6) and 2 cm (Figure 2.7). The larger size is responsible for a higher value of the Gr number, leading to a turbulent motionless flow. The profiles of temperature developed through the thickness are slightly different from the previous obtained in laminar mode, a bit lower.

$$\mathrm{Pr} = 0.71 \quad \text{and} \quad \mathrm{Gr.Pr} = 1.75 \cdot 10^8 \cdot \Delta T_{inter} > 10^9 \ \text{ turbulent flow}$$

$$\text{Then, } \mathrm{Nu} = 0.12 \cdot (Gr \cdot \mathrm{Pr})^{0.33} = 70 \cdot \Delta T^{0.33}_{inter} \ \text{and } h = 1.6\, \Delta T^{0.33}_{inter} \ \ \mathrm{W/m^2} \cdot \deg$$

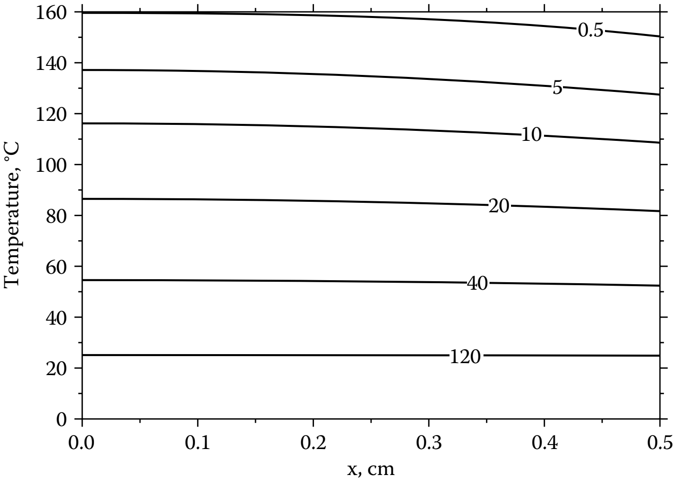

FIGURE 2.4 Profiles of temperature developed through the thickness of a rubber sheet at various times (min), when the rubber sheet initially at 160°C is cooled down in motionless air at 20°C. Thickness = 1 cm. Free convection is in laminar mode. Half the thickness is shown.

Thus, the equation expressing the boundary at the rubber–air interface becomes:

$$-\lambda \cdot \frac{\partial T}{\partial x} = 1.6 \cdot (T_{rs} - T_{air})^{1.33} \tag{2.27''}$$

In the same way as for the previous case, the problem is resolved using a numerical treatment.

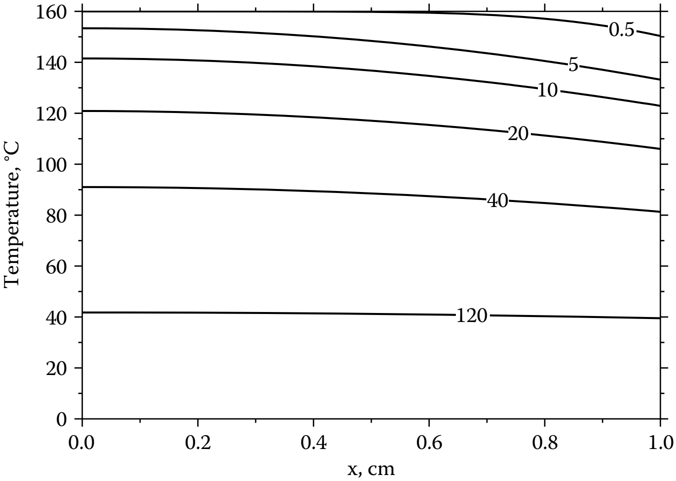

FIGURE 2.5 Profiles of temperature developed through the thickness of a rubber sheet at various times (min), when the rubber sheet initially at 160°C is cooled down in motionless air at 20°C. Thickness = 2 cm. Free convection is in laminar mode. Half the thickness is shown.

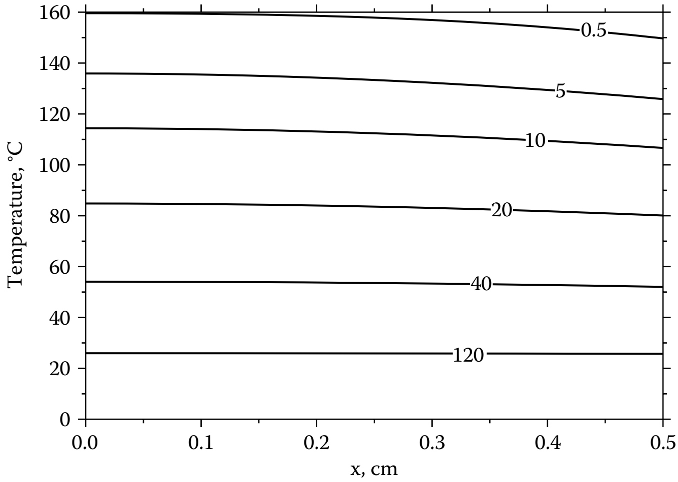

FIGURE 2.6 Profiles of temperature developed through the thickness of a rubber sheet at various times (min), when the rubber sheet initially at 160°C is cooled down in motionless air at 20°C. Thickness = 1 cm. Free convection is in turbulent mode. Half the thickness is shown.

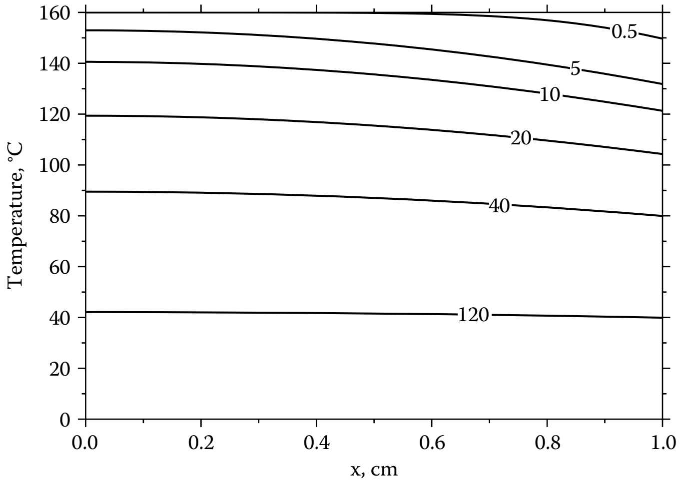

FIGURE 2.7 Profiles of temperature developed through the thickness of a rubber sheet at various times (min), when the rubber sheet initially at 160°C is cooled down in motionless air at 20°C. Thickness = 2 cm. Free convection s in turbulent mode. Half the thickness is shown.

2.6.2 COOLING OF PERFECTLY CURED RUBBER IN STIRRED FLUID

2.6.2.1 Case of Stirred Air in a Vertical Position

This is the case of a square rubber sheet 1 cm thick with 10-cm sides, initially at 160°C, immersed in stirred air at 20°C on both sides, in a vertical position.

The Reynold's number should be used and evaluated, and from the value obtained for this number, it is possible to calculate the Nüsselt number.

$$\mathrm{Re} = \frac{L \cdot u \cdot \rho}{\mu} \tag{2.30}$$

With $\mu = 1.8 \cdot 10^{-4}$ Po $\quad \rho = 1.2 \cdot 10^{3}$ g/cm^3 $\quad \lambda = 2.7 \cdot 10^{-4}$ W/cm.deg
and the linear speed of air $U = 10^3$ cm/s $\quad L = 10$ cm $\quad \mathrm{Re} = 66$
then $\mathrm{Nu} = a \cdot (\mathrm{Re})^n = 4.4 = R$ $\quad$ and $h = 12$ W/m^2 · deg

Equations 2.45 and 2.48 can be used for calculating the profiles of temperature as well as the heat released by the rubber to the surrounding air.

The equations of heat transfer in the rubber thickness and on the surface are:

$$\frac{T_{x,t} - T_{sur}}{T_{in} - T_{sur}} = \sum_{n=1}^{\infty} \frac{2R \cdot \cos \beta_n \frac{x}{L}}{\cos \beta_n \cdot (\beta_n^2 + R^2 + R)} \exp\left[-\beta_n^2 \frac{\alpha \cdot t}{L^2}\right] \tag{2.45}$$

$$\frac{Q_\infty - Q_t}{Q_\infty} = \sum_{n=1}^{\infty} \frac{2R^2 \cdot \exp\left[-\beta_n^2 \frac{\alpha \cdot t}{L^2}\right]}{\beta_n^2 (\beta_n^2 + R^2 + R)} \tag{2.48}$$

with the dimensionless number $R = 4.4$ (Figure 2.8).

2.6.2.2 Case of Stirred Water in a Vertical Position

This is the case of a square rubber sheet 2 cm thick with 10-cm sides, initially at 160°C, immersed in stirred water at 20°C on both sides, in a vertical position.

With the following values of the parameters for the water:

$\mu = 10^{-2}$ *Po* $\quad \rho = 1$ g/cm^3 $\lambda = 6.10^{-3}$ W/cm · deg
and U = 10 cm/s $\quad L = 10$ cm $\quad$ there is: Re = 10^4
and then $Nu = 0.61 \cdot (10^4)^{0.47} = 46$ $\quad$ and $h = 276$ W/m^2 · deg

Equations 2.45 and 2.48 can be used for calculating the profiles of temperature developed through the thickness of the rubber, with $R = Nu = 46$ (Figure 2.9).

Whatever the thickness of the rubber sheet, the cooling is far more efficient in stirred water, as shown by the profiles of temperature developed through the thickness.

2.6.3 HEATING STAGE OF THE CURED RUBBER IN THE MOLD

The mold temperature is assumed to be initially uniform when the rubber sheet at a lower temperature is placed between the two heated slabs. The heat flux is equal between the two surfaces in contact, according to Equation 2.26.

The equations are as follows:

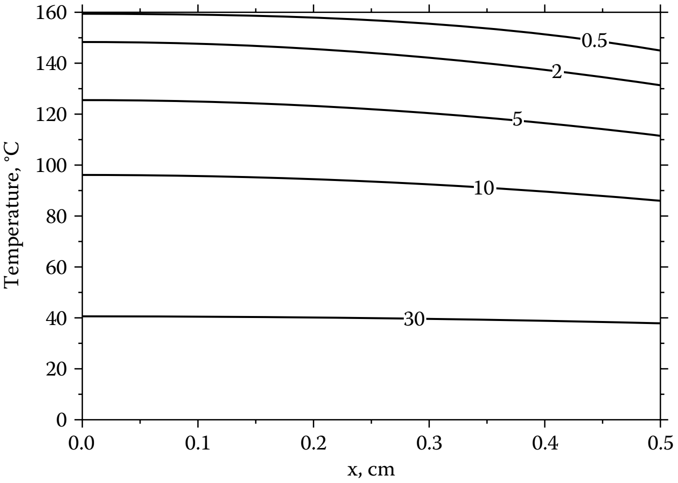

FIGURE 2.8 Profiles of temperature developed through the thickness of a rubber sheet at various times (min), when the rubber sheet initially at 160°C is cooled down in stirred water at 20°C. Thickness = 1 cm. Forced convection has constant surface convection coefficient.

The heat flux through the thicknesses of the rubber and of the mold is expressed by the same Equation 2.8, with their respective values for the thermal diffusivity α_r and α_m

$$\frac{\partial T}{\partial t} = \alpha \cdot \frac{\partial^2 T}{\partial x^2} \tag{2.8}$$

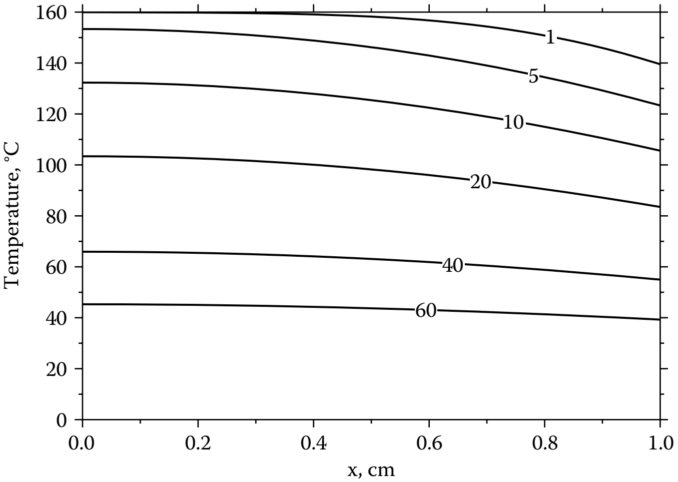

FIGURE 2.9 Profiles of temperature developed through the thickness of a rubber sheet at various times (min), when the rubber sheet initially at 160°C is cooled down in stirred water at 20°C. Thickness = 2 cm. Forced convection has constant surface convection coefficient.

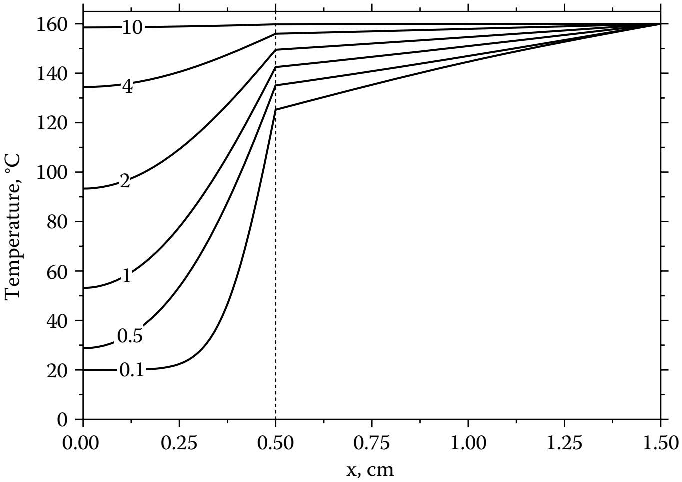

FIGURE 2.10 Profiles of temperature developed through the thickness of a rubber sheet and of the mold, when the rubber sheet previously at 20°C is placed between the slabs of the mold initially at 160°C. Rubber thickness = 1 cm. Mold thickness = 1 cm. Half the thickness of the system is drawn because of the symmetry. Time is expressed in minutes.

And the equality of the heat flux on both sides at the rubber–mold interface, as soon as the rubber is placed through the slabs of the heated mold, leading to the rewritten Equation 2.26:

$$t > 0 \quad \lambda_m \cdot \left[\frac{\partial T}{\partial x}\right]_m = \lambda_r \cdot \left[\frac{\partial T}{\partial x}\right]_r \tag{2.26'}$$

The main results are expressed in terms of profiles of temperature developed through the mold and rubber, either in Figure 2.10 where the rubber thickness is 1 cm or in Figure 2.11 where it is 2 cm, while the mold thickness is 1 cm in both cases.

The thermal characteristics of the rubber and mold are given in Table 2.1.

These profiles of temperature lead to conclusions of interest:

i. At low times, a decrease in temperature at the rubber–mold interface as well as through the mold is observed while the heating system of the mold is located on its external surface. This result shows the necessity to heat the mold at a given part inside the mold so as to keep the temperature constant on the surface of the mold.
ii. The effect of the relative thicknesses of the rubber sheet and mold on this decrease in the mold temperature is important, being 10 or 30 min when the rubber thickness is 1 or 2 cm.

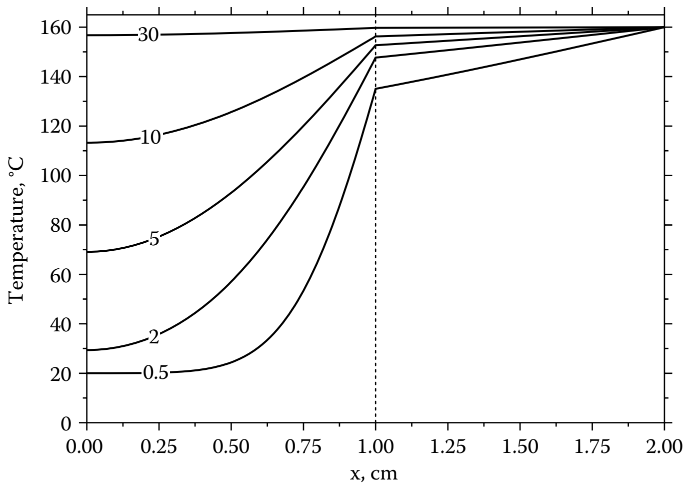

FIGURE 2.11 Profiles of temperature developed through the thickness of a rubber sheet and of the mold, when the rubber sheet previously at 20°C is placed between the slabs of the mold initially at 160°C. Rubber thickness = 2 cm. Mold thickness = 1 cm. Half the thickness of the system is drawn, because of the symmetry. Time is expressed in minutes.

2.7 CONCLUSIONS ON HEAT TRANSFER BOUNDARY CONDITIONS

As shown in this chapter, the boundary conditions which rule the conditions of heat transfer at the interface separating two media are of great importance. The equations which express these conditions have been presented as clearly as possible. It should be repeated as already said in the Preface that these conditions are presented only in a few books. The first published was from Carslaw and Jaeger [15] in which the theoretical treatment of the conduction of heat in solids was described and demonstrated in detail, but only a few lines were concerned with the problems of convection, and the numerical methods with finite differences were not known at that time. On the other hand, the heat transmission from McAdams [2] is fully focused on the calculation of heat transfer taking place in tubings and other heat exchanger apparatus, and contains various graphs and equations, but could still be considered as a primer by specialists in these areas; the section devoted to numerical treatment, however, has aged along with the book. It [3] is fine for either conduction or convection work, but

TABLE 2.1
Thermal Characteristics of the Rubber and Mold cm²/s g

Rubber	$\alpha = 10^{-3}$ cm²/s	$\rho = 0.9$ g/cm³	$C_p = 2.2$ J/g. deg	$\lambda = 2 \cdot 10^{-3}$W/cm. deg
Steel	$\alpha = 0.04$	$\rho = 7.9$	$C_p = 0.12$	$\lambda = 0.038$

is written in French, and calculations are made under stationary conditions only. In another book [4], devoted to the cure of thermosetting resins, a large part is concerned with numerical treatments, using the explicit finite differences methods that were current at that time.

In short, heat exchange takes place at the boundary separating two media, in such a way that when one medium is heated, the other in contact is cooled to the same degree, so that heat conservation is maintained. This is shown in Equation 2.26 when two solid media are in contact and the heat flux is the same on both sides of the interface; this equality also stands at the solid–fluid interface shown in Equation 2.27, where the surface heat convection appears in the fluid. In this case, the problem is more complex, as the fluid may be either motionless or stirred, leading to heat convection into the fluid, expressed in different ways. As a result, when the fluid is motionless, expressions as complex as Equations 2.27′ or 2.27″ are obtained with an nth power different from one for the temperature difference between the solid surface and the fluid far away from this surface, the nth power value depending on the nature of the regime, which may be either laminar or turbulent. Only in the case of stirred fluid can Equation 2.45 be used for the profiles of temperature and Equation 2.48 for the heat quantities exchanged, but in this more simple case, the values of the parameter β should be evaluated before their introduction in the terms of the series. A table is provided for the six roots of $\tan\beta \cdot \beta = R$ necessary for calculation. And, finally, it is understandable that numerical methods would be used for achieving these calculations.

From a practical point of view, two provisional and obvious conclusions concerned with heat transfer between two media are worth noting. One applies to the case of two solid media in perfect contact, using the example of a rubber sample heated in a mold: the heat transferred from the mold to the rubber is responsible not only for an increase in the rubber temperature but also for a decrease in the mold temperature, which is perfectly sensible next to the interface. A heating system should be placed somewhere within the mold in order to maintain its temperature as constant. The question is to know where the right place is. Another question concerns the cooling period of the sample in the fluid after the heating and cure stage when an appreciable time is necessary for the rubber temperature to decrease; in Chapter 4, it will be seen that this long cooling period could be managed to improve the extent of cure throughout the rubber, especially in the middle.

A few papers have been published showing the effect of the cooling period on the temperature in the rubber. The temperature history was measured and calculated at the mid-plane of rubber sheets set in the vertical position under various cooling conditions: for a 2-cm-thick rubber sheet initially at 180°C immersed in motionless air at 25°C [16]; for a 2-cm-thick rubber at 180°C immersed in motionless air at either 20 or 100°C [17]; and for a 1-cm-thick rubber sheet initially at 160°C immersed either in motionless water at 13°C or in motionless air maintained at 125°C [18]. In all these cases, good agreement was obtained between the experimental and calculated curves. Moreover, during the long period of cooling over which the temperature remained high, especially at the mid-plane of the rubber sheet, an increase in the state of cure was evaluated; this advantage will be considered in Chapter 4, which is devoted to the cure process.

REFERENCES

1. Fourier J.B. 1822. *Théorie analytique de la Chaleur*, Gauthier-Villars Ed. English translation by Freeman, Cambridge (1878).
2. McAdams W.H. 1954. *Heat Transmission*, McGraw Hill series in chemical engineering, Tokyo. Chapter 1–3, 1–57.
3. Wuithier P. 1972. *Raffinage et Génie chimique, Science et Techniques du Pétrole*, Editions Technip, Paris. Chapter 3: Transferts de Matière 274–347.
4. Vergnaud J.M. and J. Bouzon. 1992. *Cure of Thermosetting Resins*. Springer Verlag, London.
5. Hands D. 1977. The thermal properties of polymers. *Rubber Chem. Technol.* 50: 480–522.
6. Gehman S.D. 1967. Heat transfer in processing and use of rubber. *Rubber Chem. Technol.* 40: 36–97.
7. Sircar A.K. and J.L. Wells. 1982. Thermal conductivity of elastomer vulcanizates by differential scanning calorimetry. *Rubber Chem. Technol.* 55: 191–207.
8. Frensdorff H.K. 1974. Thermal diffusivity measurements on elastomers. *Rubber Chem. Technol.* 47: 849–57.
9. Brown R.P. 1979. *Physical Testing of Rubbers*, Chapter 14: 239–245. Applied Science Publishers, London.
10. BS 874. Determining Thermal Insulating Properties with Definitions and Thermal Insulating Terms (1973).
11. BS 4370. Part 2. Methods of Test for Rigid Cellular Materials (1973).
12. ASTM C177-71. Test for Thermal Conductivity of Materials by Means of the Guarded Hot Plate.
13. Hands D. and F. Horsfall. 1975. A thermal conductivity apparatus for solid and molten polymers. *J. Phys. E. Scientific Instruments*. 8: 687–690.
14. Hands D. and F. Horsfall. 1977. The thermal diffusivity and conductivity of natural rubber compounds. *Rubber Chem. Technol.* 50: 253–65.
15. Carslaw, H.S. and J.C. Jaeger, 1959. *Conduction of Heat in Solids*, Clarendon Press, Oxford, U.K. Chapters 2–9, 51–230.
16. Khouider A., J. Bouzon, and J.M. Vergnaud. 1986. Effect of cure enthalpy on cure progress during the cooling period in motionless air. *Thermochim. Acta*. 102: 83–92.
17. Khouider A. and J.M. Vergnaud. 1986. Effect of temperature of motionless air on the increase in state of cure of vulcanizates. *J. Appl. Polym. Sci.* 32: 5301–5313.
18. Khouider A. and J.M. Vergnaud. 1988. Increase in the state of cure in vulcanizates after removal from the mold. *J. Polym. Eng.*, 8: 19–39.

NOMENCLATURE

A	area through which heat is transferred
α	thermal diffusivity, defined in Equations 2.7 and 2.8
β	term used in Equation 2.47
C	heat capacity
$F_{x,t}$	heat flux at position x and time t
h	surface heat convection
L	main dimension in Equations 2.29–2.31. Half the thickness of the sheet in Equation 2.34

λ, λ_1, λ_2	thermal conductivity, thermal conductivity in position 1 or 2
λ_r, λ_m	thermal conductivity of the rubber, of the mold, respectively
μ	viscosity of a gas in Equation 2.30
Q, Q_t, Q_∞	heat, heat transferred at time t, after infinite time
R	dimensionless number defined in Equation 2.46
ρ	density
$T, \frac{\partial T}{\partial t}, \frac{\partial T}{\partial x}$	temperature, increase in temperature with time, gradient of temperature.
$T_{x,t}, T_x, T_t$	temperature, function of both position and time, of position, of time (Equation 2.13)
T_{in}, T_∞	temperature, initially, after infinite time, respectively
t	time
x	abscissa characterizing the position

DIMENSIONLESS NUMBERS

Nu	Nusselt's number defined in Equation 2.29
Re	Reynold's number defined in Equation 2.30
Gr	Grashof's number defined in Equation 2.31
Pr	Prandtl's number defined in Equation 2.32

3 Kinetics of the Cure Reaction

The cure of vulcanization of elastomers is a process whereby chemical crosslinks are introduced between the elastomer chains, resulting in the formation of a three-dimensional network. Overall, the chemistry accompanying sulfur vulcanization is extremely complex and although several techniques have been developed to monitor the process and to analyze the products formed, most are time-consuming and tedious.

There are various ways to determine the parameters of the kinetics of the cure reaction. The parameters to consider are: the cure enthalpy, which is the heat evolved from the overall cure reaction; the order of the reaction which is concerned with the concentration of active agent remaining free during the reaction at time *t*; and the two parameters that allow defining of the effect of the temperature on the rate of the reaction, that is, the energy of activation and a constant that depends only on the compound, by following the Arrhenius expression. Thus, by considering all these parameters, the cure of rubbers is considered a simple reaction.

Various techniques have been developed in turn: the Mooney viscometer, the Wallace–Shawbury curometer, the oscillating disc rheometer (ODR), and the moving disc rheometer (MDR), in addition to the calorimetry techniques. The isothermal calorimetry and its counterpart in scanning mode, the isothermal moving disc rheometer (MDR), and the improvement of this last technique with the rubber process analyzer run in scanning mode, are considered.

3.1 CALORIMETRY: PRINCIPLE, THEORY, AND TECHNIQUES

3.1.1 Principle of Calorimetry

In calorimetry techniques, enthalpy changes accompanying physical or chemical events, whether they are exothermic or endothermic, are measured and monitored either as a function of temperature or time. Thus, a calorimeter is able to collect a heat flux exchanged between the sample and the sensible part of the apparatus, generally made of thermocouples, and to register it. The result is a profile of the rate of enthalpy change, either as a function of temperature as the sample is heated at a known linear rate in differential scanning calorimetry (DSC), or as a function of time when the calorimeter is held at constant temperature in isothermal differential calorimetry (DC).

On the whole, two types of calorimeters exist: one is where the sample, located in a flat holder, is placed upon the sensitive part of the calorimeter, shaped as a horizontal plate. Thus, the sample may exchange a vertical heat flux between this temperature-sensitive plate. The other consists of a cylindrical sample surrounded by a temperature-sensitive cylinder, and the heat flux exchanged is radial. When this cylindrical sample is long enough, the heat transfer developed longitudinally can be neglected, and only the radial heat transfer and heat flux is of concern. A drawback with this type of apparatus comes from the thin air layer necessary for dropping the sample in the calorimeter in a smooth manner; the effect of this air layer on the heat flux and its consequences on the enthalpy and the kinetics was considered theoretically in detail [1–3]. The main advantage of the cylindrical sample stands for the amount which may be around 150–250 mg, depending on the density of the material. On the other hand, the calorimeter with the horizontal plate has two inconveniences: one comes from the small amount of the sample; the other is brought by the possible loss in heat from the sample to the air located above it [4]. In both types of calorimeters, the problem stands with the quality of the thermal contact between sample and the sensitive part of the calorimeter.

3.1.2 THEORETICAL CONSIDERATIONS IN CALORIMETRY

The process of cure in the sample set in the calorimeter is similar to that taking place in a mold. The rubber should be heated to a temperature at which the exothermal cure reaction starts, provoking an increase in temperature through the rubber, as well as a heat flux on the rubber surfaces. It should be especially mentioned that the surface must be kept in contact with the sensible part of the calorimeter. We will consider the case of each of the two types of calorimeters.

3.1.2.1 Case of the Calorimeter with a Cylindrical Sample

The equation of transient heat conduction through the cylindrical cross-section of the sample, even if the calorimeter is maintained isothermal, is expressed as follows:

$$\frac{\partial T}{\partial t} = \frac{\alpha}{r} \cdot \frac{\partial}{\partial r}\left[r \frac{\partial T}{\partial r}\right] + \frac{1}{C} \cdot \frac{\partial Q}{\partial t} \tag{3.1}$$

The heat flux at the rubber–calorimeter interface is given by:

$$HF = -\lambda \cdot \frac{\partial T}{\partial r} \tag{3.2}$$

where λ is the thermal conductivity of the rubber, and the radial gradient of temperature is developed in the rubber sample at the surface in contact with the calorimeter.

The assumption in the calorimeter calculation is that the partial enthalpy evolved up to time t, as a fraction of the total enthalpy evolved, represents the conversion up to time t. The overall rate of cure is given by:

$$\frac{dQ}{dt} = k_T \cdot (Q_\infty - Q_t)^n \tag{3.3}$$

where the rate of the heat evolved by the overall cure reaction is expressed as a function of the rate constant of the cure reaction k_T at temperature T, n is the order of the reaction, Q_t is the partial enthalpy evolved up to time t, and Q_∞ is the total enthalpy of the cure reaction.

3.1.2.2 Case of the Calorimeter with a Horizontal Sensible Detector, Plane in Shape

In this case, the problem is quite different from the previous one for two reasons at least: the thermal conduction through the rubber sample is monodirectional through its thickness; the heat flux occurs on both surfaces of the plane rubber sample, the one being the rubber–calorimeter sensor interface and the other taking place at the rubber surface in contact with the surrounding air. It could be said at that time that this air is generally heated by the heating system of the calorimeter, and thus it can only be expected that the air temperature is constantly equal to that of the heating plate. Because of the exothermal cure reaction shown in Equation 3.3, an increase in temperature appears through the rubber mass, leading to the production of the two heat fluxes on both surfaces.

$$\frac{\partial T}{\partial t} = \alpha \cdot \frac{\partial^2 T}{\partial x^2} + \frac{1}{C} \cdot \frac{\partial Q}{\partial t} \tag{3.4}$$

with the same expression for the rate of heat generated by the cure reaction

$$\frac{dQ}{dt} = k_T \cdot (Q_\infty - Q_t)^n \tag{3.3}$$

The heat flux evolved from the rubber surface to the sensor surface is somewhat similar to that for the cylindrical sample, with the difference that this flux is expressed linearly:

$$H.F. = -\lambda_r \cdot \left[\frac{\partial T}{\partial x}\right]_r = -\lambda_c \cdot \left[\frac{\partial T}{\partial x}\right]_c \tag{3.5}$$

where the heat flux at the surface of the rubber with the thermal conductivity of the rubber is shown, as well as the corresponding heat flux associated in the calorimeter sensor.

Moreover, the heat flux occurring at the rubber surface in contact with the surrounding air is:

$$H.F. = -\lambda_r \cdot \left[\frac{\partial T}{\partial x}\right]_r = h \cdot (T_{rs} - T_{air}) \tag{3.6}$$

where h is the surface coefficient of convection in air, T_{rs} is the temperature at the rubber surface, and T_{air} the temperature of air.

We have to understand that if the heat flux defined by Equation 3.5 at the rubber sensor is of interest, because it provides the intensity and shape of the cure exotherm, the other taking place in the air, expressed by Equation 3.6, is characterized by the loss in heat for the cure reaction. From a first approach, based on a logical consideration, this loss in heat affects essentially the values of the enthalpy of cure which is reduced somewhat. The shape of the exotherm, which gives rise to the kinetics of the reaction, should not be affected; as in Equation 3.6, the loss in heat is proportional to the difference in temperatures, in the same way as for the gradient of temperature shown in Equation 3.5. The loss in heat could follow kinetics similar to that observed on the sensor of the calorimeter.

Calculation of this heat loss can be made by evaluating the Grashof and Prandtl numbers, and then the Nusselt number, leading to the value of the coefficient of convective transfer *h*. Then, using the method described in Chapter 2, Section 2.6, it is possible to obtain the heat loss by convective effect.

3.1.3 ISOTHERMAL CALORIMETRY TECHNIQUES

The calorimetry techniques have been used for many purposes in the cure of rubber, including to measure the heat of the overall cure reaction, but also for evaluating the kinetics of the heat evolved from the overall reaction. The only question at first was what way to use the calorimetry? In the early eighties, it seemed to a majority of the authors that the isothermal condition would be preferable, but finally the operation in scanning mode was preferred.

3.1.3.1 Measure of the Cure Enthalpy under Isothermal Conditions

The calorimeter is generally run in differential, and the heat flux is measured by comparison with a known system. In the DC experiment, the enthalpy of all reactions occurring at a constant applied temperature up to some given time is determined. But the applied temperature is the set calorimeter temperature and not the true sample temperature during the cure because of local heating arising from the exothermic reaction [4]. This enthalpy, ΔH, corresponds with the overall enthalpy of all formation and degradation reactions up to the time of the experiment. The process is as follows: while the calorimeter is maintained at the desired temperature, the rubber sample at room temperature is dropped in the sensible part of the calorimeter. Thus, the rubber is strongly heated, leading to steep gradients of temperature developed through the sample, without thinking of the cooling of the calorimeter for awhile, and an endothermic heat flow can be observed; following the increase in temperature in the rubber, the exothermic reaction takes place, accompanied by the heat flux from the rubber to the sensible set of the calorimeter. It is thus possible that some heat losses, essentially by convection, modify the result. Finally, because of the internal heat generated by the exothermic cure reaction, the temperature in the sample is increased and becomes higher than that of the calorimeter, leading to the exothermic heat flux which is recorded. After the rubber sample has been given this precure, it is removed from the calorimeter, cooled down, and replaced in the calorimeter maintained under the same conditions, in order to obtain the baseline. As a result, two curves are obtained, one with a peak during the cure and the other with a linear curve corresponding with the postcure. The enthalpy of cure is thus obtained by integrating the area located between these two curves. The first difficulty of this technique results from the low value of the cure enthalpy of rubbers.

Another fact of high concern appears with the small sample used with some calorimeters; it has been said that the question that always arises is how representative of the homogeneity of the batch is a 5 to 10 mg sample taken from a large batch (typically from 100–2000 g, as mixed on laboratory equipment).

An improvement has been made for the calorimeter by making the sample cylindrical in shape and long enough so that the heat flux meter is placed at mid-height of

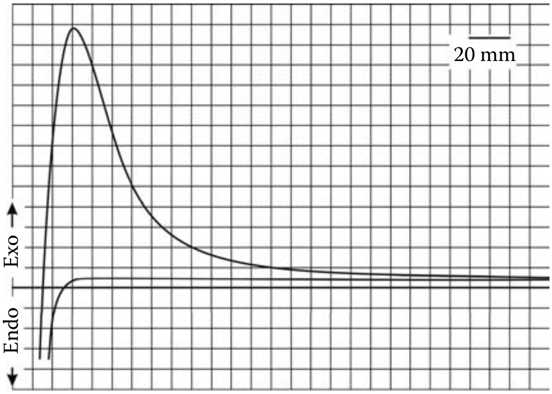

FIGURE 3.1 Measurement of the cure enthalpy using a DC calorimeter. Isotherms at 180°C; the one obtained with the fresh rubber, the other with the already cured rubber (Figure 11, private paper SETARAM from P. Le Parlouer and J. M. Vergnaud).

the sample. In this case, no loss in heat occurs, and the sensitivity of the apparatus is improved by using a rather large sample, around 150–200 mg [5].

An example of heat flux obtained with this apparatus is shown in Figure 3.1, with the two curves [5] for rubber cured with 2% sulfur and $Q_\infty = \Delta H = 20$ J/g

3.1.3.2 Kinetics of the Overall Cure Reaction

The kinetic parameters of the cure reaction should be determined from the DC experiments. As there are three parameters to be known, three isothermal experiments at different temperatures are necessary to achieve the objective.

Figure 3.2 illustrates DC exotherms obtained on the same time scale for a compound with 2% sulfur. These temperatures (160, 170, 180°C) were chosen so that the

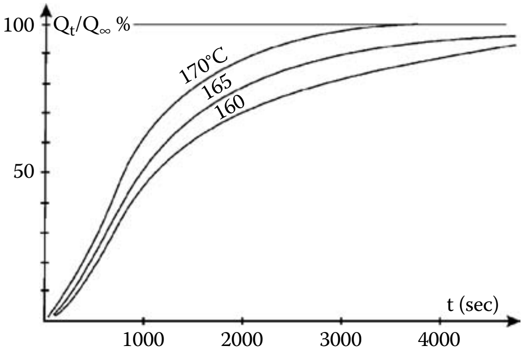

FIGURE 3.2 DC experimental curves expressing Q_t/Q_∞ against time at 160, 170, 180°C for the cure of rubber. (With permission of Elsevier, Figure 1, *Thermochim. Acta,* 1982. 59:149–56. A. Accetta, P. Le Parlouer, and J. M. Vergnaud.)

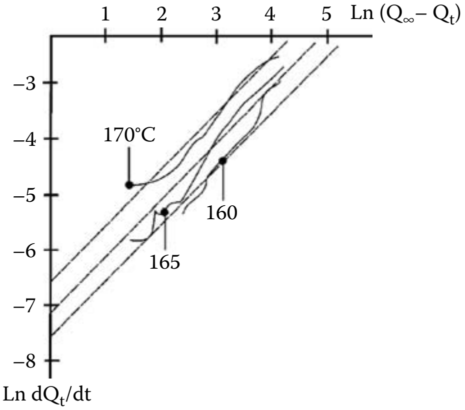

FIGURE 3.3 Evaluation of the order of the overall reaction, by plotting $\log(\frac{dQ}{dt})$ versus $\log(Q_\infty - Q_t)$. (With permission of Elsevier, Figure 2, *Thermochim. Acta* 1982. 59:149–56. A. Accetta, P. Le Parlouer, and J. M. Vergnaud.)

vulcanization rate would be sufficiently high to allow a short cure time for industrial applications.

By plotting log (heat rate) against log $(Q_\infty - Q_t)$, linear curves are obtained for these three temperatures with a slope equal to 1 (Figure 3.3), leading to a first-order cure reaction.

In earlier studies, the decrease of free sulfur was found to follow a first-order law with respect to time, for natural rubber and for SBR with sulfamide accelerators [6].

The values of the temperature coefficient k_T at these three temperatures are obtained by measuring the ordinate intercept in this figure for the three temperatures. The energy of activation E is found from the slope of Ln k_T versus $1/T$ plots [Figure 3.4]. This value is of the order of magnitude with corresponding values reported for natural rubber [6]. The other values concerned with the thermal

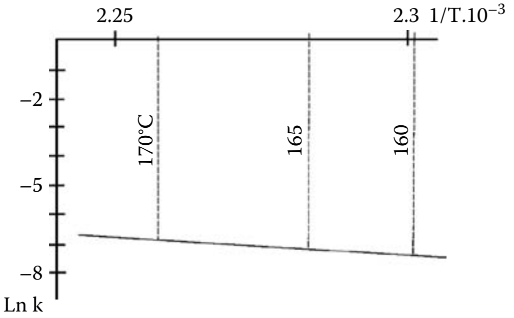

FIGURE 3.4 Evaluation of the energy of activation by plotting Lnk_T vs. $\frac{1}{T}$ (T in Kelvin). (With permission of Elsevier, Figure 3, *Thermochim. Acta* 1982. 59: 149–56. A. Accetta, P. Le Parlouer and J. M. Vergnaud.)

TABLE 3.1
Kinetic Parameters Obtained by DC Calorimetry

at 160°C $k(s^{-1}) = 5.5 \cdot 10^{-4}$; at 165°C $k(s^{-1}) = 7.7 \cdot 10^{-4}$; at 170°C $k(s^{-1}) = 10.6 \cdot 10^{-4}$; order $n = 1$; $k_0(s^{-1}) = 3 \cdot 10^9$; $E = 25.4$ kcal/mole; $Q_\infty = 20$ J/g; $\lambda = 0.2$W/m.deg; $C = 2.2$ J/g.deg; $\rho = 0.9$ g/cm^3; $\alpha = 10^{-3}$ cm^2/s $= 10^{-7}$ m^2/s

properties, which are in agreement with the earlier values published in the literature [7–9], are also collected in this Table 3.1.

3.1.4 CALORIMETRY IN SCANNING MODE

In the DSC experiment, starting with fresh uncured stock, the sample is scanned at a selected heating rate up to a temperature at which the reaction exotherm is complete. The cure exotherm is usually observed in the 150–240°C range, depending upon the accelerator type and level. In this first DSC curve, an exotherm may be observed in the normal cure temperature range. After the sample has been given a precure for a known time and temperature, it is quenched-cooled to prevent further reactions and then scanned under conditions identical to the initial scan. Thus, this second scan is obtained with the cured rubber sample. The new figure obtained for this vulcanized rubber is then used as the baseline, which is generally flat, with a slight change in the slope, depending on the change in the thermal properties of this material with temperature change (Figure 3.5).

3.1.4.1 Measure of the Cure Enthalpy in Scanning Mode

The value of the cure enthalpy of the overall cure reaction is obtained in the same way as previously done by using the isothermal condition process. The area measured between the two curves shown in Figure 3.5 is the basis for the measure of the cure enthalpy.

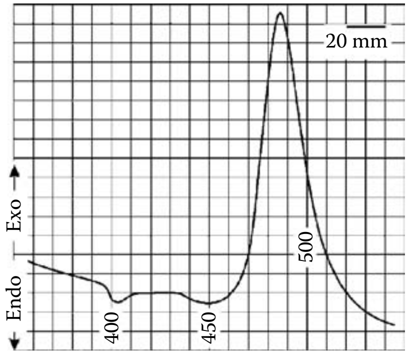

FIGURE 3.5 Exotherm obtained with calorimetry in scanning mode. (Figure 3 SETARAM, private paper SETARAM from P. Le Parlouer and J. M. Vergnaud.)

3.1.4.2 Kinetics of the Cure Reaction

The heat flux is expressed as a function of temperature, as shown in Figure 3.5. As the heating rate for the sample is the same as for the calorimeter,

$$b = \frac{dT}{dt} \tag{3.7}$$

Equation 3.3, representing the rate of cure, is thus written in terms of temperature:

$$\frac{dQ}{dT} = \frac{k_0}{b} \cdot (Q_\infty - Q_T)^n \cdot \exp\left[-\frac{E}{RT}\right] \tag{3.8}$$

The above equation, written in the logarithm form,

$$Ln\frac{dQ}{dT} = Ln\frac{k_0}{b} + n \cdot Ln(Q_\infty - Q_T) - \frac{E}{RT} \tag{3.9}$$

by using finite differences, becomes:

$$\Delta\left[Ln\frac{dQ}{dT}\right] = n \cdot \Delta[Ln(Q_\infty - Q_T)] - \frac{E}{R} \cdot \Delta\left[\frac{1}{T}\right] \tag{3.10}$$

This equation can be rewritten as follows:

$$\frac{\Delta\left[Ln\frac{dQ}{dT}\right]}{\Delta[Ln(Q_\infty - Q_T)]} = n - \frac{E}{R}\frac{\Delta\left[\frac{1}{T}\right]}{\Delta[Ln(Q_\infty - Q_T)]} \tag{3.11}$$

Thus, by plotting the values of the left-hand side of the above equation as a function of $\frac{\Delta\left[\frac{1}{T}\right]}{\Delta[Ln(Q_\infty - Q_T)]}$, a straight line can be obtained. The activation energy can be calculated from the value of the slope of this straight line, and the order n is given by the intercept with the ordinate axis. The value of the constant preexponential k_0 can be determined easily by writing that the rate of enthalpy change at a given temperature, obtained either by experiment or calculation using the values found for the kinetic parameters, is the same.

A good way of testing the validity of the kinetic parameters determined by the method consists of comparing the experimental curve with that obtained by calculation using the kinetic parameters [10,11].

For a given size of the sample, the main parameter in the DSC technique is the heating rate, which has various effects on the heat flux temperature, as shown in Figure 3.6 [12].

- Thus, an increase in the heating rate is responsible for a shift of the heat flux towards the highest temperature; this is especially important for the maximum of the heat flux.
- Nevertheless, the heat flux describing the rate of the reaction starts at about the same temperature, whatever the value selected for the heating rate.

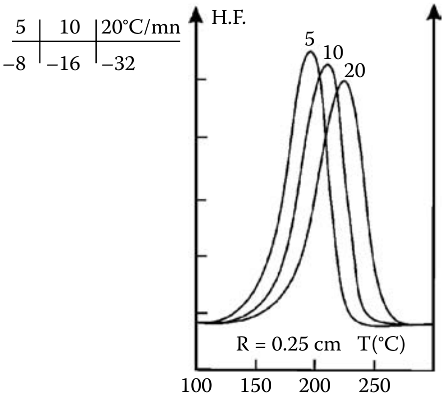

FIGURE 3.6 Calorimetry in scanning mode. Effect of the heating rate on the heat flux-temperature history. (With permission of Elsevier, Figure 9, *Thermochim. Acta* 1987. 116: 111–24. J.Y. Armand and J.M. Vergnaud.)

- The sensitivity of the technique, measured by the height of the heat flux at its maximum, is directly proportional to the heating rate, as shown in Figure 3.7.
- Two types of gradients of temperature through the radius of the sample (or the thickness when the sample is a thin sheet) are developed during the process for two reasons:
    i. During the first stage of heating, the difference between the temperature on the face and at the middle varies as a linear function of the heating rate and of the square of the radius of the sample [13].

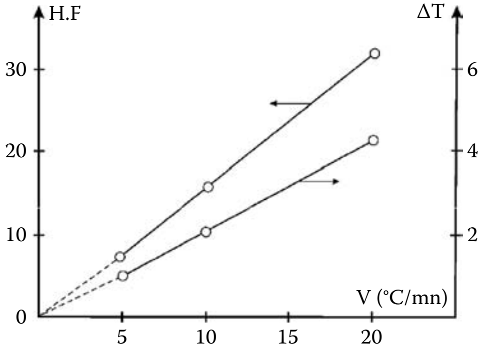

FIGURE 3.7 Effect of heating rate on the height of maximum heat flux, and on the maximum value of the difference between the temperature on the face and at the middle of the sample. (With permission of Elsevier, Figure 11, *Thermochim. Acta* 1987. 116:111–24. J.Y. Armand and J.M. Vergnaud.)

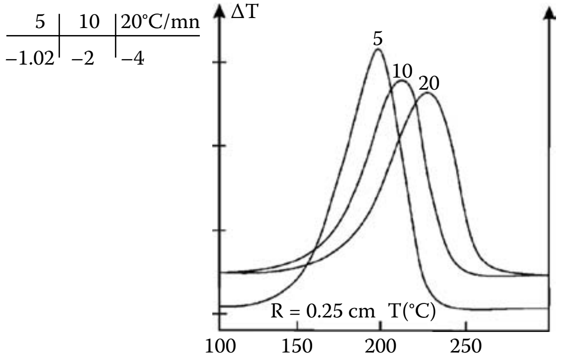

FIGURE 3.8 Calorimetry in scanning mode. Effect of heating rate on the difference between the temperature on the face and at the middle of the sample. (With permission of Elsevier, Figure 10, *Thermochim. Acta* 1987. 116: 111–24. J.Y. Armand and J.M. Vergnaud.)

ii. As a result of the internal heat generated from the cure reaction, other gradients of temperature are developed and superimposed on the first gradients. The difference between the temperature at the middle and on the face is shown in Figure 3.8 as a function of the temperature of the calorimeter. This difference of temperature is found to vary linearly with the heating rate (Figure 3.7).

iii. The gradients of temperature developed through the radius of the sample are shown at various times for two values of the heating rate: left 10°C/min, and right 20°C/min (Figure 3.9).

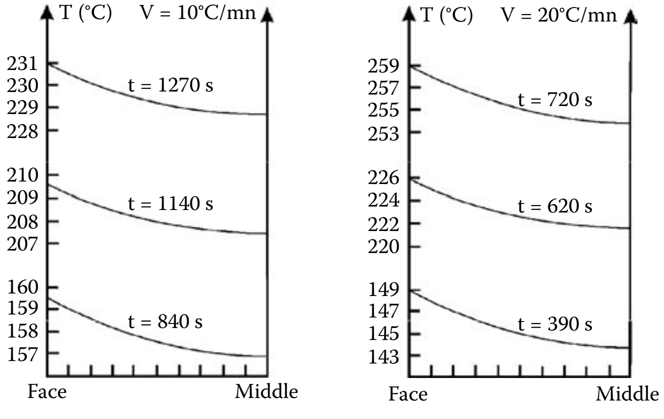

FIGURE 3.9 Gradients of temperature developed through the radius of the sample at various times, for the heating rate of 10°C/min (left) and of 20°C/min (right). (With permission of Elsevier, Figure 12, *Thermochim. Acta* 1987. 116: 111–24. J.Y. Armand and J.M. Vergnaud.)

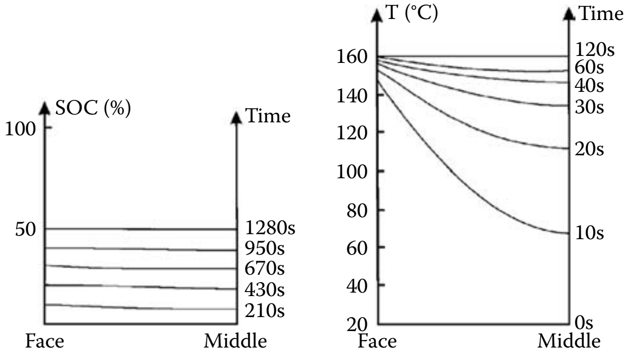

FIGURE 3.10 Profiles of temperature developed through the radius of the sample in DC calorimetry at 170°C. (With permission of Elsevier, Figure 8, *Thermochim. Acta* 1987. 116: 111–24. J.Y. Armand and J.M. Vergnaud.)

3.1.5 CONCLUSIONS ON CALORIMETRY TECHNIQUES

In the early eighties, many workers preferred using the DC technique rather than the DSC calorimetry for studying the kinetics of reactions, essentially because the temperature would be supposed constant, which simplifies the kinetic study.

In fact, there are various important disadvantages in the DC technique. The sample at room temperature is introduced in the calorimeter maintained at the selected temperature, and in spite of the steep gradients of temperature developed through the thickness of the sample, it takes some time for the sample to establish thermal equilibrium. The temperature of the sample is not the set calorimeter temperature, especially at the beginning of the process. This fact is especially obvious in Figure 3.10 where the profiles of temperature developed through the radius of the sample are calculated at various times, necessitating 100 s for thermal equilibrium to become establish. Moreover, as the cure reaction starts within a narrow temperature window, it is not easy to select the three temperatures necessary for determining the kinetics of the reaction.

In the DSC technique, some gradients of temperature are developed through the thickness of the sample, but they are not so steep as in the DC technique, and after a certain period, they become constant. Moreover, as these temperature gradients are proportional to the heating rate, they can be controlled by choosing an appropriate heating rate.

After a few studies, among them these contribution [3,14], almost all researchers were inclined to use the calorimetry in scanning mode.

Let us note that this question about the temperature—either to be kept constant or programmed with a constant rate used in calorimetry—is quite general for all techniques initially run under isothermal conditions. Thus, this problem arising in calorimetry will be also considered in the same way with the moving die rheometer (MDR) technique.

3.2 INCREASE IN STIFFNESS DURING CURE: ISOTHERMAL MDR

3.2.1 PRESENTATION OF THE TECHNIQUE

As noted [15], when a compounded rubber is subjected to a plasticity measurement at a high enough temperature and for a long time, it will cure, and consequently a plasticity test can be used as a test for scorch or rate of cure. Thus, the Mooney viscometer is used to measure scorch (i.e., the onset of vulcanization), and an oscillating disc rheometer will measure the plasticity of the compound before the onset of cure, as well as the increase in stiffness as curing takes place. Moreover, tests for scorch and rate of cure should be distinguished from tests for degree of cure or optimum cure measured on the vulcanized material.

The most obvious changes in a rubber mix when vulcanization sets in are an increase in stiffness and an increase in the elastic component of the visco-elastic deformation. The Mooney viscometer offered a convenient way of measuring scorch and even rate of cure according the standard method given in ISO 667.

Laboratory measurement of curing characteristics have been somewhat revolutionized by the introduction of the cure meters. There were two types of cure meter: the reciprocating paddle type as in the Wallace–Shawbury curometer, and the oscillating disc type such as the Monsanto rheometer. In the oscillating disc type (ODR) a biconical disc is embedded in the rubber in a closed cavity. The disc is oscillating through constant angular displacement, and the torque required monitored.

The oscillating die rheometer (ODR) and the moving die rheometer (MDR) have been developed and marketed by Monsanto, the MDR being introduced in 1985 [16]. In the MDR, a thin sheet of rubber, around 2 mm thick, is placed between the two dies kept at the desired temperature; the lower disc oscillates and a reaction torque/pressure transducer is positioned above the upper disc. It has been found that the MDR gives shorter times of cure than the ODR because of better heat transfer and higher torque values, owing to the die design.

Another reason may come from a different thickness of the rubber sample. The torque–time curves obtained with these two apparatus shown in Figure 3.11 clearly show this strong difference. All these two apparatus work under isothermal conditions. Thus the MDR is used at three temperatures to allow evaluation of the kinetic parameters of the cure reaction.

An example is given where the activation energy and the preexponential factor have been calculated from the fractional modulus obtained with this MDR and EPDM compounds [17]. The modulus value was assumed to vary with time, following first-order kinetics, and the rate constant varies with temperature according to the Arrhenius equation. A reference time conversion of 1.3/10°C was found for sulfur vulcanization with a reference temperature of 150°C. The enthalpy of cure was not considered as being a significant drawback because the percent of vulcanizing agent was low associated with a low enthalpy.

3.2.2 PROCESS OF CURE IN ISOTHERMAL MDR

The process of cure taking place in the rubber sample in the isothermal MDR has been deeply studied in a previous paper [18], and some results obtained are reported.

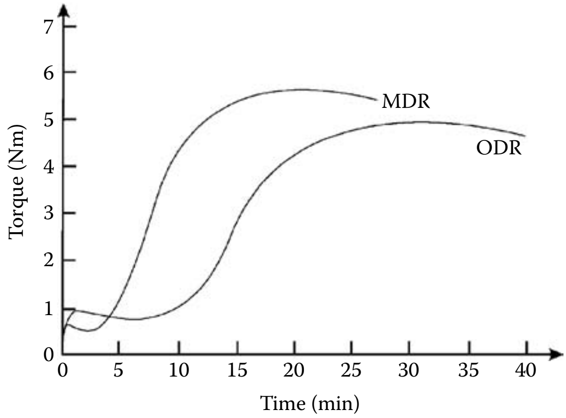

FIGURE 3.11 Torque–time curves obtained with the oscillating disc rheometer (ODR) and with the moving die rheometer (MDR) with the same rubber compound.

The first objective was an in-depth study of the process of cure in the sample between the MDR dies, by considering not only heat transfer through the sample but also the heat generated by the overall cure reaction. Three various EPDM samples were selected with different percentages of peroxide ranging from 2 to 19%, associated with a cure enthalpy between 14 and 51 J/g. Another purpose was to evaluate the state of cure in the sample at various times, and thus profiles of temperature and of state of cure developed through the thickness of the rubber can be obtained at various times, especially associated with typical values of the torque (5, 50 and 95% of maximum torque). Comparison could be made between the values of the state of cure and the value of the torque.

3.2.2.1 Experimental

The materials used for curing (Hutchinson) are described in Table 3.2

The peroxide used was *bis*(ter-butyl-peroxy-isopropyl) benzene: Perkadox 14-40. For these samples, the density is 1.18 g/cm^3, the heat capacity is 2 J/g.deg and the heat conductivity is 0.25 W/m.deg.

TABLE 3.2
Main Components of Three EPDM Samples Used (wt %)

EPDM	C black	Plasticizer	Chemicals	Peroxide
100	50	13	3	2
100	46	11	3	9
100	42	9	2	19

The two apparatus used for curing were:

- A Monsanto 2000 E MDR (Alpha Technologies) run under isothermal conditions within the 170–190°C range. The sample, initially at room temperature, is placed between the dies kept at the selected temperature. The thickness of the sample is around 0.2 cm. The torque value is monitored as a function of time.
- A calorimeter C 80 (SETARAM) run in scanning mode with a heating rate of 0.2°C/min. The heat flux is recorded as a function of temperature and time. Samples around 6 g are placed into a cylindrical holder with an internal diameter of 1.7 cm. Two holders are placed into the heating block, one containing the reactive sample, the other alumina.

3.2.2.2 Theoretical Treatment

The rate of increase of the modulus m_t is given by the first-order equation:

$$\frac{dm}{dt} = k'_T \cdot (m_\infty - m_t)^n \tag{3.12}$$

at constant temperature. After integration by assuming temporarily that $n = 1$, it gives:

$$\frac{m_t}{m_\infty} = 1 - \exp(-k'_T \cdot t) \tag{3.13}$$

where k'_T is expressed in terms of temperature by:

$$k'_T = k'_0 \cdot \exp\left[-\frac{E'}{RT}\right] \tag{3.14}$$

E' being the energy of activation, and k'_0 the preexponential constant.

In the calorimeter the equation of radial heat conduction is:

$$\frac{\partial T}{\partial t} = \alpha \cdot \left[\frac{\partial^2 T}{\partial r^2} + \frac{1}{r} \cdot \frac{\partial T}{\partial r}\right] + \frac{1}{C} \cdot \frac{\partial Q}{\partial t} \tag{3.4}$$

The rate at which heat is generated by the cure reaction is:

$$\frac{dQ}{dt} = k_T \cdot (Q_\infty - Q_t)^n \tag{3.3}$$

with the constant k_T expressed as follows:

$$k_T = k_0 \cdot \exp\left[-\frac{E}{RT}\right] \tag{3.14}$$

The integration of Equation 3.3 when $n = 1$ is written as follows:

$$1 - Y = 1 - \frac{Q_t}{Q_\infty} = \exp(-k_T \cdot t) \tag{3.15}$$

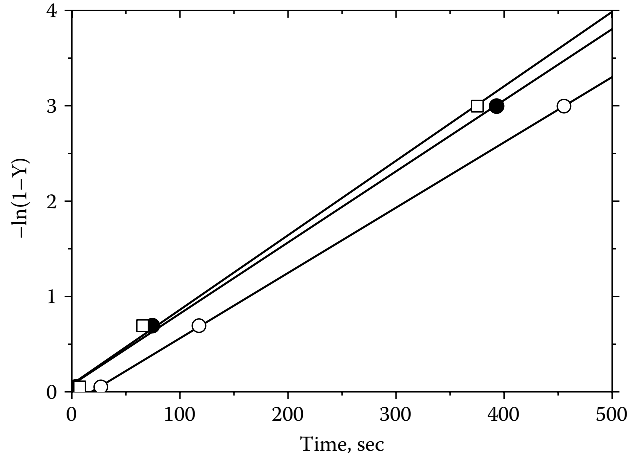

FIGURE 3.12 Plot of Ln(1-Y) vs. time for various % peroxide in EPDM from MDR under isothermal conditions at 170°C. (With permission, Institute of Materials, Minerals and Mining, original publication, Figure 1, in *Plastics, Rubber and Composites*. 2001. 30: 275–81. I.D. Rosca and J.M. Vergnaud.)

Let us note that the two values given to the couples E and E', k_T and k'_T, as well as k'_0 and k_0, are not assumed to be the same without a deep verification.

Calculation is made by using a numerical method, as the mathematical treatment is not feasible.

3.2.2.3 Results Obtained by Calorimetry

Two types of parameters are of interest that are connected with the kinetics of the overall cure reaction and the enthalpy of cure. Parameters such as order of reaction, energy of activation, and preexponential factor are evaluated from calorimetry measurements carried out under isothermal conditions at temperatures ranging from 170 to 190°C. As an example, a plot of $L_n(1 - Y)$ as a function of time, shown in Figure 3.12, gives straight lines for the EPDMs with various percents of peroxide (1, 9, and 19%) at 180°C. Similar curves are obtained at 170 and 190°C. Thus, the assumption for the order to be 1 is right; the slope of these curves provides the value of the rate constant k_T at various temperatures. The values of k_T in the logarithm form are plotted versus the reciprocal absolute temperature in Figure 3.13. Straight lines are observed with approximately the same slope, giving the values of the activation energy, whereas the value of the preexponential factor k_0 are obtained by using Equation 3.14 and the above values of the activation energy.

The values of the kinetic parameters obtained from calorimetry measurements are collected in Table 3.3.

These results lead to the following comments:

i. The values of the rate constant are nearly similar whatever the percent of peroxide.

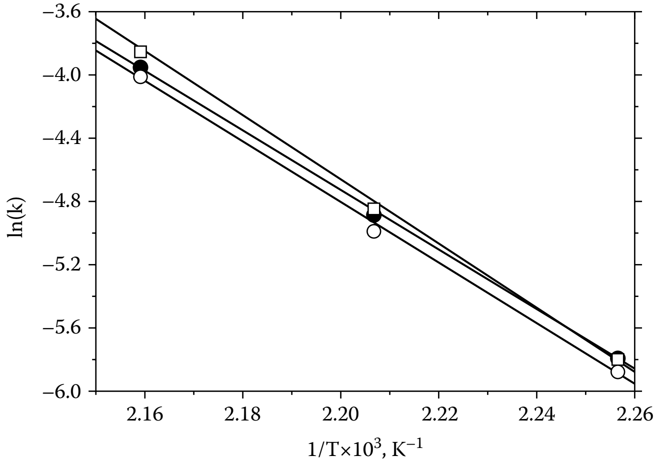

FIGURE 3.13 Lnk versus 1/T from MDR under isothermal conditions within 170-190°C range. (With permission, Institute of Materials, Minerals and Mining, original publication, Figure 2 in *Plastics, Rubber, and Composites*, 2001. 30: 275–81. I.D. Rosca and J. M. Vergnaud.)

ii. The order of the overall cure reaction is 1, as proved by the straight lines obtained in Figure 3.12 that were drawn by using Equation 3.15 established by making this assumption.
iii. The activation energy is about the same for the three EPDM compounds within the 170–190°C range; these values are of the same order of magnitude as those published for EPDM [17–19].
iv. The enthalpy of cure strongly increases with the percent of peroxide, but not proportionally with this percentage.
v. The values of the energy activation and of the preexponential factor are of the same order of magnitude, whatever the temperature and the percent of peroxide.

3.2.2.4 Results Obtained by Using Either MDR or Calorimetry

The results are expressed in terms of profiles of temperature and of state of cure developed through the thickness of the sample located in the dies of the MDR. These

TABLE 3.3
Parameters of Cure Obtained by Calorimetry

% peroxide	Lnk_0	E/R	ΔH(J/g)
2	37.3	19150	14.3
9	36.7	18850	44.7
19	40	20300	56.7

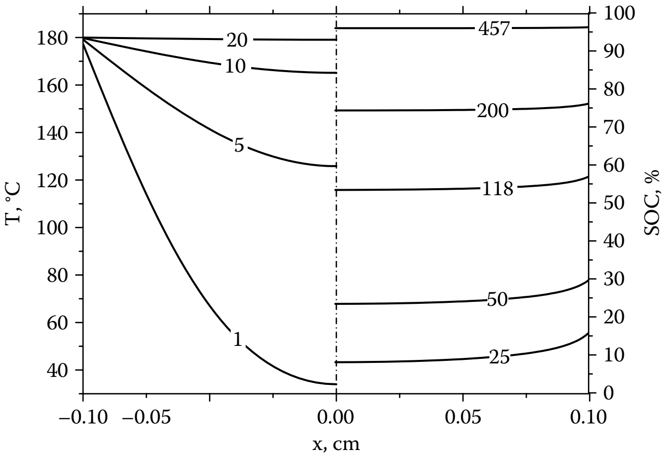

FIGURE 3.14 Profiles of temperature (left) and of state of cure (right) developed through the dies of the MDR at 180°C. (With permission, Institute of Materials, Minerals and Mining, Original Publication, Figure 3 in *Plastics, Rubber, and Composites*, 2001. 30: 275–81. I.D. Rosca and J. M. Vergnaud.)

values of temperature and state of cure are calculated using a numerical treatment taking all the facts into account, and especially the heat transfer at the rubber–die interface given by Equation 3.5, as well as the values in Table 3.3 for the enthalpy of cure.

The profiles of temperature (left) and of state of cure (right) developed through the rubber sheet with 2% peroxide are shown when the MDR temperature is 180°C (Figure 3.14) and 170°C (Figure 3.15). In Figure 3.16 are drawn the profiles of state of cure developed through the thickness of the rubber sample heated in the MDR at 180°C when the percent of peroxide is 9 (left) and 19 (right).

These profiles lead to the following observations:

i. Only half the thickness of the rubber sheet is shown, because of the symmetry.
ii. When the sample, initially at room temperature, is placed between the dies kept at the desired temperature, it takes some time for thermal equilibrium through the rubber to establish. Thus steep temperature gradients are developed through the thickness of the sample, especially at the beginning of the process and after 15–20 s, the temperature is uniform.
iii. Steep profiles of state of cure are developed through the sample, especially at the beginning of the process. Thus, either these profiles of temperature or states of cure make measurement of the 5% modulus difficult to define.
iv. In the same way, as shown in Figure 3.17 where *Ln*(1−*Y*) is plotted versus time, nearly straight lines are obtained, being a proof for the first-order reaction of cure.

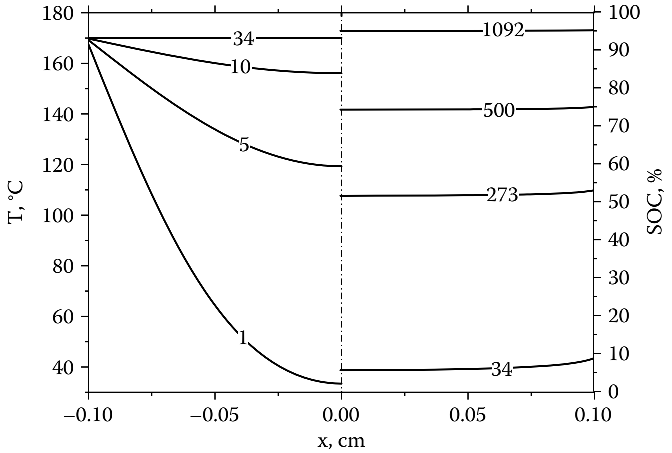

FIGURE 3.15 Profiles of temperature (left) and of state of cure (right) developed through the dies of the MDR at 170°C. (With permission, Institute of Materials, Minerals and Mining, Original Publication, Figure 5 in *Plastics, Rubber, and Composites*, 2001. 30: 275–81. I.D. Rosca and J.M. Vergnaud.)

The effect of the percent peroxide and of the enthalpy associated with this percentage can be appreciated by comparing the times of 95% modulus, either in Figures 3.14–3.16 or in Table 3.4, where the values obtained by MDR are collected.

On the other hand, the values of the activation energy and of the preexponential factor calculated from these times for 95% modulus by using the Equation 3.13 and 3.14 are collected in Table 3.5.

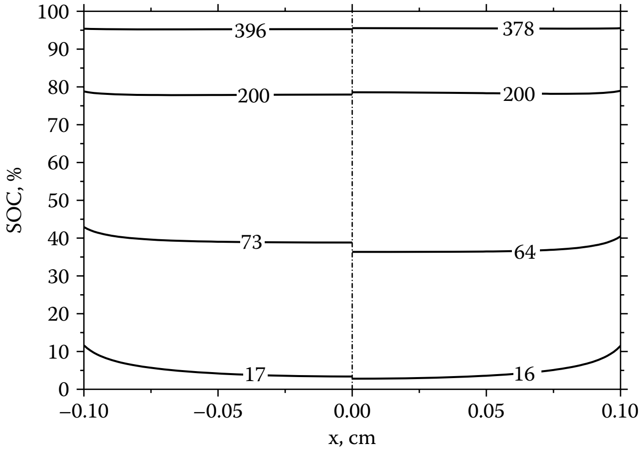

FIGURE 3.16 Profiles of state of cure developed through rubber sheet in MDR dies at 180°C, for 9% peroxide (left) and 19% (right). Times in s. (With permission, Institute of Materials, Minerals and Mining, original publication, Figure 4 in *Plastics, Rubber, and Composites*, 2001. 30: 275–81. I.D. Rosca and J.M. Vergnaud.)

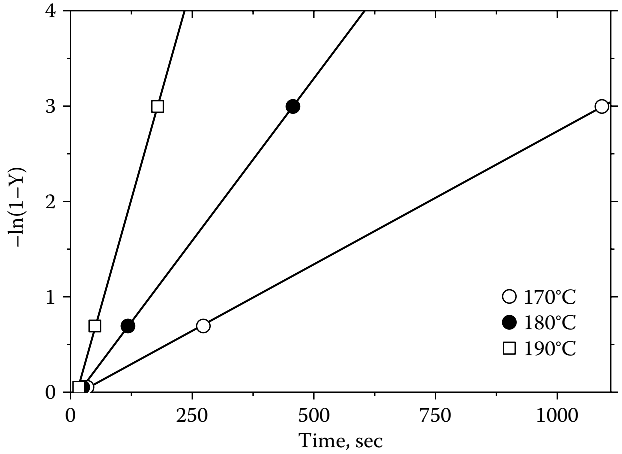

FIGURE 3.17 Ln(1-Y) vs. time with MDR under isothermal conditions within the 170–190°C range. Y is defined by Equation 3.16. (With permission of Elsevier, Figure. 1, *Polymer* 2002. 43: 195–202., I.D. Rosca and J. M. Vergnaud.)

TABLE 3.4
Times (s) for 95% Modulus Obtained from MDR Measurement

% peroxide	170°C	180°C	190°C
2	1092	457	179
9	965	396	152
19	960	378	142

TABLE 3.5
Parameters of the Cure Kinetics Obtained by MDR

% peroxide	Lnk_0	E/R
2	36	19000
9	36.7	18950
19	38.5	19600

TABLE 3.6
Times (s) Necessary for the Modulus to Reach 50% its Maximum Value

% peroxide	170°C	180°C	190°C
2	252	105	41
9	223	91	35
19	222	87	33

Some conclusions of interest can be made:

i. Comparison between the results obtained using either calorimetry or MDR is of great interest, as the values obtained for the kinetic parameters are of the same order of magnitude for the various values of the percentage of peroxide.
ii. In the same way, the order of the overall cure reaction is proved to be one.
iii. The times for the modulus to attain 50% of its maximum are similar to those obtained by calorimetry, in spite of the fact that the profile of the state of cure is not uniform (Table 3.6).
iv. In short, in conclusion, it can be said that the process of cure is described in a same way by considering either the state of cure or the modulus. Thus, the following statement holds: the change in the modulus is intimately connected with the state of cure.

3.2.3 CONCLUSIONS ON THE PROCESS IN ISOTHERMAL MDR

The process of the cure of rubbers taking place in the MDR is similar to that in a mold or in the calorimeter: heat transfers by conduction through the rubber with equality of the heat flux on each face of the die–rubber interface, followed by the cure reaction. With the MDR run under isothermal conditions, the sample initially at room temperature is introduced between the heated dies, and strong heat transfer occurs through the rubber, without considering a decrease in die temperature. The cure reaction starts at a given temperature and gradients of state of cure are expanded with a higher value on the surfaces in contact with the dies. After sufficient time, the profiles of state of cure become more and more uniform. In the present instance, for the times at which the modulus reaches 5 and even 50% of the maximum torque modulus, the gradient of state of cure is still not uniform [18].

Some parameters are of considerable interest, regardless of the nature of the rubber and vulcanizing agent, such as the temperature of the dies, the thickness of the sample, and the quality of the contact between the rubber and the dies. They were considered using the data given by calorimetry, using a numerical treatment taking all the facts into account.

The nature of the vulcanizing agent and of the rubber (i.e., EPDM compounds with peroxide in this instance) is of prime importance to the kinetics of cure: the activation energy and the preexponential factor play major roles, and the cure enthalpy is also of some importance in spite of its low value, whereas the order of the overall reaction is 1. Thus, because of the kinetics of cure, the time of cure varies considerably with the temperature, and thus there is a narrow temperature window through which meaningful data can be obtained. The cure enthalpy is rather low and thus does not intervene much in the process. Nevertheless, DSC experiments, which are based on measuring the enthalpy evolved, are also commonly used for determining the kinetics of cure [12].

Two parameters that are not often considered in MDR were examined: the quality of contact between the rubber and dies, and the thickness of the sample. Both these parameters play a role at the beginning of the course, being responsible for a change in the process of heating and thus the progress in the cure. The times for the values of 5 and even 50% maximum modulus can be strongly affected by these two parameters.

3.3 MDR IN SCANNING MODE WITH CONSTANT HEATING RATE

3.3.1 Presentation of the Technique

In the same way as for a calorimeter for which the scanning mode has brought some interesting advantages, it seemed to the authors that an attempt should be made with the MDR in using it with a linear increase in temperature [20]. Thus, the theory of the method has been developed, leading to results of concern, proving at least that this method is feasible.

The main drawbacks in the isothermal MDR comes from these facts, which cannot be eliminated, but only reduced:

- Three experiments at different temperatures are necessary which should be selected within a narrow temperature window, meaning that more than three may be required.
- To suppose that with isothermal MDR, the temperature through the rubber sample reaches quickly that of the dies consists of deluding oneself. In fact, it takes some time for the sample initially at room temperature to reach that of the apparatus.
- Steep gradients of temperature and of state of cure are developed through a large part of the process, so that the values of the torque modulus at 5%, and even at 50% of the maximum are obtained when the sample is not vulcanized uniformly.

The first objective of this study [20] was to show that the MDR could be used in scanning mode with a constant heating rate in order to eliminate the drawbacks of the MDR run under isothermal conditions, and to show that the kinetic parameters can be obtained from this torque–temperature curve.

The other purpose was to evaluate mathematically the torque change as a function of temperature, as well as the kinetic parameters from this curve. Moreover, the profiles of temperature and of state of cure developed through the sample cured in the MDR dies either in scanning mode or under isothermal conditions are evaluated numerically.

3.3.2 THEORETICAL TREATMENT

3.3.2.1 Assumptions

The following assumptions are made:

i. Perfect contact is obtained between the rubber and heating dies, and thus the temperature is constantly the same on each face of the die–rubber interface.
ii. The rate of heating of the new MDR is constant between the initial and final temperature T_0 and T_f.
iii. The increase of the rate of torque with temperature is expressed by an Arrhenius equation.
iv. As shown in the previous chapter devoted to the study of EPDM cured with a peroxide, the torque increases in the same way as does the state of cure.

3.3.2.2 Mathematical Treatment

By putting

$$Y = \frac{Torque_t}{Torque_\infty} = \frac{SOC_t}{SOC_\infty} \tag{3.16}$$

the differential equation under isothermal condition

$$\frac{dY}{dt} = k_0 \cdot (1-Y)^n \cdot \exp\left[-\frac{E}{RT}\right] \tag{3.17}$$

becomes with the constant heating rate b

$$b = \frac{dT}{dt} \tag{3.18}$$

$$\frac{dY}{dT} = \frac{k_0}{b} \cdot (1-Y)^n \cdot \exp\left[-\frac{E}{RT}\right] \tag{3.19}$$

expressing the ratio of the torque or of the state of cure as a function of temperature.

By integrating between the temperatures T_0 and T, when in addition the order of the overall cure reaction is 1, it comes:

$$Y_T = 1 - \exp\left[-\frac{k_0}{b}\int_{T_0}^{T} \exp\left(-\frac{E}{RT}\right) dT\right] \tag{3.20}$$

Equation 3.19 in logarithm form is

$$Ln\frac{dY}{dT} = Ln\frac{k_0}{b} + n \cdot Ln(1-Y) - \frac{E}{RT} \tag{3.21}$$

which becomes with finite differences:

$$\Delta Ln\frac{dY}{dT} = n \cdot \Delta Ln(1-Y) - \frac{E}{R} \cdot \Delta\left[\frac{1}{T}\right] \tag{3.22}$$

rewritten as follows:

$$\frac{\Delta Ln\frac{dY}{dT}}{\Delta Ln(1-Y)} = n - \frac{\frac{E}{R} \cdot \Delta\left[\frac{1}{T}\right]}{\Delta Ln(1-Y)} \tag{3.23}$$

Schematized in a simple way, this equation becomes:

$$A_T = n - \frac{E}{R} \cdot B_T \tag{3.24}$$

By plotting A_T as a function of B_T, the slope gives the activation energy and the intercept n.

The preexponential factor can be calculated finally in Equation 3.21.

3.3.3 RESULTS OBTAINED WITH MDR IN SCANNING MODE

3.3.3.1 Material and Apparatus Used for the Study

The rubber used was the EPDM compound described in Table 3.2 with 2% peroxide. The Monsanto 2000 E MDR is used under isothermal conditions, while the simulation is done by calculation. The thickness of the sample is taken as equal to 0.2 cm. A calorimeter C 80 was used in scanning mode with a heating rate of 0.2°C/min and a sample of around 6 g.

The characteristics of cure and of heat transfer are shown in Table 3.7.

In scanning mode of the MDR, the temperature of the dies and the rubber starts at room temperature (25°C) and increases constantly with time.

3.3.3.2 Calculation of the Torque–Temperature Curve

The value of the torque at time t, Y_t, as a fraction of its maximum value, expressed in percent, is drawn as a function of the die temperature. The curves are shown in Figure 3.18 for various values of the heating rate ranging from 2 to 10°C/min. Calculation is made using Equation 3.20 and the values collected in Tables 3.3 and 3.5.

TABLE 3.7
Characteristics of the Cure and of Heat Transfer

Enthalpy: 14.3 J/g	$\rho = 1.18 g/cm^3$	C = 2 J/g.deg	$\lambda = 0.25$ W/m.deg

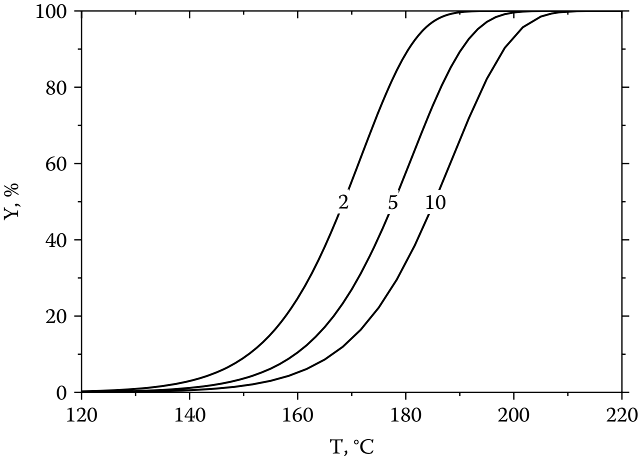

FIGURE 3.18 MDR in scanning mode. Torque vs. temperature with various heating rates. (With permission of Elsevier, Figure 5, *Polymer* 2002. 43: 195–202. I.D. Rosca and J.M. Vergnaud.)

Some comments are worth noting:

i. Calculation is made using Equation 3.20, based on the assumption that thermal equilibrium through the rubber is obtained at any time. In fact, as shown more precisely in Figure 3.19, a gradient of temperature is developed through the thickness during the scan, this gradient being proportional to

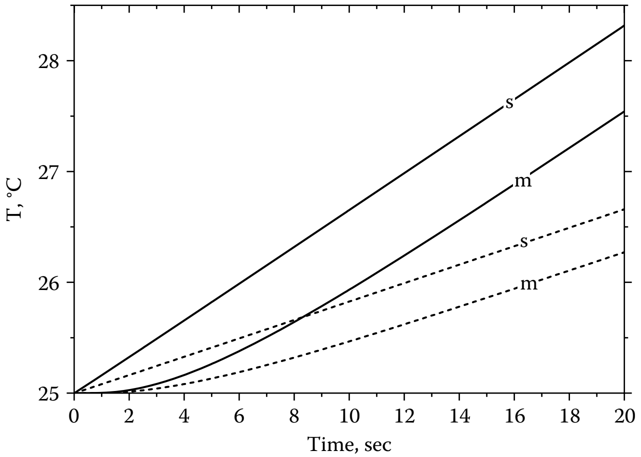

FIGURE 3.19 MDR in scanning mode. Increase in temperature of the rubber for various heating rates, at the surface (s) at the mid-plane (m). (With permission of Elsevier, Figure 6, *Polymer* 2002. 43: 195–202. I.D. Rosca and J.M. Vergnaud.)

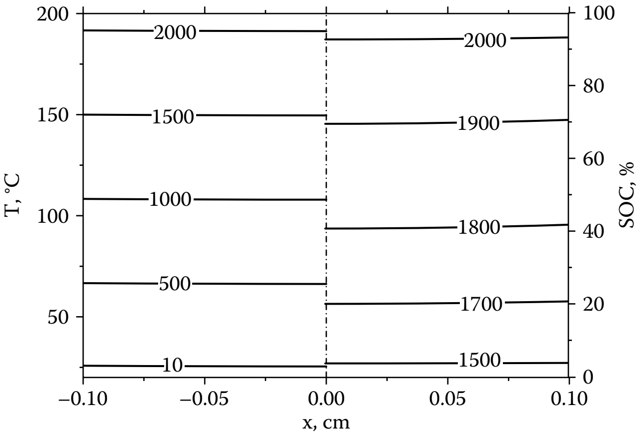

FIGURE 3.20 MDR in scanning mode. Profiles of temperature (left) and of state of cure (right) developed through the rubber with heating rate of 5°C/min. (With permission of Elsevier, Figure 7, *Polymer* 2002. 43: 195–202. I.D. Rosca and J. M. Vergnaud.)

the heating rate in the same manner as in a calorimeter [3]. Nevertheless, the larger temperature difference through the rubber thickness is rather low (i.e., 0.3 and 0.6°C, when the heating rate is 5 and 10°C, respectively). This fact also appears in Figure 3.20 where the profiles of temperature and state of cure are shown using a larger scale.

ii. Typical S-shaped curves are obtained, starting at around the same temperature of the dies. Whatever the heating rate, these torque–temperature curves have a similar shape.
iii. The value selected for the heating rate is of great interest, in the same way as for the calorimeter. A very wide range is used in Figure 3.18 from 2 to 10°C/min. An increase in the heating rate shifts the S-curve toward a higher temperature through a translational way [3].
iv. The temperature of the die, for which the torque is maximum, highly depends on the value of the heating rate, with the statement being true that the higher the value of the heating rate, the higher the value of the maximum temperature necessary for the die to reach.

3.3.3.3 Profiles of Temperature and State of Cure in the Rubber Sample

It is of interest to determine the temperature profiles developed in the rubber sample when the MDR is driven in scanning mode. This calculation is made by considering the heat transfer by conduction through the rubber sample using numerical calculation. The results are shown in Figure 3.19 with the temperatures on the surface in contact with the die and at the mid-plane of the rubber, plotted as a function of time. In addition, the profiles of temperature (left) and of the state of cure (right) developed through the thickness of the rubber sample are drawn at various times in Figure 3.20 when the heating rate is 5°C/min.

The following facts deserve mention:

i. The temperature on the surface of the rubber is constantly the same as that of the die whatever the value of the heating rate. This fact results from the good contact at the rubber–die interface and, above all, because the rubber and dies are at the same temperature at the beginning of the process.
ii. The temperature at the mid-plane, initially at 25°C, does not follow exactly the temperature of the die at the beginning of the process. It takes some time for the temperature at the mid-plane to vary, because of the slow rate of heat transfer through the rubber, as shown in Figure 3.19. The temperature at the mid-plane is thus shifted to a lower value during the process of scanning of the MDR. The difference between the temperature at the mid-plane and on the surface of the rubber increases with the value of the heating rate, as already found in the calorimetry run in the scanning mode [3]. After a rather short time of 20 s., this difference becomes constant to around 0.7 and 0.35°C when the heating rate is 10 and 5°C/min, respectively. This difference is in fact proportional to the heating rate [3].
iii. These results for the temperature profiles are also shown in Figure 3.20 (left) when the heating rate is 5°C/min. The profiles of temperature are nearly flat during the whole process with a difference of 0.35°C between the surface end the mid-plane of the rubber.
iv. The gradients of the state of cure shown in Figure 3.20 (right) are nearly flat during the whole process, this fact resulting from the flat profiles of temperature through the rubber.

3.3.3.4 Evaluation of the Kinetic Parameters from the Curves Obtained in Scanning Mode

Of course, it is of great interest to determine the kinetic parameters from the torque–temperature curves obtained with the MDR run in scanning mode. These parameters can be calculated from the curves shown in Figure 3.18 by using either the method based on Equation 3.11, called the Freeman–Carroll method, or the simple method based on fitting the parameters in Equation 3.19.

Another method of interest, based on Equation 3.21, is plotting $Ln\frac{dY}{dT}$ as a function of the reciprocal temperature. As shown in Figure 3.21, a straight line is obtained with a slope proportional to the activation energy E/R, when the value of $Ln(1-Y)$ is negligible. This fact occurs when Y is less than 60% [20].

The interest of these methods is worth discussing

i. The Freeman–Carroll method [**21**] is very well known, but tedious to use.
ii. The method based on fitting the parameters in Equation 3.19 is a method of least squares linear or nonlinear. It is very simple when the order of the overall cure reaction can be considered to be one.
iii. The method shown in Figure 3.21, using the plots of $Ln(\frac{dY}{dT})$ as a function of the reciprocal temperature is easy to use, especially for a first-order cure reaction. The value of the activation energy is obtained from the slope of

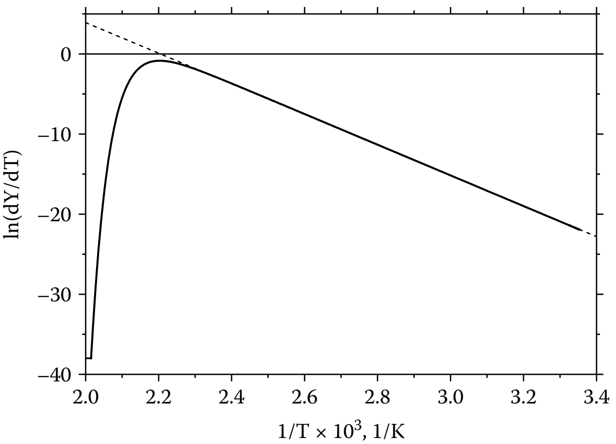

FIGURE 3.21 MDR in scanning mode. Evaluation of the kinetic parameters. (With permission of Elsevier, Figure 8, *Polymer* 2002. 43: 195–202., I.D. Rosca and J.M. Vergnaud.)

the straight line. The value of the preexponential factor k_0 is determined by using Equation 3.19 or from the value of the intercept of this straight line on the $Ln\left(\frac{dY}{dT}\right)$ axis when $1/T$ tends to zero.

iv. The effect of a change in the order of the overall cure reaction around one, within the 0.7–1.3 range, was found to be small on the rate of the reaction of rubber, and on the profiles of temperature and of state of cure developed through the thickness of the sheets [22].

3.3.4 CONCLUSIONS ON THE MDR IN SCANNING MODE

The MDR can be driven in scanning mode in the same way as a calorimeter, with only one experiment with the same sample, whereas at least three experiments are necessary when using the MDR under isothermal condition. The main parameter of interest for this new way of using the MDR is the heating rate. As a conclusion, a value ranging from 2 to 10°C/min—or much better, from 2 to 5°C/min—should be selected. Of course, a lower value of the heating rate is responsible for a longer time of experiment.

The profiles of temperature and state of cure are interesting pieces of information. In scanning mode for the MDR, a slight gradient of temperature is developed at the beginning of the experiment, but after a short time it becomes constant.

The method of scanning mode for the MDR has been applied successfully to the other rubber compounds shown in Table 3.2 and 3.3. The kinetic parameters of the cure were obtained by using Equation 3.21, and the method of least squares was proved to be the best [23].

The effect of the heating rate as well as the quality of the rubber–die contact was also seriously considered [24] by using a rubber compound made of 100 parts EPDM with 2 parts sulfur and 50 parts C black. The kinetics of cure was expressed by Equation 3.19 and the parameters obtained using Equation 3.21.

Finally, the history has been similar both with the MDR or the calorimeter. After being utilized under isothermal conditions a few decades ago, the calorimetry technique is now widely used in the scanning mode, and the MDR, quite recently, could be used in scanning mode with the rubber process analyzer.

3.4 IMPROVEMENTS FOR MDR IN SCANNING MODE

3.4.1 MDR Scanned with Change in Heating Rate

In spite of the advantages brought by the scanning mode to the MDR technique, it is also true that it takes a rather long experimental time to heat the sample up to the final temperature at which the cure reaction has come to an end, especially in starting at room temperature. Further, thinking that the heating stage between room temperature and the temperature at which the cure reaction starts—for example, around 120–140°C—is little use and, basically lost time; it is understandable that other improvements on the scanning mode technique have to be made. This is the reason why the method has been improved by changing the heating rate along the process of cure [25].

The linear temperature programming is used with the following improvement: the MDR starting at room temperature is heated at a rather high heating rate up to a temperature at which the cure reaction is assumed to take place, and at that time, the heating rate is considerably reduced. An advantage of this method over the linear temperature programming appears in reducing the time of experiment without detriment to the process.

In the case of the new method with the two heating stages process, with the first stage of 50°C/min and the second of 5°C/min, the profiles of temperature (left) and of the state of cure (right) drawn in Figure 3.22 are not flat for times lower than 120 s,

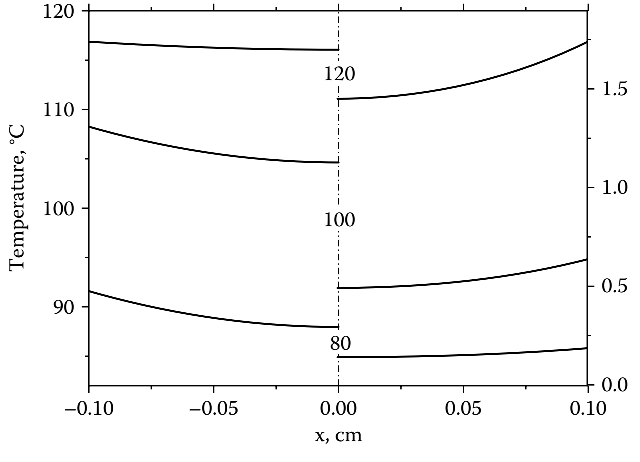

FIGURE 3.22 MDR in scanning mode with two heating rates in succession: 50 and 5°C/min. Profiles of temperature (left) and of state of cure (right) through the rubber. (With permission of Elsevier, Figure 7, *Polym. Testing*, 2004. 23: 59–67. I.D. Rosca and J.M. Vergnaud.)

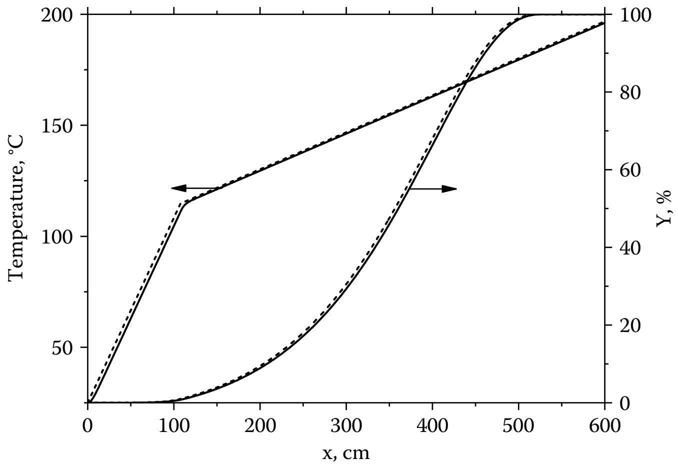

FIGURE 3.23 MDR in scanning mode with two heating rates in succession: 50 and 5°C/min. Temperature–time (left) and of state of cure–time histories (right) through the rubber. (With permission of Elsevier, Figure 8, *Polym. Testing*, 2004. 23: 59–67. I.D. Rosca and J.M. Vergnaud.)

during the strong heating stage. This fact results from this fast heating rate of 50°C/min, as already shown in calorimetry with a fast heating rate [3,14]. The temperature–time (left) and the state of cure–time (right) histories drawn in Figure 3.23 either at the mid-plane (full line) or on the surface in contact with the die (dotted line), are able to give information over the whole process of cure. Thus, it clearly appears that during the fast heating stage, up to 110 s, a small but significant difference exists between these two different temperature–time histories, which becomes nearly negligible during the second low heating rate. The state of cure–time history is not so different at the mid-plane and on the surface of the sample during this period of cure. And it has been possible to obtain the parameters of the cure reaction from the curve drawn with the MDR, as it has been previously calculated [25] in the same way as it has been done with the MDR run in scanning mode with only one constant heating rate.

3.4.2 MDR WITH SQUARE-ROOT TIME–TEMPERATURE DEPENDENCE [26]

It should be said that, if the constant heating rate has been selected for programming the temperature in various techniques, as the gas phase chromatography and calorimetry, and proposed as well for the MDR [18,20], it is perhaps not the best way to increase the temperature. The drawback of the linear heating rate results from its principle, as the rate of increase in temperature remains the same, irrespective of the phenomenon that takes place in the sample. On the contrary, it seems better to increase the rate of heating during the stage of heating and to decrease it when the reaction occurs. Thus, a reduction in time during the heating stage also reduces the time of experiment, and the stage of reaction is considered over a longer time.

This new method was developed [26] for the MDR by increasing the temperature with the square root of time. The theory of the process of heating and of the resulting cure is established, enabling the evaluation of the kinetic parameters of the cure reaction. On the other hand, the process has been deeply studied, allowing the determination of the profiles of temperature developed through the thickness of the rubber sample, as well as the profiles of the state of cure.

3.4.2.1 Theoretical Treatment of the Process

The assumptions are the same as those that have been made for the MDR in scanning mode, with the exception of the temperature which varies with the square root of time.

By putting

$$Y = \frac{Torque_t}{Torque_\infty} = \frac{SOC_t}{SOC_\infty} \tag{3.16}$$

with the rate of heating b defined by

$$T = T_0 + b \cdot t^{0.5} \tag{3.25}$$

the differential equation under isothermal condition

$$\frac{dY}{dt} = k_0 \cdot (1-Y)^n \cdot \exp\left[-\frac{E}{RT}\right] \tag{3.17}$$

becomes with the square root of time–temperature dependence:

$$\frac{dY}{dT} = \frac{2k_0}{b^2} \cdot (1-Y)^n \cdot (T-T_0) \cdot \exp\left[-\frac{E}{RT}\right] \tag{3.26}$$

Integrating between T_0 and T, leads the function Z as a function of temperature T.

By plotting $Ln\frac{dY}{dT}$ versus $Ln(1-Y)$ in Equation 3.26, the order n of the overall cure reaction can be obtained, being equal to the slope.

In the same way, by plotting $Ln\frac{dY}{dT}(1-Y)^{-n}$ versus the reciprocal temperature in Equation 3.26, the slope gives the value of the energy of activation

3.4.2.2 Materials and Apparatus

The EPDM compound containing 2% sulfur (Hutchinson) as described in Table 3.2 is used for calculation, and the values of the kinetic parameters k_0 and E are shown in Table 3.5.

A calorimeter C 80 (SETARAM) is run in scanning mode with a heating rate of 0.2°C/min for measuring the enthalpy of cure.

3.4.3 RESULTS CALCULATED WITH THE MDR RUN WITH THIS METHOD

Three different values for the heating rate are selected between the large 10–50°C/min$^{0.5}$ range. The following conclusions are worth noting:

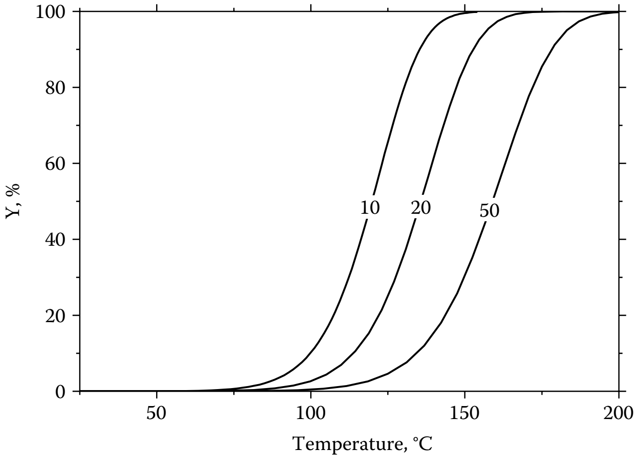

FIGURE 3.24 MDR in scanning mode with square root of time–temperature programming. Torque–temperature histories for various heating rates. (With permission of Elsevier, Figure 1, *Polymer*, 2003. 44: 4067–74. I.D. Rosca and J.M. Vergnaud.)

i. The change in torque with temperature, as shown in Figure 3.24, follows S-curves, starting at about the same temperature of the die.
ii. The effect of the heating rate is of great importance, the curves being shifted to higher values when the heating rate is increased, in the same manner as with the linear temperature programming. However, the curves are not exactly shifted through a translation way as for the linear programming of temperature [20].
iii. The change in torque with this method, expressed as a function of time, in Figure 3.25, is of interest. Thus, other S-shaped curves are also obtained. However, the effect of the value of the heating rate appears to be of great importance. Because of the square root of time temperature dependence, the curves are obtained at a much lower time when the heating rate is larger.
iv. As shown previously for the linear programming temperature, using the single method based on Equation 3.26, all the kinetic parameters calculated are similar to those introduced for calculation in torque when the temperature is varied with the square root of time.
v. The profiles of temperature, as well as the corresponding profiles of state of cure, are drawn in Figure 3.26 for half the thickness of the sample, as the system is symmetric, when the sample thickness is 0.2 cm. The profiles of temperature are nearly flat during the whole process of heating. In the same manner, the profiles of state of cure are flat, meaning that the rubber is homogeneously cured.
vi. The value of the heat evolved from the cure reaction is not taken into account for the evaluation of the temperature, as usual with the MDR. This fact can be done because of the low value of the enthalpy of cure of the rubber. Of course, in case of thermosetting resins whose reaction is highly exothermic, accounting the enthalpy is mandatory.

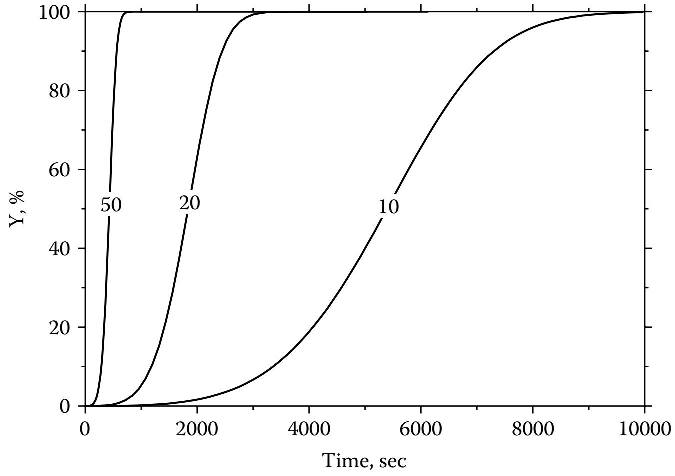

FIGURE 3.25 MDR in scanning mode with square root of time–temperature programming. Torque-time histories for various heating rates. (With permission of Elsevier, Figure 2, *Polymer*, 2003. 44: 4067–74. I.D. Rosca and J.M. Vergnaud.)

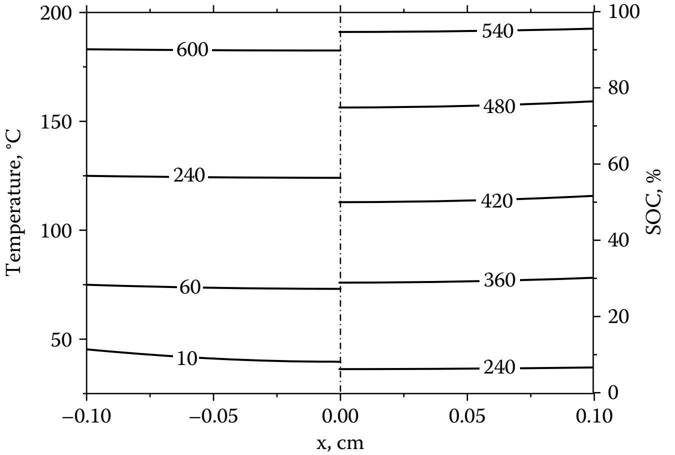

FIGURE 3.26 MDR in scanning mode with square root of time–temperature programming. Profiles of temperature (left) and of state of cure (right) in the rubber with the heating rate of 50°C/min$^{0.5}$. Time in s. and thickness of 0.2 cm. (With permission of Elsevier, Figure 6, *Polymer*, 2003. 44: 4067–4. I.D. Rosca and J.M. Vergnaud.)

3.5 CONCLUSIONS

In conclusion, it could be said that two main methods and apparatus exist for evaluating the kinetic parameters of the cure of rubbers.

The calorimetry, especially used in scanning mode, is the technique appropriated for measuring the enthalpy of the overall reaction. It may also be used for evaluating the kinetic parameters of this reaction, in spite of the low value of the enthalpy. For this last reason, rather large samples should be used so as to get more sensible and precise measurements.

The moving die rheometer (MDR), run under isothermal conditions, is widely used for evaluating the kinetic parameters of the overall cure reaction. The main drawback of this method comes from the fact that the experiments should be performed at three temperatures at least selected within a narrow temperature window through which the reaction takes place.

Based on theoretical studies, it has been proved that the MDR could be driven in scanning mode with a constant heating rate, leading to interesting benefits. This fact was found to be true since the rubber process analyzer (RPA) is now launched on the market. Moreover, other more sophisticated modes of heating seem to be still of greater interest than the constant heating rate.

Some results of interest should be pointed out:

i. In the calorimeter, the sensitive part is submitted to the heat flux emitted from the cure reaction, which results from the increase in temperature at the surface of the rubber sample during the exothermic cure reaction.
ii. It has been observed that the properties of the rubber sample, and especially its stiffness with the MDR, or its resistance to liquids [7] (Chapter 1), vary in a proportional way with the state of cure, expressed in terms of partial heat evolved as a fraction of the total heat evolved.
iii. With the MDR operated in programmed temperature, whatever the law of programming, it is more possible to evaluate the characteristics of the scorch, i.e., the onset of vulcanization than with the isothermal MDR. In fact, not only the scorch time is registered, but also the temperature of the rubber at this time can be evaluated by using the temperature versus time law of programming.
iv. The rubber process analyzer (RPA 2000 from Alpha Technologies) is now available on the market. It is able to measure the properties of rubber compounds before, during the cure, and even after cure, by registering the torque in the same way as does the MDR, but with a programmed temperature.

REFERENCES

1. Liu H., J.Y. Armand, J. Bouzon, and J.M. Vergnaud. 1988. Effect of the layer of air between the calorimeter and cylindrical samples in DC experiments. *Thermochim. Acta*. 130: 355–366.
2. Armand J.Y., J. Bouzon, and J.M. Vergnaud. 1989. Modelling of the process in DC experiments by considering the layer of air between the calorimeter and holder. *Thermochim. Acta*. 147: 291–302.

3. Vergnaud J.M. and J. Bouzon. 1992. *Cure of Thermosetting Resins*, Springer Verlag, London. Chapter 12, 200.
4. Brazier D.W., in Grassie. 1981. *Developments in Polymer Degradation*–Tome 3. Chapter 2: Calorimetric studies of rubber vulcanisation and vulcanisates, Applied Science Publ., London. 27.
5. Accetta A., P. Le Parlouer and J.M. Vergnaud. 1982. Kinetic parameters of the overall reaction of scrap rubber vulcanization by 2% sulfur. *Thermochim. Acta*. 59: 149–156.
6. Bhatnagar S.K. and S. Banerjee. 1968. Kinetics of accelerated vulcanization. III. *N*-cyclohexyl-benzothiazole-2-sulfenamide accelerated sulphur vulcanization of rubbers. *J. Inst. Rubber Ind.* 2: 177–193.
7. Hands D. and F. Horsfall. 1980. A new Method for simulating industrial cure processes. *Kautschuk Gummi Kunststoffe*. 33: 440–46.
8. Prentice G.A. and M.C. Williams. 1980. numerical evaluation of the state of cure in a vulcanizing article. *Rubber Chem. Technol.* 53: 1023–31.
9. Gehmann S.D. 1967. Heat transfer in processing and use of rubber. *Rubber Chem. Technol.* 40: 36–97.
10. Kretzschmar K. and K.W. Hoffmann. 1989. Kinetic aspects arising during the differential scanning calorimetry investigation of curing epoxy resins with anhydride. *Thermochim. Acta*. 83: 139–53.
11. Chataing G. and J.M. Vergnaud. 1985. Effect of heating rate on the separation of various phenomena in the DSC technique. *Thermochim. Acta*. 94: 379–86.
12. Armand J.Y. and J.M. Vergnaud. 1987. Compared study of the process in DC and DSC in case of a reaction of low enthalpy (cure of rubber by DC and DSC). *Thermochim. Acta*. 116: 111–24.
13. Armand J.Y., R. Gonnet, R. Jones, J. Bouzon, M. Touchard, and J.M. Vergnaud. 1986. Effect of heating rate and sample size on heat transfer through the sample in DSC. *Thermochim. Acta*. 103: 341–351.
14. Vergnaud J.M. 1987. Modelling in calorimetry working under isothermal conditions or in scanning mode. *Thermochim. Acta*. 114: 15–27.
15. R.P. Brown. 1979. *Physical Testing of Rubbers*, Applied Science Publ. London. Chapter 6.4.
16. Di Mauro P. 1985. *Proc. Int. Rubber Conf.*, Kyoto, Japan. Japan Society of the Rubber Industry. 50.
17. Sengupta A. and B.B. Konar. 1997. Cure characteristics of ethylene propylene diene rubber-polypropylene blends. *J. Appl. Polym. Sci*. 66: 1231–36.
18. Rosca I.D. and J.M. Vergnaud. 2001. Study of process of cure of EPDM rubbers in moving die rheometer. *Plastics, Rubber Composites*. 30: 275–81.
19. Mishra S., B. Baweja and R.J. Chandra. 1999. Studies on dynamic and static crosslinking of EVA and EP diene ter-polymer blends. *J. Appl. Polym. Sci*. 74: 2756–63.
20. Rosca I.D. and J.M. Vergnaud. 2002. New way of using rheometers in scanning mode for the cure of rubbers. *Polymer*. 43: 195–202.
21. Freemann E.S. and B.J. Carroll. 1958. Equation with finite differences. *J. Phys. Chem.* 62: 394–97.
22. Chater M., G. Chataing, and J.M. Vergnaud. 1985. Enhanced study of differential scanning calorimetry with determination of heat flux-time curves, profiles of temperature and state of cure. *Thermochim. Acta*. 90: 135–47.
23. Rosca I.D., R. Granger, and J.M. Vergnaud. 2004. Linear temperature programming rheometers for the cure of rubbers: Effect of various parameters. *Polym. Polym. Composites*. 12: 87–98.
24. Rosca I.D., R. Granger, and J.M. Vergnaud. 2004. Rheometers in scanning mode for cure of rubbers with low enthalpy: Effect of heating rate and rubber-die contact. *Plastics, Rubber Composites*. 33: 130–37.

25. Rosca I.D. and J.M. Vergnaud. 2004. Rheometers in scanning mode by changing the rates of linear temperature programming for the cure of rubbers. *Polym. Testing*. 23: 59–67.
26. Rosca I.D. and J.M. Vergnaud. 2003. Rheometers with square-root of time-temperature programming for the cure of rubbers. *Polymer*. 44: 4067–74.

NOMENCLATURE

α	thermal diffusivity of the rubber
b	rate of increase in temperature
C	heat capacity
$F_{x,t}$	heat flux at position x and time t
h	surface heat convection
E	energy of activation of the cure reaction
k_T, k_0	rate constant at temperature T, rate constant of the reaction, respectively
λ_r, λ_m	thermal conductivity of the rubber, of the mold, respectively
m_t, m_∞	modulus at time t, after infinite time
Q, Q_t, Q_∞	heat, heat transferred at time t, after infinite time
n	order of the cure reaction
r	for radial dimension
R	perfect gas constant
ρ	density of the rubber
$T, \frac{\partial T}{\partial t}, \frac{\partial T}{\partial x}$	temperature, increase in temperature with time, gradient of temperature
T, T_0	temperature, temperature at time 0
T_{rs}, T_{air}	temperature on the rubber surface, in air, respectively
T_{in},T_∞	temperature, initially, after infinite time, respectively
t	time
x	abscissa characterizing the position
Y	partial heat evolved at time $t = Q_t/Q_\infty$

4 Cure of Rubber in Mold

4.1 RUBBER–MOLD RELATION

4.1.1 Process of Heating and Cure

In this chapter we will consider what happens when the rubber previously at room temperature (20°C) is introduced in the heated mold. In Chapter 5 we observe conditions in injection molding, when the melted rubber is injected at a higher temperature in the heated mold. Comparison of these two cases will illustrate the reduction in time for the cure of rubbers of various thicknesses.

4.1.1.1 Mathematical Treatment

We begin by considering the heat transfer by conduction through the mold and the rubber with a typical condition at the mold–rubber interface, without forgetting the internal heat evolved from the cure reaction.

The following assumptions are made:

i. Heat is transferred through the steel mold and the rubber by one-dimensional conduction, with either constant or temperature-dependent parameters. The equation of thermal conduction is partial derivative, as the temperature depends on both time and position.
ii. Internal heat generated by the cure reaction is described by an equation with an order and energy activation.
iii. The temperature dependence of the rate of heat evolved by the cure reaction is described by the Arrhenius relation.
iv. The order of the reaction is applied to the remaining curing agent.
v. At the rubber–mold interface, there is equality of heat transfer by conduction on both faces of this interface.
vi. Heat convection from the external surface of the mold in the surrounding is neglected.
vii. There is a heating system able to maintain the temperature constant in the mold.

The equations for the transient conduction heat transfer are:

In the rubber sheet:

$$\rho_r \cdot C_r \cdot \frac{\partial T}{\partial t} = \lambda_r \cdot \frac{\partial^2 T}{\partial x^2} + \rho_r \cdot \frac{\partial Q}{\partial t} \tag{4.1}$$

which is simplified when the thermal parameters are constant:

$$\frac{\partial T}{\partial t} = \alpha_r \cdot \frac{\partial^2 T}{\partial x^2} + \frac{1}{C_r}\frac{\partial Q}{\partial t} \tag{4.1$'$}$$

In the mold

$$\rho_m \cdot C_m \cdot \frac{\partial T}{\partial t} = \lambda_m \cdot \frac{\partial^2 T}{\partial x^2} \tag{4.2}$$

which is simplified when the thermal parameters are constant:

$$\frac{\partial T}{\partial t} = \alpha_m \cdot \frac{\partial^2 T}{\partial x^2} \tag{4.2$'$}$$

At the mold–rubber interface, assumption *v* is written as follows:

$$\lambda_m \cdot \left[\frac{\partial T}{\partial x}\right]_m = \lambda_r \cdot \left[\frac{\partial T}{\partial x}\right]_r \tag{4.3}$$

while t represents time and T the temperature, λ is for the thermal conductivity, ρ the density and C the specific heat at constant pressure, in each material.

The internal heat generated by the cure reaction is described by the equation:

$$\frac{dQ}{dt} = k_0 \cdot (Q_\infty - Q_t) \cdot \exp\left[-\frac{E}{RT}\right] \tag{4.4}$$

where the order of the overall reaction n is taken as 1, E is the energy of activation, k_0 the rate constant, while Q_t and Q_∞ represent the heat of reaction evolved at time t and infinite time, respectively. In fact, Q_∞ is the enthalpy of the overall cure reaction.

4.1.1.2 Numerical Treatment of the Problem

Because of the presence of the heat of the cure reaction whose rate is a function of the reciprocal temperature, there is no analytical solution for the problem, and it is resolved by way of a numerical treatment taking into account all the facts.

4.1.2 EFFECT OF THE POSITION OF THE HEATING SYSTEM

4.1.2.1 Mold–Rubber System

The scheme of the mold–rubber system is described in Figure 4.1. The mid-plane of the rubber sheet is a plane of symmetry. Two systems of heating are considered for the mold in order to maintain the temperature of the mold at a constant: the one where the heating system is on the external surface of the mold in contact with the surrounding, and the other where this heating system is on the surface in contact with the rubber.

Comparison between these two heating systems is thus possible.

At the same time, the effect of the thickness of the rubber sheet is considered, whereas the thickness of the slabs of the mold is kept constant.

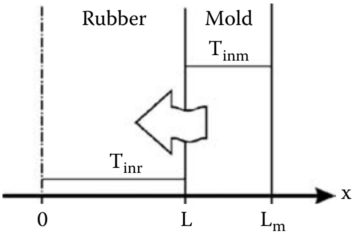

FIGURE 4.1 Scheme of the mold–rubber system, the mid-plane of the rubber being a plane of symmetry for the system (vertical dotted line).

4.1.2.2 Results Obtained for the Cure of the Rubber Sheet

The results are expressed in terms of profiles of temperature developed through the thickness of the mold–rubber system, and of profiles of the state of cure, obtained at various times. The thickness of the rubber sheet is varied within the 1–4 cm range, whereas the thickness of each slab of the mold is 1 cm. The initial temperature is 20°C for the rubber and 180°C for the slabs of the mold. The system of heating is different for the mold: on the one hand, it is on the external surface in contact with the surroundings (Figures 4.2–4.4), and on the other hand, it is on the surface in contact with the rubber (Figures 4.5–4.7).

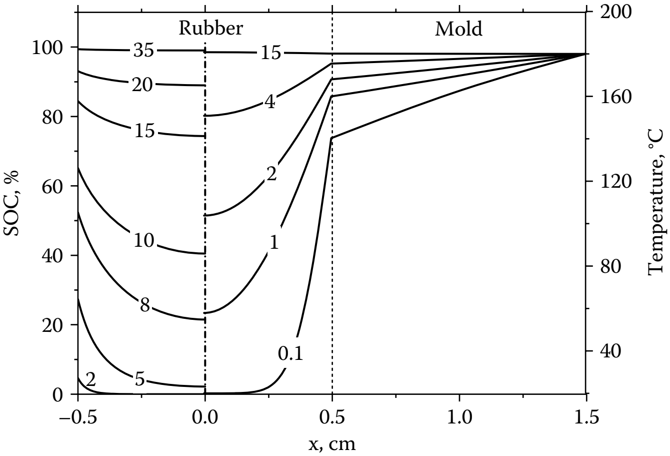

FIGURE 4.2 Profiles of temperature either in the mold (extreme right) or in the rubber (right) and of state of cure (left) with a thickness of the rubber of 1 cm with the thickness of 1 cm for each slab of the mold, whereas the initial temperature is 20°C for the rubber and 180°C for the mold. The heating system is on the external surface of each slab. Thermal and kinetic parameters are in Table 4.1 with enthalpy of 14.3 J/g. Because of the symmetry, only half the thickness of the rubber–mold is shown, with the plane of symmetry at position 0.

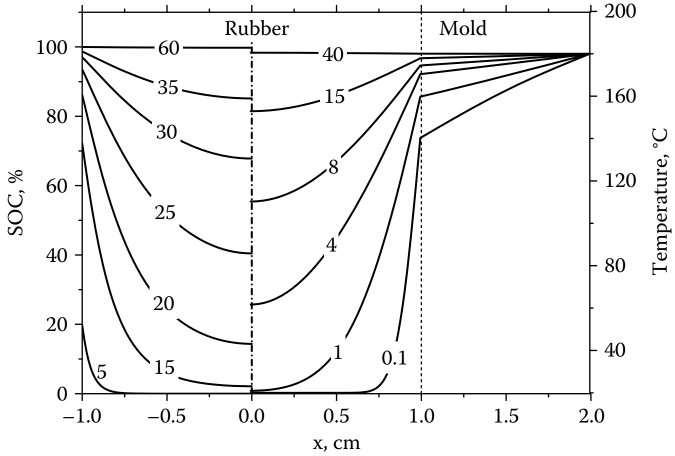

FIGURE 4.3 Profiles of temperature either in the mold (extreme right) or in the rubber (right) and of state of cure (left) with a thickness of the rubber of 2 cm with the thickness of 1 cm for each slab of the mold, whereas the initial temperature is 20°C for the rubber and 180°C for the mold. Heating system on the external surface of each slab. Thermal and kinetic parameters in Table 4.1 with enthalpy of 14.3 J/g. Because of the symmetry, only half the thickness of the rubber–mold is shown, with the plane of symmetry at position 0.

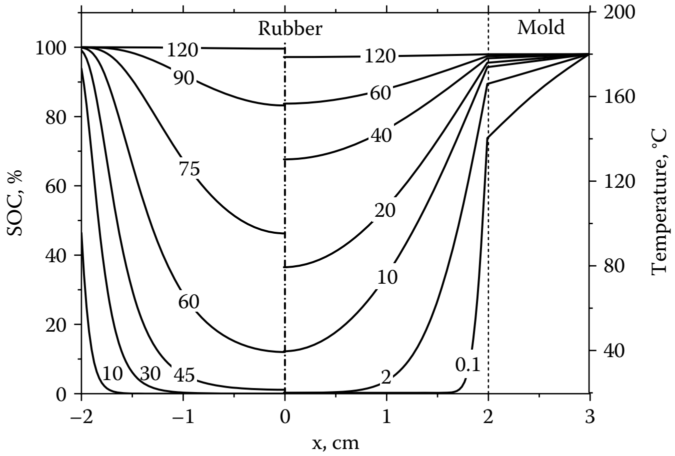

FIGURE 4.4 Profiles of temperature either in the mold (extreme right) or in the rubber (right) and of state of cure (left) with a thickness of the rubber of 4 cm with the thickness of 1 cm for each slab of the mold, whereas the initial temperature is 20°C for the rubber and 180°C for the mold. Heating system on the external surface of each slab. Thermal and kinetic parameters in Table 4.1 with enthalpy of 14.3 J/g. Because of the symmetry, only half the thickness of the rubber–mold is shown, with the plane of symmetry at position 0.

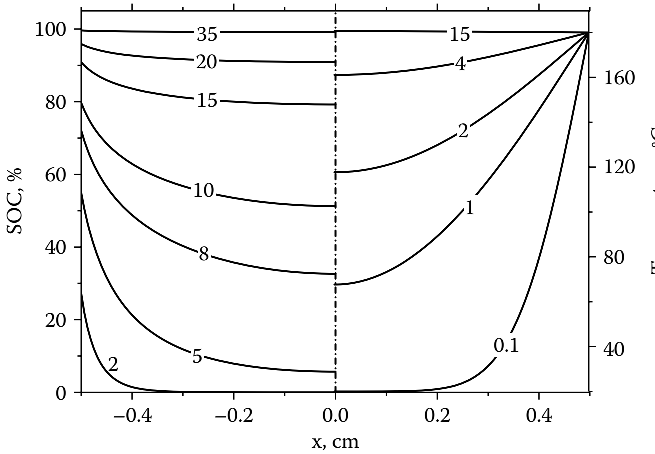

FIGURE 4.5 Profiles of temperature (right) and of state of cure (left) developed through the rubber with a thickness of the rubber of 1 cm with the thickness of 1 cm for each slab of the mold, whereas the initial temperature is 20°C for the rubber and 180°C for the mold. Heating system on the surface of the slabs of the mold is in contact with the rubber. Thermal and kinetic parameters shown in Table 4.1 with enthalpy of 14.3 J/g. Only half the thickness of the rubber is shown because of the symmetry with the plane of symmetry at position 0 on the abscissa. The mold is not shown, because of the constant temperature on the rubber surface.

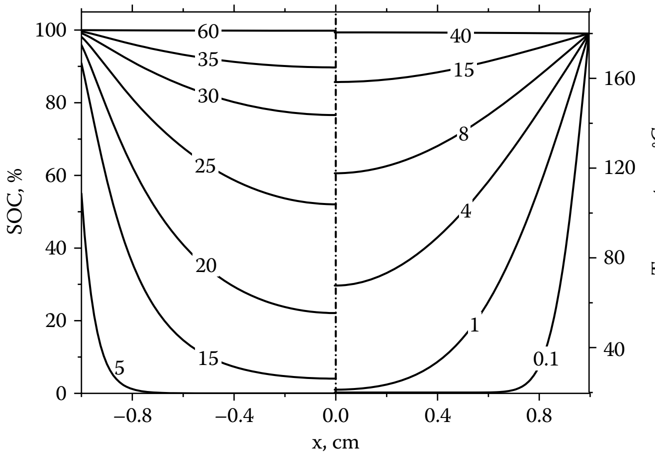

FIGURE 4.6 Profiles of temperature (right) and of state of cure (left) developed through the rubber with a thickness of the rubber of 2 cm with the thickness of 1 cm for each slab of the mold, while the initial temperature is 20°C for the rubber and 180°C for the mold. Heating system on the surface of the slabs of the mold is in contact with the rubber. Thermal and kinetic parameters shown in Table 4.1 with enthalpy of 14.3 J/g. Only half the thickness of the rubber is shown, because of the symmetry with the plane of symmetry at position 0 on the abscissa. The mold is not shown because of the constant temperature on the rubber surface.

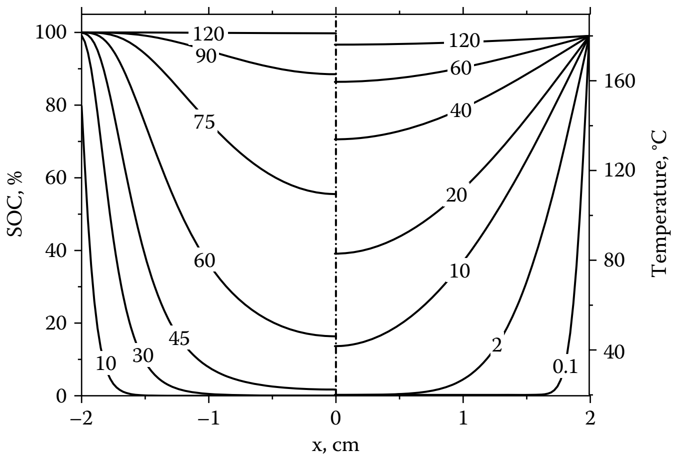

FIGURE 4.7 Profiles of temperature (right) and of state of cure (left) developed through the rubber with a thickness of the rubber of 4 cm with the thickness of 1 cm for each slab of the mold, while the initial temperature is 20°C for the rubber and 180°C for the mold. Thermal and kinetic parameters shown in Table 4.1 with enthalpy of 14.3 J/g. Only half the thickness of the rubber is shown, because of the symmetry with the plane of symmetry at position 0 on the abscissa. The mold is not shown because of the constant temperature on the rubber surface.

For this study, the thermal parameters for the mold and rubber, as well as the kinetic parameters of the cure reaction, are shown in Table 4.1, by taking the value of ΔH = 14.3 J/g.

The following conclusions are drawn from these figures:

i. All these Figures 4.2 to 4.7 are drawn by taking into account the plane of symmetry at position 0 of the abscissa.
ii. It is clear that the introduction of the rubber sheet initially at 20°C between the slabs of the mold at 180°C is responsible for a decrease in temperature through the mold thickness, while this temperature is kept constant on the external surface of the slabs where the heating system is active. Moreover,

TABLE 4.1
Thermal and Kinetic Parameters Used for Calculation

λ_r = 0.2 W/m.deg	C_r = 2.2 J/g.deg	ρ_r = 0.9 g/cm^3	$\alpha_r = 10^{-7}$ m^2/s
λ_m = 3.8 W/m.deg	C_m = 0.12 J/g.deg	ρ_m = 7.9 g/cm^3	α_m = 4.10 m^2/s
% peroxide 2	9	19	$Lnk_0 = 36$
ΔHJ/g 14.3	44.7	56.7	E/R = 19,000

TABLE 4.2
State of Cure at the Mid-Plane Thickness Versus time "Minute"

Thickness	1 cm				2 cm				4 cm			
SOC%	90.1	95	99	100	90.2	95	99	100	90	95	99	100
Time (1)	20.7	25	35	54	37	41	51	70	95	101	113	134
Time (2)	19.5	24	33	52.5	35	39	49	68	91	97	109	130

Note:

1: The heating system is on the external surface of the slabs of the mold.

2: The heating system is on the slab surface in contact with the rubber.

it takes some time for the temperature on the surface of the mold to reach 180°C. This recovery time depends on the thickness of the rubber: it takes more than 4 minutes for rubber 1 cm thick, and 60 minutes for rubber 4 cm thick.

iii. By comparing the Figures 4.2–4.4 with the Figures 4.5–4.7 which differ only by the position of the heating system, the profiles of temperature and of state of cure developed through the thickness of the rubber look similar at the end of the process of cure. The slight difference can be distinguished using Table 4.2
iv. The time necessary for the state of cure to reach 100% is far longer than that for 90 or 95%, whatever the thickness of the rubber sheet.

4.2 EFFECT OF THE THICKNESS OF THE RUBBER SHEET

The effect of the thickness of the rubber sheet can be determined by comparing either Figures 4.2–4.4 or Figures 4.5–4.7 obtained with different heating systems of the mold, or more precisely by using the values shown in Table 4.2.

The following comments can be made:

i. Whatever the thickness of the rubber sheet, steep gradients of temperature and of state of cure develop through the thickness during the cure.
ii. Of course, longer times are necessary for the temperature at the mid-plane of the sheet to attain the mold temperature. The law resulting from the ratio $\frac{\alpha \cdot t}{L^2}$, which appears in Equation 2.41 for heat transfer, proves that the time necessary to attain the same value for the temperature is proportional to the square of the thickness and is not easy to find.
iii. Following these profiles of temperature, other profiles of state of cure are developed, with a higher value on the surface in contact with the slabs of the mold.

The effect of the thickness of the rubber on the cure is also determined in Figure 4.8 by drawing the temperature–time histories obtained either at the rubber surface in

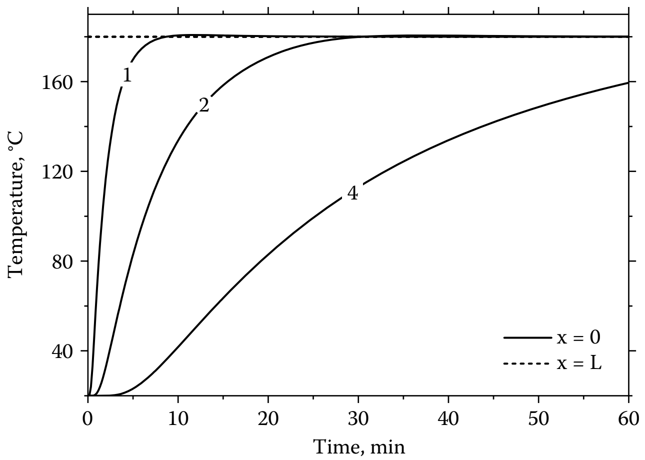

FIGURE 4.8 The temperature–time history at the surface of the rubber in contact with the mold ($x = L$ dotted line) and at the mid-plane of the rubber ($x = 0$ full line) for various thicknesses of the rubber sheet. Mold temperature = 180°C. Enthalpy = 14.3 J/g. Heating system on the face of the mold is in contact with the rubber.

contact with the mold (dotted line) or at the mid-plane of the rubber sheets (full line), when the temperature of the mold is 180°C, and the enthalpy of cure is 14.3 J/g. The corresponding state of cure–time histories either at the rubber surface (dotted line) or at the mid-plane of the rubber sheets are drawn in Figure 4.9. The values of the thickness of these rubber sheets are shown in these two figures. The heating system is on the mold–rubber interface.

It is also of interest to evaluate the effect of the thickness of the rubber sheet when the heating system is on the external surface of the mold in contact with the surroundings, as shown in Figure 4.10 for the temperature–time history and in Figure 4.11 for the state of cure–time history. These curves are drawn as they are calculated at the mold temperature of 180°C with the rubber compound containing 2% sulfur responsible for an enthalpy of cure of 14.3 J/g.

A few complementary observations are drawn from these Figures 4.8 to 4.11:

i. Because of the position of the heating system at the rubber–mold interface, the temperature on the rubber surface (dotted line) reaches instantaneously that of the mold (Figure 4.8).
ii. A given time is necessary for the temperature to start at the mid-plane of the rubber, resulting from the time necessary for heat to reach this position.
iii. The state of cure–time history at the surface of the rubber in contact with the mold is the same whatever the thickness of the rubber sheets (dotted line in Figure 4.9).
iv. S-shaped curves are obtained for the state of cure–time histories at the mid-plane of the rubber sheets as shown in Figure 4.9 (full lines).

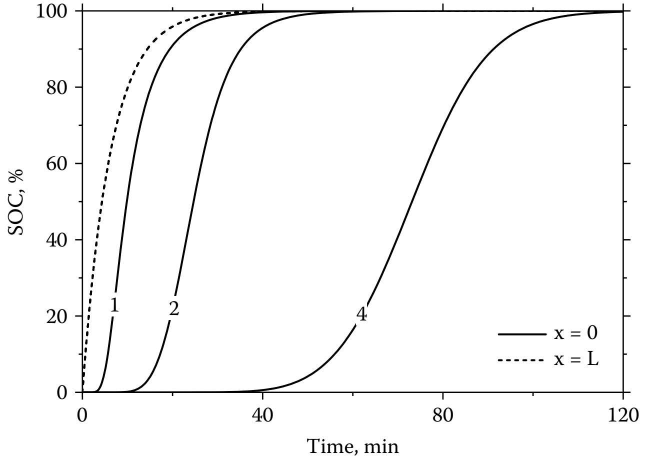

FIGURE 4.9 State of cure–time history at the surface of the rubber in contact with the mold ($x = L$ dotted line) and at the mid-plane of the rubber ($x = 0$ full line) for various thicknesses of the rubber sheet. Mold temperature = 180°C. Enthalpy = 14.3 J/g. Heating system on the face of the mold is in contact with the rubber.

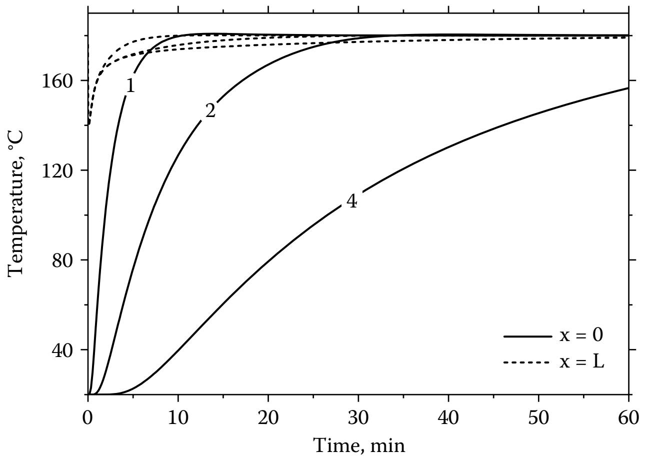

FIGURE 4.10 Temperature–time history at the surface of the rubber in contact with the mold ($x = L$ dotted line) and at the mid-plane of the rubber ($x = 0$ full line) for various thicknesses of the rubber sheet. Mold temperature = 180°C. Enthalpy = 14.3 J/g. Heating system is on the external face of the mold.

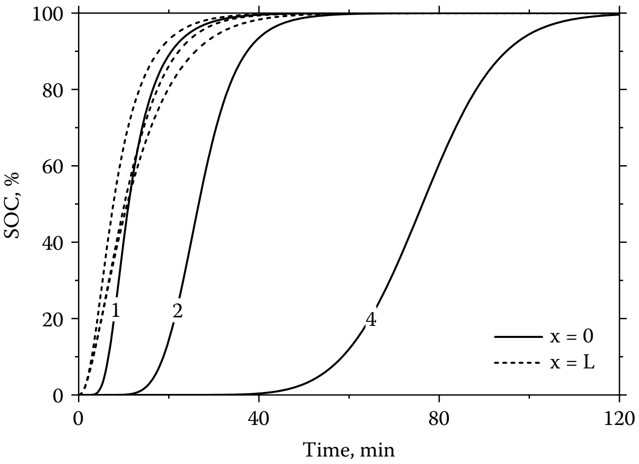

FIGURE 4.11 State of cure–time history at the surface of the rubber in contact with the mold ($x = L$ dotted line) and at the mid-plane of the rubber ($x = 0$ full line) for various thicknesses of the rubber sheet. Mold temperature = 180°C. Enthalpy = 14.3 J/g. Heating system is on the external face of the mold.

v. When the heating system is on the external surface of the mold, it takes some time for the temperature to increase on the surface of the rubber, as shown with the dotted lines in Figure 4.10. Moreover, these temperature–time histories are not the same when the thickness of the rubber sheet is varied. The temperature on the rubber surface increases more quickly when the thickness of the rubber is lower.

vi. The effect of the position of the heating system also appears for the state of cure–time history by comparing the curves drawn in Figures 4.9 and 4.11. Not only the state of cure–time histories in Figure 4.11 differ from those drawn in Figure 4.9 at the rubber surface, but the external position of the heating system is responsible for curves, which depend on the thickness of the rubber sheet. This result follows the temperature–time histories obtained in Figure 4.10, which also depend on the thickness of the rubber sheet. Moreover, this effect is also sensible at the mid-plane of the rubber sheets.

4.3 EFFECT OF THE ENTHALPY OF CURE

The effect of the enthalpy of cure, associated with the value of the percent curing agent, can be observed by comparing the profiles of temperature and of state of cure drawn in the following figures, when the heating system of the mold is on the rubber surface, while the mold temperature is kept constant at 180°C:

- In Figure 4.5 (14.3 J/g) with the other Figures 4.12 (44.7J/g) and 4.13 (56.7 J/g) when the thickness is 1 cm for the rubber sheet,

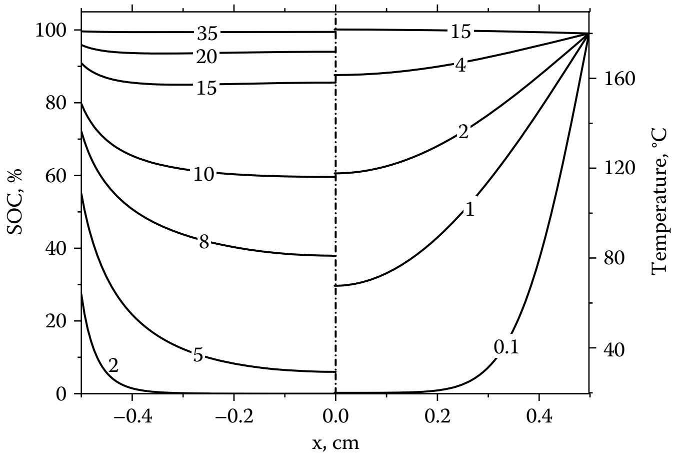

FIGURE 4.12 Profiles of temperature (right) and of state of cure (left) developed in the rubber with a thickness of the rubber of 1 cm and the thickness of 1 cm for each slab of the mold, whereas the initial temperature is 20°C for the rubber and 180°C for the mold. Heating system on the surface of the slabs of the mold in contact with the rubber. Thermal and kinetic parameters shown in Table 4.1 with enthalpy of 44.7 J/g. Only half the thickness of the rubber is shown because of the symmetry with the plane of symmetry at position 0 on the abscissa.

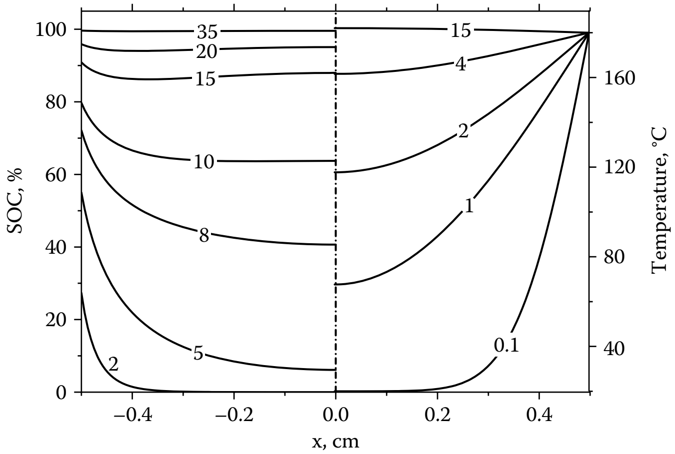

FIGURE 4.13 Profiles of temperature (right) and of state of cure (left) developed in the rubber with a thickness of the rubber of 1 cm and the thickness of 1 cm for each slab of the mold, while the initial temperature is 20°C for the rubber and 180°C for the mold. Heating system on the surface of the slabs of the mold is in contact with the rubber. Thermal and kinetic parameters shown in Table 4.1 with enthalpy of 56.7 J/g. Only half the thickness of the rubber is shown because of the symmetry with the plane of symmetry at position 0 on the abscissa.

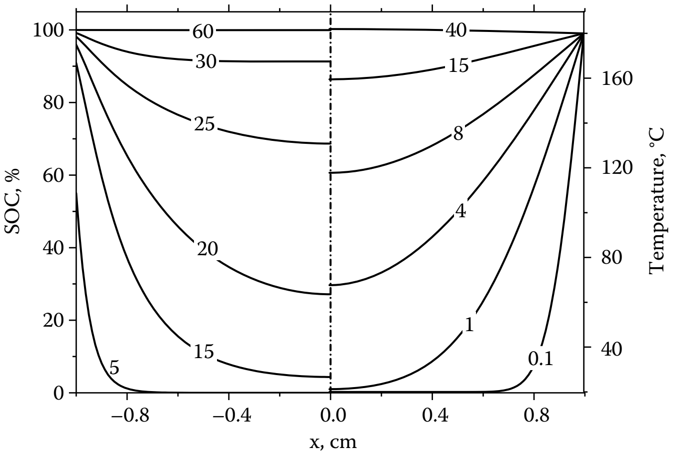

FIGURE 4.14 Profiles of temperature (right) and of state of cure (left) developed in the rubber with a thickness of the rubber of 2 cm and the thickness of 1 cm for each slab of the mold, while the initial temperature is 20°C for the rubber and 180°C for the mold. Thermal and kinetic parameters shown in Table 4.1 with enthalpy of 44.7 J/g. Only half the thickness of the rubber is shown because of the symmetry with the plane of symmetry at position 0 on the abscissa.

- In Figure 4.6 (14.3 J/g) with the other Figures 4.14 (44.7 J/g) and 4.15 (56.7 J/g) when the thickness is 2 cm for the rubber, and in the Figures 4.7 (14.3 J/g) with the other Figures 4.16 (44.7 J/g) and 4.17 (56.7 J/g) when the thickness is 4 cm.

As shown in Table 4.1, the thermal and the kinetic parameters are similar for these rubber compounds, whatever the percent curing agent.

From the curves drawn in these figures, the following comments can be made:

i. Comparison between the curves of the Figures 4.5, 4.12, and 4.13, obtained with the same thickness of the rubber (1 cm), shows that the profiles of temperature are nearly similar, except at the end of the process, as the temperature is slightly higher at the mid-plane than on the rubber–mold interface when the enthalpy of cure is larger.
ii. Comparison between the curves of the Figures 4.5, 4.12, and 4.13 obtained with the same thickness of the rubber (1 cm) shows that the profiles of state of cure are quite different, especially at the end of the process, since the value of the state of cure at the mid-plane is slightly higher than on the rubber–mold interface when the enthalpy of cure is larger.
iii. Comparison between the curves of the Figures 4.5, 4.12, and 4.13 obtained with the same thickness of the rubber (1 cm) shows that at 20 minutes the value of the state of cure is nearly uniform when the enthalpy of cure is larger. Moreover, at the same time of 20 minutes, the state of cure is higher in Figure 4.13 for the larger enthalpy of cure.

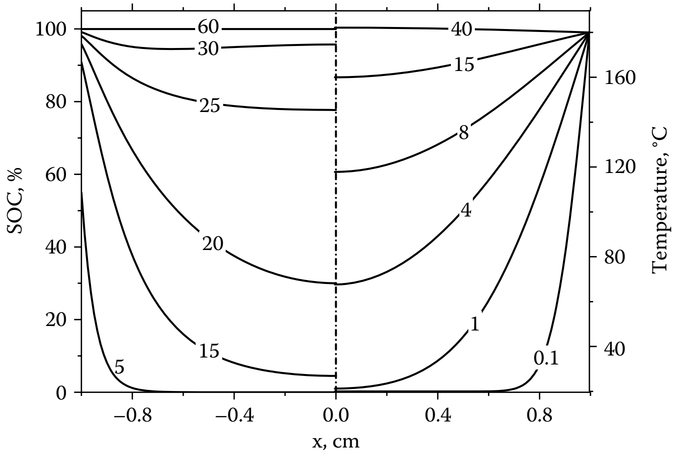

FIGURE 4.15 Profiles of temperature (right) and of state of cure (left) developed in the rubber with a thickness of the rubber of 2 cm and the thickness of 1 cm for each slab of the mold, whereas the initial temperature is 20°C for the rubber and 180°C for the mold. Heating system on the surface of the slabs of the mold is in contact with the rubber. Thermal and kinetic parameters shown in Table 4.1 with enthalpy of 56.7 J/g. Only half the thickness of the rubber is shown because of the symmetry with the plane of symmetry at position 0 on the abscissa.

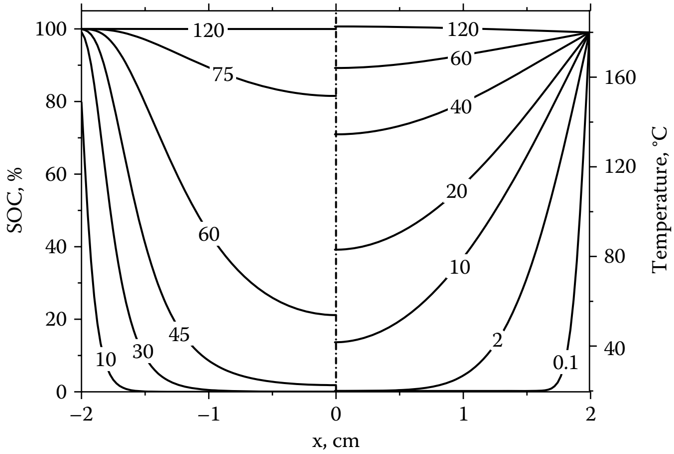

FIGURE 4.16 Profiles of temperature (right) and of state of cure (left) developed in the rubber with a thickness of the rubber of 4 cm and the thickness of 1 cm for each slab of the mold, whereas the initial temperature is 20°C for the rubber and 180°C for the mold. Heating system on the surface of the slabs of the mold is in contact with the rubber. Thermal and kinetic parameters shown in Table 4.1 with enthalpy of 44.7 J/g. Only half the thickness of the rubber is shown because of the symmetry with the plane of symmetry at position 0 on the abscissa.

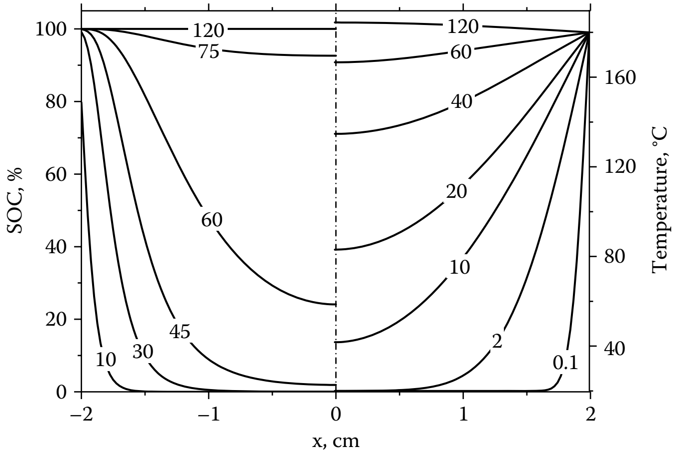

FIGURE 4.17 Profiles of temperature (right) and of state of cure (left) developed in the rubber with a thickness of the rubber of 4 cm and the thickness of 1 cm for each slab of the mold, while the initial temperature is 20°C for the rubber and 180°C for the mold. Heating system on the surface of the slabs of the mold is in contact with the rubber. Thermal and kinetic parameters shown in Table 4.1 with enthalpy of 56.7 J/g. Only half the thickness of the rubber is shown because of the symmetry with the plane of symmetry at position 0 on the abscissa.

iv. Comparison between the curves of the Figures 4.6, 4.14, and 4.15 obtained with the same thickness of the rubber (2 cm) shows that the profiles of temperature are nearly similar, except at the end of the process, since the temperature is slightly higher at the mid-plane than on the rubber–mold interface, when the enthalpy of cure is larger.

v. Comparison between the curves of the Figures 4.6, 4.14, and 4.15 obtained with the same thickness of the rubber (2 cm) shows that the profiles of state of cure are quite different, except at the very beginning of the process, for times lower or equal to 15 minutes. For times higher than 20 minutes, the values of the state of cure largely depend on the value of the enthalpy of cure, following the statement: the higher the enthalpy of cure, the higher the value of the state of cure.

vi. Comparison between the curves of the Figures 4.7, 4.16, and 4.17 obtained with the same thickness of the rubber (4 cm) shows that if the profiles of temperature are nearly similar for times lower than 40 minutes, they become quite different for times longer than 60 minutes. At the end of the process, the temperature is higher at the mid-plane than on the rubber–mold interface when the enthalpy of cure is larger.

vii. Comparison between the curves of the Figures 4.7, 4.16, and 4.17 obtained with the same thickness of the rubber (4 cm) shows that the profiles of state of cure are nearly similar for times lower than 45 minutes, but they become quite different for times equal or longer than 60 minutes. On the

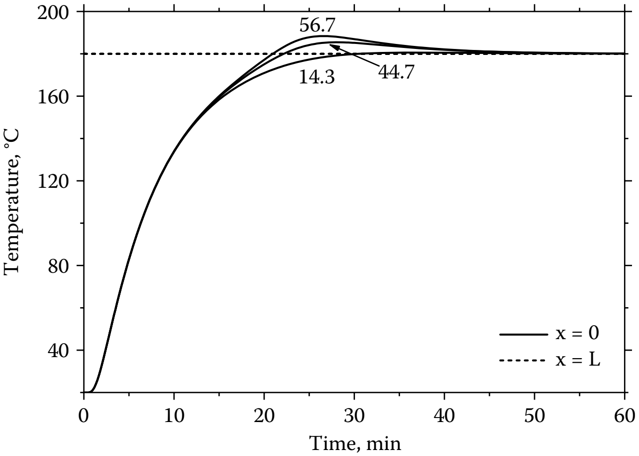

FIGURE 4.18 Temperature–time history at the surface of the rubber in contact with the mold (x = L dotted line) and at the mid-plane of the rubber (x = 0 full line) for various values of the enthalpy of cure. Mold temperature = 180°C. Thickness of rubber = 2 cm. Heating system on the face of the mold is in contact with the rubber.

whole, after this time of 60 minutes, higher values of the state of cure are attained at shorter times when the enthalpy of cure is larger.

viii. These differences in the profiles of the temperature and of state of cure result from the effect of the enthalpy of cure, whatever the thickness of the rubber sheet. However, they are enhanced when the rubber thickness is larger.

ix. The increase in temperature at the mid-plane of the rubber sheet (2 cm heated at 180°C) is clearly shown in Figure 4.18, where the temperature–time histories are drawn either on the rubber–mold interface or at the mid-plane. A peak is attained for the temperature at the mid-plane, while the temperature is kept constant at the rubber–mold interface, when the heating system is on this interface.

x. The effect of the cure enthalpy on the state of cure is shown in Figure 4.19 where the state of cure–time histories are drawn either at the surface of the rubber in contact with the mold for $x = L$ (dotted line) or at the mid-plane (full line) of sheets (2 cm thick heated at 180°C with the heating system on the mold surface in contact with the rubber). Thus the same curve is shown at the rubber surface. But, if the curves drawn at the mid-plane (x = 0) start at the same time, around 10 minutes, they diverge, and the state of cure increases more rapidly when the cure enthalpy is increased. This fact results from the higher increase in temperature attained with the higher cure enthalpy.

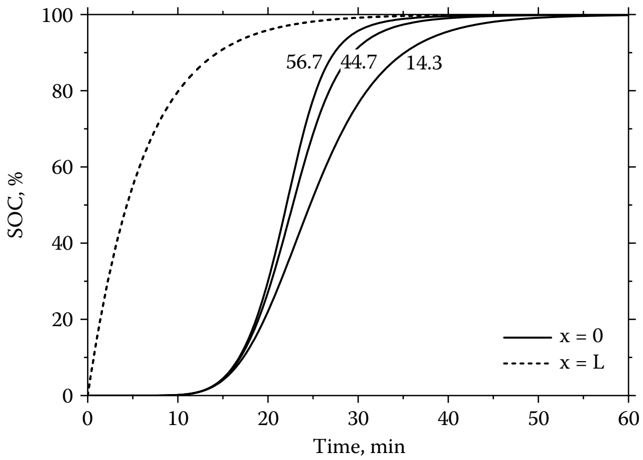

FIGURE 4.19 State of cure–time history at the surface of the rubber in contact with the mold (x = L dotted line) and at the mid-plane of the rubber (x = 0 full line) for various values of the enthalpy of cure. Mold temperature = 180°C. Thickness of rubber = 2 cm. Heating system on the face of the mold is in contact with the rubber.

4.4 EFFECT OF THE TEMPERATURE ON THE CURE

The temperature of the mold is of great importance to the rate of cure, and thus to the time necessary to get a given value for the state of cure.

The effect of the mold temperature is studied by considering the profiles of temperature and of the state of cure developed through rubber sheets of the same thickness (2 cm) with the same percent curing agent and the same enthalpy of cure (14.3 J/g). The heating system is placed at the rubber–mold interface, and thus the temperature at the rubber surface attains instantaneously that of the mold.

The following figures are shown:

- Figure 4.6, when the temperature is 180°C
- Figure 4.20, when the temperature is 170°C
- Figure 4.21, when the temperature is 160°C

The comparison of these three figures leads to some observations of interest:

i. The profiles of temperature in these three figures are similar, if they are reported as a fraction of the mold temperature, as predicted by the Equation 2.41.
ii. The profiles of the state of cure developed through the thickness of these three figures show that the rate of cure is increased by increasing the temperature. Thus, the value of nearly 100% for the state of cure is reached at 60 minutes at 180°C, while times of 120 minutes and 210 minutes are necessary to obtain the same value at 170°C and 160°C, respectively.

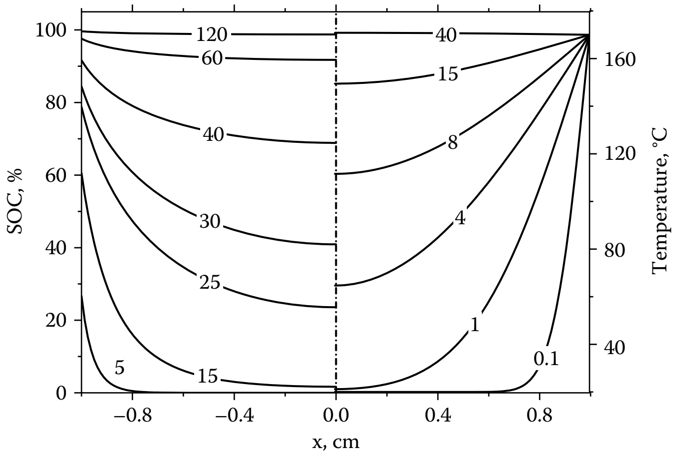

FIGURE 4.20 Profiles of temperature (right) and of state of cure (left) developed in the rubber with a thickness of the rubber of 2 cm with the thickness of 1 cm for each slab of the mold, while the initial temperature is 20°C for the rubber and 170°C for the mold. Heating system on the surface of the slabs of the mold is in contact with the rubber. Thermal and kinetic parameters shown in Table 4.1 with enthalpy of 14.3 J/g. Only half the thickness of the rubber is shown, because of the symmetry with the plane of symmetry at position 0 on the abscissa.

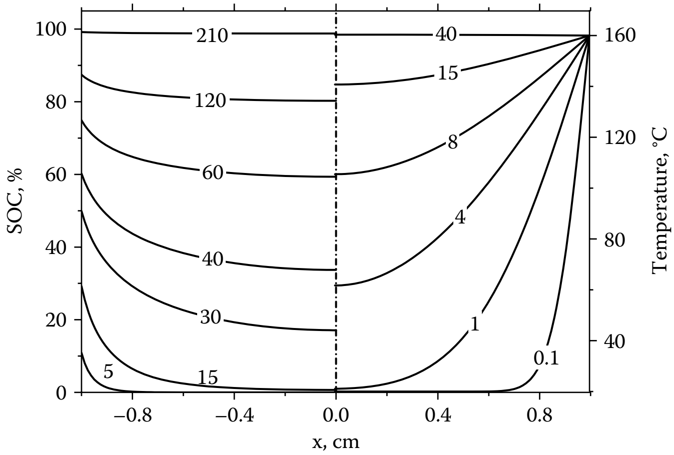

FIGURE 4.21 Profiles of temperature (right) and of state of cure (left) developed in the rubber with a thickness of the rubber of 2 cm with the thickness of 1 cm for each slab of the mold, while the initial temperature is 20°C for the rubber and 160°C for the mold. Heating system on the surface of the slabs of the mold in contact with the rubber. Thermal and kinetic parameters shown in Table 4.1 with enthalpy of 14.3 J/g. Only half the thickness of the rubber is shown because of the symmetry with the plane of symmetry at position 0 on the abscissa.

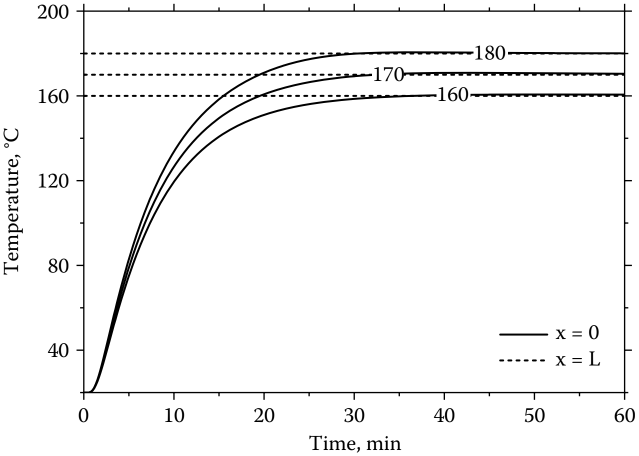

FIGURE 4.22 Temperature–time history at the surface of the rubber in contact with the mold (x = L dotted line) and at the mid-plane of the rubber (x = 0 full line) for various values of the mold temperature. Thickness of rubber = 2 cm. Enthalpy = 14.3 J/g. Heating system on the face of the mold in contact with the rubber.

iii. Steeper gradients of temperature are obtained for the higher temperature of the mold, while nearly uniform values of the state of cure are shown at the lower temperature of 160°C.

The effect of the temperature of the mold can also be defined by drawing on the same Figure 4.22 the temperature–time histories obtained either at the rubber–mold interface or at the mid-plane of the rubber, as well as the corresponding histories for the state of cure in Figure 4.23.

The following results are thus obtained:

i. The temperature on the surface of the rubber (position $x = L$) reaches instantaneously that of the mold, as shown by the dotted line in Figure 4.22. In fact, the increase in temperature at the surface is nearly constant from the beginning, and thus obeys Equation 4.5 (already shown in Chapter 2 as Equation 2.41).

$$\frac{T_{x,t} - T_\infty}{T_{in} - T_\infty} = \frac{4}{\pi} \cdot \sum_{n=0}^{\infty} \frac{(-1)^n}{2n+1} \cdot \cos\frac{(2n+1)\pi x}{2L} \cdot \exp\left[-\frac{(2n+1)^2\pi^2}{4L^2}\alpha \cdot t\right] \quad (4.5)$$

ii. The temperature in the mid-plane of the rubber (position x = 0) increases by following a S-shape, and the same time is necessary for this temperature increase to begin. In fact, as said already, it takes some time for heat to get through the rubber, and thus for the temperature to increase.

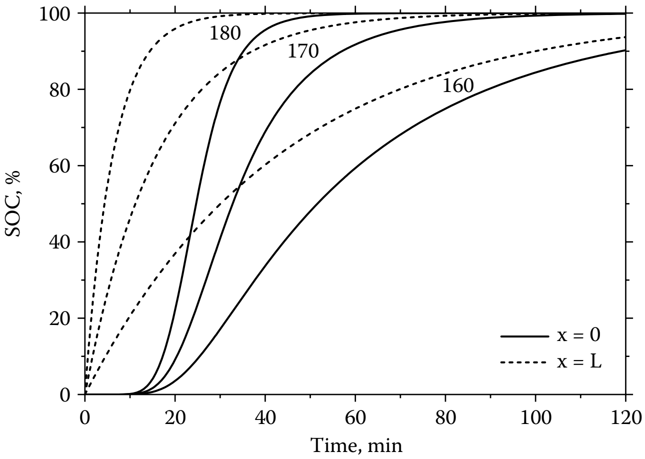

FIGURE 4.23 State of cure–time history at the surface of the rubber in contact with the mold (x = L dotted line) and at the mid-plane of the rubber (x = 0 full line) for various values of the mold temperature. Thickness of rubber = 2 cm. Enthalpy = 14.3 J/g. Heating system on the face of the mold in contact with the rubber.

iii. The state of cure–time histories drawn on the surface of the rubber in contact with the mold (dotted lines for $x = L$) exhibit a vertical tangent at the beginning of the process, as predicted by the Equation 2.44 in Chapter 2, and rewritten in 4.6:

$$\frac{Q_t}{Q_\infty} = 1 - \frac{8}{\pi^2}\sum_{n=0}^{\infty}\frac{1}{(2n+1)^2}\cdot\exp\left[-\frac{(2n+1)^2\pi^2}{4L^2}\alpha\cdot t\right] \tag{4.6}$$

iv. The state of cure–time histories obtained at the mid-plane of the rubber sheet (full lines for $x = 0$) follow a S-shape profile for these three temperatures. Associated with the time necessary for the temperature to increase at the mid-plane, a lag time is necessary for the state of cure to start; this lag time is nearly similar for the three temperatures.

4.5 EFFECT OF THE KINETIC PARAMETERS OF THE CURE

As shown in depth in the first chapter, as well as in the third, it is not easy to determine the kinetic parameters of the cure reaction. This is why the principle of a reference temperature was established by various authors [1–3].

When the cure was assumed to follow an overall reaction, taking into account not only the amount of the curing agent but also its temperature dependence, the kinetic parameters were considered. First, the value of 1 for the order was taken for granted [4], and nearly at the same time the activation energy was supposed to play an important role so as to evaluate the effect of the temperature on the rate of cure [4–6].

Other workers have built nomograms, in addition to their numerical models [7–9].

Finally, using the above results and theoretical consideration, the kinetics of the cure reaction was established and used for evaluating either the profiles of temperature developed through the material or the corresponding profiles of state of cure [10–12]. At that time the kinetics of the cure reaction was determined by calorimetry run under isothermal conditions and finally in scanning mode with a constant temperature program. As the enthalpy of the cure reaction is rather low for rubbers, the problem was tedious, leading to results with sometimes a low level of accuracy.

Rather than look for a more accurate method for obtaining data for the kinetics of cure, attention was given to evaluating the effect of the lack of accuracy in the kinetic parameters. Some studies were conducted by using calorimetry [13–15]. Thus, the effect of the order of the overall cure reaction on the rate of cure was determined, and profiles of temperature and state of cure were evaluated by varying the value of the order around the value found from experiments made with a rubber compound cured with 3% sulfur [13]. By using the same approach and the same method, the effect of a variation of the activation energy on the profiles of temperature and of state of cure was also studied [14,15].

The effect of the kinetic parameters on the cure is evaluated in this subsection by using the values collected in Table 4.1, which are the basis values around which they are varied. The mold–rubber is considered with the heating system placed on the mold surface in contact with the rubber sheet. The results are expressed in terms of temperature–time histories and of state of cure–time histories calculated either at the rubber surface or at the mid-plane of this rubber sheet. The rubber thickness is 2 cm, and the mold temperature is 170°C. The cure enthalpy is 14.3 J/g associated with sulfur at 2%.

4.5.1 EFFECT OF THE ORDER OF THE OVERALL REACTION

The effect of the order of the overall cure reaction on the process is evaluated by varying the order around 1, by taking the values of 1.25, 1, and 0.75, as shown in the following two figures:

Figure 4.24, where the temperature–time history at the rubber surface and at the mid-plane are drawn as they are calculated with these three values of the order n, with $n = 1.25$ (curve 1); $n = 1$ (curve 2); $n = 0.75$ (curve 3).

Figure 4.25, where the state of cure–time history at the rubber surface and at the mid-plane are drawn as they are calculated with the three values of the order n, with: $n = 1.25$ (curve 1); $n = 1$ (curve 2); $n = 0.75$ (curve 3).

These curves deserve the following comments:

i. As shown in Figure 4.24, the effect of the position of the heating system at the rubber–mold interface on the temperature–time history at the rubber surface appears clearly. It is necessary to extend the scale of time to 0.10 minute to be able to distinguish a decrease in the temperature at the rubber surface, which is short in time and small in extent. This fact is also shown in Figure 4.5 where the profiles of temperature developed through the rubber thickness are drawn.

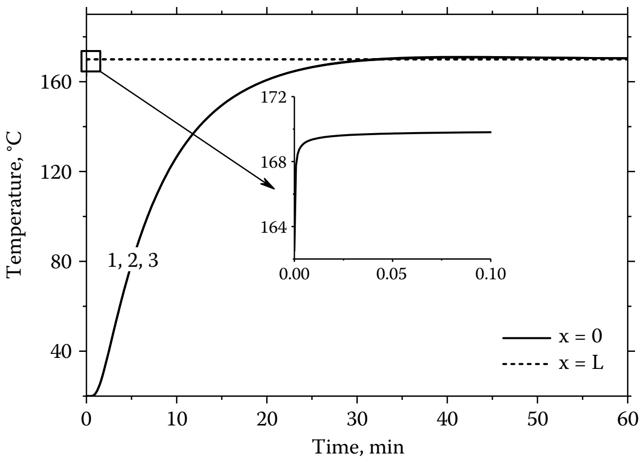

FIGURE 4.24 Temperature–time history on the surface (dotted line) and at the mid-plane (full line) with the order $n = 1.25$ (curve 1), 1 (curve 2), and 0.75 (curve 3). Rubber thickness (2L) = 2 cm. Enthalpy = 14.3 J/g $T_m = 170°C$. Heating system on the rubber surface.

ii. The temperature–time history at the mid-plane of the rubber exhibits an S-shape, starting at a time that depends on the thickness of the rubber.

iii. The effect of the value given to the order of the overall reaction of cure, n, on the temperature–history does not appear significantly, the reason being that the value of the cure enthalpy is very low. Calculation made with 3% sulfur associated with a much larger enthalpy leads to a highly visible change in the temperature–time history [13].

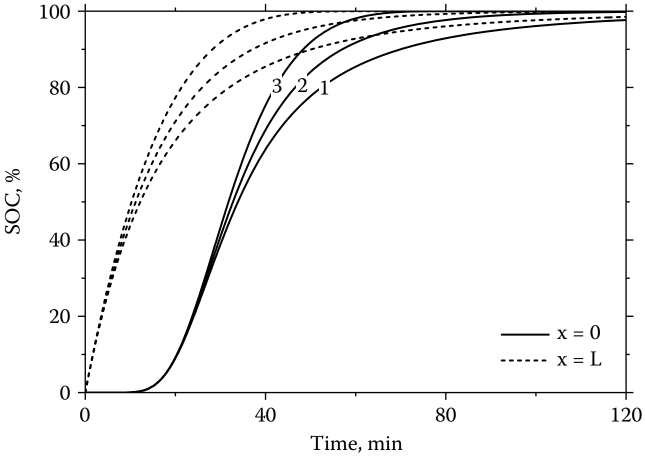

FIGURE 4.25 State of cure–time history on the surface (dotted line) and at the mid-plane (full line) with the order $n = 1.25$ (curve 1), 1 (curve 2), and 0.75 (curve 3). Rubber thickness (2L) = 2 cm. Enthalpy = 14.3 J/g. $T_m = 170°C$. Heating system on the rubber surface.

iv. The curves in Figure 4.25 show the strong effect of the value given to the order of the cure reaction on the state of cure obtained either at the rubber surface or at the mid-plane.

v. Either at the mid-plane (full line) or at the surface (dotted line), the SOC–time curves strongly diverge at a value of the SOC around 40%.

vi. The effect of the order of the overall reaction can be determined by the statement: the higher the order, the lower the value of the state of cure. This fact is of great importance to the process. For instance, the time necessary for the SOC to reach the value of 90% is increased by 20% when the order is varied from 1 to 1.25; on the other hand, this time is decreased by 20% when the order is varied from 1 to 0.75. Similar results were obtained by considering another rubber compound with different kinetic parameters [13].

4.5.2 EFFECT OF THE ACTIVATION ENERGY

Let us recall that the activation energy is determined by plotting the rate constant expressed in logarithm form, Lnk_T, versus the reciprocal temperature, $\frac{1}{T}$, this temperature being expressed in kelvin. An error can be made on the value obtained for the slope of this curve, which is equal to $\frac{E}{R}$; and thus another error is made for the value of the exponential factor k_0, which compensate for the previous error, so as to keep the same value of k_T.

The effect of the value of the activation energy on the process is evaluated by taking the value of $Lnk_T = -5.94$ obtained at 180°C and the couples of the associate values calculated from the relationship: $k_T = k_0 \cdot \exp\left[-\frac{E}{RT}\right]$:

$\frac{E}{R} = 19{,}000$ and $Lnk_0 = 36$; $\frac{E}{R} = 20{,}000$ and $Lnk_0 = 38.2$; $\frac{E}{R} = 18{,}000$ and $Lnk_0 = 33.79$.

Thus, the temperature–time history and the state of cure–time history are calculated either at the mid-plane or on the surface of a rubber sheet of thickness (2L) 2 cm, during the cure at 170°C, by taking the three couples of values shown above.

The effect of the activation energy on the cure of the rubber sheets can be appreciated in the following figures:

- Figure 4.26 with the temperature–time history at the rubber surface and at the mid-plane obtained with the three values of the activation energy.
- Figure 4.27 with the state of cure–time history at the rubber surface and at the mid-plane obtained with the three values of the activation energy.

The following conclusions can be drawn from these curves:

i. The temperature–time histories obtained either at the surface of the rubber or at the mid-plane are nearly similar, whatever the values given to the kinetic parameters Lnk_0 and $\frac{E}{R}$, as shown in Figure 4.26.

ii. The state of cure–time histories slightly vary with the values given to the couple of parameters Lnk_0 and $\frac{E}{R}$. Thus, the times necessary for the state of cure to reach 90% at the mid-plane of the rubber sheet with the two

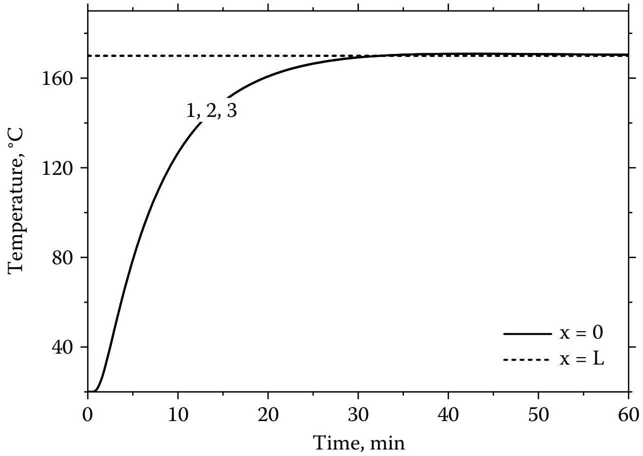

FIGURE 4.26 Temperature–time history on the surface (dotted line) and at the mid-plane (full line) with the order n = 1 and the following couples Ln(/s) = 36 with E/R = 19,000 (curve 2), 38.2 with 20,000 (curve 3), 33.79, and 18,000 (curve 1). Thickness (2L) = 2 cm. Enthalpy = 14.3 J/g T_m = 170°C. Heating system on the rubber surface.

extreme values of the couple of parameters (curves 3 and 2) vary only by 2% around the mean time obtained with the original values of the couple shown in curve 2.

iii. This slight difference in the times obtained in ii) results from the way of determining the parameters, by considering that the value of the rate

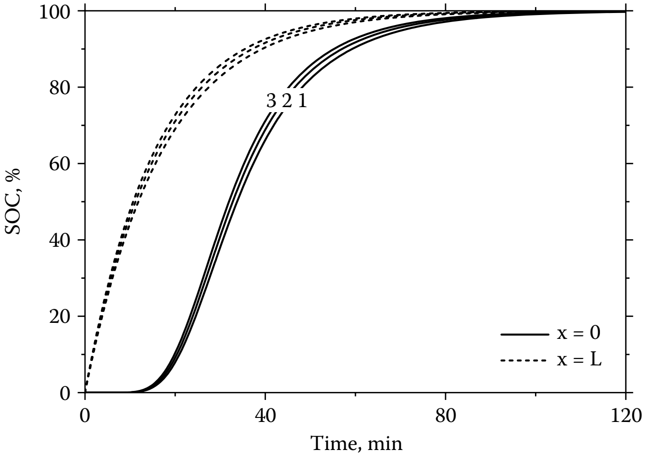

FIGURE 4.27 State of cure–time history on the surface (dotted line) and at the mid-plane (full line) with the order n = 1 and the following couples Ln(/s) = 36 and E/R = 19,000 (curve 2); 38.2 with 20,000 (curve 3); 33.79 and 18,000 (curve 1). Thickness (2L) = 2 cm. Enthalpy = 14.3 J/g T_m = 170°C. Heating system on the rubber surface.

constant LnK_T is correctly measured. In a previous study [14] where the values of LnK_T were different at the beginning of the calculation, the effect of a change in each of these two parameters Lnk_0 and $\frac{E}{R}$ on the state of cure–time histories was much stronger, leading to very different values of the time necessary to reach a given value.

4.6 EFFECT POSTCURE OF A RUBBER SHEET

Sometimes the possibility exists to increase the value of the state of cure of a rubber material without prolonging the time along which it is cured in the mold. This fact is worth considering because the cure operation in a mold is essentially costly, especially for the large pieces. A few years ago, it was said [16] that for final rubber products, the cost of the process associated with heating and time was found to be higher than the contribution of the raw materials. Thus, any shortening of the vulcanizing cycle without detriment to quality could provide an opportunity to increase productivity for a large capital investment. Several methods could be used to reduce the cure–time cycle:

- Using a higher temperature for the mold [17–19], with a limitation in this increase because of the possibility of burning.
- Choosing accelerators having ultra strong activity [20,21].
- Ensuring that the process of cure was properly carried out and stopped at the correct time [11,22].
- Developing injection molding systems [23]. This method is so important and so widely employed that it will be studied in Chapter 5.

Early works [24,25] concerned with the study of the profiles of temperature and state of cure developed through the rubber mass, after it was extracted from the mold and allowed to cool down in motionless air at room temperature, already showed that an increase in the state of cure could be expected during the cooling period. Moreover, an improvement in physical properties such as the swelling in toluene and mechanic properties measured either under static or dynamic conditions [16] has been found.

Some other studies were made with the objective to determine the increase in the state of cure associated with the conditions of the post cure as well as the value of the state of cure of the material when removed from the mold [24–26].

Thus, two parameters were especially considered, such as the value of the cure enthalpy [25] and the value of the temperature of the motionless air in which the post cure is achieved [26]. Thus the increase in the state of cure obtained at the mid-plane of the rubber sheet was found to vary linearly with the value of the cure enthalpy. Obviously the lowest value of the coefficient of surface heat transfer at the rubber surface during the period of postcure is desirable

The increase in the state of cure in vulcanizates after removal from the mold is evaluated when the rubber sheet thickness is rather large, this thickness being of 4 cm. The other characteristics are as follows: Temperature of the mold = 170°C

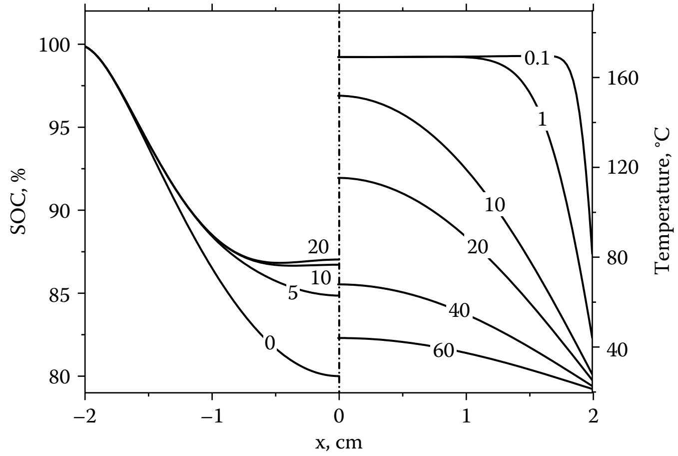

FIGURE 4.28 Cooling of a rubber sheet of thickness (2L) = 4 cm and postcure in stirred water at 20°C. Cure at 170°C in such a way that the SOC = 80% at the mid-plane. Heating system on the rubber surface. Surface thermal coefficient h = 276W/(m^2·deg). Profiles of SOC (left) and temperature (right) during the postcure.

during the cure with the heating system at the surface of the mold in contact with the rubber. The time of cure in the mold is defined so that the value of the state of cure at the mid-plane of the rubber sheet is equal to 80%. The conditions of the postcure are varied, by either the nature of the fluid in which the rubber is immersed after removal from the mold or the temperature of this fluid. Four cases are especially examined, by drawing the profiles of temperature (right) and the profiles of state of cure (left) developed through the thickness of the rubber sheets during the stage of cooling:

- By cooling the rubber sheet in stirred water at 20°C with a high coefficient of heat transfer at the rubber surface: $h = 276$ W/(m^2·deg) (Figure 4.28).
- By cooling the rubber sheet in motionless air kept at 20°C, with a low thermal coefficient at the rubber surface: $h = 2.2 \cdot \Delta T^{0.25}$ W/(m^2·deg) (Figure 4.29).
- By cooling the rubber sheet in motionless air kept at 100°C with the low thermal coefficient at the rubber surface: $h = 2.2 \cdot \Delta T^{0.25}$ W/(m^2·deg) (Figure 4.30).
- By cooling the rubber sheet in motionless air kept at 120°C with the low thermal coefficient at the rubber surface: $h = 2.2 \cdot \Delta T^{0.25}$ W/(m^2·deg) (Figure 4.31).

The calculations are made in two stages:

- The first is made when the rubber sheet is cured in the mold up to time t_{ex} by using the Equations 4.1–4.4.
- The second is made when the rubber sheet is removed from the mold, and let cool down in a fluid, by using Equations 4.1 or 4.1′ and 4.4′, with the

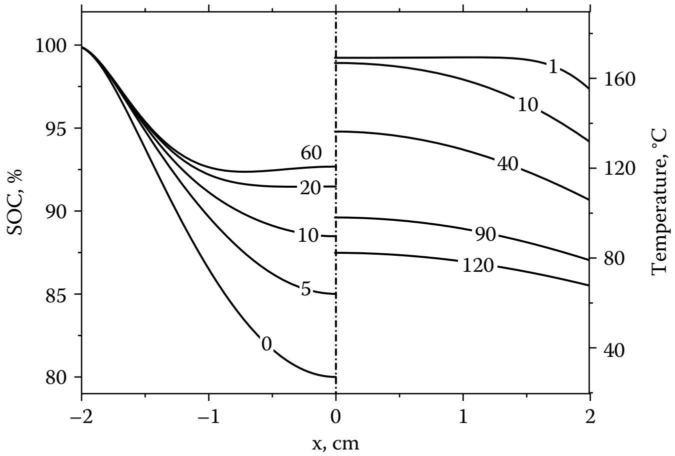

FIGURE 4.29 Cooling of a rubber sheet of thickness (2L) = 4 cm and postcure in motionless air at 20°C. Cure at 170°C in such a way that the SOC = 80% at the mid-plane. Heating system on the rubber surface. Surface thermal coefficient $h = 2.2 \cdot \Delta T^{0.25}$ $W/(\text{m}^2 \cdot \text{deg})$. Profiles of SOC (left) and temperature (right) during the postcure.

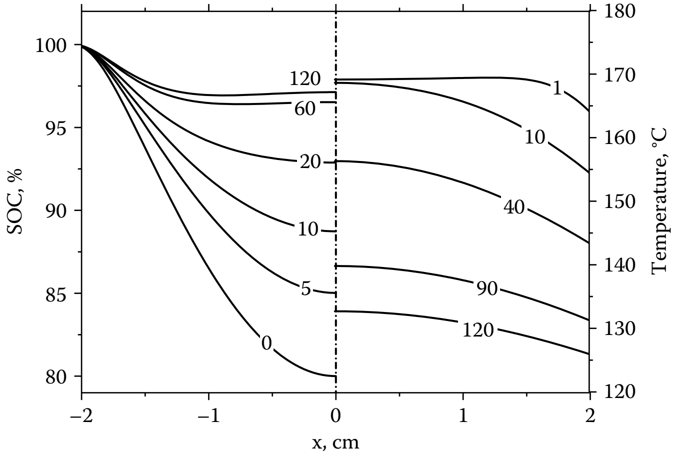

FIGURE 4.30 Cooling of a rubber sheet of thickness (2L) = 4 cm and postcure in motionless air at 100°C. Cure at 170°C in such a way that the SOC = 80% at the mid-plane. Heating system on the rubber surface. Surface thermal coefficient $h = 2.2 \cdot \Delta T^{0.25}$ $W/(\text{m}^2 \cdot \text{deg})$. Profiles of SOC (left) and temperature (right) during the postcure.

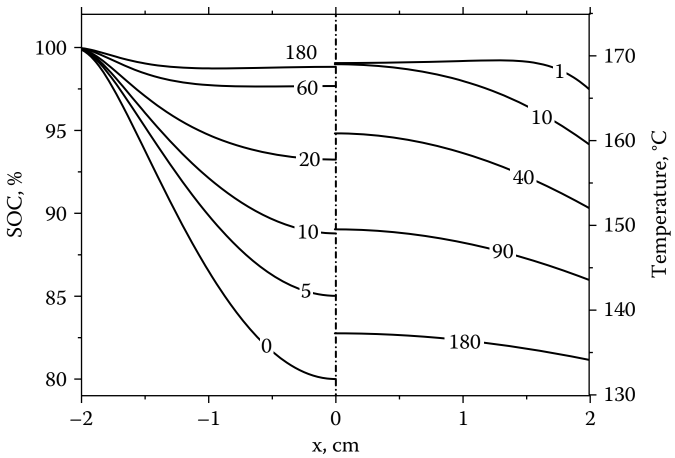

FIGURE 4.31 Cooling of a rubber sheet of thickness (2L) = 4 cm and post-cure in motionless air at 120°C. Cure at 170°C in such a way that the SOC = 80% at the mid-plane. Heating system on the rubber surface. Surface thermal coefficient $h = 2.2 \cdot \Delta T^{0.25}$ $W/(\mathrm{m}^2 \cdot \mathrm{deg})$. Profiles of SOC (left) and temperature (right) during the postcure.

boundary condition taking into account the heat convection effect on the surface defined by the value of h, written in Equation 4.7.

$$\mathrm{t} > 0 - \lambda \cdot \left[\frac{\partial T}{\partial x}\right]_s = h \cdot (T_s - T_{ext}) \tag{4.7}$$

$$\frac{dQ}{dt} = k_0 \cdot (Q_\infty - Q_{tex}) \cdot \exp\left[-\frac{E}{RT}\right] \tag{4.4'}$$

Let us remark that Equation 4.4′ is similar to Equation 4.4, except for the value of the extent of heat evolved from the cure reaction at time t_{ex}, which represents the time at which the rubber is removed from the mold and allowed to cool.

The profiles of temperature (right) and of state of cure (left) developed through the rubber sheet 4 cm thick in these four cases leads to the following interesting comments:

i. The profiles of temperature and of state of cure developed at different times are the best way to define the increase in the cure during the postcure. Thus, a complete view of the inside of the rubber mass is shown in these four figures, in good agreement with the temperature–time histories and state of cure–time histories previously drawn in the former papers [24–26].
ii. In the worst case of cooling as far as the postcure is expected, that is, in stirred cold water, the temperature, initially uniform at 170°C, drops rapidly at the rubber surface up to 1 minute. And 60 minutes are necessary

for the temperature through the rubber thickness to reach that of the water. [Figure 4.28].

iii. In the case of cooling in stirred water kept at 20°C, a slight increase in the value of the state of cure can be appreciated from 80 to 87% in around 20 minutes. After this time, the temperature in the rubber is too low for the cure reaction to take place. [Figure 4.28]. Let us note that a time of cooling of 10 minutes is enough for a significant postcure in this case.

iv. In the case of cooling in motionless air kept at 20°C, the effect of the lower coefficient of thermal transfer at the rubber surface appears [Figure 4.29]. The temperature at the rubber surface slowly declines, while the temperature at the mid-plane remains constant at 170°C during a period of 10 minutes. As a result of this low temperature decrease, the value of the state of cure increases notably through the rubber mass, and especially at the mid-plane, growing from 80 up to 93 during a period of time of 60 minutes.

v. When the rubber sheet is allowed to cool down in motionless air kept at 100°C [Figure 4.30], not only the rate of the decrease in temperature at the rubber surface is very low, but the temperature at the mid-plane remains rather high over a long period of time. As a result, the state of cure increases regularly with time up to around 97% at the mid-plane.

vi. When the rubber sheet is cooled down in motionless air kept at 120°C [Figure 4.31], the rate of the decrease in temperature throughout the rubber thickness is still lower. And obviously the consequence is a rather high increase in the state of cure, especially at the mid-plane, from 80 to nearly 98%.

vii. By considering Equation 4.4′, obviously the rate of increase in the cure reaction is a function of the amount of reactive agent remaining in the rubber at the time of removal from the mold. This is the reason why the increase in the state of cure is higher at the mid-plane of the rubber sheet where the initial value of the state of cure is lower.

viii. The main parameters of the postcure system are the nature of the fluid, its temperature, and the value of the coefficient of thermal transfer at the rubber–fluid interface.

ix. From an economical point of view, it should be said that it is not necessary to heat the atmosphere in which the rubber sheets are immersed. When the rubber pieces are placed in a closed room, the atmosphere is heated by these materials, and the problem that arises consists of evaluating the number of pieces to be cooled down at the same time.

4.7 CURE OF RUBBER–METAL SANDWICHES

Undesired vibrations and shocks may originate from a wide variety of sources, such as unbalance and reciprocal motions in mechanical machinery, aerodynamic turbulence, rough sea movements, earthquakes, road and rail transportations, and tough handling of equipment.

Rubber products are used in special applications for protecting housings and large buildings from the motion of earthquakes, for example. Whichever way the earth shifts—horizontal or vertical, the horizontal being worse—it is necessary to isolate a building from the ground by a special system made of rubber and metal in a sandwich configuration. The stability of the system against horizontal motion is increased by using systems where the thickness of the rubber is rather thin, its elasticity used to absorb shock and motion.

4.7.1 THEORETICAL STUDY OF THE PROCESS OF CURE

The rubber–metal system is made of sheets of rubber alternating with sheets of metal, as shown in Figure 4.32. Generally, the thickness of each layer of rubber is the same, as well as that of the metal. But the problem can be resolved whatever the thickness of the rubber–metal components.

The system with the extreme layers made of metal is heated in the same way as it is made in a mold so as to cure the rubber and increase the adherence between the rubber–metal interface. Thus, the equations are as follows:

In the rubber sheet:

$$\rho_r \cdot C_r \cdot \frac{\partial T}{\partial t} = \lambda_r \cdot \frac{\partial^2 T}{\partial x^2} + \rho_r \cdot \frac{\partial Q}{\partial t} \tag{4.1}$$

which becomes simplified when the thermal parameters are constant:

$$\frac{\partial T}{\partial t} = \alpha_r \cdot \frac{\partial^2 T}{\partial x^2} + \frac{1}{C_r}\frac{\partial Q}{\partial t} \tag{4.1'}$$

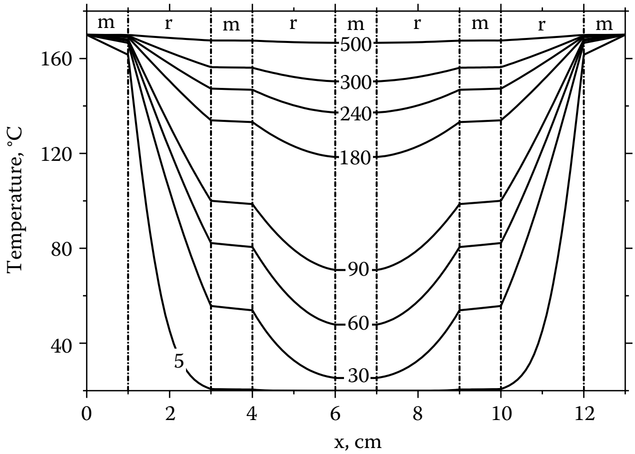

FIGURE 4.32 Cure of metal–rubber in sandwich form: metal of thickness 1 cm and rubber sheets of thickness 2 cm, made of 5 metal sheets and 4 rubber sheets. The external metal sheets are heated at 170°C. Temperature profiles developed through the thickness of the system. The parameters are shown in Table 4.1.

In the metal sheet:

$$\rho_m \cdot C_m \cdot \frac{\partial T}{\partial t} = \lambda_m \cdot \frac{\partial^2 T}{\partial x^2} \tag{4.2}$$

which becomes simplified when the thermal parameters are constant:

$$\frac{\partial T}{\partial t} = \alpha_m \cdot \frac{\partial^2 T}{\partial x^2} \tag{4.2$'$}$$

At the metal–rubber interface, because of the perfect contact, the assumption v is written as follows, the heat flux being the same on both sides of the interface.

$$\lambda_m \cdot \left[\frac{\partial T}{\partial x}\right]_m = \lambda_r \cdot \left[\frac{\partial T}{\partial x}\right]_r \tag{4.3}$$

whereas t represents time and T the temperature, λ is for the thermal conductivity, ρ the density, and C the specific heat at constant pressure, in each material.

The rubber–metal system is heated on both extreme metal surfaces, and when the heating system of the new mold is at the mold–metal interface, the temperature is kept constant on the extreme metal surfaces.

The internal heat generated by the cure reaction is described by the equation:

$$\frac{dQ}{dt} = k_0 \cdot (Q_\infty - Q_t) \cdot \exp\left[-\frac{E}{RT}\right] \tag{4.4}$$

where the order of the overall reaction is taken as 1, E is the energy of activation, and k_0 the rate constant, whereas Q_t and Q_∞ represent the heat of reaction evolved at time t and infinite time, respectively, Q_∞ being the enthalpy of the overall cure reaction.

In the same way as for the problem of the cure of rubber in a mold, there is no analytical solution, and this problem should be resolved by using a numerical method.

4.7.2 RESULTS

The results are expressed in terms of profiles of temperature and of state of cure, as they are developed through the thickness of the rubber–metal system made of five metal sheets and of four rubber sheets.

- The temperature of the system is kept at 170°C,
- The thicknesses are as follows: metal = 1 cm; rubber = 2 cm

The thermal parameters of the rubber and of the metal, as well as the kinetic parameters of the cure of rubber are shown in Table 4.1.

The profiles of temperature developed through the thickness of the rubber–metal system at various times are drawn in Figure 4.32, and the profiles of the state of cure developed at the same times appear in Figure 4.33.

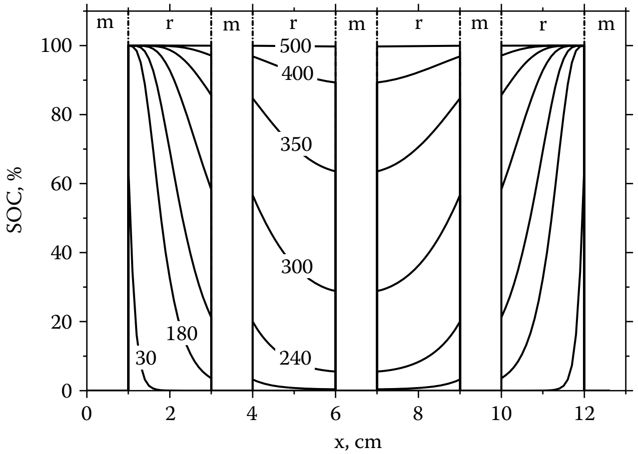

FIGURE 4.33 Cure of metal–rubber in sandwich form: metal of thickness 1 cm and rubber sheets of thickness 2 cm, made of 5 metal sheets and 4 rubber sheets. The external metal sheets are heated at 170°C. State of cure profiles developed through the thickness of the system. The parameters are shown in Table 4.1.

These profiles can lead to the following conclusions:

i. As heat is transferred from the extreme surfaces, the temperature starts increasing at these two surfaces, as well as the state of cure in the rubber sheets.
ii. The effect of the higher heat diffusivity through the metal appears with the change in the gradient of temperature either at the interface or within the thickness. The change in the temperature gradient at the metal–rubber interface is mathematically described by the Relation 4.3 expressing that the heat flux is the same on both sides of this interface. Thus, the gradient in each material is inversely proportional to the thermal conductivity.
iii. Because of the rather important thickness of the system, it takes a long time for heat to be transferred.
iv. Of course, in Figure 4.33 where the profiles of state of cure are drawn, there is a blank in the metal sheets. A discontinuity is observed in the profiles of state of cure in the successive sheets of rubber, resulting from the fact that there is also a discontinuity in the profiles of temperature in these rubber sheets due to the presence of the metal sheets.
v. Beyond the particular process of cure in this case, the important problem which should not be neglected is the bonding of the rubber to the metal. This problem of adhesion of rubbers to metals is very well covered in Reference [27] where a full description of the various tests is given.
vi. Another case of interest appears with the cure of a rubber when the cure is bound to various fabrics in order to get proofed materials such as hose.

In this case, the process of cure is similar as that described with a metal. The fabric–rubber system is heated under the conditions necessary for the rubber to be cured, and the theory of the process is also similar as that described in this subsection; all that is changed are the thermal properties of the fabric material.

4.8 SIMULTANEOUS CURE OF VARIOUS KINDS OF RUBBERS

The problem of curing various sorts of rubber compounds simultaneously sometimes arises, for instance, when bilayers with different properties on each side are desired. In one particular example shown in the literature, two thin EPDM rubber discs are cured together, the one containing 2% sulfur as a vulcanizing agent whereas the other has 10 or 20% sulfur [28,29].

4.8.1 THEORETICAL APPROACH OF THE PROCESS

The problem is somewhat similar to those considered either in Section 4.1 when the rubber is cured in a mold or in Section 4.7 when the rubber is cured in a rubber–metal sandwich. In fact, a kind of sandwich is obtained with two various rubber compounds.

The process consists of a heat transfer through the rubber compounds and the cure in each of these compounds. The problem is studied in the case of two sheets of rubber cured together under the same conditions.

When the thermal parameters are constant, there are these equations for heat transfer:

For the rubber in sheet 1 with the values of the thermal diffusivity α_1 and of the thermal capacity C_1

$$\frac{\partial T}{\partial t} = \alpha_1 \cdot \frac{\partial^2 T}{\partial x^2} + \frac{1}{C_1}\frac{\partial Q}{\partial t} \tag{4.8}$$

For the rubber in sheet 2, the same equation stands with the corresponding thermal parameters

$$\frac{\partial T}{\partial t} = \alpha_2 \cdot \frac{\partial^2 T}{\partial x^2} + \frac{1}{C_2}\frac{\partial Q}{\partial t} \tag{4.8'}$$

At the interface between the two rubbers, the equality of the heat flux on both sides leads to:

$$\lambda_1 \cdot \left[\frac{\partial T}{\partial x}\right]_1 = \lambda_2 \cdot \left[\frac{\partial T}{\partial x}\right]_2 \tag{4.9}$$

The cure reaction is described by the general equation:

$$\frac{dQ}{dt} = k_0 \cdot (Q_\infty - Q_t)^n \cdot \exp\left[-\frac{E}{RT}\right] \tag{4.4}$$

where the kinetic parameters of the cure should be taken for each rubber compound.

4.8.2 RESULTS FOR BILAYER RUBBER COMPOUNDS

A bilayer system is made of two rubber compounds with the same thickness, which are cured simultaneously under the same conditions: 170°C and the heating system of the mold placed at the mold surface in contact with the rubber.

Two rubber compounds are selected whose thermal and kinetic parameters are shown in Table 4.1. These rubber compounds differ only in the value of the percent sulfur and the corresponding value of the cure enthalpy.

The cure enthalpy is 14 J/g for the first rubber compound, called r1, and 56.7 J/g for the second rubber compound called r2.

The results are expressed in terms of profiles of temperature in Figure 4.34 when the thickness is 0.2 cm for each sheet, and in Figure 4.36 for a larger thickness of 2 cm for each sheet. The corresponding profiles of state of cure are drawn for these two rubber systems in Figure 4.35 for the thinner bilayer and in Figure 4.37 for the thicker one.

A few conclusions can be drawn from these profiles:

i. The profiles of temperature are similar in the two rubber sheets for two reasons: the thermal parameters are the same for the rubbers r1 and r2, and the internal heat evolved from the low cure enthalpy has a little effect.
ii. Of course, the effect of the thickness is shown by comparing the Figures 4.34 and 4.36.
iii. The bilayer rubber sheet is heated in a mold with the heating system acting at the mold–rubber interface, so that the temperature on the rubber surfaces is almost that of the mold.

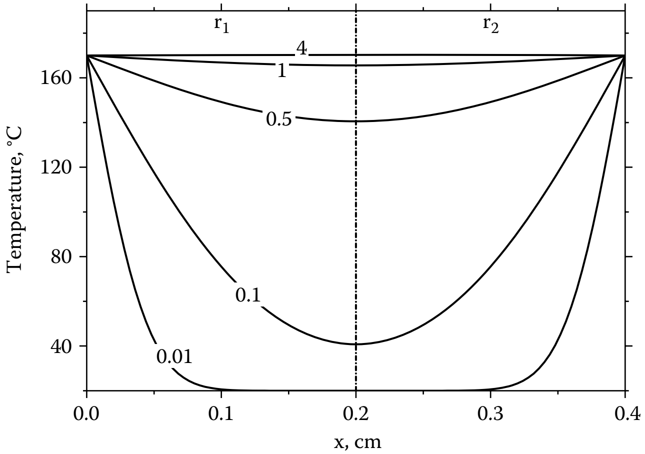

FIGURE 4.34 Cure of a system made of two rubber compounds: thickness (2L) of each rubber sheet: 0.2 cm with the enthalpy of 14 J/g (r1) and 56.7 J/g (r2). Profiles of temperature at various times T_m = 170°C. Heating system on the rubber surfaces.

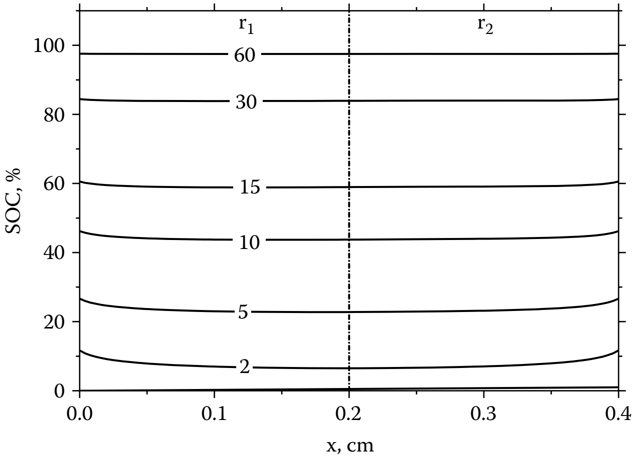

FIGURE 4.35 Cure of a system made of two rubber compounds: thickness (2L) of each rubber sheet: 0.2 cm with the enthalpy of 14 J/g (r1) and 56.7 J/g (r2). Profiles of state of cure at various times $T_m = 170°C$. Heating system on the rubber surfaces.

iv. The profiles of state of cure shown in Figure 4.35 for the thinner thickness of 0.2 cm are identical for each rubber of the bilayer. This fact results from the profiles of temperature which are identical and from the cure enthalpy of rubber which are rather low.

v. For the larger thickness of 2 cm for each rubber layer, a slight difference can be observed in the profiles of state of cure shown in Figure 4.37. Thus,

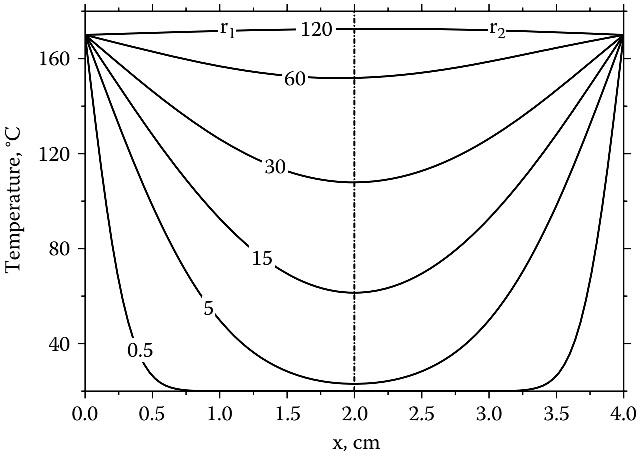

FIGURE 4.36 Cure of a system made of two rubber compounds: thickness (2L) of each rubber sheet: 2 cm, with the enthalpy of 14 J/g (r1) and 56.7 J/g (r2). Profiles of temperature at various times $T_m = 170°C$. Heating system on the rubber surfaces.

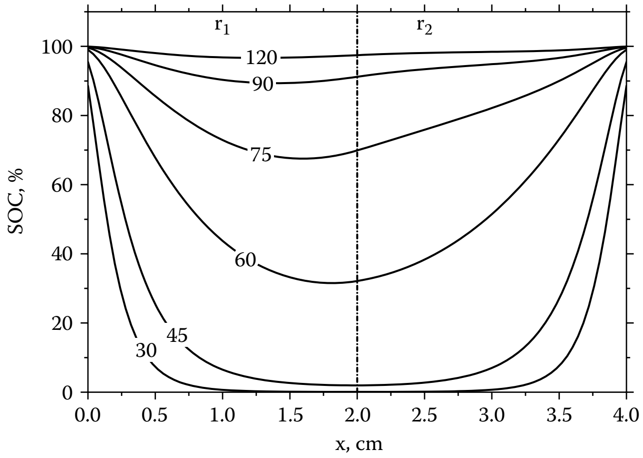

FIGURE 4.37 Cure of a system made of two rubber compounds: thickness (2L) of each rubber sheet: 2 cm, with the enthalpy of 14 J/g (rl) and 56.7 J/g (r2). Profiles of state of cure at various times T_m = 170°C. Heating system on the rubber surfaces.

the profiles are not symmetrical with regards to the mid-plane of the bilayer sheet, being higher in the layer r2 where the cure enthalpy is larger.

vi. Thus the effect of the thickness of the component of the bilayer on the profiles of state of cure can be observed in this Figure 4.37.

vii. These profiles of state of cure are calculated by considering that there is no transfer of the active agent through the bilayer system during the cure. It will be shown in Chapter 7 that a diffusion of the curing agent takes place during the cure, leading to interesting properties in terms of mechanics or liquid resistance.

4.9 GENERAL CONCLUSIONS

Various conclusions can be drawn from the results shown in this Chapter 4.

i. The process of cure is well established with the stages of heating by conduction through the mold and the rubber associated with the stage of the cure reaction.

ii. The cure reaction is expressed by the general kinetics, with an order, enthalpy of cure, energy of activation, and preexponential term. The effect of these parameters on the cure is evaluated, so as to support this assumption. Nevertheless, this method looks more efficient than the other one using the temperature reference.

iii. As the cure reaction is slightly exothermic, various profiles of temperature and of state of cure are expanded through the mass of the rubber.

iv. Hence, it could be found to some advantages in the postcure after removal of the rubber piece from the mold to place it in a closed room, so that the cooling period was reduced, enabling the cure to progress especially at the middle of the piece.
v. The position of the heating system in the mold is considered, as it may be of importance, especially for large pieces of rubber.
vi. The injection system is considered in Chapter 5, although the process of heating and cure in the mold is the same as that developed in this Chapter 4. The main difference comes from the fact that is desirable to heat the rubber mass before its injection in the mold at a temperature at which the viscosity is minimal so as to fill up the mold.
vii. The simultaneous cure of various rubber compounds is studied, by taking into account the heating conditions at their interface. In this case, a diffusion of the active agent occurs from the part with the higher concentration to the other part. This diffusion can be increased by maintaining for a while the temperature of the system at a value for which the diffusion takes place without noticeable cure. The mechanical properties of the final compound, especially at the junction of the components, are increased as shown precisely in Chapter 7.
viii. The metal–rubber sandwich is considered, as these components are generally used in various energy-absorbing systems, and, for instance, to reduce the effects of earthquakes. As a house is built over them, they are very effective in protecting the structure from the effects of the vertical motions of an earthquake.

REFERENCES

1. Hands D. and F. Horsfall. 1980. A new Method for simulating industrial cure processes. *Kautschuk gummi Kunststoffe* 33: 440–46.
2. Ambelang J.C., K.C. Beach, and D.F. Sullivan. 1962. Temperature coefficient of vulcanization for present-day tire compounds. *Rubber Chem. Technol.* 35: 92–104.
3. Kong D., J.L. White, F.C. Weissert, and N. Nakajima. 1987. An experimental and theoretical study of heat conduction and vulcanization of rubber compounds in molds. *Rubber Chem. Technol.* 60: 140–58.
4. Claxton W.E. and J.W. Liska. 1973.Calculation of state of cure in rubber under variable time-temperature conditions. *Rubber Age*. 95: 267–43.
5. Frank A., K. Hafner, and W.F. Kern.1962. The activation energy of vulcanization. *Rubber Chem. Technol.* 35: 76–91.
6. Barker L.R. 1973. Effect of temperature on vulcanization time. *J. Institution Rubber Industry*. 7: 121–23.
7. Prentice G.A. and M.C. Williams.1980. Numerical evaluation of the state of cure in a vulcanizing article. *Rubber Chem. Technol.* 53: 1023–31.
8. Conant F.S., J.F. Svelik, and A.E. Juve. 1958. Equivalent cures in specimens of various shapes. *Rubber Chem. Technol.* 31: 562–568.
9. Claxton W.E. and H.C. Holden. 1973. An analog heat-flow and cure controller simulator for rubber. *Rubber Chem. Technol.* 46: 1103–1113.

10. Accetta A., P. Le Parlouer, and J.M. Vergnaud. 1982. Kinetic parameters of the overall reaction of scrap rubber vulcanization by 2% sulfur. *Thermochim. Acta*. 59: 149–56.
11. Accetta A. and J.M. Vergnaud. 1983. Calculation of the temperature and extent of reaction during the vulcanization of powdered rubber. *Rubber Chem. Technol.* 56: 689–02.
12. Accetta A. and J.M. Vergnaud. 1982. Rubber recycling. Upgrading of scrap rubber powder by vulcanization. II. *Rubber Chem. Technol.* 55: 961–66.
13. Rochette B., A. Sadr, M. Abdul, and J.M. Vergnaud. 1984. Effect of a variation of the order of the overall reaction of cure on the profiles of temperature and state of cure developed at the midplane of rubber sheets. *Thermochim. Acta*. 79: 187–95.
14. Ferradou C. and J.M. Vergnaud. 1983. Effect of variation in the kinetic parameters on the vulcanization of rubber sheets. *Thermochim. Acta*. 68: 283–90.
15. Abdul M., B. Rochette, A. Sadr, and J.M. Vergnaud. 1984. Effect of variation in the values of the thermal properties of rubber on the vulcanization of thin and thick sheets. *Thermochim. Acta*. 80: 287–96.
16. Khouider A.. and J.M. Vergnaud. 1988. Increase in the state of cure in vulcanizates after removal from the mould. *J. Polym. Eng*. 8: 19–39.
17. Mukhopadhyay R. and S.K. De. 1978. Effect of elevated temperature on the unaccelerated and accelerated sulphur vulcanization of natural rubber. *Rubber Chem. Technol.* 51: 704–17.
18. Bhowmick A.K., R. Mukhopadhyay, and S.K. De. 1979. High temperature vulcanization of elastomers. *Rubber Chem. Technol.* 52: 725–34.
19. Sadr A., M. Hivert, and J.M. Vergnaud. 1983. Effect of mould temperature and cure enthalpy on the state of cure at the midplane of rubber sheets. *Thermochim. Acta*. 71: 237–45.
20. Lautenschlaeger F.K. and P. Zeeman. 1979. Model compound vulcanization. Part II. Comparison of accelerators. *Rubber Chem. Technol.* 52: 1030–43.
21. Bhatnagar S.K. and S. Banerjee. 1968. Kinetics of accelerated vulcanizates. Sulphur vulcanization with 2-mercatobenthiazole and its Zn salts in presence of ZnO and stearic acid. *Angewandte Makromol. Chemie*. 3: 177–21.
22. Ferradou C., B. Rochette, and J.M. Vergnaud.1985. Effect of a variation in kinetic parameters (rate constant, energy of activation) on the vulcanization of rubber sheets in injection moulding process. *J. Appl. Polym. Sci*. 30: 2663–74.
23. Sadr A., R. Granger, and J.M. Vergnaud. 1985. ACS Symposium Series No. 270, *Reaction Injection Molding: Polymer Chemistry and Engineering*, Ed. E. Lresta. 18: 279–291.
24. Abdul M. and J.M. Vergnaud. 1984. Vulcanization progress in rubber sheets during cooling in motionless air after extraction from the mould. *Thermochim. Acta*. 76: 161–70.
25. Khouider A., J. Bouzon, and J.M. Vergnaud. 1986. Effect of cure enthalpy on cure progress during the cooling period in motionless air. *Thermochim. Acta*. 102: 83–92.
26. Khouider A. and J.M. Vergnaud. 1986. Effect of temperature of motionless air on the increase in state of cure of vulcanizates after their extraction from the mould. *J. Appl. Polym. Sci.*. 32: 5301–13.
27. Brown R.P. 1979. *Physical Testing of Rubbers*. Applied Science Publishers, London. Chapter 18.
28. Azaar K., I.D. Rosca, and J.M. Vergnaud. 2002. Anisotropic swelling of thin EPDM rubber discs by absorption of toluene. *Polymer*. 43: 4261–67.
29. Azaar K., R. Granger, I.D. Rosca, and J.M. Vergnaud. 2000. Effect of the state of cure on the hardness and resistance to liquids of EPDM rubbers. *Polym. Polym. Composites*. 8: 325–31.

NOMENCLATURE

α, α_r, α_m	thermal diffusivity, of the rubber, of the mold
C, C_r, C_m	heat capacity, of the rubber, of the mold
ΔH	enthalpy of the cure reaction
h	surface heat convection
E	energy of activation of the cure reaction
k_T, k_0	rate constant at temperature T, rate constant of the reaction, respectively
L	thickness of half of the sheet
λ_r, λ_m	thermal conductivity of the rubber, of the mold, respectively
Q, Q_t, Q_∞	heat, heat transferred at time t, after infinite time
n	order of the cure reaction
R	perfect gas constant
ρ, ρ_r, ρ_m	density, of the rubber, of the mold
SOC	state of cure
$T, \frac{\partial T}{\partial t}, \frac{\partial T}{\partial x}$	temperature, increase in temperature with time, gradient of temperature
T, T_0, $T_{x,t}$	temperature, temperature at time 0, at position x and time t
T_{rs}, T_{air}	temperature on the rubber surface, in air, respectively
T_{in}, T_∞	temperature, initially, after infinite time, respectively
t	time
x	abscissa characterizing the position

DIMENSIONLESS NUMBERS

$\frac{a \cdot t}{L^2}$	dimensionless time, in Equations 4.5 and 4.6

5 Cure of Rubber with Injection Molding

5.1 PRINCIPLES OF THE TECHNIQUE

As shown in Chapter 4, the cure operation takes place in the mold where the rubber compound is heated to a temperature at which the reaction starts with a significant rate. But a drawback arises when the rubber, initially at room temperature, is placed in the slabs of the mold previously heated at the desired temperature, because it takes some time for the rubber to be heated to the mold temperature. Moreover, the mold may be so complex in size that it is not possible to introduce the rubber compound in a solid state. For these two reasons, the technique of injection molding is applied.

The process of injection molding consists of three stages [1–4]:

i. The rubber compound is heated in a reservoir and strongly stirred.
ii. The heated compound with a low viscosity is injected into the mold under the appropriate pressure, sufficient to fill the various parts of the mold.
iii. The rubber compound is cured in the heated mold.

As the viscosity of the rubber compound increases with the stage of cure, it is important to know exactly the temperature at which the cure takes place, as heat increases viscosity, so as to inject into the mold the rubber with an appropriately low viscosity.

Thus, the main challenge is to select the right temperature at which the rubber compound should be injected, keeping in mind these two points: too low a temperature will necessitate a longer cure time in the mold, and too high a temperature brings the risk of blocking the injection system with the rubber partially cured.

Finally, three aspects of the process are considered in succession:

i. Evaluation of the time necessary for the rubber compound to be heated to the convenient temperature for injection, that is, the scorch time, or onset time of vulcanization. This scorch time can occur at various temperatures. Alpha Technologies' rubber process analyzer (RPA) is the most appropriate apparatus for determining the temperature–time value convenient for this purpose because of its programmed temperature feature.
ii. Conditions for injection of the rubber in the mold (i.e., the pressure and temperature, depending on the plasticity of the rubber).
iii. Calculation of the optimal conditions of cure of the rubber compound in the mold, with the time of cure associated with the mold temperature.

5.2 EVALUATION OF THE OPERATIONAL CONDITIONS IN THE INJECTION SYSTEM

5.2.1 THEORY

The theory of the process of heating has already been considered in Chapter 4, but it is more deeply developed in this chapter devoted to injection molding.

The process of cure results from the heating stage in the reservoir followed by the stage of cure in the mold; parts of these two stages are simultaneous.

Two parameters are of interest and are connected with each other, the temperature of the rubber in the reservoir, which will be the injection temperature T_i, and the time t_i over which the rubber is maintained in the reservoir before injection.

5.2.1.1 Heating Stage in the Reservoir before Injection

The equations describing the heating process alone could be used, but it is preferable to use the equation of heating with the simultaneous cure reaction, so as to be capable of determining exactly the right temperature at which the rubber could be injected into the mold.

$$\frac{\partial T}{\partial t} = \alpha \cdot \frac{\partial^2 T}{\partial x^2} + \frac{1}{C} \cdot \frac{\partial Q}{\partial t} \tag{5.1}$$

The rate of the internal heat generated by the cure reaction is given by:

$$\frac{dQ}{dt} = k_0 \cdot (Q_\infty - Q_t) \cdot \exp\left[-\frac{E}{RT}\right] \tag{5.2}$$

The value of the state of cure of interest is expressed by the partial heat evolved at time t_i as a fraction of the total heat evolved when the heating stage in the reservoir is achieved:

$$\text{SOC} = \frac{Q_t}{Q_\infty} 100 \tag{5.3}$$

As the temperature of the rubber in the reservoir increases from room temperature to the desired temperature, it is assumed that the increase in temperature is linear with time. Moreover, because of the strong rate of stirring of the rubber in the storage bulb, the temperature is uniform throughout the rubber mass.

Thus, by calling the rate of increase in temperature b such as:

$$b = \frac{dT}{dt} \tag{5.4}$$

the Equation 5.2 is rewritten as follows:

$$\frac{dQ}{dT} = \frac{k_0}{b} \cdot (Q_\infty - Q_t) \cdot \exp\left[-\frac{E}{RT}\right] \tag{5.5}$$

5.2.1.2 Injection Stage of the Rubber in the Mold

Calculations are possible only for evaluating the time necessary t_i to heat the rubber compound at the desired temperature of injection T_i. Of course, it will be necessary to determine experimentally the viscosity of the rubber at this temperature T_i because this material should be injected into the cavity of the mold. This value can be obtained from the experiment made with the RPA.

5.2.2 RESULTS FOR THE HEATING STAGE IN THE RESERVOIR

The rate of increase in temperature of the rubber in the reservoir could be very high, so that the final temperature of the reservoir T_i is rapidly reached, and the main parameter of interest is the time over which the rubber remains in the reservoir at the selected value of the temperature T_i.

The result is expressed in terms of the state of cure–time history obtained at various values of the temperature of the reservoir T_i. The curves drawn in Figure 5.1 show the increase in the state of cure of the rubber with time, as they are calculated under isothermal condition by using the kinetic parameters of the cure reaction collected in Table 5.1.

Some comments of interest are worth noting from Figure 5.1:

i. The values chosen for the temperature T_i of the reservoir range from 80 to 140°C, and a rather long value of the time over which the rubber could be maintained at these temperatures is considered 20 hours. Thus, these curves allow the users to determine the time t_i selected at each temperature T_i for the rubber sample whose kinetic parameters are defined in Table 5.1.

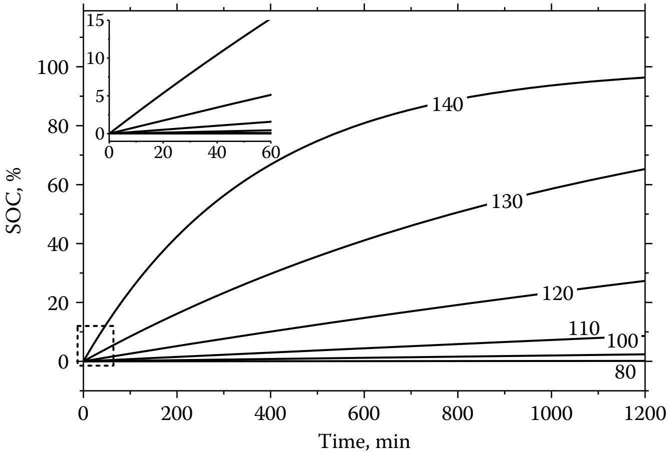

FIGURE 5.1 Uniform value of the state of cure of the rubber compound as a function of time during the heating and storing stage in the reservoir, for the injection temperatures: 80, 100, 110, 120, 130, 140°C.

TABLE 5.1
Thermal and Kinetic Parameters Used for Calculation

$\lambda_r = 0.2$ W/(m.deg)	$C_r = 2.2$ J/g·deg	$\rho_r = 0.9$ g/cm^3	$\alpha_r = 10^{-7}$ m^2/s
$\lambda_m = 3.8$ W/(m.deg)	$C_m = 0.12$ J/g·deg	$\rho_m = 7.9$ g/cm^3	$\alpha_r = 4 \cdot 10^{-6}$ m^2/s
% peroxide 2	9	19	$Lnk_0 = 36$
ΔHJ/g 14.3	44.7	56.7	E/R = 19,000

ii. Two scales are used, the larger one up to 1200 min for time, and a smaller one up to 60 min which is especially of value for the higher temperatures.

iii. Of course, the dilemma appears for the user with the obvious statement: the higher the temperature of the reservoir, the lower the residence time of the rubber.

iv. As shown in the figure with the smaller scale, a temperature up to 130°C could be used in the reservoir when the residence time of the rubber is lower than 20 min, when the maximal value of the state of cure of the sample could be lower than 2%.

v. The Equation 5.1 is related to one-dimensional heat conduction through a sheet, but obviously any other equation can be used for the heating stage of the rubber sample in the reservoir.

5.3 HEATING STAGE AND CURE IN THE MOLD

5.3.1 Theoretical for the Stage of Cure in the Mold

The Equations 5.5 (or 5.2) to 5.7 describe the process and allow the calculation of the final value of the state of cure obtained in the mold when the sample is spherical in shape. Calculation is made by using the above three equations, when the process of heating and cure starts from the temperature of injection T_i to the mold temperature T_m for the rubber sample. The total time necessary for the process of molding injection is thus the time t_i in addition to the time necessary for the rubber to be cured in the mold, called t_m. However, it should be said already that the stage of heating in the reservoir for the nth material is done simultaneously during the stage in the mold of the (n–1)th rubber previously injected

The equation for heat transfer through the rubber mass in the mold depends on the shape of this rubber. The case of a rubber sample spherical in shape is considered.

The rubber sphere initially at temperature T_i in the mold is in contact with the mold at temperature T_m, so that heat transfer is radial through the rubber mass:

$$\frac{\partial T}{\partial t} = \alpha \cdot \left[\frac{\partial^2 T}{\partial r^2} + \frac{2}{r} \cdot \frac{\partial T}{\partial r} \right] + \frac{1}{C} \cdot \frac{\partial Q}{\partial t} \tag{5.6}$$

The boundary condition at the rubber–mold interface is written by considering that the heat flux at the rubber–mold interface is equal on the two spherical surfaces:

$$\lambda_r \cdot \left[\frac{\partial T}{\partial r}\right]_r = \lambda_m \cdot \left[\frac{\partial T}{\partial r}\right]_m \tag{5.7}$$

$$\frac{dQ}{dt} = k_0 \cdot (Q_\infty - Q_t) \cdot \exp\left[-\frac{E}{RT}\right] \tag{5.2}$$

No analytical solution exists for this problem, and it is resolved numerically.

5.3.2 RESULTS OBTAINED BY CALCULATION

The results are expressed in terms of temperature–time history obtained for the rubber at the center of the spherical sample when it is located in the mold, and in terms of state of cure–time history, either in the reservoir before injection or at the center of the sphere in the mold. Complementary results are provided with the profiles of temperature developed through the radius of the sphere and with the associated profiles of state of cure, at various times, during the cure stage in the mold.

For calculation, the thermal and kinetic parameters of the rubber are collected in Table 5.1 with 14.3 J/g for the enthalpy of cure. The heating system of the mold is placed on the surface of the mold in contact with the rubber.

The following figures are drawn:

- Figure 5.2, showing the increase in temperature at the center of the spherical rubber sample in the mold for various values of the injection temperature T_i and for three temperatures of the mold T_m ranging from 160 to 180°C, when the radius is 1 cm.
- Figure 5.3, showing the state of cure–time history at the rubber surface of the spherical sample in contact with the mold for two values of the injection temperature T_i (80 and 120°C) for various temperatures of the mold T_m ranging from 160 to 180°C, when the radius is 1 cm.
- Figure 5.4, showing the state of cure–time history at the center of the spherical rubber sample for various values of the temperature of the mold T_m (160, 170, 180°C) and of the injection system T_i (80, 120°C), when the radius is 1 cm.
- Figure 5.5, where the profiles of temperature developed through the radius (1 cm) of the rubber sample are drawn at various times for two temperatures of injection T_i (80, 120°C) for the temperature of the mold T_m of 170°C.
- Figure 5.6, showing the profiles of state of cure developed through the radius (1 cm) of the rubber sample at various times, when the temperature of the mold T_m is 170°C for two values of the injection temperature T_i (80, 120°C).
- Figure 5.7, where the profiles of temperature developed through the radius (2 cm) of the rubber sample are drawn at various times for two temperatures of injection T_i (80; 120°C) when the temperature of the mold T_m is 170°C.

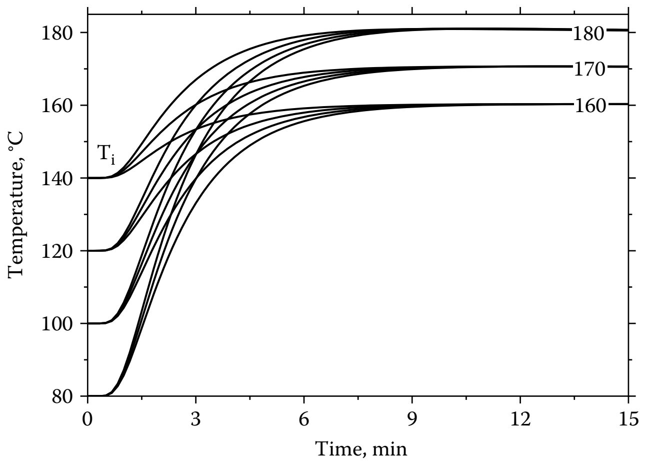

FIGURE 5.2 Temperature–time history at the center of the spherical rubber, when the heating system is on the mold surface in contact with the rubber for various values of the mold temperature (160, 170, 180°C) and of (80, 100, 120, 140°C). Radius = 1 cm.

- Figure 5.8, showing the profiles of state of cure developed through the radius (2 cm) of the rubber sample at various times, when the temperature of the mold T_m is 170°C for two values of the injection temperature T_i (80, 120°C).
- Figure 5.9, where the state of cure–time histories are drawn at the center of the spherical rubber sample when the mold temperature T_m is 170°C for various values of the injection temperature T_i (20, 80, 100, 120°C). The radius of the sphere is 2 cm.

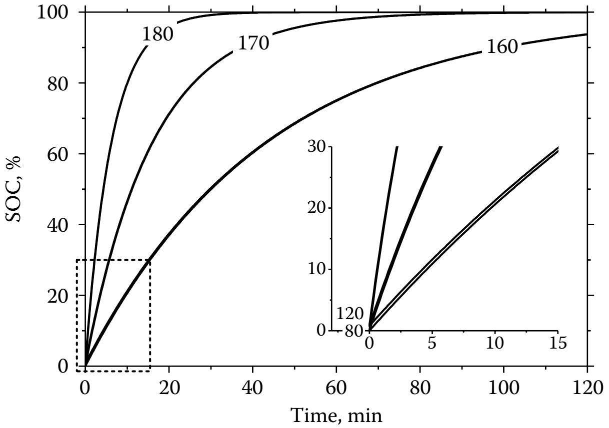

FIGURE 5.3 State of cure–time history at the rubber surface in contact with the mold, with the heating system on the mold surface in contact with the rubber, for various values of the mold temperature: 160, 170, 180°C. Radius = 1 cm for = 80, 120°C.

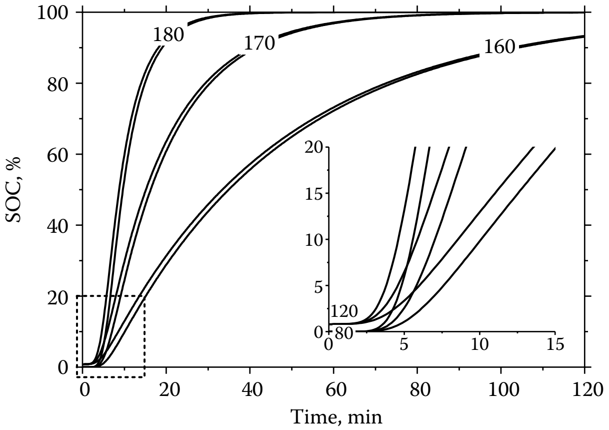

FIGURE 5.4 State of cure–time history at the center of the spherical rubber, when the heating system is on the mold surface in contact with the rubber, for various values of the mold temperature = 160, 170, 180°C. Radius = 1 cm = 80, 120°C.

- Figure 5.10, showing the profiles of temperature developed through the radius (4 cm) of the rubber sample at various times, when the temperature of the mold T_m is 170°C for two values of the injection temperature T_i (80, 120°C).
- Figure 5.11, showing the profiles of state of cure developed through the radius (4 cm) of the rubber sample at various times, when the temperature of the mold T_m is 170°C for two values of the injection temperature T_i (80, 120°C).
- Figure 5.12 where are drawn the state of cure–time histories calculated at the center of the spherical rubber sample of radius 4 cm, when the temperature of the mold T_m is 170°C for various values of the injection temperature T_i (20, 80, 100, 120°C).

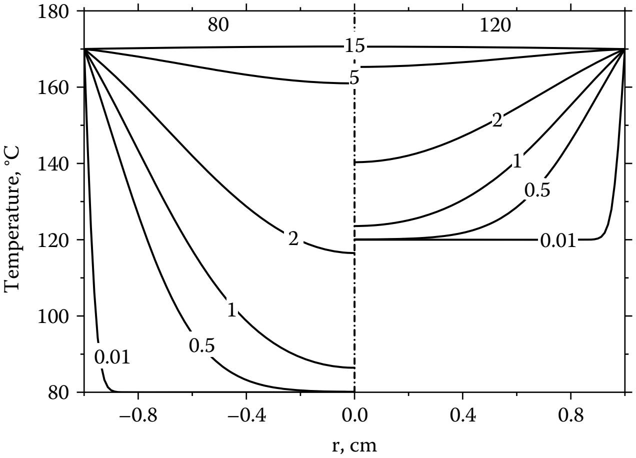

FIGURE 5.5 Profiles of temperature in the mold at different times for two values of the temperature = 80, 120°C, when T_m = 170°C; the radius = 1 cm. The center is at position 0.

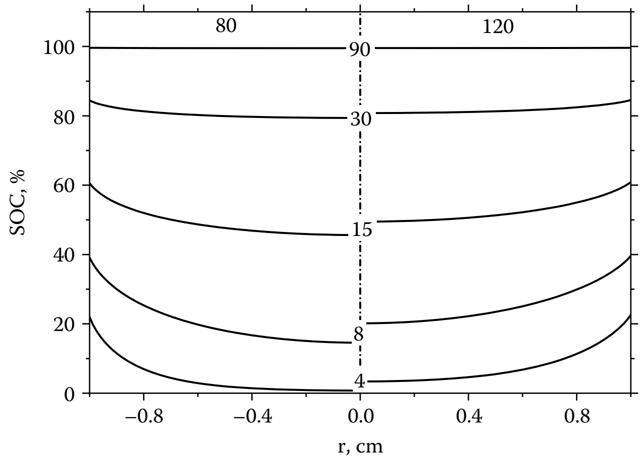

FIGURE 5.6 Profiles of state of cure of the rubber in the mold at different times for two values of the temperature = 80, 120°C, when T_m = 170°C; radius = 1 cm. Center at 0.

The following conclusions can be drawn from these figures:

i. In Figure 5.2, the effect of either the mold temperature T_m in the 160–180°C range or the temperature of injection in the 80–140°C range on the temperature–time histories at the center of the spherical rubber sample clearly appears, when the radius of the sample is 1 cm.
ii. In Figure 5.3, the effect of either the mold temperature T_m in the 160–180°C range or the temperature of injection in the 80–120°C range on the

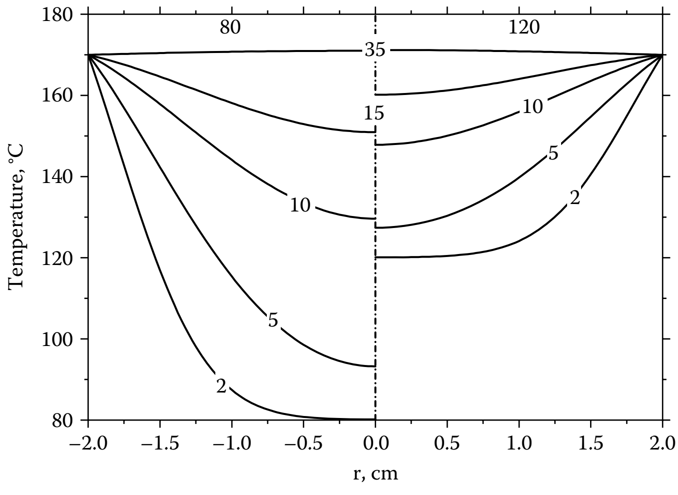

FIGURE 5.7 Profiles of temperature in the mold at different times for two values of the temperature = 80, 120°C, when T_m = 170°C; radius = 2 cm. The center is at position 0.

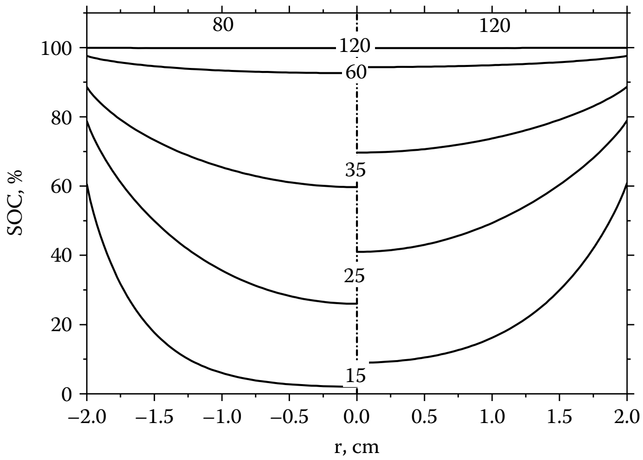

FIGURE 5.8 Profiles of state of cure of the rubber in the mold at different times for two values of the temperature = 80, 120°C, when T_m = 170°C; radius = 2 cm. Center at 0.

state of cure–time histories on the rubber surface in contact with the mold appears, when the radius of the sample is 1 cm. The rate of increase in the state of cure is very high at the beginning of the process. Let us remark that these curves are the same whatever the value of the radius of the rubber sample.

iii. In Figure 5.4, the effect of either the mold temperature T_m in the 160–180°C range or the temperature of injection in the 80–120°C range on the

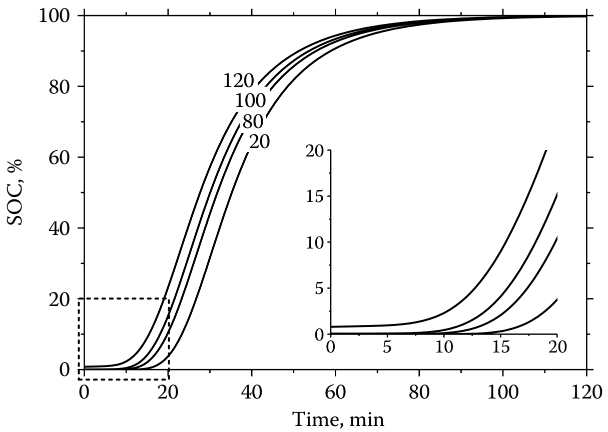

FIGURE 5.9 State of cure–time history at the center of the spherical rubber, for various values of the injection temperature = 20, 80, 100, 120°C when the heating system is on the mold surface in contact with the rubber. T_m = 170°C; radius = 2 cm.

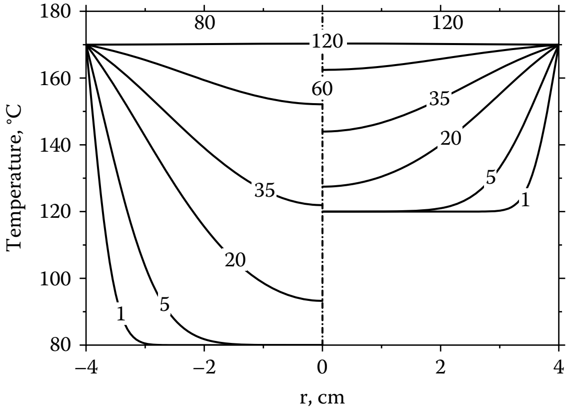

FIGURE 5.10 Profiles of temperature in the mold at different times for two values of the temperature = 80, 120°C, when T_m = 170°C; radius = 4 cm. The center is at position 0.

state of cure–time histories in the center of the rubber appears, when the radius of the sample is 1 cm. Of course, a delay in the increase of the state of cure is observed with regard to the corresponding one obtained on the surface, at the beginning of the process. It takes some time for heat to be conducted through the radius.

iv. The profiles of temperature developed through the radius of the sample (1 cm) at various times drawn in Figure 5.5 complement the results shown in Figure 5.2.

v. In the same way as for the profiles of temperature, the profiles of state of cure developed through the radius of the sample (1 cm) drawn in Figure 5.6 give complementary information to the results shown in Figures 5.3 and 5.5.

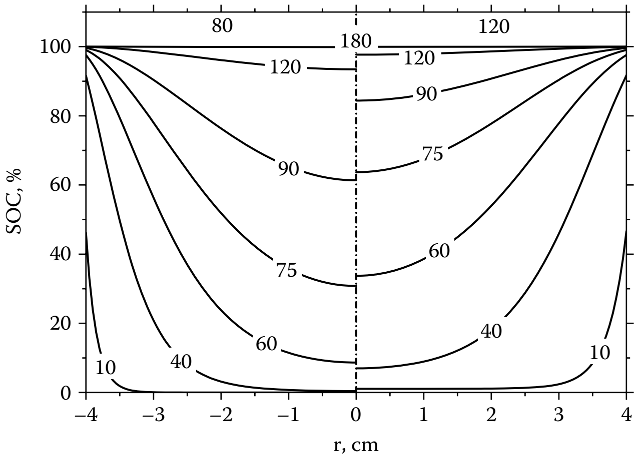

FIGURE 5.11 Profiles of state of cure of the rubber in the mold at different times for 2 values of the temperature = 80, 120°C, when T_m = 170°C; Radius = 4 cm. Center at 0.

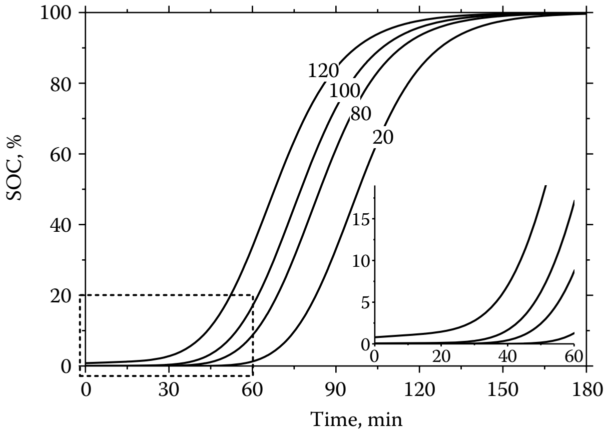

FIGURE 5.12 State of cure–time history at the center of the spherical rubber, for various values of the injection temperature = 20; 80; 100, 120°C when the heating system is on the mold surface in contact with the rubber. T_m = 170°C. Radius = 4 cm.

vi. The effect of the value of the radius can be appreciated by comparing the profiles of temperature developed through the radius, either in Figure 5.7 (2 cm) or in Figure 5.5 (1 cm). Of course, a longer time is necessary for the temperature at the center of each sphere to reach that of the mold (170°C), whatever the injection temperature (80 or 120°C).

vii. Following the result obtained for the temperature profiles shown in Figure 5.7 (2 cm) and in Figure 5.5 (1 cm), comparison between the profiles of state of cure developed through the radius at various times drawn either in Figure 5.8 (2 cm) or in Figure 5.6 shows the effect of the value of the radius of the spherical rubber sample. The time necessary for the state of cure to reach around 100% is nearly two times longer when the radius goes from 1 to 2 cm.

viii. The effect of the injection temperature T_i on the state of cure–time history at the center of the spherical rubber sample is also shown when the mold temperature is 170°C and the radius is 2 cm in Figure 5.9. Of course, the cure reaction starts at a lower time with a higher rate when the injection temperature is greater.

ix. The effect of a larger size for the rubber sample (radius of 4 cm) can be appreciated in Figure 5.10 with the profiles of temperature developed through the radius of the sample and in Figure 5.11 with the corresponding profiles of state of cure.

x. Finally, the effect of the injection temperature T_i on the state of cure–time history at the center of the large spherical sample (4 cm) clearly appears in Figure 5.12 when the mold temperature is 170°C and T_i is varied within the 20–120°C range.

xi. More precisely, the time necessary for the state of cure of the rubber to reach 90% at the center, is shown in Table 5.2 for various values of the radius of the spherical rubber sample and various values of the injection temperature T_i.

TABLE 5.2
Time Necessary for the SOC to Reach 90% at the Center (min) $T_m = 170°C$

Radius of the Sphere (cm) T_i°C	1	2	4
20	42.3	58.8	127.2
80	41.5	55.3	113.3
100	41	53.7	106.5
120	40.3	51.3	97.2

In all cases the cure of the rubber has the characteristics described in Table 5.1 with 14.3 J/g, with the mold temperature T_m of 170°C.

Thus, the time of cure in the mold is significantly reduced by using a higher injection temperature T_i. For instance, the reduction in time resulting from using the injection system with the temperature T_i of 120°C with regard to the molding system (when the initial temperature of the rubber in the mold is 20°C) depends on the value of the radius of the sample: if it is only 5% when the radius is 1 cm, it comes to 15% for a radius of 2 cm, and attains 30% for the larger radius of 4 cm.

5.4 CONCLUSIONS ON INJECTION MOLDING

The injection system offers various advantages over the usual molding system:

- Of course, injecting the rubber sample to a temperature higher than the room temperature used with the molding system enables a reduction in time, because there is to be considered not only the time necessary for the rubber to be heated from room temperature to the injection temperature, but also the temperature T_i must be uniform through the rubber mass with the injection system. This last fact also explains that the reduction in time highly increases with the radius (or the thickness) of the rubber sample.
- Another advantage of the injection system comes from the fact that the rubber can be injected into a mold with a complex shape, provided that the viscosity is low enough not to necessitate too high a pressure.
- Ultimately, whatever the size of the final samples or their shape, the injection system can be controlled when the kinetic parameters of the cure reaction are known, in the same way as for the cure of a rubber sample in the usual mold [1–4].
- Various applications of the injection molding system have been developed outside the scope of the cure of rubbers, and a few examples are given, with the substitution of thermoset rubbers by thermoplastic elastomers: a range of thermoplastic elastomer compounds were introduced and processed using reaction compounding technology. They are called reaction modified thermoplastic elastomers or ReMoTE [5].

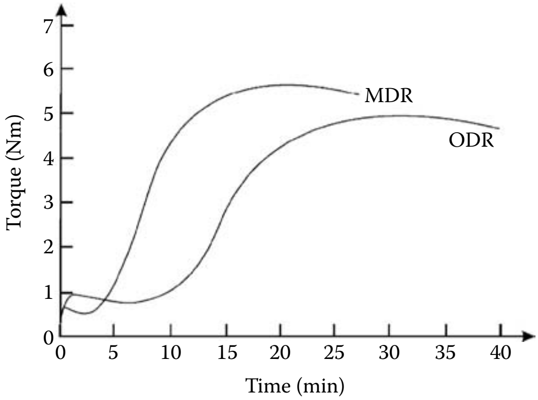

FIGURE 5.13 Torque–time curves obtained with the same rubber sample using the oscillating die rheometer (ODR) and the moving die rheometer (MDR).

- Another application of the injection system consists of recycling old and waste rubber. The reactive mixing of crumb rubber with a melted polymer represents an innovative way of recycling these waste rubbers [6]. Some thermoplastic elastomer may contain up to 60% recycled rubber derived from used vehicle tires, and thus through the reactive injection system the rubber scrap is revulcanized [7].
- As shown in Figure 5.13, with the torque versus time obtained with the ODR and MDR run under isothermal conditions, only the time of the minimum value of the torque can be appreciated, but it is not possible to get the value of the temperature of the rubber sample associated with this minimum torque.
- Finally, it should be repeated that the best apparatus available, in our opinion, for determining simultaneously the conditions of temperature and time at which the rubber can be stored without an increase in stiffness is the rubber process analyzer (RPA) from Alpha Technologies, as it can be run with a programmed temperature.

REFERENCES

1. Sadr-Bazaz A., R. Granger, and J.M. Vergnaud. 1984. Calculation of profiles of temperature and state of cure developed within the rubber mass in injection molding process. *J. Appl. Polym. Sci.* 29: 955–63.
2. Sadr A., R. Granger, and J.M. Vergnaud. 1985. Profiles of temperature and state of cure developed within rubber in injection molding systems. American Chemical Society Symposium series: *Reactive Injection Moulding and Reactive Processes*. 18: 279–91.
3. Ferradou C., B. Rochette, and J.M. Vergnaud. 1985. Effect of a variation in kinetic parameters (rate constant, activation energy) on the vulcanization of rubber sheets in injection molding process. *J. Appl. Polym. Sci.* 30: 2663–74.
4. El Brouzi A., R. Granger, J. Bouzon, and J.M. Vergnaud. 1989. Modelling and simulation of the process of reactive injection moulding in case of composite with low enthalpy. *Plastics Rubber Process. Appl.* 12: 7–13.

5. TPE for soft-touch applications. 2005. *High Performance Plastics*, September 4.
6. Wiessner S. and H. Michael. 2003. Thermoplastic elastomer from rubber crumb and propylene. *KGK: Kautschuk Gummi Kunststoffe*. 56: 514–18.
7. Ng W. 2000. Recycling technology employs tire scrap to manufacture TPV. *Modern Plastics Int*. 30: 37.

NOMENCLATURE

$\alpha, \alpha_r, \alpha_m$	thermal diffusivity, of the rubber, of the mold
b	rate of increase in temperature
C, C_r, C_m	heat capacity, of the rubber, of the mold
ΔH	enthalpy of the cure reaction
E	activation energy of the cure reaction
h	surface heat convection
k, k_T	rate constant of the cure reaction, at temperature T
k_0	constant rate of the cure reaction, independent of temperature
L	half the thickness of the sheet
λ_r, λ_m	thermal conductivity of the rubber, of the mold, respectively
Q, Q_t, Q_∞	heat, heat transferred at time t, after infinite time
r	radius
R	ideal gas constant
ρ, ρ_r, ρ_m	density, of the rubber, of the mold
$T, \frac{\partial T}{\partial t}, \frac{\partial T}{\partial x}$	temperature, rate of increase in temperature, gradient of temperature
T_{in}, T_∞, T_i	temperature initially, after infinite time, of injection, respectively
t	time
x	abscissa characterizing the position

6 Mechanical Properties of Rubbers

6.1 MECHANICAL PROPERTIES OF UNVULCANIZED RUBBERS

6.1.1 PRINCIPLE OF VISCOELASTIC BEHAVIOR

The ease of deformation called *plasticity* characterizes the unvulcanized rubber compound, and causes the highly plastic rubber to flow easily. Viscosity is the resistance to plastic deformation or flow and, hence, the inverse of plasticity. Unvulcanized rubbers are not totally viscous but exhibit some elastic behavior. Rubber does not exhibit Newtonian flow as the shear rate is not proportional to the shear stress. Moreover, measurements of flow properties should be made at the shear rate of interest.

As interestingly shown in Reference [1], to get an accurate idea of how a rubber behaves in the die of an extruder is a difficult problem that has not been solved by existing plasticity tests. Hence, plasticity tests have mostly been used as a check on the uniformity of repeated batches.

6.1.2 MEASURE OF PLASTICITY AND FLOW RATE WITH PLASTIMETERS

Various plastimeters are able to measure the plasticity of rubber compounds.

6.1.2.1 Compression Plastimeters: Plate Test and Disc Test

Their technique is very simple but has great disadvantages, and thus these plastimeters have been found useful only for routine testing, especially of uncompounded rubber, where just similar materials are compared.

With the plate test, the test piece is compressed between parallel plates under a constant force, and the compressed thickness measured. The test-piece area increases, and hence the pressure decreases as the rubber spreads out.

With the disc test, the test piece area remains constant, and the compression pressure remains constant. However, the shear stresses in the rubber vary as its thickness is decreased. The main advantage of the disc test is that the result is less affected by variations in test-piece volume.

6.1.2.2 Rotation Plastimeters: Mooney Viscometer

The Mooney viscometer is extensively used for routine quality control purposes. The apparatus consists of a rotor and a stator. The rotor turns at a constant rate inside a closed cavity containing the test piece so that a shearing action takes place between the surfaces of the rotor and the walls of the chamber. The torque required to rotate the rotor is monitored by a transducer. It is standardized in ISO R 289 [2].

6.1.2.3 Extrusion Plastimeters and Die Swell

In this apparatus, rubber is forced through a small cylindrical die under a known pressure, and the volume extruded in a given time is measured. As it is similar in action to extruders in the factory, it is a test of extrudibility rather than plasticity. It also resembles the classical capillary viscometer. Apart from the rate of extrusion, it is also possible to visually estimate the quality of extrusion, and moreover, the cylindrical die could be replaced with one having a more complicated cross section. It is apparent that the advantage of the extrusion plastimeter is that it simulates to some extent the processing operations of extrusion and injection molding. Additionally, higher shear rates are possible than are obtained in compression or rotation plastimeters; the shear rate can be comparable with those encountered in processing, and heat buildup is not a great problem as the passage of the rubber through the die is very rapid. Small instrumented extruders, which are available commercially, are also used in the laboratory to measure extrudibility. The best known special die, the Garvey die [3], is worth mentioning. Methods of test for extrudibility are given in ASTM D2230 [4] using a screw type laboratory extruder, and standard compounds are included for use as comparison.

6.1.2.4 Miscellaneous Processibility Tests

Another approach is to use a small scale internal mixer and to monitor the torque required to turn the rotors which gives a measure of the effective viscosity. These instruments are most appropriate in estimating mixing behavior, in spite of the fact that they have been used more for plastics than rubbers.

Commercial instruments are available: the Brabender Plastograph, and Plasticorder, this latter allowing use of an extruder head; the RAPRA variable torque rheometer [5]. The advantages of these instruments are based on the similarity of their action to full-scale extrusion equipment and on the fact that they can be operated at shear rates appropriate for factory equipment. But because of the difficulty of matching exactly the range of shear rates which exist in full-scale plant, successful scaling-up is difficult. Elongation flow measurements have been reported by several workers, in which a sample is stretched in uniaxial tension at a constant strain rate [6].

Curemeters, oscillating disc, and reciprocating paddle types are forms of plastimeter that measure plasticity before the onset of cure, as well during the cure. The viscoelastic behavior of uncured rubber tested by dynamic measurement is characterized by in-phase and out-of-phase moduli and loss tangent.

6.1.2.5 Correlation between Plastimeters

From the number of plastimeters in use, it is obvious that there is a demand to know the relationship between the readings obtained with them. The problem is that the flow properties of rubber cannot be defined by a single parameter. Several correlations between readings of various plastimeters are shown in Brown's book devoted to the physical testing of rubbers [1].

6.1.3 SCORCH TIME MEASURE [1]

When the compounded rubber is heated at a high enough temperature and for long enough time, it will cure. Hence, there is not a clear distinction between a plasticity test and a test for scorch or rate of cure. Thus, the Mooney viscometer is used to measure scorch, that is, the onset of vulcanization, whereas an oscillating disc rheometer measures the plasticity of the compound before the onset of cure, as well the increase in stiffness when cure takes place.

Parallel plate compression plastimeters have been used for measuring the rate of cure at various times and temperatures. The test pieces are heated for various times and then tested in the plastimeter. The change in plasticity is then plotted against time of heating to give a scorch curve. The Mooney viscometer offers a more convenient way of measuring scorch, and a standard method is given in ISO 667 [7].

Other laboratory instruments able to measure the curing characteristics, the so-called curemeters, are widely used for the routine control of fully compounded rubbers.

Two types of curemeters are in common use: the reciprocating paddle type, such as the Wallace–Shawbury curometer, and the oscillating disc type, such as the Monsanto rheometer.

In the reciprocating paddle, a small paddle embedded in the rubber, which is itself enclosed in a heated cavity, is reciprocated. Either the change in amplitude of oscillation at constant force or the change in force to produce constant amplitude is monitored as a measure of change in stiffness.

In the oscillating disc a bi-conical disc is embedded in the rubber in a closed cavity, such as with the Mooney. The disc is oscillated through constant angular displacement and the torque monitored.

The British standard, BS 1673, Part 10 [8] covers reciprocating paddle, as well as oscillating disc curemeters.

However, as shown in Figure 6.1, tracing the torque as a function of time obtained with the isothermal oscillating disc rheometer (ODR), the temperature of the sample varying with time according to an unknown law, it is not easy to determine the conditions of time and temperature for the scorch of cure, which are associated with the minimum torque value. Moreover, the moving die rheometer (MDR), gives a shorter

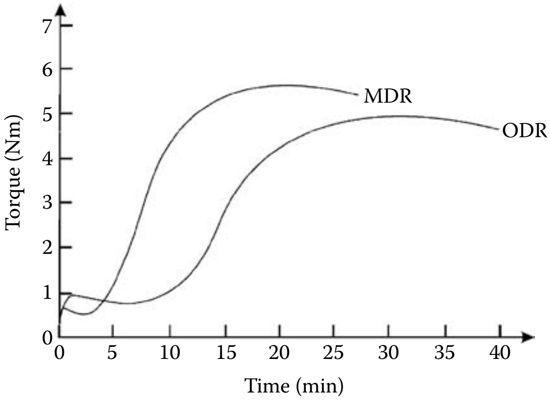

FIGURE 6.1 Torque–time (temperature) curves obtained with the oscillating disc rheometer (ODR) and the moving disc rheometer (MDR).

time, resulting perhaps from a different shape and more surely from a thinner thickness of the sample.

The rubber process analyzer (RPA 2000), recently available on the market, can be run either under isothermal temperature or with a programmed temperature, the time and temperature of the scorch of the cure of reaction are easily and precisely obtained.

6.2 MECHANICAL PROPERTIES OF VULCANIZED RUBBERS

There are two types of tests of interest for characterizing the vulcanized rubbers:

- The tests run under static conditions
- The tests run under dynamic conditions

6.2.1 Tests Run under Static Conditions

These tests, also called *short-term stress and strain properties* tests, are perfectly described in a special book devoted to the physical testing of rubbers [1], so that only a brief description will be given in this subsection. Such tests have been of enormous value, particularly in quality control tests, and have been studied and standardized for many years.

Stress/strain relationships are commonly used in tension, compression, shear, or indentation. It should be said that all stress/strain relationships are a function of the elastic modulus, with the exception of the breaking point, which measures the resistance to breaking.

6.2.1.1 Hardness of Rubber

By determining its resistance to a rigid indentor to which a force is applied, the hardness measurement is obtained, giving the measure of the elastic modulus of the rubber. Hardness may be regarded as depending simply on Young's modulus, as the cured rubber is perfectly elastic. Indentation involves deformation in tension, shear, and compression.

For a perfectly elastic rubber, various geometries of indentors are described, with the relationships related to Young's modulus [1].

The indenting force can be applied in three ways:

- Measurement of the indentation resulting from the application of a constant force
- Measurement of the force required to produce a constant indentation
- Measurement of the indenting force associated with the depth of indentation

An application of the measure of hardness showing how useful it could be appears in Reference [9], as researchers were able to demonstrate the diffusion taking place between two sheets of rubber containing different percent curing agents during the cure process. The measurements made along the thickness of the two half sheets with 2% and 10% peroxide cured together are of interest. The hardness expressed in terms of Shore D does not discontinuously vary at the interface; on the contrary, the hardness

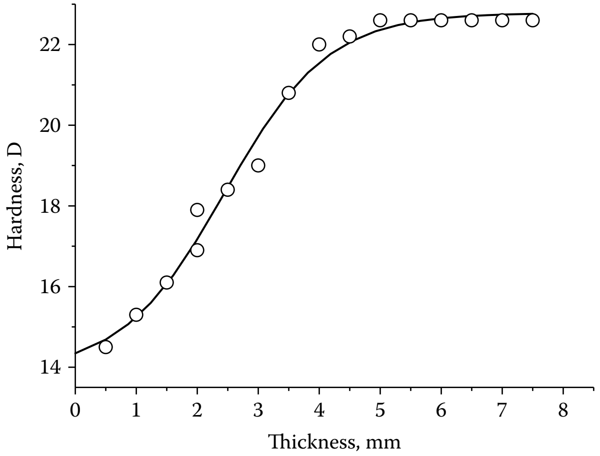

FIGURE 6.2 Hardness versus the thickness of the bilayer sheet containing 2% and 10% peroxide.

varies continuously along the thickness from 22 on the 10% peroxide rubber surface to 14.5 on the 2% peroxide rubber surface. This gradient of hardness along the thickness of the bilayer EPDM sheet can be explained by a diffusion of the peroxide during the heating period of the cure process when the rubber is less viscous (Figure 6.2).

The hardness measured with the small pocket type of hardness meter is associated with the durometer tests. Although there is not an international standard [1] that covers durometers, there is one for plastics, ISO R868 [10], which was used [9]. The two durometers specified are the Shore A and D which are also described in ASTM D2240 [11] where they are intended to cover both rubbers and plastics. The A scale corresponds approximately to the IRHD (International Rubber Hardness Degrees) scale and the D scale can be conveniently be used for hard rubbers above about 90 IRHD.

An example is given for the variation of the hardness samples either with the percentage sulfur or with the percentage plasticizer introduced in the rubber (Figure 6.3). These samples were prepared from rubber powder recovered from old tires (ultra-fine tire scrap with 90% of the particles smaller than 20 microns), by curing them under pressure after addition of various percentages sulfur ranging from 0 to 5 [12]. As shown in this figure, the hardness expressed in terms of Shore D not only increases with the percentage of sulfur as usual but also slightly decreases with the percentage of plasticizer, the plasticizer being the dioctyl phthalate (DOP).

6.2.1.2 Tensile Stress/Strain

After indentation hardness, the most common type of stress strain measurements is that made in tension. The ability of rubber to stretch to several times its original length is one of its chief characteristics, but it is worth noting that at least as many rubber products are used in compression or shear as are used in tension [1].

Essentially, dumb-bell shaped or, less often, ring-shaped test pieces are strained at a constant rate of traverse and force with the corresponding extension recorded.

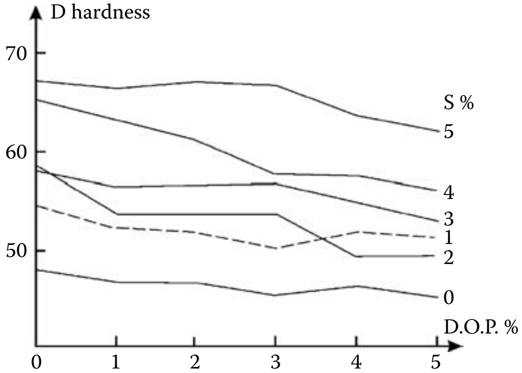

FIGURE 6.3 Hardness as a function of plasticizer concentration (% DOP) for different percentages of sulfur in rubber samples. (Reproduced with permission from *Rubber Chemistry and Technology,* Copyright 1982. 55: 328–36. A. Accetta and J. M. Vergnaud, Figure 8, Rubber Division, ACS.)

It is usual in rubber testing to calculate tensile stresses, including those at break, on the initial cross-sectional area of the test piece, and these stresses are sometimes called *nominal stresses.*

Extension is always recorded as percentage of elongation, which is the increase in length as a percentage of original gauge length.

An example of the variation of the ultimate tensile strength (or tensile stress at break, expressed in M Pascal) as a function of plasticizer concentration (%DOP) is given for different percentages of sulfur used for curing the samples [12]. As shown in Figure 6.4, the ultimate tensile strength increases rather strongly with the percent of sulfur up to 5%, and it slightly decreases with the percentage of plasticizer (DOP) added to the final material. The variation of the elongation at break (expressed in percentage of the original length) as a function of either the percentage of plasticizer or the percentage of sulfur used for curing the samples is drawn in Figure 6.5. In this example, the elongation at break does not depend on the per cent plasticizer when it is between 0 and 5%, and it varies in a rather complex way with the percentage of sulfur used for curing.

6.2.1.3 Compression Stress/Strain [1]

The compression stress/strain is in many ways easier to carry out than a tensile test; moreover, in view of the large number of applications of rubber in compression, they should be more often used.

Frequently, the test piece is the complete product, and in that case there is no problem regarding shape of the test piece. A compressive force is applied, usually at constant rate of deformation, and the force and corresponding deformation recorded.

Test pieces are specially prepared in the form of a disc or short cylinder, the compressive force being applied to the circular faces. The compression can be operated under two conditions: either with perfect slippage between the rubber and the compressing members or with complete absence of slip. As perfect slippage is impossible

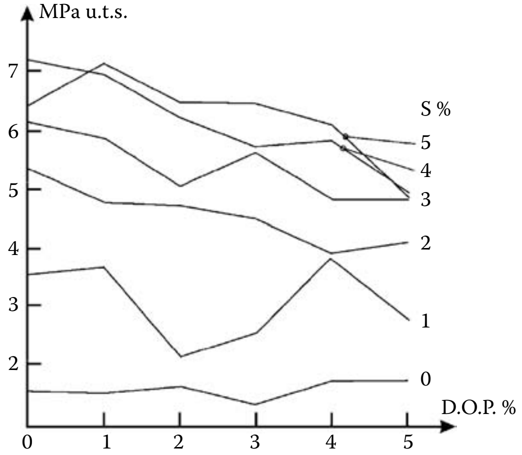

FIGURE 6.4 Ultimate tensile strength (MPa) as a function of plasticizer concentration (% DOP) for different percentages of sulfur in the vulcanized rubber. (Reproduced with permission from *Rubber Chemistry and Technology,* Copyright 1982. 55: 328–36. A. Accetta and J. M. Vergnaud, Figure 9, Rubber Division, ACS.)

to achieve, most applications involve either rubber bonded to metal or compressed between surfaces that could possibly eliminate slip.

Let us note that this kind of test measures the behavior of the special rubber pieces supporting housings in case of earthquake. And, thus, special attention has been given to the cure process of these kinds of rubber–metal pieces in sandwich form in Chapter 4. It should be said that the motion due to earthquake is far from being vertical, as the horizontal component of the motion is essential and is also the most destructive.

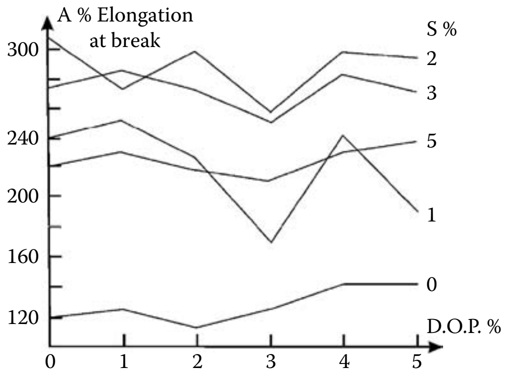

FIGURE 6.5 Elongation at break (% of the initial length) as a function of plasticizer (% DOP) for different percentages of sulfur used for curing. (Reproduced with permission from *Rubber Chemistry and Technology,* Copyright 1982. 55: 328–36. A. Accetta and J. M. Vergnaud, Figure 7, Rubber Division, ACS.)

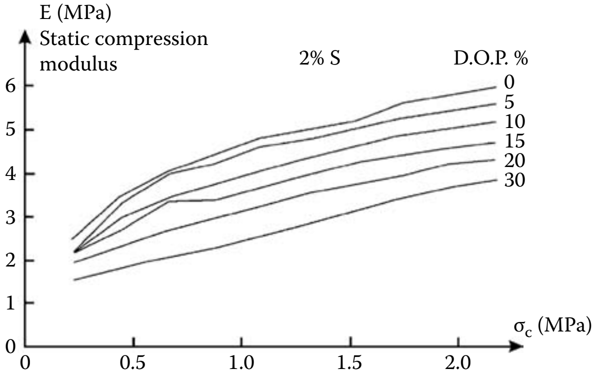

FIGURE 6.6 Static compression modulus E (MPa) as a function of pressure (MPa) for various percentage plasticizer (DOP) in rubber samples cured with 2% sulfur. (Reproduced with permission from *Rubber Chemistry and Technology,* Copyright 1982. 55: 328–36. A. Accetta and J. M. Vergnaud, Figure 1, Rubber Division, ACS.)

An example is given in Figure 6.6 showing the static compression modulus E expressed in MPa as a function of the pressure σ_c (MPa) for different percentages of plasticizer (DOP) with rubber samples cured with 2% sulfur. There is a significant increase in the static modulus E with the compression pressure σ_c; on the other hand, for each compression value the static compression modulus progressively decreases with percentage DOP as plasticizer [12].

6.2.1.4 Shear Stress/Strain [1]

Shear-like compression is a more important mode of deformation for engineering applications than tension. Testing in shear is not more difficult than testing in tension, and the only practical difficulty comes from the necessity to bond the rubber test piece to rigid members to provide attachments for applying the shearing force.

Let us remark that this kind of test is of interest for predicting the resistance of rubber–metal pieces in case of an earthquake.

6.2.1.5 Tear Tests [1]

Unlike the normal tensile test when the force to produce failure in a flawless test piece is measured, in a tear test the force is not applied evenly but concentrated on a deliberate flaw or sharp discontinuity, and the force to continuously produce a new surface is measured. This force to start tearing depends in a complex manner on the geometry of the test piece and on the nature of the discontinuity. This last discontinuity is a cut, notch, or reentrant angle. As a result, the tear strength measured is not a fundamental property of the material, and it is difficult to correlate the results obtained with these tests with performance of products in service. For an article in service, the force necessary to initiate a tear as distinct from that to propagate a tear is of greater interest, as it could be argued that once a tear has started, the product has failed and the force or energy needed to continue the tear is of little interest.

But in most standard tests, the maximum force measured during the test is recorded, and no distinction made between the stages of initiation and propagation.

6.2.2 Dynamic Stress and Strain Properties

In dynamic tests the rubber is subjected to cyclic deformation, and the stress and strain are monitored. Dynamic properties are important in a large number of engineering applications of rubber, including springs and dampers, and are generally much more useful from a design point of view than the results given by the static tests.

Basically, there are two classes of dynamic motion:

- Free vibration in which the test piece is set into oscillation and the amplitude allowed to decay due to damping in the system
- Forced vibration in which the oscillation is maintained by external means

The force vibration machines may operate at resonance or away from resonance.

There is an international standard ISO 2856 [13] dealing with general requirements for dynamic testing which can be referred to for the classification of test machines, preferred conditions, and recommended test shapes [1].

The static tests considered in this chapter treat the rubber as being essentially an elastic, or rather, high elastic material, whereas it is in fact visco-elastic and hence its response to dynamic stressing is a combination of an elastic response and of a viscous response, so that energy is lost in each cycle. The Maxwell model represents this behavior as spring and dashpot in parallel.

For sinusoidal strain the motion is described by the equation:

$$\gamma = \gamma_0 \cdot \sin \omega t \tag{6.1}$$

where γ is the strain, γ_0 the maximum strain amplitude, ω the angular frequency, and t time.

If the rubber were a perfect spring, the stress τ would be similarly sinusoidal and in phase with the strain. However, because the rubber is visco-elastic the stress will not be in phase with the strain but can be considered to precede it by the phase angle δ, so that Equation 6.1 is rewritten as follows:

$$\tau = \tau_0 \cdot \sin(\omega t + \delta) \tag{6.2}$$

In other words, the deformation lags behind the force by the angle δ.

It is convenient [1] to consider the stress as a vector having two perpendicular components, one in phase with the displacement τ' and one 90° out of phase τ'' and to define corresponding in-phase, out-of-phase, and the resultant modulus.

The Young's moduli in compression are defined by:

$$E^x = E' + iE'' \tag{6.3}$$

where

E^x is the complex resultant Young's modulus,

E' in phase or storage modulus,

and E'' is out of phase or loss modulus.

The loss factor β is defined by the relation:

$$\beta = \tan \partial = \frac{E''}{E'} \tag{6.4}$$

6.2.2.1 Dynamic Compression Property of Vulcanized Rubber

To reduce undesirable vibration effects, the source may be isolated by means of vibration absorbers. The answer to the isolation problem is the correct mounting of the source (machine) on springs and dampers, that is, on rubber blocks [14]. Because dynamic properties are of great concern in engineering applications, including springs and dampers, dynamic tests are much more useful than the simple static tests. As said above, there are two classes of dynamic motions: free vibration and forced vibration.

In the following example [15], a forced vibration test is chosen in which the oscillation frequency is maintained away from resonance.

The rubber material is obtained by curing a scrap rubber powder at various times and temperatures, and the various values of the state of cure are calculated from the partial heat evolved from the cure reaction measured by calorimetry, as already shown in Chapter 4. The dynamic properties in compression are determined at room temperature by using several samples for which the state of cure is ranging from 36 to 90%. The apparatus used enables the measurement of the visco-elasticity of the rubber sample under various conditions such as compression, traction, shear (viscoelasticimeter from Metravib, France).

The effect of the state of cure on in-phase modulus E' is shown in Figure 6.7 for different frequencies while the displacement amplitude was kept constant (4 μm).

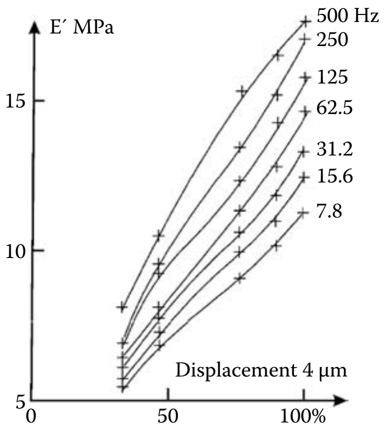

FIGURE 6.7 In-phase modulus in dynamic compression as a function of the state of cure, SOC, of the samples, for different values of the frequency.

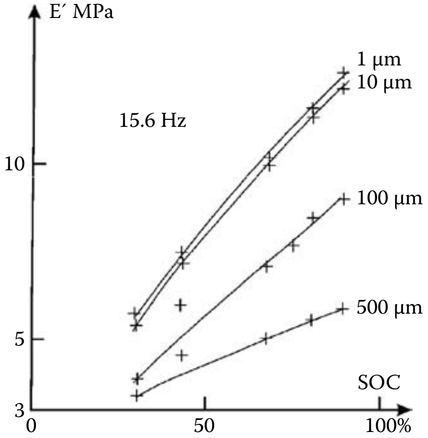

FIGURE 6.8 In-phase modulus in dynamic compression as a function of the state of cure, SOC, of the samples, for different values of the displacement, at constant frequency (16.5 Hz).

These couples of values can be accommodated on straight lines, which slopes vary with frequency, according the following relation:

$$E' = \text{b. SOC} + \text{a} \tag{6.5}$$

The correlation factor is about 1, indicating a good correlation for this linear function between the state of cure and in phase modulus.

6.3 CONCLUSIONS ON THE MECHANICAL PROPERTIES OF RUBBERS

Only a part of the mechanical properties of rubbers is considered in this chapter; in order to get a full knowledge on these properties of rubbers, and on how to determine these properties, we refer to the excellent book cited as Reference [1].

Two kinds of information are useful: one concerned with the unvulcanized rubber, so as to determine the best operational conditions of temperature and time for the injection molding and the other characterizing the final vulcanized rubber compound.

6.3.1 Conclusions Concerned with Unvulcanized Rubber

As already said, there was some difficulty in evaluating the conditions of the scorch time (i.e., the onset of vulcanization at a given temperature with the isothermal ODR and the isothermal MDR) as the scorch time obtained was not associated with a known temperature. This has been an argument for developing the rubber process analyzer (RPA, Alpha Technologies), which can be run not only under isothermal conditions but also with a programmed temperature, giving then simultaneously the temperature and time for the scorch.

6.3.2 CONCLUSIONS CONCERNED WITH VULCANIZED RUBBER

On the whole, two kinds of mechanical properties are of interest to characterize the rubber materials: those measured under static conditions, and the others measured under dynamic conditions.

A few examples are given for the usual mechanical properties of rubber samples measured under static conditions: the hardness, the ultimate tensile strength, and the elongation at break. Let us note that the measurement of the hardness through the thickness of a bilayer sample made of rubber cured with different percentages of curing agent, was able to explain the particular strength in adhesion of the final material leading to the final conclusion: the curing agent diffuses during the cure through these two layers.

The mechanical properties measured under dynamic conditions are of high interest, as they allow the use of the rubber samples in engineering applications.

In all these applications, the value of the state of cure of the rubber samples is considered as a reference, with the final conclusion being that the properties of the rubber samples increase with the state of cure. This fact brings some additional interest to the problems set by the cure of rubber.

REFERENCES

1. Brown R.P.1979. *Physical Testing of Rubbers*, Applied Science Publishers, London. Chapters 6, 8, 9.
2. ISO R289. 1963. Determination of Viscosity of Natural and Synthetic Rubbers by the Shearing Disc Viscometer.
3. Garvey B.S., M.H. Whitlock, and J.A. Freese. 1942. Processing characteristics of synthetic tire rubber. *Ind. Eng. Chem.* 34: 1309–12.
4. ASTM D 2230. 1977. Extrudibility of Unvulcanised Compounds.
5. Paul K.T. 1973. *RAPRA Bulletin*, February 1972. *RAPRA Members Journal.* March 1973.
6. White J.L. 1977. Processability of rubber and rheological behaviour. *Rubber Chem. Technol.* 50: 163–85.
7. ISO 667. 1975. Determination of Rate of Cure Using the Shearing Disc Rheometer.
8. BS 1673. Part 10. 1977. Measurement of Prevulcanising and Curing Characteristics by Means of Curemeters.
9. Azaar K., R. Granger, I.D. Rosca and J.M. Vergnaud. 2000. Effect of the state of cure on the hardness and resistance to liquids of EPDM rubbers. *Polym. Polym. Composites.* 8(5): 325–331.
10. ISO R868. 1968. Determination of Indentation Hardness of Plastics by Means of a Durometer (Shore Hardness).
11. ASTM D2240. 1975. Indentation Hardness of Rubber and Plastics by Means of a Durometer.
12. Accetta A. and J.M. Vergnaud. 1982. Vibration isolation properties of vulcanizates of scrap rubber powder. *Rubber Chem. Technol.* 55: 328–36.
13. ISO 2856. 1975. Elastomers. General Requirements for Dynamic Testing.
14. Snowdon J.C.1980. Vibration isolation: Use and characterization. *Rubber Chem. Technol.* 53: 1041–87. Reprinted from *J. Acoustical Soc. of America* (1979) 66: 1245–74.
15. Rochette B., M. Abdul, F. Fesquet, and J.M. Vergnaud. 1984. Correlation of the dynamic properties in compression of vulcanizates with their state of cure. Int. Rubber Conference, Moscow.

NOMENCLATURE

β	loss factor, defined in Equation 6.4
δ	angle representing the lag in Equation 6.2
E^x, E', E''	complex resultant Young's modulus, in-phase, out of phase component
γ, γ_0	used to characterize the strain, its maximum amplitude in Equation 6.1
τ, τ_0	used to represent the stress, its maximum amplitude
ω	angular frequency of the motion, in Equation 6.1
SOC	state of cure

7 Resistance of Rubber to Liquids

7.1 EFFECT OF LIQUIDS ON RUBBER AND ITS MEASURES

When a rubber sample is in contact with a liquid, a complex interaction between these two materials may take place. The action of the liquid on rubber results in absorption of the liquid by the rubber, sometimes followed by extraction of soluble constituents from the rubber. As usual, absorption is greater than extraction, so an increase in volume (or weight) results. It should be said that a decrease in volume or in weight of the rubber under these conditions implies more serious damage to the rubber than when swelling is observed.

7.1.1 MEASUREMENT OF THE SWELLING

Tests in which rubber samples are exposed to liquids are called "swelling tests" because of the resulting change in volume of the test pieces. The liquids generally used are aromatic compounds, the most common being toluene, as it is less volatile than benzene. These tests are also called "oil ageing" when standard grades of mineral oil are the liquids [1].

Volume change (or weight change) is a very good measure of the resistance of a rubber to a given liquid, a high degree of swelling clearly indicating that the rubber is not suitable for use in that environment. In addition, the degree of swelling can be related to the state of cure of the rubber, the crosslink density being estimated by use of the Flory–Rehner equation [2]. Let us recall that the value of the state of cure was determined by measuring the swelling of thin sheets of rubber samples immersed in toluene [3].

The degree of volume change with time is the best way, if not the only way, of determining the resistance of a rubber to a given liquid. The preferred method for volume change is the gravimetric method, which consists of weighing the test piece in air before and after immersion in the liquid. The curve obtained expresses the kinetics of absorption of the liquid. The time to reach equilibrium, where maximum swelling occurs, is proportional to the square of the thickness of a sheet [4,5]. Moreover, this kinetics will be represented by a few parameters of diffusion, which enable the measurement of not only the maximum swelling but also of the rate at which it is attained.

Discontinuous measurements of the dimensions, or volume, or weight, necessitate a short interval after the extraction of the sample from the liquid, as the liquid evaporates rather strongly from the rubber sample [6]. Then, the most useful method consists of measuring the change in length of a long and thin test piece when it is continuously immersed in the liquid.

7.1.2 STANDARD TESTS

The international method for resistance to liquids is ISO 1817 [7], which has been revised [1]. The method gives general clauses covering conditioning, choice of test liquid, temperatures and duration of test, and then details separate routines for determining the change in physical properties. ISO 1817 specifies two procedures for determination of tensile properties and hardness, one immediately after immersion and the other after immersion and subsequent drying.

The equivalent British Standard BS 903 Part A 16 [8] is similar to ISO 1817 but includes three additional procedures [9].

A second ASTM method DI 1460 [10] gives a procedure for change in length after immersion, using a long and thin test piece. The advantage of this method is that measurement can be made through the transparent walls of the container and hence can be used with liquids under pressure.

Various standard liquids are defined, such as ASTM oils and pure toluene, this last liquid being the most useful liquid, as standard oils are so complex in composition that it is necessary to know the provenance of these oils.

Note the nonstandard methods described and reviewed [1,11,12].

7.2 LIQUID TRANSPORT BY DIFFUSION

7.2.1 PRINCIPLE OF DIFFUSION

Very often, the transport of the liquid through the rubber is controlled by diffusion with either a constant or concentration-dependent diffusivity. This transport can be performed under stationary conditions when the concentration of the liquid varies with position, and under transient conditions when the liquid concentration varies with position and time.

The diffusion of liquid through a rubber can differ strongly according to its nature. Rubbers usually have a wide spectrum of relaxation times associated with their structural changes and especially with the motion of polymer segments. All of these relaxation times decrease as temperature or the liquid concentration in the rubber is increased, and the motion of the chain segments is enhanced. The diffusion of liquids in rubbers is thus associated with the finite rates at which the rubber structure changes in response to the motion of the liquid. An important feature of rubbers is their glass transition temperature. Above this temperature, the rubbers are in a rubbery state, and below this temperature they are in a glassy state.

The diffusion behaviour of polymers in a rubbery state is described by Fick's laws with constant or concentration-dependent diffusivity.

As shown in Chapter 2, transfer of heat by conduction is due to random molecular motions, and there is an obvious analogy between the two processes of heat conduction and of mass transport by diffusion. Fick in 1855 recognized this fact, and put diffusion on a quantitative basis by adopting the mathematical equation of heat conduction derived some years earlier by Fourier (1822).

The rate of transfer of a substance diffusing through a unit area of a section is proportional to the gradient of concentration normal to the section:

$$F = -D \cdot \frac{\partial C}{\partial x} \tag{7.1}$$

where F is the rate of transfer per unit area of section, C the concentration of diffusing substance, and D is called the diffusion coefficient, or diffusivity.

If F, the amount of material diffusing, and C, the concentration, are both expressed in terms of the same unit of quantity, then the diffusivity D is independent of this unit and has the following dimensions : $(\text{length})^2 \cdot (\text{time})^{-1}$ or in the CGS system $\text{cm}^2 \cdot s^{-1}$.

7.2.2 DIFFERENTIAL EQUATIONS OF DIFFUSION

7.2.2.1 Case of a One-Dimensional Diffusion through a Thin Sheet

In the element of volume taken within the very thin sheet of thickness dx, separated by the planes of abscissa x and $x + dx$, perpendicular to the axis of diffusion (Figure 7.1), the flux of diffusing substance are F_x and F_{x+dx}, respectively. The mass balance during the short time dt gives:

$$A \cdot (F_x - F_{x+dx}) = -A \cdot \frac{\partial F}{\partial x} \cdot dx = A \cdot \frac{\partial C}{\partial t} \cdot dx, \tag{7.2}$$

A being the area through which the heat flux is transmitted, and $A \cdot dx$, the volume of the solid considered. The change in concentration dC during the time dt through this solid, results from these flux.

This equality can be written as follows:

$$-\frac{\partial F}{\partial x} = \frac{\partial C}{\partial t} \tag{7.3}$$

By considering the value of the flux expressed in Relation 7.1, it comes:

$$\frac{\partial C}{\partial t} = \frac{\partial}{\partial x}\left[D \cdot \frac{\partial C}{\partial x}\right] \tag{7.4}$$

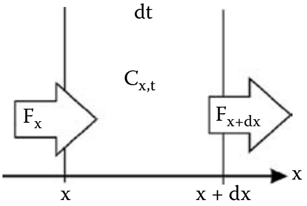

FIGURE 7.1 Scheme of one-dimensional transport of diffusing substance through a thin sheet.

This equation is the fundamental equation of one-directional diffusion through a sheet, when the diffusivity D is concentration-dependent. When the diffusivity is constant, this equation simplifies, leading to:

$$\frac{\partial C}{\partial t} = D \cdot \frac{\partial^2 C}{\partial x^2} \tag{7.4'}$$

7.2.2.2 Radial Diffusion through the Section of a Cylinder or a Sphere

The radial diffusion through a cylinder long enough so as the longitudinal diffusion may be neglected, is obtained in the same way by evaluating the mass balance:

$$\frac{\partial C}{\partial t} = \frac{1}{r} \cdot \frac{\partial}{\partial r}\left[r \cdot D \cdot \frac{\partial C}{\partial r} \right] \tag{7.5}$$

which becomes when the diffusivity is constant:

$$\frac{\partial C}{\partial t} = \frac{D}{r} \cdot \frac{\partial}{\partial r}\left[r \cdot \frac{\partial C}{\partial r} \right] = D \cdot \left[\frac{1}{r} \cdot \frac{\partial C}{\partial r} + \frac{\partial^2 C}{\partial r^2} \right] \tag{7.5'}$$

The equation of radial diffusion through a sphere

$$\frac{\partial C}{\partial t} = \frac{1}{r^2} \cdot \frac{\partial}{\partial r}\left[r^2 \cdot D \cdot \frac{\partial C}{\partial r} \right] \tag{7.6}$$

becomes, with the constant diffusivity,

$$\frac{\partial C}{\partial t} = \frac{D}{r^2} \cdot \frac{\partial}{\partial r}\left[r^2 \cdot \frac{\partial C}{\partial r} \right] = D \cdot \left[\frac{2}{r} \cdot \frac{\partial C}{\partial r} + \frac{\partial^2 C}{\partial r^2} \right] \tag{7.6'}$$

7.2.3 INITIAL AND BOUNDARY CONDITIONS

The initial conditions represent mathematically the nature of the profiles of concentration initially throughout the sheet. Either the profile of concentration is uniform or not. In the first case, an analytical solution can be found, while in the second case, generally a numerical method should be used.

With constant initial concentration, it is written, with a sheet of thickness 2 L:

$$t > 0 \quad -L < x < +L \quad C = C_{in} \tag{7.7}$$

The boundary conditions represent mathematically the conditions on the surfaces of the sheet. Generally, three conditions may appear:

- When the rate at which the diffusing substance enters an external fluid by convection is equal to the rate at which the substance is brought by internal diffusion to the surface:

$$-D \cdot \frac{\partial C}{\partial x} = h \cdot (C_s - C_{ext}) \quad \text{surface} \tag{7.8}$$

where h is the coefficient of surface convection at the sheet–fluid interface, C_s and C_{ext} are the concentrations of the diffusing substance on the sheet surface and in the external fluid, respectively.

Note that the concentration in a fluid, because of the convection which acts much faster than diffusion through a solid, may be considered as uniform.

- When there is no transport of diffusing substance at the surface of the solid, the coefficient h in Equation 7.8 is equal to 0, leading to:

$$\frac{\partial C}{\partial x} = 0 \tag{7.9}$$

- When two solids, called 1 and 2, are in perfect contact, the rates of transport are equal on both sides of their interface, which is written as follows:

$$D_1 \cdot \left[\frac{\partial C}{\partial x}\right]_1 = D_2 \cdot \left[\frac{\partial C}{\partial x}\right]_2 \tag{7.10}$$

- When a solid is in contact with a fluid strongly stirred, the value of the coefficient of surface convection is so large than it may be considered as infinite, and the concentration on the surface of the solid is constantly equal to the concentration in the fluid:

$$C_s = C_{ext} \tag{7.11}$$

7.2.4 GENERAL SOLUTION OF THE EQUATIONS OF DIFFUSION IN SHEETS

The general solution is obtained for the one-directional diffusion through a sheet of thickness 2L, when the sheet is immersed in a fluid of very large volume, with the following assumptions:

i. The volume of the external fluid is so large with respect to that of the rubber sheet that the concentration of the diffusing substance remains constant, a particular case being 0.
ii. The diffusivity of the substance through the sheet is constant.
iii. The initial profile of concentration in the rubber sheet is uniform.
iv. The effect of the edges is negligible with respect to the one-directional transport through the thickness of the rubber sheet.
v. The thickness of the rubber sheet is taken as 2L, so as to take advantage of the symmetry of the problem. This thickness remains constant during the process, meaning that the volume of the diffusing substance exchanged is small.
vi. The boundary condition is expressed by Equation 7.8, which takes into account the equality of the rates of transport of the diffusing substance on the two sides of the interface.

The equation of diffusion through the thickness of the rubber sheet is:

$$\frac{\partial C}{\partial t} = D \cdot \frac{\partial^2 C}{\partial x^2} \tag{7.4'}$$

and the boundary equation is defined by Equation 7.8:

$$-D\cdot\frac{\partial C}{\partial x}=h\cdot(C_s-C_{ext}) \tag{7.8}$$

The solution of the problem is expressed by the equation

$$\frac{C_\infty-C_{x,t}}{C_\infty-C_{in}}=\sum_{n=1}^{\infty}\frac{2K\cdot\cos\left[\beta_n\frac{x}{L}\right]}{\cos\beta_n\cdot(\beta_n^2+K^2+K)}\exp\left[-\beta_n^2\frac{D\cdot t}{L^2}\right] \tag{7.12}$$

where the β_ns are the positive roots of:

$$\beta\cdot\tan\beta=K \tag{7.13}$$

and the dimensionless number K is given by:

$$K=\frac{h\cdot L}{D} \tag{7.14}$$

The kinetics of transfer of diffusing substance is expressed in terms of the dimensionless number $\frac{D\cdot t}{L^2}$ by using the other dimensionless number $\frac{M_t}{M_\infty}$:

$$\frac{M_\infty-M_t}{M_\infty}=\sum_{n=1}^{\infty}\frac{2K^2}{\beta_n^2\cdot(\beta_n^2+K^2+K)}\exp\left[-\beta_n^2\frac{D\cdot t}{L^2}\right] \tag{7.15}$$

The value M_t represents the amount of diffusing substance after time t, whereas M_∞ is the corresponding value attained after infinite time, at equilibrium.

Let us remark again that L represents half the thickness of the rubber sheet (Figure 7.2).

7.2.5 SOLUTION OF DIFFUSION IN SHEETS WITH INFINITE COEFFICIENT OF CONVECTION

When the fluid in contact with the rubber sheet is strongly stirred, the coefficient of surface convection at the rubber–fluid interface is infinite. Then the β_ns are equal

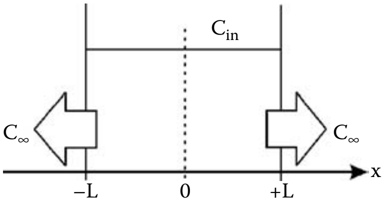

FIGURE 7.2 Scheme of the sheet of thickness 2L, with: $-L < x < +L$ and $C = C_{in}$ is the uniform concentration of diffusing substance initially in the sheet, when the problem of release of the liquid from the rubber sheet is considered.

to $(n+0.5)\cdot\pi$ and the equations are reduced, either for the profiles of concentration developed through the thickness or for the kinetics of mass transported:

$$\frac{C_\infty - C_{x,t}}{C_\infty - C_{in}} = \frac{4}{\pi}\cdot\sum_{n=0}^{\infty}\frac{(-1)^n}{2n+1}\cdot\cos\frac{(2n+1)\pi\cdot x}{2L}\cdot\exp\left[-\frac{(2n+1)^2\pi^2}{4L^2}D\cdot t\right] \tag{7.16}$$

$$\frac{M_\infty - M_t}{M_\infty} = \frac{8}{\pi^2}\cdot\sum_{n=0}^{\infty}\frac{1}{(2n+1)^2}\cdot\exp\left[-\frac{(2n+1)^2\pi^2}{4L^2}D\cdot t\right] \tag{7.17}$$

7.2.6 CASE OF RUBBER SHEETS IN CONTACT WITH A LIQUID

Three cases appear for a rubber sheet in contact with a liquid:

i. No liquid enters the rubber sheet.
ii. A small amount of liquid enters (or leaves) the rubber sheet (e.g., a few percent), and in this case, Equations 7.12 and 7.15 should be used to represent the process when the liquid is not stirred, whereas Equations 7.16 and 7.17 can be used when the liquid is strongly stirred.
iii. A large amount of liquid enters (or leaves) the rubber sheet, for example, more than 10–20%. Then, the volume of the rubber sheet changes, as well as its thickness. Moreover, the nature of the solid is modified, and the liquid diffuses through the solid–liquid compound, so as the diffusivity becomes concentration-dependent following this statement: the diffusivity increases with the liquid concentration. These two facts, the change in dimension and the concentration-dependent diffusivity, make the problem impossible to be mathematically considered, and so, only numerical solutions are able to resolve it.

Let us remark that in the third case, as gradients of liquid concentrations are developed through the thickness of the rubber, the rubber sheet becomes heterogeneous, with a gradient of change in the thickness and gradient of change in the diffusivity.

7.2.7 DETERMINATION OF THE PARAMETERS OF DIFFUSION

The following parameters are necessary for expressing the kinetics of diffusion of liquid for rubbers:

i. The diffusivity D is the main parameter, either constant or concentration-dependent.
ii. The amount of liquid absorbed at equilibrium by the rubber, after infinite time of contact with the liquid, theoretically speaking, M_∞.
iii. The thickness of the sheet, initially when it is free from liquid, and at the end of the process when it is saturated.

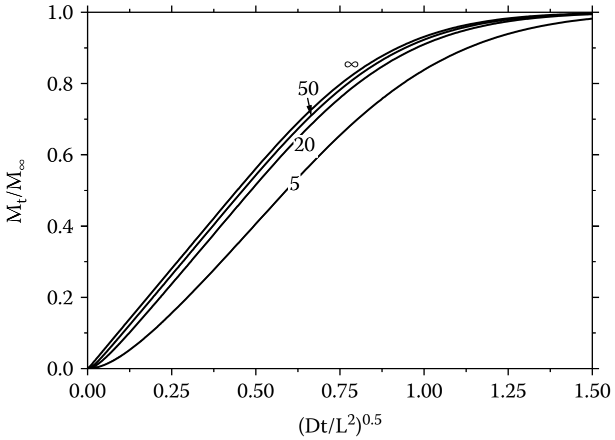

FIGURE 7.3 Kinetics of transfer of the diffusing substance into (or out from) the sheet with a thickness 2L, with different values of the dimensionless number $K = \frac{h \cdot L}{D}$. The values of K are shown on the figure. These master curves are drawn by using the dimensionless numbers $\frac{M_t}{M_\infty}$ and $\frac{D \cdot t}{L^2}$ (or rather its square root) as coordinates.

iv. The density of the rubber and of the liquid, as the change in dimension of the rubber is concerned by the volume of liquid.

v. Moreover, the rate of stirring of the liquid should be evaluated, in order to get knowledge on the coefficient of surface transfer h. In fact, it is obtained from the slope of the curve drawn by putting the amount of liquid absorbed versus time or versus the square-root of time, at very short times. The curves drawn in Figure 7.3 for various values of the dimensionless number $K = \frac{h \cdot L}{D}$ show the effect of the coefficient of surface h. The straight line for K infinite is obtained by using Equation 7.17 while the others are obtained using Equation 7.15 with various values of K.

vi. Dimensionless numbers appear in the various equations of diffusion:

$\frac{D \cdot t}{L^2}$ which means that the time necessary for a given transport is proportional to the square of the thickness of the sheet;

$\frac{h \cdot L}{D}$ which characterizes the importance of the convection at the rubber surface with respect to the diffusion.

7.2.8 EQUATION OF RADIAL DIFFUSION WITH CHANGE IN DIMENSION OF THE SPHERE

The equation of radial diffusion 7.6 established for a sphere when the amount of liquid absorbed is so small that it may be negligible should be modified when this amount of liquid becomes large with respect to the volume of the rubber sphere. This Equation 7.6 should be established in the new case where the concentration of the liquid is so large in the rubber that it cannot be ignored [13,14].

Each point in the rubber sphere is defined by two radial abscissae: the one, u, when the sphere is free from liquid, and the other, r, which varies with the amount of liquid absorbed as $r = f(u, t)$. In the same way, the radius of the sphere R free from liquid becomes $r = f(R, t)$.

The membrane of radius $r(u, t)$ of initial thickness du has a total volume $V(u, t)$ made of the volumes of the rubber and of the liquid, at time t, such as:

$$V(u, t) = V(u, rubber) + V(u, t) \cdot C(u, t) \tag{7.18}$$

where $C(u, t)$ is the per unit volume concentration of liquid at time t in this membrane.

As the volumes of this membrane are, respectively:

$$V(u, rubber) = 4\pi \cdot u^2 \cdot du \tag{7.19}$$

$$V(u, t) = 4\pi \cdot r^2 \cdot dr \tag{7.19$'$}$$

the volume expansion resulting from the presence of the liquid is expressed by:

$$\frac{V(u,t)}{V(u,rubber)} = \frac{r^2 \cdot dr}{u^2 \cdot du} = \left[1 - C(u,t)\right]^{-1} \tag{7.20}$$

and the linear expansion becomes:

$$\frac{dr}{du} = \frac{u^2}{r^2}[1 - C(u,t)]^{-1} \tag{7.21}$$

The liquid balance within the membrane during lapse of time dt, by considering the volume which enters and leaves, gives:

$$\frac{\partial}{\partial t}[V(u,t) \cdot C(u,t)] = \frac{\partial}{\partial u}\left[A \cdot D \cdot \frac{\partial C}{\partial r}\right] du \tag{7.22}$$

By replacing in Equation 7.22 the area A by $4\pi \cdot r^2$ and the volume $V(u, t)$ defined in 7.20, Equation 7.22 becomes:

$$\frac{\partial}{\partial t}[C \cdot (1 - C)^{-1}] = \frac{1}{u^2}\frac{\partial}{\partial u}\left[r^2 \cdot D \cdot \frac{\partial C}{\partial r}\right] \tag{7.23}$$

By expressing $\frac{\partial C}{\partial r}$ in terms of $\frac{\partial C}{\partial u}$ and considering the linear expansion in Equation 7.21, Equation 7.23 is rewritten as follows:

$$\frac{\partial}{\partial t}[C \cdot (1 - C)^{-1}] = \frac{1}{u^2}\frac{\partial}{\partial u}\left[\frac{r^4}{u^2} D \cdot (1 - C)\frac{\partial C}{\partial u}\right] \tag{7.24}$$

This Equation 7.24 is the general equation of radial diffusion in a sphere when the volume of liquid is so large that a change in dimension occurs.

When the concentration of liquid C in the rubber is small and negligible, r and u are similar, and the Fick's equation for radial diffusion is obtained:

$$\frac{\partial C}{\partial t} = \frac{1}{u^2}\frac{\partial}{\partial u}\left[u^2 \cdot D \cdot \frac{\partial C}{\partial u}\right] \tag{7.25}$$

7.2.9 GENERAL EQUATION OF ONE-DIMENSION DIFFUSION

The rubber being isotropic, the local linear expansion resulting from the absorption of liquid is the same in all directions [15]. Thus, the surface expansion $A(u,t)$ is as follows:

$$A(u,t) = \left[\frac{\partial x}{\partial u}\right]^2 \tag{7.26}$$

The additivity of the volumes of rubber and of liquid gives:

$$V(u,t) = V(u,0) + V(u,t) \cdot C(u,t) \tag{7.27}$$

In each place at time t, the volume extent due to the swelling is:

$$\frac{V(u,t)}{V(u,0)} = [1 - C(u,t)]^{-1} \tag{7.28}$$

and the subsequent linear dilatation and surface extent are, respectively:

$$\frac{\partial x}{\partial u} = [1 - C(u,t)]^{-1/3} \quad A(u,t) = [1 - C(u,t)]^{-2/3} \tag{7.29}$$

The element of volume of thickness du and unit area $A(u,0)$ becomes trapezoidal.

By evaluating the liquid balance during this element of volume during the time dt, it is found:

$$\frac{\partial}{\partial t}[C \cdot (1-C)^{-1}] = (1-C)^{-2/3} \cdot \frac{\partial}{\partial u}\left[(1-C)^{1/3} \cdot D \cdot \frac{\partial C}{\partial u}\right] \tag{7.30}$$

This Equation 7.30 is general, whatever the swelling. When the concentration of liquid is small and negligible, $x = u$, and $C = 0$, Fick's equation is obtained:

$$\frac{\partial C}{\partial t} = \frac{\partial}{\partial x}\left[D \cdot \frac{\partial C}{\partial x}\right] \tag{7.4}$$

7.3 DIFFUSION OF THE CURING AGENT DURING THE CURE

It is very important to determine a possible transport of the curing agent during the cure period of the compound. To obtain this information [16], which is difficult, if not impossible to get directly, the following indirect experiment has been made. Two discs of rubber each containing a different percent curing agent, around 2% and 10%, are pressed together, and this system is cured.

The composition (Hutchinson) of these two compounds is described in Table 7.1.

The peroxide is Perkadox.

Two discs with a thickness of 0.4 cm for each and a diameter of 6 cm are pressed and cured together in the slabs of a heated press kept at 187°C during a period of time enough for the state of cure to reach 95%.

TABLE 7.1
Composition of two EPDM Compounds Cured together

EPDM	C black	Plasticizer	Chemicals	Peroxide
100	49	13	3	2
100	46	11	3	10
100	42	9	2	20

The hardness is measured on the plane surfaces of the 0.8 cm thick sheet made of the two layers with 2% and 10% peroxide. The sheet is cut through the thickness, and the hardness is measured along the section parallel with the thickness. The results for the hardness along the thickness of the bilayer sheet are given in Table 7.2.

These results shown in Table 7.2 lead to a few observations:

i. Of course, the material cured with 10% peroxide is much harder than that with 2% peroxide. The values appear on position 0 for the 2% peroxide and 8 for the 10% peroxide.
ii. The measurements made along the thickness of the two half sheets with 2% and 10% peroxide cured together show something of interest. The hardness varies progressively along the thickness from 22.6 on the 10% peroxide rubber surface to 14.5 on the 2% peroxide surface. The gradient of hardness along the thickness of the bilayer EPDM sheet can be explained by a diffusion of the peroxide during the heating period of the cure process when the rubbers are less viscous. Thus, the property of the bilayer sheet does not vary with a sharp discontinuity at the interface, at the position 4 mm. This fact can be responsible for a rather homogeneous material with good adhesion at the interface between the two layers.
iii. When the bilayer system is immerged in toluene, a diffusion of the liquid is observed leading to a different swelling depending on the nature of each component of the bilayer, as precisely described in Section 7.4.1. As a result of this difference in the swelling of each component of the bilayer, a strong torsion is observed so as to enable the surface with 2% peroxide to dilate more than the other with 10% peroxide. When the bilayer

TABLE 7.2
Hardness (Shore D) Along the Thickness (X mm) of the Bilayer Sheet

X (mm)	0	0.5	1	1.5	2	2.5	3	3.5	4
Shore D	14.5	14.5	15.3	16.1	16.9	17.9	18.4	19	20.8
X (mm)	4.5	5	5.5	6	6.5	7	7.5	8	
Shore D	22	22.2	22.6	22.6	22.6	22.6	22.6	22.6	

is removed from the liquid and let into the surrounding atmosphere, the liquid evaporates while the shape of the bilayer is becoming similar to the original one.

iv. It should be pointed out that the strength during the adsorption is considerable. But it is not sufficient to delaminate the two layers. An industrial application could be drawn from this observation, especially for retreading the huge tires used for trucks, as the external rubber-band in contact with the road is changed many times and cured with the whole tire.

v. It could be noticed that similar results have been obtained for thermosetting resins [17]. In order to repair broken pieces made of thermosetting resins, the following operation was made: put pure resin of the fresh, uncured thermoset without filler in contact with the surface of the precured thermosetting resin so it may diffuse into it; finally press together the two layers, the one made of the fresh uncured thermosetting resin and the other already cured, so as to cure themselves in a mold. As a result, the mechanical properties of the final bilayer material, such as elongation in flexion, elongation in traction, were as good as for the original sample, when the time of diffusion for the pure resin was long enough (i.e., around 24 hours).

7.4 EXAMPLES OF DIFFUSION OF LIQUIDS IN RUBBERS

7.4.1 Diffusion of Liquids through a Sheet with Change in Dimensions

7.4.1.1 Experimental Procedures

Sheets of EVAc (ethylene-vinyl acetate, of type 28-40 with 28% vinyl acetate and a melt index of 40) are used (Atochem). The thickness of the sheets is around 0.05 cm when they are free from liquid. Sheets of 3 × 3 × 0.051 cm are immersed in *n*-heptane (density = 0.684 g/cm^3. As the thickness of these sheets is smaller than the other dimensions, the effect of transfer through the edges is negligible, and all the diffusing substance enters through the plane faces.

The sheets are immersed in the liquid, and the kinetics of absorption followed either by weighing at intervals or by measuring the dimensions. The values obtained for the sample are given in the Table 7.3 [15].

TABLE 7.3
Characteristics of the Experiment

	Empty Sheet	Liquid at Equilibrium	Final Sheet
Volume (cm^3)	0.4623	0.4096	0.8719
Volumic expansion factor	1		1.886
Linear expansion factor	1		1.235
Dimensions (cm × cm × cm)	3.01 × 3.01 × 0.051		3.72 × 3.72 × 0.063
Diffusivity (cm^2/s)	$D = 4.5 \cdot 10^{-7}$		—

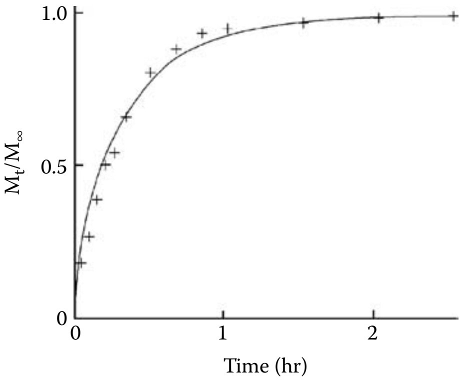

FIGURE 7.4 Kinetics of absorption of *n*-heptane by the EVAc sheet obtained either by experiment (dots) or by calculation (full line) taking into account the swelling and diffusion, with the diffusivity $D = 4.5 \cdot 10^{-7}$ cm^2/s. (With permission of Elsevier, Figure 2, *Europ. Polym. J.*, 1992, 28, 809, A. Bakhouya, A. El Brouzi, J. Bouzon, and J. M. Vergnaud.)

7.4.1.2 Results and Conclusions

A numerical treatment is made, taking into account the diffusion, and the change in dimension. The results are expressed by way of two figures, the one (Figure 7.4) representing the kinetics of absorption obtained either by experiment or calculated with the numerical treatment, and the other (Figure 7.5) showing the profiles of concentration of liquid developed within the thickness of the sheet as they are calculated.

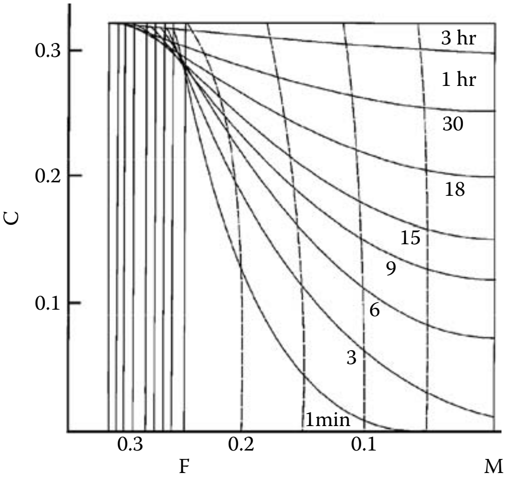

FIGURE 7.5 Profiles of concentration of liquid developed through the thickness of the sheet, as they are calculated by taking into account the diffusion and swelling, with the diffusivity $D = 4.5 \cdot 10^{-7}$ cm^2/s. (With permission of Elsevier, Figure 5, *Europ. Polym. J.*,1992, 28, 809, A. Bakhouya, A. El Brouzi, J. Bouzon, and J. M. Vergnaud.)

These figures lead to the following observations:

i. The first with the validity of the numerical model taking into account the absorption of the liquid whose kinetics is controlled by diffusion and the subsequent change in dimensions. In fact, a good agreement is obtained in Figure 7.4 between the experimental and calculated kinetics.
ii. In Figure 7.5, are drawn not only the profiles of concentration of the liquid developed at various times through the thickness of the sheet, but also the change in the thickness of the sheet, connected with the linear expansion factor of 1.235.
iii. The surface expansion factor of 1.525 is not shown, but the surface of the sheet in contact with the liquid increases in this way.

7.4.2 Diffusion of Liquids in EPDM Sheets with Different Percentages of Peroxide

7.4.2.1 Experimental

The three EPDM formulations (Hutchinson) described in Table 7.1 with the percentage of peroxide varying within the 2–20% range are used, while toluene is the liquid. Discs with a thickness of 0.2 cm and a diameter of 6 cm previously cured in the slabs of a heated press kept at 187°C are immersed in the liquid with a slight stirring. During the stage of absorption, the discs are weighed at intervals, and the dimensions measured at given places in order to follow the kinetics of absorption and the kinetics of the change of dimensions as the thickness and diameter [18].

7.4.2.2 Results on Kinetics of Absorption and Discussion

The kinetics of absorption of toluene by the EPDM rubber discs are drawn (Figure 7.6) as they are obtained from experiments (dots) and by calculation (full line) when the percentage of peroxide is 2, 10, and 20. The dimensionless number $\frac{M_t}{M_r}$ is used, expressing the weight of toluene absorbed as a fraction of the initial weight of the discs free from liquid.

These results obtained either by calculation or by experiments are also expressed in terms of the square root of time, using the weight of toluene absorbed at time t as a fraction of the corresponding value extrapolated for infinite time (Figure 7.7) [18].

These curves lead to the following conclusions:

i. Calculation is made by assuming an isotropic behavior of the rubber disc with respect to the swelling. The data are shown in Table 7.4.
ii. Good agreement is shown between the kinetics of absorption obtained from experiments and by calculation for the three EPDM samples, whatever the percentage of peroxide (Figure 7.6).
iii. The slope at the beginning of the stage of absorption is oblique in Figures 7.6 and 7.7. This is due to the finite coefficient of convective transfer on the surface of the rubber discs [4–6,19]. It should be recalled that a vertical tangent is associated with an infinite value of the coefficient h in

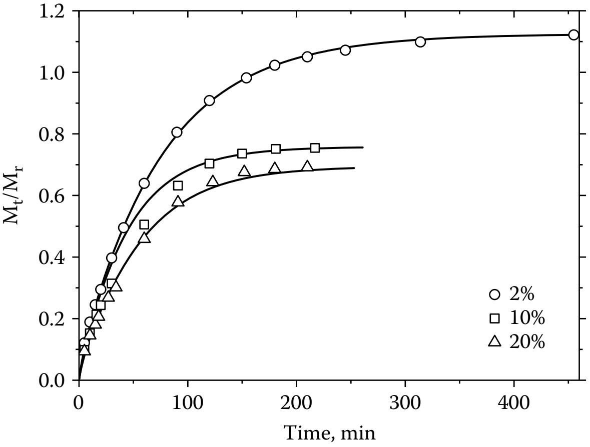

FIGURE 7.6 Kinetics of toluene absorption by three EPDM rubber discs with 2, 10, and 20 parts peroxide. Amount (w/w) of toluene absorbed as a fraction of the initial weight of rubber free from liquid. (With permission of Elsevier, Figure 2 in *Polymer*, 2002, 43, p. 4261; K. Azaar, I. D. Rosca, and J. M. Vergnaud.)

Equation 7.8 leading to the kinetics expressed by Equation 7.17. This fact is also proved by the shape of the curves in Figure 7.7, since the straight lines do not pass through the origin.

iv. The effect of the percentage of peroxide on the resistance of the EPDM discs is shown in these Figures 7.6 and 7.7 and Table 7.4.

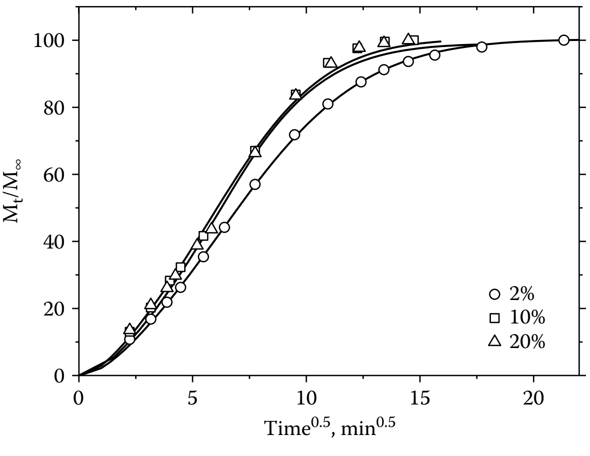

FIGURE 7.7 Amount of toluene absorbed by three EPDM rubber discs as a fraction of the square root of time (w/w percentage of initial rubber free from liquid) for 2, 10, and 20% peroxide. (With permission of Elsevier, Figure 3 in *Polymer,* 2002, 43, p. 4261, K. Azaar, I. D. Rosca, and J. M. Vergnaud.)

TABLE 7.4
Parameters of Diffusion

% Peroxide	$D_0(x10^7\ \text{cm}^2/\text{s})$	α	$h(x10^4\ \text{cm/s})$	$\frac{V_\infty}{V_r}$	$\frac{L_\infty}{L_0}$	$\frac{R_\infty}{R_0}$
2	7.9	2.5	1	1.5	1.3	1.56
10	8.7	2.5	1	1.03	1.24	1.46
20	8.6	2.5	1	0.945	1.21	1.42

v. The diffusivity slightly varies with the percent peroxide, as well as the factor α which characterizes its concentration-dependence shown in Equation 7.31 used for calculation:

$$D = D_0 \cdot \exp\left[\alpha \frac{C}{C_\infty}\right] \tag{7.31}$$

vi. The main parameter is the amount of liquid absorbed that decreases when the percentage of peroxide is increased.
vii. The process of absorption is thus controlled by radial and longitudinal diffusion through the disc, and convective transfer on the surface with a concentration-dependent diffusivity.

7.4.2.3 Anisotropic Swelling of EPDM Rubber Discs

The kinetics of absorption of toluene have been determined by weighing the uptake of liquid as a function of time, which is the more accurate method [1]. Nevertheless, at this time also, measurements are made in the same position for the thickness and the diameter. The results for these values are shown in Figures 7.8–7.10 for the discs with 2, 10, and 20% peroxide. The kinetics of the change in dimension for the thickness and radius are also drawn, as they are calculated by considering the anisotropic behavior of the rubber discs to the swelling. Various conclusions can be drawn from these curves:

i. From the experimental values, there are two kinetics for the swelling, the one expressed in terms of the change in the thickness, and the other in terms of the change in the radius.
ii The kinetics of these changes in dimensions can be calculated by using the same parameters of diffusion shown in Table 7.4, except for the increments of thickness and radius Δx and Δr shown in Table 7.5 to take into account the anisotropy of the rubber disc to swelling. Rather good agreement is thus obtained between the calculated and experimental kinetics, by considering that accuracy is not so favorably attained for these measurements of dimensions that those made on the weight.

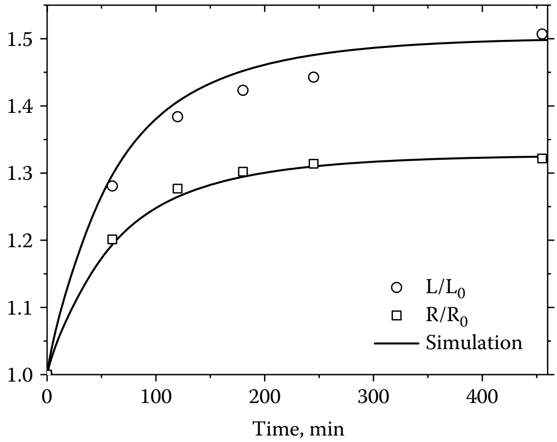

FIGURE 7.8 Kinetics of the increase in dimensions of EPDM rubber discs with 2% peroxide. Experiments (dots); calculated (full line). (With permission of Elsevier, Figure 4 in *Polymer*, 2002, 43, p. 4261, K. Azaar, I. D. Rosca, and J. M. Vergnaud.)

iii. A large and significant difference appears between the kinetics of swelling expressed in terms of the thickness and of the radius. The increase in the thickness is more important than that in the diameter. The ratio of these ultimate values, when equilibrium is attained, is around 1.18, this ratio being about the same whatever the percent peroxide used for the cure of the rubber discs (Figure 7.11) [20].

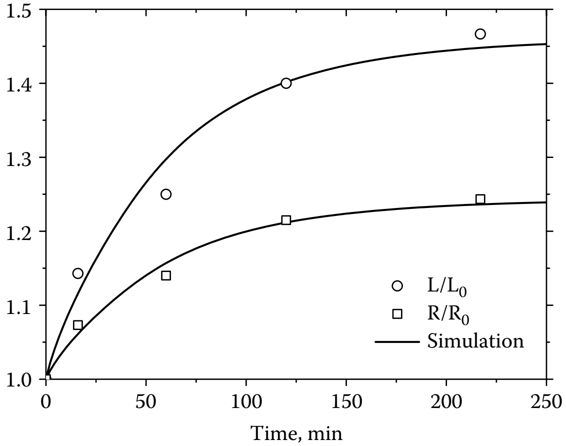

FIGURE 7.9 Kinetics of the increase in dimensions of EPDM rubber discs with 10% peroxide. Experiments (dots); calculated (full line). (With permission of Elsevier, Figure 5 in *Polymer*, 2002, 43, p. 4261 K. Azaar, I. D. Rosca, and J. M. Vergnaud.)

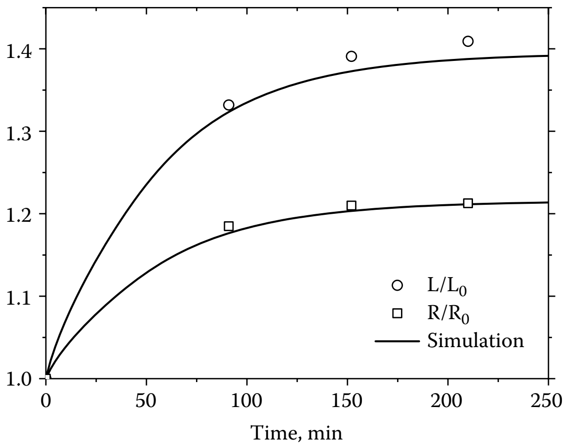

FIGURE 7.10 Kinetics of the increase in dimensions of EPDM rubber discs with 20% peroxide. Experiments (dots); calculated (full line). (With permission of Elsevier, Figure 6 in *Polymer*, 2002, 43, p. 4261, K. Azaar, I. D. Rosca, and J. M. Vergnaud.)

iv. Of course, the kinetics of swelling expressed in terms of volume is located between the other kinetics describing the change in dimensions of the thickness and of the radius, with the following ratio:

$$\left[\frac{R_t}{R_0}\right]^2 \cdot \left[\frac{L_t}{L_0}\right] = \left[\frac{V_t}{V_0}\right] \tag{7.32}$$

v. The anisotropy of these rubber discs, the swelling being larger in the thickness than in the radius, whatever the percent peroxide used for the cure, may be explained by an orientation of the macromolecules along the flat parallel faces of the discs, which is obtained during the cure when the rubber is pressed into the slabs of the mold.

TABLE 7.5

Parameters Used for Calculation the Kinetics of Swelling

Increments	Isotropic	Anisotropic
Δr	1	0.853
Δx	1	1.353

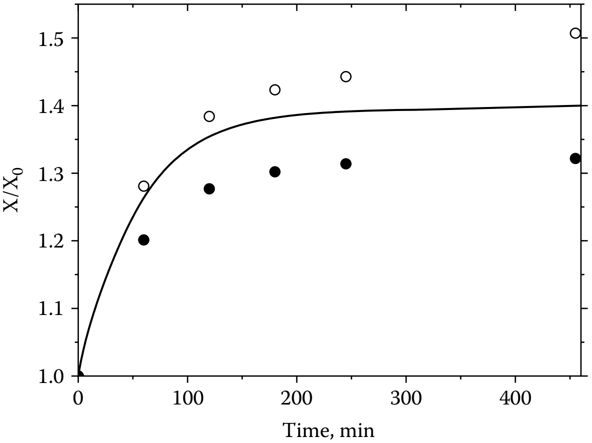

FIGURE 7.11 Kinetics of increase in dimensions of EPDM rubber disc with 2% peroxide obtained by considering the rubber disc either isotropic or anisotropic towards swelling. Kinetics of change in volume (full line), in the thickness (white) and in the radius (black). (With permission, Institute of Materials, Minerals and Mining, original publication, Figure 4 in *Plastics, Rubber, and Composites*, 2002, 31, 220, K. Azaar, I. D. Rosca, and J. M. Vergnaud.)

7.5 DRYING OF RUBBERS CONTAINING A LIQUID

As shown in Reference [6], a book devoted to the subject of drying polymers and rubbers the process is rather complex. In fact, the process of drying a rubber is controlled either by diffusion of the liquid through the solid or by evaporation of the liquid in the vapor state at the surface. The diffusivity can be concentration-dependent when the liquid concentration in the rubber is large or constant when this concentration is small. The rate of vaporization appears in the coefficient of surface convection in Equation 7.8.

Thus, the process is defined for a sheet by the following two equations:

$$\frac{\partial C}{\partial t} = D \cdot \frac{\partial^2 C}{\partial x^2} \tag{7.4'}$$

$$-D \cdot \frac{\partial C}{\partial x} = h \cdot (C_s - C_{ext}) \quad surface \tag{7.8}$$

where the coefficient of surface h is equal to the rate of drying of the liquid in pure state, C_s represents the surface concentration of the liquid in the rubber, and C_{ext} is the surface concentration of the liquid required to maintain equilibrium with the surroundings. Of course, in the case of the external atmosphere constantly free from vapor, there is:

$$C_{ext} = 0 \tag{7.33}$$

In fact, in order to get the surrounding atmosphere free from vapor, it is necessary to stir the solid surface so as to eliminate the vapor from the rubber surface.

As the evaporation is endothermic, the surface of the rubber is cooled differently during the stage of drying, depending on the rate of evaporation.

The problem cannot be resolved mathematically, and a numerical model taking into account the following stages: the diffusion through the thickness of the rubber, evaporation at the surface, and change in dimension of the rubber sheet, should be built and tested.

The results concerned with the process of drying are usually expressed either in terms of kinetics of drying, i.e., of loss of liquid, or of profiles of concentration developed through the rubber with the subsequent change in dimension.

7.5.1 OPERATIONAL CONDITIONS

An example is shown, drawn from a recent paper [16] where EPDM rubbers cured separately with 2% and 10% peroxide are submitted to the stages of absorption of toluene up to equilibrium, followed by the stage of drying. These two rubber discs, 0.235 cm thick, cured at 187°C so as to have a state of cure of 90% and 96%, are immersed into toluene over more than 300 minutes, this time being necessary to attain equilibrium with a flat profile of liquid concentration through the thickness of the discs. These discs presaturated of toluene are thus exposed to air at room temperature (25°C) with a slight agitation.

7.5.2 EXPERIMENTAL RESULTS AND DISCUSSION

The results are given by way of two figures: Figure 7.12 for the kinetics of drying, where the ratio $\frac{M_t}{M_r}$ of the weight of liquid as a fraction of the weight of the rubber free from liquid is plotted as a function of time; and Figure 7.13 where the profiles of

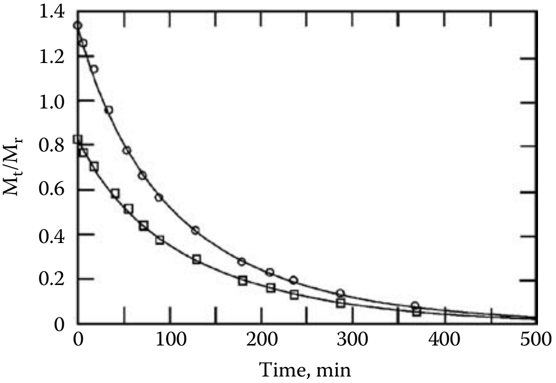

FIGURE 7.12 Kinetics of evaporation of toluene from the presaturated EPDM rubber discs for two types of rubbers, cured either with 2 or 10% peroxide. Experimental (dots); theoretical (full line). (With permission of RAPRA, Figure 6 in *Polymers and Polymer Composites*, 2000, 8, 325, K. Azaar, R. Granger, I. D. Rosca, and J. M. Vergnaud.)

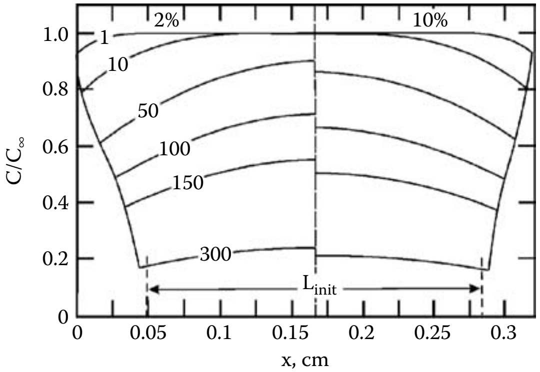

FIGURE 7.13 Profiles of concentration developed through half the thickness of the sheets, with the subsequent change in dimension, at different times. Left: rubber cured with 2% peroxide; Right: rubber cured with 10% peroxide. (With permission of RAPRA, Figure 3 in *Polymers & Polymer Composites*, 2000, 8, 325, K. Azaar, R. Granger, I. D. Rosca, and J. M. Vergnaud.)

concentration of liquid are drawn at various times, as well as the subsequent shrinkage of the rubber. Some results are worth noting:

i. The kinetics of evaporation are described by the process of diffusion through the solid, with a finite rate of evaporation. Thus, at the beginning of the stage, there is an oblique tangent for these two kinetic curves.
ii. The values of the diffusivity are the same for the stages of absorption and desorption in these two rubbers. As precisely shown in Reference [6], the diffusion of the liquid through the rubber thickness is similar during these two stages.
iii. Moreover, the diffusivity is nearly the same, whatever the percentage peroxide.
$D = 2.7 \cdot 10^{-6}$ cm^2/s for 2% peroxide $D = 2.5 \cdot 10^{-6}$ cm^2/s for 10% peroxide
$h = 5 \cdot 10^{-3}$ cm/s
iv. Similar kinetics of absorption and of desorption are obtained when these two rubber compounds are cured with either 90% or 96% for the state of cure.
v. The profiles of concentration developed through the thickness of the sheets lead to some observations: the rate of evaporation of the liquid is finite; a decrease in the thickness of the sheets is observed during this stage. The time necessary for the stage of desorption is longer than that of absorption, resulting from the rather low rate of evaporation of toluene.
vi. The kinetics obtained by calculation and experiments are in good agreement, as shown in Figure 7.12. And, finally, at the end of this stage of evaporation, the thickness of the rubber sheet is equal to that of the rubber before the stage of absorption.
vii. Half the thickness of the two different sheets is shown in Figure 7.13, as this is made possible because of the symmetry. Moreover, this presentation makes easy the comparison for the sheets cured either with 2% or 10% peroxide.

7.6 PERMEABILITY OF RUBBERS TO VAPORS AND GASES

7.6.1 PRINCIPLE OF THE TRANSFERS

As pointed out in Reference [1], rubbers are by no means impermeable to vapors and gases, although in many cases the rate of transmission is low and slow. In a number of applications even a small loss of gas may be important, for example, tires, and consequently the rate of transmission needs to be measured. Gas or vapors can flow through a rubber in the same way as does a liquid, by following the slight motions of segments of the polymer.

7.6.2 THEORETICALS OF THE PROCESS

The process can be considered as the flow of the diffusing substance through a membrane. If one face $x = 0$ of the membrane is kept at a constant concentration C_0 and the other $x = L$, C_L, is maintained at 0, and the membrane is initially free from this substance, the equation of diffusion 7.4′ applies:

$$\frac{\partial C}{\partial t} = D \cdot \frac{\partial^2 C}{\partial x^2} \tag{7.4′}$$

With the boundary conditions, written as follows:

$$x = 0 \quad \mathrm{C} = C_0 \quad \text{and} \quad x = L \quad C_L = 0 \tag{7.34}$$

and the initial conditions $0 < x < L \;\; C_{x,0} = C_{in} = 0$
the solution of the problem is given by Equation 7.35 for the profile of concentration developed through the thickness of the membrane [4–6,19,21]:

$$\frac{C_{x,t}}{C_0} = 1 - \frac{x}{L} - \frac{2}{\pi} \cdot \sum_{n=1}^{\infty} \frac{1}{n} \cdot \sin \frac{n \cdot \pi \cdot x}{L} \cdot \exp\left[-n^2\pi^2 \frac{D \cdot t}{L^2}\right] \tag{7.35}$$

The amount of substance that emerges at time t from the external face, at $x = L$, is M_t:

$$\frac{M_t}{C_0} = \frac{D \cdot t}{L} - \frac{L}{6} - \frac{2L}{\pi^2} \cdot \sum_{n=1}^{\infty} \frac{(-1)^n}{n^2} \cdot \exp\left[-n^2\pi^2 \frac{D \cdot t}{L^2}\right] \tag{7.36}$$

As the concentration of substance through the membrane varies with space x and with time t, the process is said to be run under transient conditions.

After infinite time, or rather a time long enough so that the series in Equations 7.35 and 7.36 vanishes, the steady state is attained, and the simple equation is obtained:

$$M_t = \frac{D \cdot C_0}{L}\left[t - \frac{L^2}{6D}\right] \tag{7.37}$$

the slope of which is:

$$\text{Slope} = \frac{M_t}{t} = \frac{D \cdot C_0}{L} \tag{7.38}$$

and the intercept on the time-axis is:

$$t_i = \frac{L^2}{6D} \tag{7.39}$$

For a gas or a vapor, the surface concentrations C_0 and C_L may not be known but only the gas or vapor pressures P_0 and P_L on the two sides of the membrane. The rate of transfer in the steady state is then sometimes written:

$$F = Per \cdot \frac{P_0 - P_L}{L}, \tag{7.40}$$

Per, being the permeability of the membrane. Here, *Per* is expressed, in the CGS system often used in problems of diffusion, as cm^3 gas, at standard temperature and pressure, passing per second through 1 cm^2 of the surface of the membrane 1 cm thick when the pressure difference across the membrane is 1 cm of mercury.

When the diffusivity is constant, and there is a linear relationship between the external vapor pressure and the corresponding equilibrium concentration within the membrane, then the Equation 7.40 is equivalent to the equation written in terms of the concentrations:

$$F = -D \cdot \frac{\partial C}{\partial x} = D \cdot \frac{C_0 - C_L}{L} \tag{7.41}$$

The linear isotherm may be written for the vapor or gas:

$$C = S{\cdot}P \tag{7.42}$$

where C is the concentration within the rubber in equilibrium with the external pressure P.

Thus, with due regard to units, it comes:

$$Per = D{\cdot}S \tag{7.43}$$

or in other terms, the permeability is proportional to the diffusivity D and to the solubility S of the gas or vapor.

7.6.3 MEASUREMENTS OF THE PERMEABILITY OF GASES

The traditional procedures for measuring gas permeability are widely and precisely described in a book devoted to the physical testing of rubbers [1]. They involve setting up a pressure differential across the test piece and measuring by change of pressure or volume the amount of gas passing the low pressure side of the membrane system.

7.6.3.1 Constant Volume Method

The apparatus necessary for the constant volume method is described in ISO 1399 [22] and BS 903, part A17 [23]. It consists of a metal cell having two cavities separated by the test rubber sheet. The high pressure cavity is filled with the test gas at the required pressure, and this pressure is measured and should be kept constant during the measure. The increase in pressure on the low pressure side is measured as a function of time. The curve obtained follows the shape shown in Figure 7.14. Thus

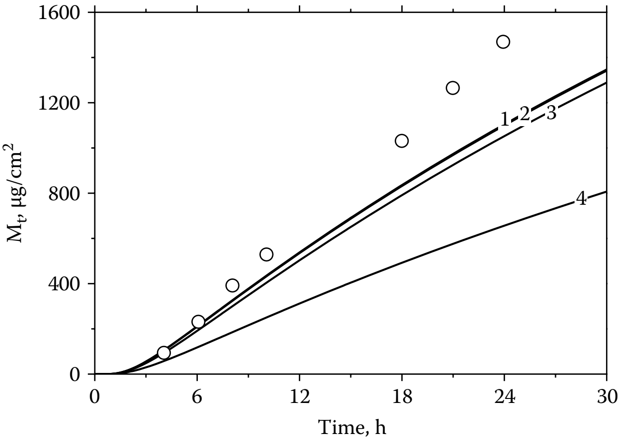

FIGURE 7.14 Kinetics of drug transfer through the skin using a patch (transdermal system) for various values of the diffusivity in the polymeric device. 1: $D = 4.4 \cdot 10^{-6}$; 2: $D = 4.4 \cdot 10^{-7}$; 3: $D = 2.2 \cdot 10^{-8}$; 4: $D = 4.4 \cdot 10^{-5}$. Skin $D = 2.2 \cdot 10^{-8}$. Units of D are in cm^2/s.

after a time longer than t_1 defined by the Equation 7.39, a straight line is obtained whose slope is proportional to $D \cdot C_0$, that is, to the permeability Per of the rubber sheet of thickness L.

7.6.3.2 Constant Pressure Method

This apparatus is similar to that used in the constant volume method, the test rubber sheet dividing the cell into high and low pressure cavities. The difference is that the low pressure side is connected to a device to measure the volume increase as gas diffuses to the low pressure side while the high pressure is kept constant. In ISO 2782 [24] and BS 903, Part A30 [25], a graduated capillary tube is used to measure the volume change.

7.6.3.3 Carrier Gas Method

Various methods using a gas chromatograph allow measurement of the flux of gas diffusing through the membrane [1].

7.6.4 Measurements of the Permeability of Vapors

The dish method [1] is used for measuring the permeability of vapors, by detecting the quantity transmitted by change in weight. Such a method is detailed in ISO 2528 [26] for sheet materials in general and also in ISO R1195 [27] for plastics film and thin sheets.

7.7 CONCLUSIONS ON RUBBER RESISTANCE TO LIQUIDS

If it is true that, more often, it is desirable to have rubber with a great resistance to liquids, sometimes it is preferable to have rubber able to control the transport of the diffusing substance. This is the case with a transdermal system (patch) for drug delivery.

In the case of these transdermal systems, the drug is dispersed through a wide variety of rubbers, the first of which is able to contain the drug in the state of a gel, and another which is in contact with the skin, to say nothing of the covering membrane. The adhesive layer in contact with the skin should at the same time adhere strongly to the skin and be highly permeable to the drug. The property of the part that contains the drug should be able not only to contain a high concentration of drug but also to deliver the drug so that a constant drug concentration is maintained on the surface of the skin. The effect of the diffusivity of the drug through the patch is shown in Figure 7.14, where the amount of drug delivered into the patient's body through its skin is shown before entering the capillaries of the patient [21].

In a few words only, as this subject is outside the scope of this book, there are various advantages for these kinds of drug delivery systems:

i. Because the liver is bypassed, the first-pass hepatic does not play the role necessary in oral dosage forms, and the drug metabolism is reduced just to that which can enter through the skin.
ii. Treatment can be started and terminated at any time by applying the patch to or removing it from the skin.
iii. Constant concentration in the patient's blood is attained, avoiding the risk of over-dosage.

On the other hand, when different rubber compounds are cured together, as seen with the components of a tire made of rubber In various compositions, a diffusion of the active agent, at least at the interface, is of great interest, as it makes the binding of these components more efficient. As shown in Section 7.3, it is possible to increase and control this diffusion phenomenon.

REFERENCES

1. Brown R.P. 1979. *Physical Testing of Rubbers*, Applied Science Publishers, London.
2. Flory P.J. and J. Rehner. 1943. Statistical mechanics of synthetic tire rubber. *J. Chem. Phys*. 11: 521–26.
3. Hands D. and F. Horsfall. 1980. A new method for simulating industrial cure processes. *Kautschuk Gummi Kunststoffe*. 33: 440–46.
4. Crank J. 1975. *The Mathematics of Diffusion*, Clarendon Press, Oxford, U.K.
5. Vergnaud J.M. 1991. *Liquid Tansport Processes in Polymeric Materials*, Prentice Hall, Englewood Cliffs, NJ.
6. Vergnaud J.M. 1992. *Drying of Polymeric and Solid Materials*, Springer-Verlag, London.
7. ISO 1817. 1975. Resistance to Liquids. Methods of Test.
8. BS 903 Part A 16. 1975. The Resistance of Vulcanised Rubber to Liquids.
9. Brown R.P. 1970. RAPRA Research Report No. 191.
10. ASTM DI 1460. 1960. Change in Length during Liquid Immersion.
11. Brown R.P. and W.L. Jones. 1972. *RAPRA Bulletin* No. 42.
12. Brown R.P. and R.C. Hughes. 1973. *RAPRA Members Journal*, (February 1973). 194.
13. Bakhouya-Sabbahi N., J. Bouzon, and J.M. Vergnaud. 1994. Absorption of liquid by a sphere with subsequent change in dimension, with radial diffusion and finite surface coefficient of mass transfer. *Plastics, Rubber Appl*. 21: 309–16.

14. Bakhouya N., A. Sabbahi, and J.M. Vergnaud. 1996. Diffusion of a liquid through an elastomeric polymer with change in dimension and concentration-dependent diffusivity. *Comput. Theoret. Polym. Sci.* 6: 109–15.
15. Bakhouya N., A. El Brouzi, J. Bouzon, and J.M. Vergnaud. 1992. Process of absorption of a liquid by a thin sheet of polymer by considering diffusion and change in dimension. *Eur. Polym. J.* 28 (7): 809–15.
16. Azaar K., R. Granger, I.D. Rosca, and J.M. Vergnaud. 2000. Effect of the state of cure on the hardness and resistance to liquids of EPDM rubbers. *Polym. Polym. Composites*. 8(5): 325–31.
17. Ben Abdelouahab J., A. El Bouardi, R. Granger, and J.M. Vergnaud. 2001. Repairing broken thermoset pieces using diffusional pre-treatment and cure with uncured resin. *Polym. Polym. Composites*. 9(8): 515–22.
18. Azaar K., I.D. Rosca, and J.M. Vergnaud. 2002. Anisotropic swelling of thin EPDM rubber discs by absorption of toluene. *Polymer*. 43: 4261–67.
19. Vergnaud J.M. and I.D. Rosca. 2006. *Assessing Food Safety of Polymer Packaging, RAPRA Technology*, Smithers Rapra Ltd, Shawbury, Shrewsbury, SY4 4NR, U.K.
20. Azaar K., I.D. Rosca, and J.M. Vergnaud. 2002. Anisotropic behaviour of thin EPDM rubber discs towards absorption of toluene. *Plastics, Rubber Composites*. 31: 220–5.
21. Vergnaud J.M. and I.D. Rosca. 2005. *Assessing Bioavailability of Drug Delivery Systems*, CRC Press, Taylor & Francis, Boca Raton, FL.
22. ISO 1399. 1976. Determination of Permeability to Gases—Constant Volume Method.
23. BS 903, Part A 17.1973. Determination of the Permeability of Rubber to Gases (Constant Volume Method).
24. ISO 2782. 2006. Rubber, Vulcanized or Thermoplastic. Determination of Permeability to Gases.
25. BS 903, Part A 30. 1975. Determination of the Permeability of Rubber to Gases (Constant Pressure Method).
26. ISO 2528. 1974. Sheet Materials—Determination of Water Vapour Transmission Rate—Dish Method.
27. ISO R1195. 1970. Determination of the Water Vapour Transmission Rate of Plastics Film and Thin Sheets.

NOMENCLATURE

A	area through which the matter diffuses
$A(u,t)$	area of the sheet at time t, for the surface expansion in Equation 7.26
α	defines in Equation 7.31 the concentration-dependency of diffusivity
β	term used in Equation 7.13
C	concentration of matter
C_s, C_{ext}	concentration on the rubber surface, in the surrounding, respectively
C_{in},$C_{x,t}$,C_∞	concentration of liquid, initial, at position x and time t, at infinite time
$C(u,t)$	concentration of liquid at position u and time t, in Equation 7.18
D	diffusivity
Δr,Δx	increments of space for calculation, in Table 7.5
$F_{x,t}$	flux of matter at position x and time t
h	coefficient of surface convection of matter
K	dimensionless number defined in Equation 7.14

L	half the thickness of the sheet in Equation 7.7
L_0,L_t	half the thickness at time 0, at time t, in Equation 7.32
M_t,M_∞	amount of liquid transferred at time t, at infinite time
Per	permeability to gas, in Equation 7.40
P_0,P_L	pressure of a gas at position 0, at position L, in Equation 7.40
R_0,R_t	radius at time 0, at time t, in Equation 7.32
r	radius of a spherical membrane with liquid in it, in Equation 7.19′
r	radial abscissa
S	solubility of a gas or of a vapor, in Equation 7.42
t	time
u	radius of spherical membrane free from liquid, in Equation 7.19
$V(u,t)$	volume of the rubber at time t with liquid in it (Equation 7.19′; 7.27)
V_0,V_t	volume at time 0, at time t, in Equation 7.32
x	abscissa characterizing the position

8 Methods of Recycling Waste Tire Rubber

8.1 GENERAL CONSIDERATION

Recycling waste rubber is a very important problem, in theory as well as economically and practically. For many years, in addition to industrial applications, theoretical studies have been carried out and sometimes developed, which would require a book exclusive to this work to describe adequately. Thus, in Chapter 8, we will focus on presenting a description of the trends in recycling up to 1974, followed by a few applications done afterward. Thus, it will be possible to visualize somewhat the scale and complexities involved.

Among the various origins of scrap rubber, those coming from tires are the most important. Thus, over the past few years, considerable attention has been given to the rubber industry's problem of disposing of this scrap.

There are various ways to recycle waste tire rubber. The first approach consists of reducing the tire rubber into scrap rubber. Sometimes, before retreading old tires with new rubber, the part of the tire that needs extracting is converted into scrap.

The cryo-grinding process is the first preference [1], the low temperature preventing the chemical-related degradation of polymer chains. Moreover, the rubber powder should preferably be ultrafine [2].

Disposal of worn-out tires and rubber products is a global problem with the main complications being that they are not biodegradable; as they are chemically cross-linked, they cannot be reprocessed like thermoplastics.

Attention will be focused on the direct cure of scrap rubber, even if the final materials are of poor quality. The properties of these second-hand materials will be measured so as to find applications of interest.

8.2 SCRAP TIRE DISPOSAL IN PREVIOUS STUDIES BEFORE 1974

8.2.1 PROBLEMS SET DOWN BY SCRAP TIRE DISPOSAL IN 1974

Several decades ago, attention had already been called to the very complicated nature of the entire disposal problem [3]. It has been said that the whole field of scrap-tire disposal is full of alternatives, compromises, legislation, and conflicting reports on technological success. An "ideal solution" would have to be based on following:

i. Waste rubber disposal processes should have no adverse effect on our environment.
ii. Preferably, the processes would conserve our natural resources via recovery and recycling raw materials.

iii. The processes should have minimum adverse impact on established industries, consistent with conservation and recycling objectives.
iv. The processes should be adapted to widespread use, and products should have commercial value.
v. Minimum cost is required to be truly competitive in our economic system.

Consequently, the following applications were presented, depending on the possible types of applications.

8.2.2 PHYSICAL APPLICATIONS

1. *Oil spills.* Shredded rubber tires in combination with polystyrene scrap have such a good capacity for absorbing oil that they have been suggested for cleaning up oil spills. After absorbing oil, the mixture is heated to form an asphaltic material that was claimed to be useful for road building [4] to avoid a secondary disposal problem.
2. *Synthetic turf.* The feasibility of using shredded scrap rubber as a component in synthetic turf for play grounds, factory floors, and park paths had also been investigated. The product Tire Turf was prepared by mixing shredded scrap tires with a binder such as polyurethane, latex, or asphalt [5], and laid like concrete. The turf covered with a fireproof material is stated to be both fungus- and rot-proof. The turf may be painted and is also porous so that water passes through for good drainage.
3. *Artificial reefs.* The use of bundled, whole scrap tires, were recommended to build artificial fish reefs [5]. Whole scrap tires, when immersed in the ocean, are rapidly encrusted with barnacles and other stationary marine life. The tires form an artificial reef which is as attractive to many fish as a natural coral reef. Protecting small fish, they provide good breeding grounds for smaller species which in turn provide food for larger fish. Thus, an ocean desert can be converted into a productive area. No toxic effects have been observed from the use of tires as fish reefs, leaching of minerals or oil from the tire being apparently prevented by the encrustation by stationary marine life.
4. *Highway abutments.* An approach to solving a safety problem by utilizing whole scrap tires was possible [5] by constructing highway abutment crash barriers made of whole scrap tires. If effective, driver fatality or severity of injury could be significantly reduced.
5. *Asphalt component.* Considerable effort has been devoted to the use of scrap tires in asphalt roads, the beneficial effect resulting from the tremendous volume which could be potentially used. Ground scrap rubber or reclaimed rubber in asphaltic paving has no appreciable beneficial effect on the durability of the asphalt pavement. However a process consisting of heating asphalt to 350–400° F and adding up to 25% of 16–25 mesh ground scrap rubber, with addition of 5.5–7.5% kerosene leads to a material able to be sprayed [6].

6. *Road base.* Another approach to the use of ground scrap rubber as a road building component was reported [6] by blending equal volumes of ground scrap rubber, sand, and emulsified asphalt.
7. *Concrete component.* Formulating ground scrap rubber in concrete gives a product of lower density than regular concrete (with poorer abrasion and poorer compression resistance), which could be cut with a saw. Rubberized concrete could find applications in architectural buildings where light weight and ease of fabrication are important [3]
8. *Sound attenuation.* An application of ground scrap rubber reduces noise due to its sound-attenuating property [3].
9. *Erosion control.* According to some references, it was suggested that whole scrap tires could be interlinked with metal clamps or other suitable means to form a mat, which could then be installed on specific areas susceptible to erosion [3,7].
10. *Splitter industry.* The splitter industry utilizes scrap tires that are rejected by retreaders. The splitter process consists of debeading the scrap tire and peeling off most of what remains of the tread. The remaining carcass is usually split into a tread section and two sidewall sections. These sections are then cut or punched in dies to form useful articles such as gaskets, shims, or ribbons from which door mats or dock bumpers are fabricated [3].
11. *Roof coatings.* The use of ground scrap rubber in asphalt for roof coating may be an outlet for scrap tires. A beneficial effect is expected to reduce the tendency of the coating to crack, the presence of the scrap rubber preventing crack propagation by elastic interference. Of course, if the scrap rubber/asphalt were treated with flame retardants the mixture would be an ideal coating. Good results have been reported on using an asphalt/rubber mixture for repairing an asphalt roof as well as sealing the flashing around chimneys.
12. *Antislip applications.* Ground scrap rubber embedded into a suitable matrix should have good antislip properties. Possible use around swimming pools represents the first effort in this application area [4].
13. *Retread industry.* Retreaded tires basically extend the useful life of the original tire and thereby tend to alleviate the scrap tire disposal problem. The retread industry would be of interest for the nonpassenger-tire segment (e.g., trucks, buses). It is obvious that if additional retreaded tires were used, the problem of scrap tire disposal would be further reduced, and a more efficient utilization of the natural resources would be realized. Based on the use of retreaded truck and airplane tires, it is technically and economically feasible to utilize retreaded tires. However, the general public considers a retreaded tire an inferior product, which is true to some extent; and, moreover, for a good quality retreaded tire, a sound tire carcass is needed [3].
14. *Trivial uses.* Some trivial uses are obvious in spite of the fact that volume requirements are expected never to be large. Examples are bumpers for small watercraft, fabrication of sandals, children's swings, flower planters, sling shots, pole guards, etc.

8.2.3 FUEL VALUE AND INCINERATION

Pollution-free direct-flame incineration offers an immediate solution to the problem of disposing of scrap tires and discarded rubber goods. Initial work on the incineration of scrap tires was conducted in England by RAPRA [8]. Disposal of used tires by this system offers the most practical solution to date to solve an immediate, pressing problem. The volume of scrap tires is drastically reduced to a sterile ash of 5% of the original weight; the gaseous by-products are carbon dioxide, water vapor, and traces of carbon monoxide. Proven technology for the removal of sulfur oxides from the stack gas is commercially available. The following design parameters must be considered for tire disposal: agitation, temperature, adequate air supply, residence time, environmental controls, mechanical stability, and the capability of incinerating an auxiliary waste oil stream.

Agitation, which is a very important design feature in any tire-burning incinerator, is usually accomplished by using a moving or rotating chamber.

However, it is believed that incineration of scrap tires is not the most desirable long-run approach when the total natural resource situation is considered. Scrap tires, a discarded resource rich in hydrocarbons, should be returned to the production cycle as useful materials, such as reclaim, reinforcing carbon black, and carbon compounds that could be chemical feed stocks. This last approach would conserve gas and oil reserves.

8.2.4 CHEMICAL APPLICATIONS

8.2.4.1 Reclaiming

Up to the time of World War II, scrap tires contained only natural rubber. Reclaiming processes were well established, and a reasonable proportion (20%) of reclaim was accepted in compounding of new tires. (Frequently, the percentage was much more in other rubber products.) In 1941 the consumption of reclaim was 32% of the consumption of new rubber.

As emulsion SBR replaced natural rubber in tires, the “devulcanization” and depolymerization stage of reclaiming technology had to change. Preparation of the feed, natural or synthetic, was essentially the same. The steps with scrap tires were removal of the metal bead, size reduction with cracking rolls or hammer mills, separation of all parts of the fiber, and grinding. The big change was in the devulcanization stage, as natural rubber and SBR vulcanizates did not respond in the same way. Natural rubber softens with heat, and heat alone can give a satisfactory reclaim, whereas SBR vulcanizates, after an initial softening with heat, quickly hardening on further heating. The alkaline process, which destroys the fabric and thus could combine defibering and devulcanization of natural rubber scrap in one step, caused a hopelessly rapid hardening of SBR vulcanizates. Because of the hardening of SBR materials, it was necessary to change the devulcanization step so that they respond in about the same way as natural rubber. Separate reclaim processes for natural and SBR were not practical, and moreover, these two types of scrap generally occurred together in the same pile of scrap tires and even in the same tire. The need for modifying the heat-softening step was met by development of various reclaiming chemicals. These developments were described in a review [9].

The significant reclaim processes in use in 1974 were the digester process, heater process, and mechanical processes [3]. But there were at that time numerous variations and combinations of these. All have similar finishing steps. The reclaim is usually further compounded, refined on tight mills, and strained to remove foreign solids.

The reclaiming industry in 1974 was in an era of decline that started about 1960. Total production of reclaim, usage of installed reclaiming capacity, and proportion reclaimed of the available scrap all fell during this period.

8.2.4.2 Pyrolysis

Pyrolysis, or the destructive distillation of scrap tires, has been proposed as a means of converting scrap tires to useful products. Pyrolysis in the absence of air is not a new technique. It was, and still remains, used as a powerful investigative tool.

Pyrolysis of scrap rubber may be conducted under significantly varied conditions of time, temperature, and pressure. It may be effected under reductive or oxidative conditions which in turn could be catalytic or noncatalytic. In considering scale-up, engineering alternatives are more important than in most chemical processes. For example, product yield and quality would be expected to be different in batch operation from that in continuous operation.

Pyrolysis of scrap tires gives as major products, gas, oil, and residue. The gas is the result of thermal cracking and dehydrogenation. The oil derives from extender oils used in the compounding of the vulcanizates as well as from the depolymerization fragments from the rubber. The residue represents recovered carbon black as well as any inorganic material used in the fabrication of the original rubber.

8.2.4.3 Carbon Black Manufacture

Some work was done on the development of a process for the utilization of scrap rubber as feed for carbon black. Ground scrap rubber, presumably fabric-free, is heated with conventional carbon black feed stock oil, and the mixture utilized in a conventional furnace type carbon black reactor. Apparently, this process is not economically attractive.

8.2.4.4 Biodegradation

Many naturally occurring polymers, such as cellulosics, animal, or plant proteins, etc., are readily attacked by a host of microorganisms in the soil, and are quantitatively degraded in relatively short periods of time. The microorganisms utilize the carbon content of these polymeric materials as a source of food and energy. As early as 1914, it was recognized that natural rubber was attacked by microorganisms. Many waste disposal processes are adaptations of natural biodegradation processes. It can be generally concluded that man has been somewhat less successful in his attempts to biodegrade the many elastomers that he has invented.

In view of these natural examples, it followed to study fermentation as a means of disposing of the vast quantities of scrap rubber arising from scrap tires. Most of the investigations were concentrated on attempts to degrade rubber with either yeasts or fungi as shown in Reference [3], a significant paper.

Yeasts appeared to metabolize the rubber without becoming physically attached to the rubber substrate, and they could be separated from the remaining rubber particles by washing. Fungi, on the other hand, became firmly bound to the rubber substrate and could not be removed by any physical treatment. Chemical digestion with hydrochloric acid, followed by digestion in hydrogen peroxide was necessary to completely remove the fungal mycelia.

Several physical and chemical changes in the rubber substrate were detectable at the conclusion of the fermentations, as a reduction in particle size.

The major factors that appear to retard the utilization of rubber by microorganisms have been assessed individually: rubber vulcanizates are hydrophobic substances that are subject to attack only at the surface; these materials are highly crosslinked and branched, and the branched structures are not conductive to biodegradation, as shown with detergents; rubber vulcanizates contain a large number of biologically active additives which retard biodegradation; finally, any scrap disposal process which depends on scrap tires as a source of raw material is dependent on a variable material.

In conclusion, it was said [3] that partial biodegradation of rubber leading to potentially useful products is technically feasible. Economically, such an approach will have to wait for significant changes in the present needs for the products of this type of process.

8.3 RECLAIMING PROCESSES IN PROGRESS

A few examples of reclaim process of scrap rubber are briefly described. However important they may be for either the quality of the process or for the amount of rubber reused, they should not be considered as a limitation in the possibilities.

8.3.1 Artificial Reefs and Highway Abutments

A discussion presented on the use of scrap tires for artificial fish reefs construction, and opposition has been carried out on this application [10]. A few years latter, it was said that some value is recovered from around 70% of the tires, with the rest going to the landfill. But in Europe, the Landfill Directive bans the disposal of shredded tires in landfills after July 2006 [11].

For highway crash barriers, the same Landfill Directive stands [11].

8.3.2 Asphalt Component and Road Base

Mixing of ground scrap rubber in asphalt was used to resurface roads in 1972 [6]. Quite recently, an overview is presented of the state-of-the-art of the asphalt-rubber production technology, and factors influencing bitumen properties are discussed [12].

Blending of waste rubber with asphalt for road building enhances the road's resistance to deformation [13]. The granulation is accomplished using a knife disintegrator, which gives particles of irregular shape and rough surface that are most suited to this process. Two processes are employed for blending the ground rough surface into the asphalt. In the wet process, the rubber is mixed with the asphalt at 170–220°C, with a typical addition of 14–20%. In the dry process, the rubber replaces part of the aggregates, and is mixed with the mineral before the latter is mixed with the asphalt. The addition of rubber particles to the asphalt gives a considerable increase in viscosity, improves the elasticity of the binder, and lowers its brittle point. Rubber-modified asphalts offer the considerable benefit of enhanced stiffness at elevated temperatures. The optimum rubber addition is 5%, and compositions with contents of 15–20% are generally very stiff. The surface is more durable, and it is possible to use thinner layers.

Recycling still struggles to make financial sense. Recycled rubber is proved to be just as versatile as the virgin material [14]. Rubber-modified asphalt is more durable and provides a quieter, smoother ride than conventional road-paving materials. Scrap tire chips in civil engineering applications afford highway and construction engineers a lightweight fill material with superb strength, durability, and drainage. Even more promising are the fine-mesh recycled rubber powders that allow rubber manufacturers to have 10% or more recycled content in their products while cutting costs and maintaining, or even enhancing, the properties of the products.

Possibilities of ground tire rubber recycling are enhanced with trans-polyoctenamer (TOR) [15]. The particular chemical properties of TOR facilitate coating of the surface of ground rubber waste by a simple technique. Moreover, the modified ground rubber can be directly molded into new rubber compounds. The ability of the TOR to crosslink the ground tire rubber (GTR) to the asphalt provides a rubberized matrix in the asphalt that prevents premature cracking, cutting, and shoving.

Mechanical properties of asphalt can be improved [16] by modification with some polymers, especially stirene-butadiene-stirene (SBS) tri-block copolymer. SBS/asphalt blends are prepared via dynamic vulcanization. Recycled tire crumb rubber is incorporated as a major component in its multi-layer construction [17] for a stadium field-turf.

Keeping environmental and economic factors in mind, it was envisaged in a review [18] that the disposal problem could be solved by incorporating ground waste rubber into virgin polymer matrices. At the end of 2001, the Asphalt Rubber Technology service has reported to be planning to use crumb rubber in several applications in the construction of its new research facility [19].

8.3.3 CURE OF SCRAP RUBBER POWDER WITH ADDITION OF NEW RUBBER

As early as 1977, a molding composition processable into a vulcanized elastomeric article such as a solid rubber article was formed by mixing together previously vulcanized scrap rubber, a vulcanizing agent such as sulfur, and suitable quantities of accelerator and/or activator. The mixture is then vulcanized under heat and pressure. An alternatively preferred embodiment of the invention comprises the addition of a small amount of virgin rubber to the composition [20]. These scrap rubbers comprise any rubber material that have been previously vulcanized and discarded for various reasons, but they come more often from large potential sources of rubber, i.e., especially tires. The vulcanizing agent (e.g., elemental sulfur) is preferably employed in an amount ranging from about 1% to about 4 % by weight of the entire composition, but better results are obtained in an amount in the range from 1% to 2%. The amount of accelerator employed in the composition may comprise as much as about 2%, based upon the total weight of the composition. Vulcanization is accomplished at molding temperatures between about 310° and about 410° F, at pressures above about

1000 pounds per square inch, and for a period of time ranging from about 5 minutes to about 20 minutes. Mold time is obviously dependent upon size of the article. The best results are obtained for the temperature of 350° F for pressures as high as 4000 psi. The mechanical properties are as follows: Tensile strength: 720–750 psi; elongation at break: 140–170%; hardness: 67 with durometer A. Let us note that a vulcanizing molding composition processable into a solid rubber tire is obtained with about 94–99% scrap rubber, 1–4% vulcanizing agent, and 0.13–2% accelerator [20].

In another study, the ground reclaim rubber was blended with stirene-butadiene rubber and cured under pressure at 160°C. The cured sheets were silica-reinforced by soaking in tetraethyl ortho silicate, then in an aqueous solution of *n*-butyl amine catalyst, followed by heat treatment at 50°C. The tensile properties of the blends containing conventionally incorporated silica, with no coupling agent, were superior to those containing silica incorporated by the sol–gel reaction [21].

Scrap rubber in the form of regenerated whole tire crumb rubber, regenerated truck tire buffings and regenerated nonblack buffings was blended with NR and the cure characteristics and physical properties of the compounded rubber blends investigated using ODR. Reclaim rubber and regenerated crumb rubber were then compounded with virgin rubber for molding [22].

The effect of reusing ground flash and scrap rubber in parent rubber compound was evaluated as early as 1976 [23]. More recently, a somewhat similar study was made [24] on natural rubber containing 0–50 phr (per hundred natural rubber) of ground waste rubber (or devulcanizate rubber). The cure characteristics, swelling, and mechanical properties measured showed the following results: the cure characteristics, including scorch time and cure time decreased slightly with increasing rubber addition, and a slight increase in the minimum torque was observed; a decrease in swelling resistance was observed with increasing rubber addition; the tensile strength and the elongation at break decreased, while the tear strength significantly increased with increasing addition; the abrasion resistance increased on addition of ground waste. It was concluded that the addition of up to 10 phr did not significantly degrade the properties of natural rubber. Another study [25] was made by incorporating mechanically ground crumb rubbers having different mesh sizes into NR-based tire tread cap compound, and the properties of the tire treads investigated. The results are discussed in terms of minimum torque, Mooney viscosity, tensile strength, fatigue to failure, and abrasion resistance, as well as the effects of mesh size and volume fraction of crumb rubber on tire properties.

On the other hand, the mechanical properties of thermoplastic vulcanizates containing ground tire rubber have been investigated with the aim of increasing use of recycled rubber. The compositions tested included passenger car combined with EPDM, SBR rubber, isoprene rubber, and butadiene rubber. It was found that the particle size of the ground tire rubber had small effect on mechanical properties, but that the choice of the sulfur accelerator was significant [26].

Using powdered factory scraps in EPDM compounds, it was found that the cost-effectiveness of this operation depends upon the method of grinding the waste rubber. Also, the size and topography of the particles depend upon the grinding technique, and these characteristics play a vital role in controlling the composite properties [27].

Virgin EPDM rubber in a thermoplastic blend of polypropylene (PP) and EPDM rubber is substituted by ground EPDM vulcanizate of known composition, after which the mechanical properties of the compound are determined. Attempts to replace amounts greater than 45% fail due to processing difficulty [28].

The efficacy of polyurethane and styrene butadiene rubber (SBR) as binders for ground rubber prepared from waste tires was compared to a formulation of a compound developed without binder. Without binder, the effect of both sulfur and accelerator content on tensile properties are studied, as well as the effect of ageing on these properties [29]. The suggested uses of the unbound product include rubber blocks, and ballast mats for railway applications.

A possible way of recycling of ground tire rubber was followed by melt blending them into various thermoplastic matrices. The influence of this addition on technical properties like yield stress, Young's modulus, notched impact strength, and damping properties is determined. The effect of swelling the particles in paraffinic plasticizing oil is also evaluated [30].

Waste ground rubber tire powder was devulcanized and mixed with 30 per hundred rubber (phr) natural rubber to give satisfactory vulcanizate properties. An intermeshing counter-rotating twin-screw extruder with constant root and flight diameters of the screw was designed and installed for waste rubber recycling [31].

8.3.4 CURE OF SCRAP RUBBER POWDER WITHOUT ADDITION OF NEW RUBBER

Other works on the same line were done in succession in the early eighties. The objective was to develop a process to upgrade the value of scrap rubber by considering the rubber powder recovered from old tires as a raw material. On the whole, it consisted of vulcanizing the rubber powder with a compound made of ultrafine sulfur impregnated with a small amount of oil, without adding new rubber [32]). By keeping the vulcanization conditions constant (160°C, 10 min, 12.5 M Pa), and by using increasing percentages of vulcanizing agent, several materials with different properties were prepared. Moreover, the change in mechanical properties with the vulcanizing composition (sulfur, accelerator) was especially studied by considering the mechanical properties measured under static conditions such as the ultimate tensile strength and the hardness [32].

8.3.4.1 Vibration Isolation Rubber Sheets

On the other hand [33], the mechanical properties were also measured in dynamic conditions. This new objective was to find valuable application for rubber stocks prepared by curing rubber powder according to the method [32]. With the purpose to obtain materials able to act in vibration isolation in buildings, the results were concerned with not only the static but also the dynamic properties of these rubber-like materials for use in antivibration mountings.

A few results are thus given in terms of the static compression modulus which is expressed as a function of the pressure for different percentage of plasticizer with 2% sulfur in Figure 8.1 and with 5% sulfur in Figure 8.2. Moreover, the dynamic in-phase modulus E' is measured as a function of the forcing frequency for different scrap rubber vulcanized with sulfur in Figure 8.3, whereas the corresponding values

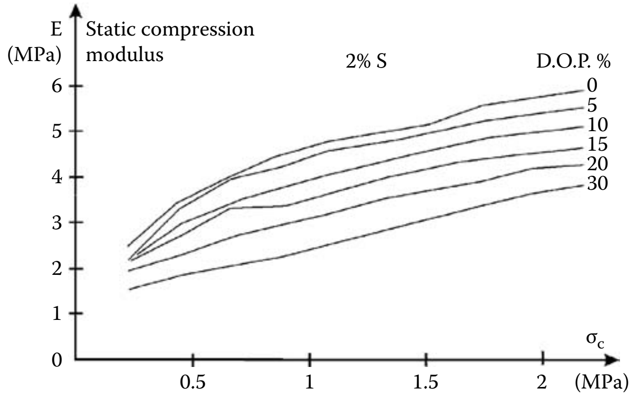

FIGURE 8.1 Static compression modulus E (MPa) as a function of pressure σ (MPa) for different percentages of plasticizer (DOP) cured with 2% sulfur. (With permission from *Rubber Chemistry and Technology*, copyright 1982, 55, 328, Figure 1. Vibration isolation properties of vulcanizates of scrap rubber powder. A. Accetta and J. M. Vergnaud, Rubber Division, ACS.)

of the loss factor are shown under the same conditions in Figure 8.4. The effect of percent sulfur on in-phase modulus appeared to be decisive when the sulfur percentage is more than 5, as shown in Figure 8.3. Three commercial rubber samples are also tested for comparison: L.R. (Linatex), rubber powder agglomerated with a thermosetting resin W (Massissol from Wattelez), and NO (Norsorex). Commercial samples made of vulcanized rubber W and NO have about the same E′ values as the other products within the 2–5% percent sulfur range. The loss factor β is dependent

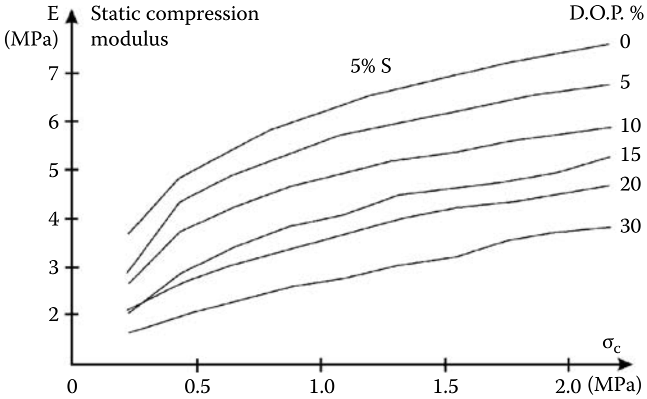

FIGURE 8.2 Static compression modulus E (MPa) as a function of pressure σ (MPa) for different percentages of plasticizer (DOP) cured with 5% sulfur. (With permission from *Rubber Chemistry and Technology*, copyright 1982, 55, 328, Figure 2. Vibration isolation properties of vulcanizates of scrap rubber powder. A. Accetta and J. M. Vergnaud, Rubber Division, ACS.)

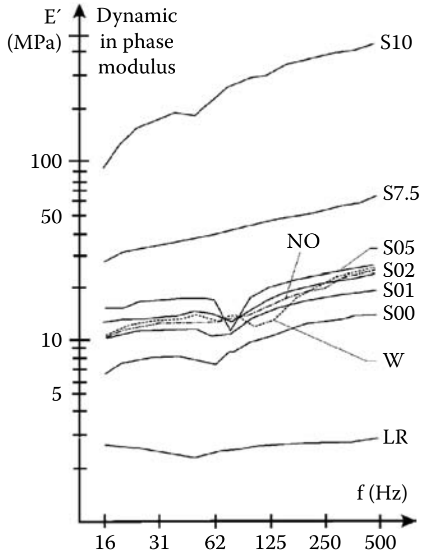

FIGURE 8.3 Dynamic in-phase modulus E′(MPa) as a function of forcing frequency (Hz) for different sulfur vulcanizates. Li: Linarex; W; Massissol; NO: Noretex; S00: 0% sulfur; S02: 2% sulfur; S07.5: 7.5% sulfur; S10: 10% sulfur. (With permission from *Rubber Chemistry and Technology*, copyright 1982, 55, 328, Figure 3. Vibration isolation properties of vulcanizates of scrap rubber powder. A. Accetta and J. M. Vergnaud, Rubber Division, ACS.)

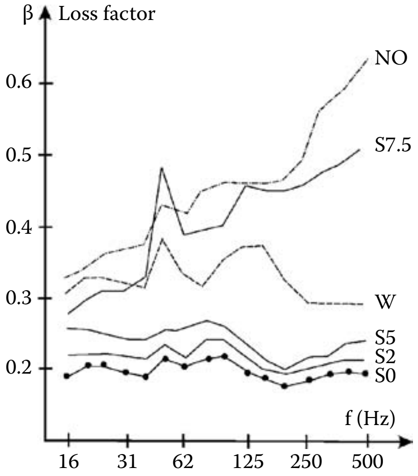

FIGURE 8.4 Loss factor β as a function of forcing frequency (Hz) for different sulfur vulcanizates. Li: Linarex; W; Massissol; NO: Noretex; SOO: 0% sulfur; SO2: 2% sulfur. S07.5: 7.5% sulfur; S10: 10% sulfur. (With permission from *Rubber Chemistry and Technology*, copyright 1982, 55, 328, Figure 4. Vibration isolation properties of vulcanizates of scrap rubber powder. A. Accetta and J. M. Vergnaud, Rubber Division, ACS.)

on both frequency and sulfur as shown in Figure 8.4. A significant increase in the loss factor is found when the percent sulfur is increased from 5% to 7.5% and 10%.

In terms of conclusions, rubber powder recovered from old tires is recognized as a valuable raw material that may be processed into useful products. Reference [33] exhibits the static and dynamic vibration properties of visco-elastic rubber materials, as well as their mechanical properties. At the optimum curing conditions (180°C, 10 min, 10 M Pa), the effect of sulfur and plasticizer on the vibration properties of the material are of interest. It is thus possible to prepare a material suitable for use in antivibration mountings, by choosing the right values of sulfur and plasticizer, according to the vibration characteristics of the machine (i.e., its mass and natural undamped resonant frequency).

8.3.4.2 Rubber Sheets Absorbing Impact Noises in Houses

Following this study on the cure of scrap rubber powder without addition of new rubber, a large range of cheap and rather good quality materials prepared with this method [34] have been used as resilient absorbing impact noises in houses. As a matter of fact, the desire to improve the comfort of housing and of working space led to stricter regulations, and so it was with acoustic problems concerning the transmission of noise in houses. Most of the materials used in order to reduce these harmful effects originated in the petrochemistry industry, including bituminous products and elastomers. A fact of interest is that the quantities required are quite important. In addition to the standard tests performed on the samples, such as static tests and dynamic tests, comparative tests on transmission of impact noises were achieved on a reduced-scale device. Acoustic pressure was measured inside a box isolated on 5 sides, with the sixth side undergoing periodic impact noises sustained by mean of the Impulse Precision Sound Level and Vibration Meter Type 2209 by Bruël-Kjaer (Copenhagen).

The tests conducted on a small scale were only comparative. The variation of acoustic pressure (dB) is plotted against the frequency [Figure 8.5]. Curve 1 is

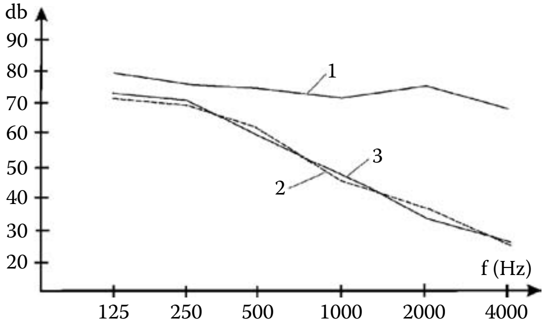

FIGURE 8.5 Acoustic pressure (dB) as a function of noise frequency (Hz). 1: original noise; 2: remaining noise with a standard material as damper; 3: remaining noise with a 2% sulfur sample as damper. (With permission from *Rubber Chemistry and Technology*, copyright 1982, 55, 328, Figure 4. Vibration isolation properties of vulcanizates of scrap rubber powder. A. Accetta and J. M. Vergnaud, Rubber Division., ACS.)

obtained without phonic isolation and curve 2 after phonic isolation by a standard material of 3 mm thickness, corresponding to French regulations on the damping of impact noise of floors in houses. Curve 3 is obtained after phonic isolation with the new product (3 mm thick, 2% sulfur). From these curves, in the usual 125 to 4000 Hz range, both materials exhibit the same absorption capacity of impact noises.

An industrial application of this process is found recently with Acoustik subflooring from Plate-Forme CPT Inc. of Canada, which is made from 100% recycled rubber and provides resistance to impact noise when installed under wood floors [35].

Another recent study was driven by pulverizing the granulates of waste rubber using a single-screw extruder in the solid state shear extrusion process, and by compressing in a mold this powder in the absence of virgin rubber. The slabs prepared in this way were subjected to mechanical and microscopic tests. Compressive creep of the powder, self-adhesion of the rubber molecules and interchange reactions of polysulfidic crosslinks were proposed as the basis of particle bonding [36].

More recently, UK developers Biotecture have designed a new housing estate using large amounts of scrap tires, expecting that the new homes will be highly energy efficient [37].

8.3.5 CONCRETE COMPONENT

In Long Beach, California, some of the concrete pavements are being replaced by recycled rubber. They have several advantages over the concrete they are replacing, including greater pedestrian safety and easier maintenance [38].

A professor has teamed up with an entrepreneur tennis player and also the California Department of Transportation to resurface a tennis court with rubberized concrete. It is said to be the first time that such a surface has been used [39].

8.3.6 PYROLYSIS OF SCRAP RUBBER

Scrap tires can be destructively distilled to give char, gas, and oil; the char can be ground to a carcass-quality carbon black, and the oil utilized as fuel or as a source of chemicals or tackifying resins [40,41]. The pyrolysis process was operated with success by using a fluidized bed, which is capable of having a uniform temperature distribution through the material [41]. Pyrolysis of old pneumatic tires was achieved in a fluidization semi-plant scale reactor [41] giving off up to 60% liquids, which consist almost totally of aromatic components. This vapor with a calorific power of about $45 \cdot 10^6\, J/\mathrm{m}^3$ is fully sufficient to work the equipment independently as for energy. As dimensions of pieces had astonishingly no effect on turbulence beds, it was possible to pyrolyze old pneumatic tires without crushing by correlative calibration of the turbulence bed.

On the whole, it could be said that the purpose of the operation was to consider the pyrolysis process as a source of chemicals either in liquid or gaseous state, as well as of char able to give carbon black [42–49].

A classical study was made to determine the domain of temperature for the pyrolysis to start, by using the loss in weight of the rubber scrap as a function of the temperature obtained with the technique of thermogravimetry with programmed temperature [50].

Another use of powders of rubber recovered from tires was presented, that is, transformation into loads of thermoplastics. The rubber should undergo a preliminary thermal treatment under nitrogen between 300 and 400°C for a few minutes, which provides a loss in weight of around 30%. Depending on the severity of the pyrolysis, the properties are different. The powder so-treated behaves as a compatible load with thermoplastics (PS, PVC, PE, PP) in the same way as a carbon black. It has interesting ultraviolet properties and tests carried out show that these powders can sometimes be better than carbon black in terms of anti ultraviolet [51]. Nevertheless, these loading powders were so poor that they cannot be used with rubber in the fabrication of tires in the same way as carbon black. More recently, using a similar technique, the solids obtained after pyrolyzation were used as filler for plastics [52,53] or even as substitute carbon black for virgin rubber compound [54].

In another work, rubber powders were examined successively by various ways: using scanning electron microscope, determining the surface-to-volume ratio by image analyzer with transmitted light illumination, nitrogen adsorption at liquid temperature using the Brunauer–Emmett–Teller method after degassing of the sample, and absorption of CTBA (acetyl trimethyl ammonium bromide). Difference in morphology between ambient and cryogenic crumbs was observed. As a result, surfaces around 0.15 m^2/g were found for these rubber powders [55]. It has been reported that cryogenic material is superior to reclaim, when the former is less than 250 microns, but at the same time as surface increases, or as particle size decreases, mixing behavior and vulcanizate mechanical performance are improved. Nitrogen adsorption surface areas are determined at the temperature of liquid nitrogen on the rubber crumb degassed for 24 hours at room temperature, rather that at elevated temperature as usual, to avoid loss of volatile components and sample modification. The results for the area of this material is around 0.12 square meter per gram, while high structure carbon black have a surface area in the range 100–150 m^2/g. The CTBA method for measurement of surface area is inexpensive, but equilibrium is only reached after more than ten hours shaking at room temperature; the adsorption isotherm is of type 1 with a plateau at a constant level.

The carbon blacks obtained by pyrolysis of special fractions of petroleum show typical properties, which are needed for reinforcing the rubber in tires, as shown in Reference [56] on this particular subject.

Recently, the carbon blacks, obtained by the pyrolysis of discarded tires and proposed for several years, have been evaluated. This process, run either at normal or reduced pressure, yields gas, oils, and chars. It was found that the carbon blacks obtained from the chars by most of the processes in operation worldwide have similar physico-chemical characteristics. Moreover, from the results published in a recent international conference devoted to this subject, it has been found that, due to their properties, these carbon blacks could be used to reinforce rubber, either alone or as additive to normal carbon blacks obtained as usual from pyrolysis of petroleum [57].

Concluding this way of reusing scrap rubber from tires, the observations made in Section 8.2.4 still stand: this process seems to be economically attractive only as long as there is a petroleum shortage.

8.3.7 Distribution of Scrap Rubber into Polymers

If the virgin rubber was considered as a potential matrix for the scrap rubber, the fine particles of this rubber waste has also been tested as an additive in polymers. Various examples following this way are examined.

Ground rubber tire was used as a partial substitute for EPDM rubber in modified EPDM—high-density polyethylene (HDPE) blends. The blends with higher rubber content showed poor processability, whereas the compositions with higher plastic content behaved like toughened plastics. It was observed that for the 60/40 rubber/plastic blend, 50% of EPDM could be replaced by the ground rubber without deterioration in properties [58].

Reactive mixing of crumb rubber with polypropylene by melting represents an innovative way of recycling old and waste rubber. A machine technology can easily be applied through injection molding. Results are examined for quasi-static and dynamic tests applied to the final materials. Moreover, the properties of this elastomer alloy remains constant after several recycling processes [59].

According to Reference [60], a sheet extruder has found a way to lower costs by compounding crumb rubber from recycled scrap tires into PE or PP, using a patented technology.

The role of compatibilization in the recycling of ground rubber from waste tires by blending with thermoplastics has been reviewed [61]. The principles of the methods involved are discussed: mechanical such as grinding, nonreactive such as the addition of block or graft copolymers, and by the addition of functionalized polymers. This compatibilization of blends of recycled high density polyethylene and ground rubber powder is improved by using gamma irradiation of the materials [62].

Thermoplastic elastomers were produced by blending low density polyethylene, fresh rubber, and ground tire rubber (GTR) in the weight proportion 50:25:25, with and without dynamic curing. Stirene butadiene rubber, natural rubber, and EPDM rubber were used as the fresh rubber fractions. The GTR was thermo-mechanically processed with and without the use of processing oil. Sulfur and peroxide agents were used for dynamic vulcanization. Samples were prepared by compression molding and assessed by dynamic mechanical thermal analysis, tensile testing, and measurement of compression set and hardness. The best results were obtained from the composition containing EPDM, GTR processed using processing oil, and dynamically vulcanized using sulfur [63].

8.4 TENTATIVE CONCLUSIONS ON TIRE RUBBER RECYCLING

Recycling waste tire rubber is such large a problem that it could be covered only by a book entirely devoted to the subject. Following the scope of the present book concerned with the cure of rubbers, only general considerations have been made by giving attention to applications employing, to some extent, the cure process.

The principles for reusing scrap rubber from tires could be established according to four criteria: amount of the rubber reused, simplicity in the process of reusing, production of material of value, and reduced pollution in the process. Another difficulty arises with the fact that better tires make recycling complex [64].

As for the amount of scrap rubber possibly reused, the method based on mixing the rubber powder with asphalt is surely of interest.

A very simple method of reusing old tires in landfills could have been a possibility. But in Europe, the Landfill Directive has banned the disposal of shredded tires in landfills since July 2006. It should be added that whole tires have been banned from landfills since 2003 [11]. Elsewhere, a high court directive [65] did not permit burning of scrap tires as a substitute fuel in cement kilns for pollution reasons.

When it comes to finding more complex systems of reusing the scrap rubber powder, recovery alternatives include pyrolysis, gasification, tire derived fuel, reuse and recycling, rubber reclaim, and retreading [3].

Pyrolysis of scrap rubber gives oil and char, from which carbon black can be obtained. The process has been tested on a small scale, more often on a laboratory scale, and sometimes on a large scale, and seems promising [57], in spite of the high quality required for the carbon black used to reinforce rubber, especially in tires [56].

The devulcanization and depolymerization processes have only been shown in brief in Section 8.2.4 [3,9].

Great attention has been given to the process of cure of scrap rubber obtained from tires, this cure being achieved in two ways: when the rubber powder is mixed with a fresh rubber [20–30]; when the rubber alone is cured at pressures higher than usual after addition of the appropriate curing agents [32–34]. In the second case, when the cure is made on the rubber powder without addition of fresh rubber, the typical properties of the final material seem to be promising in housing applications [32–37], such as vibration isolation rubber sheets and the absorbing-impact-noise rubber sheets.

Finally, it would be useful to cite the *Annual Buyer's Guide to Tire and Rubber Recycling Equipment* [66], which contains contact details and brief product information for more than a hundred companies, most North American, including manufacturers of primary and secondary tire shredding equipment, knives, and granulating and pulverizing systems.

REFERENCES

1. 2003. Hope for tired tyres. *Ind. Environ. Management.* 14(7): 10.
2. Swor R.A., L.W. Jensen, and M. Budzol. 1981. Ultrafine recycled rubber. *Rubber Chem. Technol.* 53: 1215–25.
3. Beckman J.A., G. Crane, E.L. Kay, and J.R. Laman. 1974. Scrap tire disposal. *Rubber Chem. Technol.* 47: 597–624.
4. Winkler J. Mar. 2, 1971. U.S. Patent 3,567,660. 1971. Oil cleanup method uses rubber wastes. *Chem. Eng. News.* 49(20): 29.
5. Anderson E.V.1972. Economics are bugaboo in scrap tire recycling. *Chem. Eng. News.* 50(33): 8.
6. Stokely J.A. and C.H. Mc Donald.1972. Hot rubber asphalt seal coats to cure cracking streets. *Pub. Works.* 103: 46–8.
7. Snyder J.D. and R.F. Hickox. 1969. Downwind, Akron stinks! Rubber disposal treadmill. Part 3. *Rubber World.* 161(5): 45–50.
8. Cheater G. and L.D. Loan. Technical Review (1966). Rubber and Plastics Research association of Great Britain. No. 37.

9. Le Beau D.S. 1967. Science and technology of reclaimed rubber. *Rubber Chem. Technol*. 40: 217–37.
10. Collins K. June 2002. Littoral sense. *Tire Technology Int*. 24–6.
11. Tyres. 2004. *Warmer Bulletin*. Suppl. 95: 1–4.
12. Radziszewski P., M. Kalabinska, and J. Pilat. 2001. Applications of waste tyre rubber granulate to modification of asphalts used in road building. *Elastomery*. 5(4): 8–16.
13. Gawell I. and L. Slusarki. 1999. Use of recycled tyre rubber for modification of asphalt. *Int. Polym Sci. Technol*. (1999) 26 (2): 97–103.
14. Moore M. 2006. Recycling still struggles to make financial sense. *Rubber and Plastics News*. 35: 28–30.
15. Diedrich K.M. and B.J. Burns. 2001. Possibility of ground tyre rubber recycling with trans-polyoctenamer. *Elastomery*. 5(4): 17–24.
16. Gui'an W., C. Xinzhong, Z. Yong, and Z. Yinxi. 2000. Preparation of storage stable SBS copolymer/asphalt blends. *China Synthetic Rubber Ind*. 23(4): 242.
17. 2002. New stadium to use field turf. *Scrap Tire News*. 16(4): 1–3.
18. De S.K. Fall 1999. Reuse of ground rubber waste: A review. 156th ACS Rubber Division Meeting, Orlando, FL. Paper 137.
19. Nov. 2001. More SC Projects will use recycled rubber. *Scrap Tire News*. 15(11): 6.
20. D.F. Morgan and L.S. Wolosky. July 18, 1973. U.S. Patent, 4,101,463. Molded composition and article molded therefrom. Filed June 7, 1977. Appl. No. 804,471.
21. De D., A. Das, P.K. Panda, B. Day, B.C. Roy. 2006. Reinforcing effect of silica on the properties of styrene butadiene rubber-reclaim rubber blend system. *J. Appl. Polym. Sci*. 99: 957–68.
22. Myhre M.J. 2004. Compounding with recycled scrap rubber. 166th Rubber Division Meet (Fall 2004) Columbus, paper 23: 22.
    Myhre M.J. 2005. Compounding with recycled scrap rubber. *Rubber World*. 231: 26–9.
23. Burgoyne M.D., G.R. Leaker, and Z. Krekix. 1976. The effect of reusing ground flash and scrap rubber in parent compound. *Rubber Chem. Technol*. 49: 375–78.
24. Shuyan Li, J. Lamminmaki, and K. Hanhi. 2005. Effect of ground rubber powder and devulcanizates on the properties of natural rubber compounds. *J. Appl. Polym. Sci*. 97: 208–17.
25. Bandyopadhyay S., S. Dasgupta, N. Mandal et al. 2005. Use of recycled tyre material in natural rubber based tyre tread cap compound : Part 1 (with ground crumb rubber). *Progress in Rubber, Plastics and Recycling Technology*. 21(4): 299–317.
26. Kuznetsova O.P., L.M. Tchepel, L.A. Zhorina, et al. 2004. Static and dynamic vulcanizates containing ground tire rubber. *Prog. Rubber, Plastics Recycling Technol*. 20: 85– 96.
27. Jacob C., R.S.P. De, and S.K. De. 2003. Using powdered factory scraps in EPDM compounds. *Rubber World*. 228: 21–5.
28. Jacob D., A.K. Bhowmick, and S.K. De. 2001. Recycling of EPDM waste. II. Replacement of virgin rubber by ground EPDM vulcanizate in EPDM/PP thermoplastic elastomeric composition. *J. Appl. Polym. Sci*. 82: 3304–12.
29. Kim J.K. and S.H. Lee. 2000. New technology of crumb rubber compounding for recycling of waste tires. *J. Appl. Polym. Sci*. 78: 1573–7.
30. Fuhrmann I. and J. Karger-Kocsis. 1999. Effects of ground tyre rubber (GTR) on the mechanical properties of thermoplastic blends. *Kautschuk Gummi Kunststoffe*. 52: 836–41.
31. Maridass B. and B.R. Gupta. 2003. Recycling of waste tire rubber powder. *KGK: Kautschuk Gummi Kunststoffe*. 56: 232–6.
32. Accetta A. and J.M. Vergnaud. 1981. Upgrading of scrap rubber powder by vulcanization without new rubber. *Rubber Chem.. Technol*. 54: 302–10.

33. Accetta A. and J.M. Vergnaud. 1982. Vibration isolation properties of vulcanizates of scrap rubber powder. *Rubber Chem. Technol.* 55: 328–36.
34. Accetta A. and J.M. Vergnaud. 1982. Rubber recycling. Upgrading of scrap rubber powder by vulcanization. II. *Rubber Chem. Technol.* 55: 961–66.
35. April 2003. Sound proof floors. *Scrap Tire News*. 17(4): 9.
36. E. Bilgili, A. Dybek, H. Arastoopour, and B. Bernstein. 2003. New recycling technology: compression molding of pulverized rubber waste in the absence of virgin rubber. *J. Elastomers Plastics*. 35: 235–56.
37. April 2006. UK housing estate to be built from tires. *Scrap Tire news*. 20(4): 20.
38. Dec.2004. Walking on rubber. *Scrap Tire News*. 18(12): 7.
39. June 2003. Old tires used in tennis court. *Scrap Tire News*. 17(6): 14.
40. Beckman J.A., G. Crane, E.L. Kay, and J.R. Laman. 1973. Destructive distillation. *Rubber Age*. 104: 43–8.
41. Kaminsky W. and H. Sinn. April 1978. Pyrolyse des déchets de matière plastique et de vieux pneus dans un appareil de fluidisation. *Matériaux et Techniques*.146–53.
42. D.E. Wolfson, J.A. Beckman, J.D. Walters, and D.J. Bennett. September 1969. Bureau of Mines Report of Investigation 7302.
43. Crane G. and E.L. Kay. 1975. Scrap tire disposal process. *Rubber Chem. Technol.* 48: 50–61.
44. Williams P. 2001. Pyrolysis turns scrap tyres into oil and gas. *Ind. Environ. Manag*. 12(6): 24.
45. Ondrey G. and T. Kamiya. 2002. Pyrolysis gets all fired up. *Chem. Eng*. 109: 27–31.
46. Sept. 2001. New pyrolysis technique adds value to tyre scrap. *British Plastics Rubber*. September. 86.
47. Sept. 2001. Chemicals from pyrolysed scrap tyres. *Specialty Chem*. 21(7): 6.
48. Kawser M.J. and N.A. Farid. 2000. Thermochemical processing of rubber waste to liquid fuel. *Plastics, Rubber Composites*. 29: 100–4.
49. Urbon J.P. September 23, 1970. Report to the National Industrial Pollution Control Council, Washington D.C.
50. Kleps T., Piaskiewicz and W. Parasiewicz. 2000. Use of thermogravimetry in the study of rubber devulcanization. *J. Thermal Analys. Calorim*. 60: 271–7.
51. Leger P. and J.M. Vergnaud. 1978. Traitement thermique de pneumatiques récupérés et utilisation comme charge dans les matières plastiques. *C.R. Acad. Sci. Paris*. 286: 311–14.
52. Jacob D., P.P. De, and S.K. De. 2002. Utilization of powdered rubber vulcanizates as a filler. *Rubber World*. 227: 43–5.
53. Moore M: 2001. Process yields active carbon from recycling. *Rubber Plastics News 2*. 22: 5.
54. Mandal N., S. Das Gupta, and R. Mukhopadhyay. 2002. Regenerated carbon black from scrap rubber products and its use in virgin rubber compound. Proceed. Conf. Prague Paper 89, p. 11.
55. Burford R.P. and M. Pittolo. May 1982. ACS Meeting, Rubber Division, Philadelphia, Penn., USA. Paper 56.
56. Donnet J.B., R.C. Bansal, and M.J. Wang. *Carbon Black: Science and Technology*, 2nd ed., Marcel Dekker 1993.
57. Donnet J.B., A. Santini, H. Schuster, and A. Geissler, Intern. Rubber Conf., Lyon 2006.
58. Naskar A.K., Bhowmick, A.K., and S.K. De. 2001. Thermoplastic elastomeric composition based on ground rubber tire. *Polym. Eng. Sci*. 41: 1087–98.
59. Wiessner S. and H. Michael. 2003. Thermoplastic elastomer made from crumb rubber and polypropylene. *KGK: Kautschuk Gummi Kunststoffe*. 56: 514–8.
60. July 2005. PE sheets contains 70% recycled tires. *Plastics Technol*. 51(7): 20

61. Mangaraj D. 2004. Role of compatibilization in recycling rubber waste by blending with plastics. 166th Rubber Division Meet, (Fall 2004) Columbus paper 27, 16. *Rubber Chem. Technol*. 2005. 78(3): 536–47.
62. Sonnier R., E. Leroy, L. Clerc, A. Bergeret, and J.M. Lopez-Cuesta. 2006. Compatibilization of polyethylene ground tyre rubber blends by gamma irradiation. *Polym Degradat. Stability*. 91: 2375–79.
63. Kumar C.R., I. Fuhrman, and J. Karger-Kocsis. 2002. LPDE-based thermoplastic elastomers containing ground tire rubber with and without dynamic curing. *Polym. Degradat. Stability*. 76: 137–44.
64. Moore M. 2002. Better tires make recycling complex. *Rubber and Plastics News*. 24: 5.
65. Macrory R. Sept. 2002. High court rejects cement tyre burning challenge. *ENDS Report*. 332: 48–9.
66. July 2004. Buyer's Guide: Tire and Rubber recycling equipment. *Scrap Tire News*. 18(7): 12–4.

NOMENCLATURE

β	loss factor, in Figure 8.4
DOP	plasticizer, for dioctyl phthalate
db	for decibel, in Figure 8.5
E	static compression modulus, in Figure 8.1
E'	dynamic in phase modulus, in Figure 8.3

9 Rubber

Cure and Properties

9.1 CONCLUSIONS

In summing up the cure of rubber heated in a mold, it can be said that this process consists of two main stages: the heating stage up to the temperature at which the cure reaction starts, and the cure reaction itself. If the heating stage is rather simple to describe, the cure of rubber is a complex reaction with initiation steps, followed by propagation steps, and ending in termination steps. Instead of attempting to study the cure by considering its various steps, reducing these steps to a unique "simple" reaction leads to an Arrhenius's expression with one value for the energy of activation and a given order of reaction for the remaining amount of the reaction components.

Either in simple molding or even in injection molding, the rubber material is heated within a narrow temperature window through which the cure reaction proceeds properly. Too high the temperature, the rubber is burned, and too low, the material is viscous without the elastic quality of the rubber. Thus, the cure reaction has to be considered seriously. And, as the quality of the final material depends on the cure process it has been submitted to in the mold, defining the value at the state of cure is of great concern. By considering the partial heat evolved up to time *t* as a fraction of the total heat evolved, a value of the state of cure is attained, but the enthalpy of the cure reaction is rather low. Taking for granted that expertise in the main properties of rubber is needed for evaluating the state of cure, methods through which the increase in the rubber properties is followed as a function of temperature and time have been developed. The increase in a mechanical property, such as the resistance to torsion, has been exploited in succession with two apparatuses: first, the moving die rheometer (MDR) working under isothermal conditions and, recently, with the rubber process analyzer (RPA) run in programmed temperature. In any case, the state of cure at time *t* is the value of this mechanical property attained at time *t* as a fraction of the maximal value of the corresponding property. On the other hand, as shown already, the capacity of absorption of a liquid has been used for a test, but the drawback for the diffusion is in the long duration of the experiments, this time being proportional to the square of the thickness of the sample.

The following points of have been studied extensively:

1. Heat transfer so as to know the temperature in the various parts of the rubber at any given time
2. The kinetics of the cure reaction, expressed in terms of either the heat evolved or the torque modulus obtained by the MDR and RPA

3. The mass transfer controlled by diffusion, considered as either a measure of the resistance of vulcanized rubber toward liquids or used to evaluate the migration of the curing agent during the cure

Following are some of the most significant results obtained from temperature study: The mold is actually a complex system with various means of heating. Very often, if not all the time, calculations are made with a mold kept at constant temperature without any other consideration. This assumption has been shown to be obviously wrong. When the heated mold is in contact with the cold rubber, heat is transferred from the mold to the rubber, and the temperature of the mold becomes lower than it was originally. This is particularly true on the face of the mold in contact with the rubber. Thus, not only should the mold be heated when the rubber is introduced, but it should also be heated at the right place. Two examples are shown in Chapter 4 where the mold is constantly heated, but at different places: the one with the heating system on the external surface of the mold, and the other when this heating system is placed on the mold surface in contact with the rubber. While this drawback is of little importance when the rubber sample is small (or rather when the rubber sheet is thin), it becomes most significant when the thickness of the rubber sample is greater than that of the mold.

Perhaps it would be useful to recall some simple rules concerning time as a function of the thickness of the rubber sample. This problem could be resolved by considering the boundary conditions that express what is happening on the rubber surface.

Primarily, it might be useful to recall the general equality of the heat flux on both sides of the interface between the rubber and the exterior, which plays a fundamental role when the rubber is bounded by a fluid, either in liquid or in gaseous state:

$$\lambda \frac{\partial T}{\partial x} = h \cdot (T_s - T_{ext}) \tag{9.1}$$

Another equation stands when the rubber is in contact with another solid, and the equality between the heat flux in the rubber and in the solid material is written as follows:

$$\lambda_r \left[\frac{\partial T}{\partial x} \right]_r = \lambda_m \left[\frac{\partial T}{\partial x} \right]_m \tag{9.2}$$

where are shown on the left side the product of the thermal conductivity of the rubber λ_r by the gradient of temperature in the rubber at the interface and on the right side the corresponding product in the other solid (e.g., the mold).

In Equation 9.1, we recall that h is the coefficient of convection in the fluid that bounds the rubber surface. Depending on the value of the stirring rate of the fluid, the convection may be either forced or free.

When the convection is forced, Equation 9.1 stands as it is written, and when the rate of stirring is so high that it may be considered as infinite, obviously the temperature on the surface of the rubber T_s is equal to the external temperature T_{ext} as soon as the process starts. In this particular case, a rather simple equation is obtained, with the dimensionless number $\frac{\alpha \cdot t}{L^2}$, which expresses the fact that the time necessary for the temperature to reach a given value is proportional to the square of the thickness of the rubber sheet.

When the convection is free, the value of the coefficient of convection h in the fluid is finite, and it depends on the dimensions of the rubber. The convection may be either turbulent or laminar. In both cases, a new dimensionless number is obtained connecting the time and the thickness of the rubber sheet, $\beta_n^2 \frac{\alpha \cdot t}{L^2}$, and the above rule between the time and square thickness of the sheet is slightly modified.

A fact of interest, and of value especially for large pieces of rubber, results from the potent increase in the state of cure, which can be obtained after the extraction of the rubber from the mold, during what is sometimes called the "postcure." The increase in the state of cure is sensible at the inside of the piece, and it is a function of the thickness of the rubber but also of the temperature of the surrounding material, as well as of the degree of cure at the time the cured rubber is removed from the mold. This last application may, at least theoretically, lead to economic considerations, with a reduction in the residence time of the rubber in the mold.

9.1.1 Evaluation of the State of Cure and Kinetics of Cure

Another fact is concerned with the parameters of the cure reaction, and how to evaluate them. If the thermal parameters are known, and the methods necessary to determine them are very well established, the knowledge is not so certain for the kinetics of the cure reaction. As stated by various authors, the state of cure at time t is represented as the partial enthalpy of cure generated by the cure reaction at time t as a fraction of the total enthalpy. Of course, two ways exist for measuring the cure of reaction and its parameters, with the calorimetry and any method able to follow the change in the property of the rubber with the cure. As shown in Chapter 3, if calorimetry is the main technique for determining the kinetic parameters of thermosetting resins, by following the heat evolved from the cure reaction, it becomes difficult in the case of rubber because of the low value of the cure enthalpy. It is a pity, as it would be perfect to use the partial enthalpy evolved from the cure reaction, as the rubber sample is heated through gradients of temperature. Thus, methods following a property during the cure are more adapted to the problem set by the rubber, and the viscosity or the resistance to torsion or torque remains the best—at that time, at least.

The moving die rheometer, MDR, still widely used, is only run under isothermal conditions. Thus, three experiments are necessary to determine the three parameters that are able to describe the effect of temperature on the rate of cure. A better use of the MDR technique is surely obtained by programming the temperature, in the same way as calorimetry was run. Hence, the rubber process analyzer (RPA), which can be run either under isothermal conditions or with a programmed temperature, has been recently launched on the market. Nevertheless, as shown in Chapter 3, by using various ways of heating, the usual linear temperature programming is perhaps not the best.

A characteristic of great concern and one worth pointing out is the change in the viscosity of the unvulcanized rubber with temperature. It decreases significantly with temperature, at least before the cure reaction starts. This fact has been shown several times in this book, in Chapter 6 for the mechanical properties of the rubbers, and especially in Chapter 5, as an application for the injection molding technique. As shown in Figure 6.1, for instance, where the torque–time profile is drawn as obtained with the MDR run under isothermal conditions, and much better measured with the rubber process analyzer, a minimum in the torque appears at the beginning of the process. This property is used in the injection molding technique for two reasons, at least: first, the rubber compound is heated at a temperature for which no sensible cure reaction occurs, and this increase in temperature is responsible for a decrease in time during the cure process in the mold; and secondly, and more important, the low viscosity of the rubber at the time of injection allows the rubber to be injected without too high a pressure to fill up the cavities of the mold. However, it clearly appears from this torque–time curve drawn with the isothermal MDR that if the scorch time is obtained, the temperature is not defined. It is another advantage of the rubber process analyzer, as with this new technique, both the characteristics of the scorch, time, and temperature are simultaneously acquired.

The effect of the diffusion of a liquid or other (curing agent) in rubber is of interest.

The effect of absorption of a liquid on rubber—especially in the family of aromatics such as toluene—is generally considerable, depending on the nature of the rubber. As a result, the huge amount of liquid absorbed in the rubber is responsible for considerable swelling. Calculation of the new dimensions and shape of the rubber material during the operation can be evaluated only when the value of the diffusivity is known at various times and places in the sample. In this case, as shown in Chapter 7, the problem becomes highly complex for various reasons. The process of transport of the liquid through the rubber being driven by diffusion, its concentration depends on both the time and space, and subsequently, deep gradients of concentration are developed through the sample. As the diffusivity is mainly concentration-dependent, its value varies not only with time but also with space. Moreover, resulting from a change in the volume of liquid absorbed at any place in the process, the dimensions are constantly moving at any time and any position. Two difficulties occur, the one with the calculation in such a problem, and the other with the way of evaluating the concentration-dependent diffusivity. Examples have been given or cited where this evaluation of the diffusivity has been made by using either a sheet or a sphere as the rubber sample. Of course, for this problem the sphere is of better use, because of its particularly high symmetry, whereas the sheet is far more complex because of its two dimensions, and in this usual case it is not possible to assume that the sheet is of infinite dimensions except for the thickness.

Moreover, as shown in Chapter 4 for the simultaneous cure of two different rubber compounds, a diffusion of the active agent takes place through the interface separating the two rubbers. This result has been proved in Chapter 7 where the hardness shown in Table 7.2 varies regularly through the thickness of these two layers. As a result, these two rubber layers are so highly bounded that they cannot be disconnected when submerged in a liquid such as toluene, in spite of the great difference in the swelling that takes place in these layers. This is of great concern when it is building up a complex rubber system, such as tires have, as it strongly binds all the components. This diffusion of the active agent can be controlled, as it occurs especially when the viscosity of the rubbers are at their lowest, at the scorch time. The main factor determining its effectiveness is the time of contact of these components before the cure reaction starts.

As already said in the Preface, a question arose as to the appropriateness of having a chapter in this book devoted to the cure of rubbers and to their properties concerned with the recovery of scrap rubber obtained from old tires. However, the amount of old tire rubber is so large that it could be considered as a raw material, and reclaiming will become a necessity when crude oil and natural rubber experience shortages. This problem is so vast that only a book in itself could describe all the possibilities of reusing. Nevertheless, a large number of opportunities has been identified, and the reclaiming processes based on the cure of these scrap rubbers have been considered.

In this book, the main results of research are presented in terms of equations and figures. In all cases, the theoretical treatment is presented in a didactic manner, so that the readers not familiar with terms can, nevertheless, easily understand its development. The assumptions for which calculations are made and the solutions obtained, are clearly presented. It is true that the problems of heat transfer by conduction, as well as those of diffusion of liquid through a rubber, are not easy to understand. This is the reason why the solutions of the differential equations with partial derivatives that express these transfers have been deeply explained. On the other hand, in order to facilitate the reader's generalizing the results, the figures are drawn by using dimensionless numbers as coordinates as often as possible, leading to master curves of value in various applications. Thus, by introducing the typical values of their problems, readers can obtain the particular result of the actual problem put before them.

In order to be as informative as possible, the results are presented in terms of the profiles of temperature and of state of cure (e.g., the thickness of a sheet during the process). Much better than other curves such as the temperature—or state of cure—time histories, these profiles are able to give a fuller insight into the process. Moreover, the temperature–time history at the mid-plane looks not too informative because of the low enthalpy of cure. As a matter of fact, the processes of heat transfer and cure reaction are intimately bound together, and thus, the profiles of temperature and of state of cure should be shown in parallel.

The data published by various authors are given so as to help readers make their own calculations. They concern the values that deal with the heat transfer and the kinetics of the cure reaction, or with the diffusion of liquids through the rubbers. In each case, the references of the authors are given in the usual way.

Most calculation and figures are presented in the case of a sheet; however, the equations have been given in the case of parallelepiped and cube. What is important to see at that point is that the smaller dimension plays the more important role, either for heating conduction or for diffusion of liquid, resulting from the dimensionless number $\frac{\alpha \cdot t}{L^2}$ which is rewritten by replacing the thermal diffusivity α by the diffusivity D in liquid diffusion.

It could be of interest to recall the history of this subject, followed by the various techniques considered in our book. It took a long time—up to a decade—for researchers to accept calorimetry in the scanning mode. Calorimetry run under isothermal conditions was considered for several years to be more comfortable, but some showed that in a process where heating plays a primary role, temperature is neither constant nor uniform, without speaking of the heat generated by the reaction, which dissipates. The same fact arose with the MDR, which developed by a similar history. Sometimes, history is repeated, as we can see, by comparing the development of the calorimetry and what has happened with MDR. The older author of this book was one of the researchers who most strongly recommended the scanning mode in calorimetry; now both authors have been pleading for a programmed temperature system developed in the RPA. The new technique run in the scanning mode is able to provide the same results with only one experiment, but more is obtained with the RPA. Its data of interest are of added value in evaluating the operational conditions of injection molding with the scorch conditions of time and temperature.

Appendix

The first six roots* β_n of $\beta \tan\beta = R$

R	β_1	β_2	β_3	β_4	β_5	β_6
0	0	3.1416	6.2832	9.4248	12.5664	15.7080
0.001	0.0316	3.1419	6.2833	9.4249	12.5665	15.7080
0.002	0.0447	3.1422	6.2835	9.1250	12.5665	15.7081
0.004	0.0632	3.1429	6.2338	9.4252	12.5667	15.7105
0.006	0.0774	3.1435	6.2841	9.4254	12.5668	15.7083
0.008	0.0803	3.1441	6.2845	9.4256	12.5670	15.7085
0.01	0.0998	3.1448	6.2848	9.4258	12.5672	15.7086
0.02	0.1410	3.1479	6.2864	9.4269	12.5680	15.7092
0.04	0.1087	3.1543	6.2895	9.1290	12.5696	15.7105
0.06	0.2125	3.1606	6.2927	9.4311	12.5711	15.7118
0.08	0.2791	3.1668	6.2959	9.4333	12.5727	15.7131
0.1	0.3111	3.1731	6.2901	9.4354	12.5743	15.7143
0.2	0.4328	3.2039	6.3148	9.4459	12.5823	15.7207
0.3	0.5218	3.2311	6.3305	9.4565	12.5902	15.7271
0.4	0.5932	3.2636	6.3161	9.4670	12.5981	15.7334
0.5	0.6033	3.2923	6.3616	9.4775	12.0060	15.7397
0.6	0.7051	3.3204	6.3770	9.4879	12.6139	15.7460
0.7	0.7506	3.3477	6.3923	9.4983	12.6218	15.7524
0.8	0.7910	3.3744	6.4074	9.5087	12.6296	15.7587
0.9	0.8274	3.4003	6.4224	9.5190	12.6375	15.7650
1.0	0.8603	3.4256	6.4373	9.5293	12.6453	15.7713
1.5	0.9882	3.5422	6.5097	9.5801	12.6841	15.8026
2.0	1.0769	3.6430	6.5783	9.6296	12.7223	15.8336
3.0	1.1925	3.8088	6.7040	9.7240	12.7966	15.8945
4.0	1.2646	3.9352	6.8110	9.8119	12.8678	15.9536
5.0	1.3138	4.0336	6.9096	9.8928	12.9352	16.0107
6.0	1.3496	4.1116	6.9924	9.9667	12.9988	16.0654
7.0	1.3766	4.1746	7.0640	10.0339	13.0584	16.1177
8.0	1.3978	4.2264	7.1263	10.0949	13.1141	16.1675
9.0	1.4149	4.2694	7.1806	10.1502	13.1660	16.2147
10.0	1.4289	4.3058	7.2281	10.2003	13.2142	16.2594
15.0	1.4729	4.4255	7.3959	10.3898	13.4078	16.4474
20.0	1.1961	4.4915	7.4954	10.5117	13.5420	16.5864
30.0	1.5202	4.5615	7.6057	10.6543	13.7085	16.7691
40.0	1.5325	4.5979	7.6647	10.7334	13.8048	16.8794
50.0	1.5400	4.6202	7.7012	10.7832	13.8R66	16.9519

(*Continued*)

The first six roots* β_n of $\beta \tan\beta = R$

R	β_1	β_2	β_3	β_4	β_5	β_6
60.0	1.5451	4.6353	7.7259	10.8172	13.9094	17.0026
80.0	1.5514	4.6543	7.7573	10.8606	13.9644	17.0686
100.0	1.5552	4.6658	7.7764	10.8871	13.9981	17.1093
∞	1.5708	4.7124	7.8540	10.9956	14.1372	17.2788

[*] The roots of this equation are all real if $R > 0$.

Suggested Reading

Brown R.P. 2002. *Practical Guide to the Assessment of the Useful Life of Rubbers*. RAPRA.

Brown R.P. 2005. *Physical Testing of Rubber*, 4th ed. Springer.

Brown R.P. and T, Butler. 2000. *Natural Ageing of Rubber: Changes in Physical Properties over 40 Years*. RAPRA. Plastics Design Library.

Brown R.P. *Rubber Product Failure*. RAPRA. 2002.

Chandraseharan V.C. 2007. *Essential Rubber Formulary: Formulas for Practitioners*. Plastics Design Library.

Datta R.N. 2002. *Rubber Curing Systems*. RAPRA.

De S.K., A.I. Isayev, and K. Kheit. 2005. *Rubber Recycling*. CRC, Taylor & Francis.

Dick J.S. 2001. *Rubber Technology: Compounding and Testing for Performance*. Hanser Gardner.

Donnet J.B. and A. Vidal. 1986. *Carbon Black. Advances in Polymer Science*. Springer.

Donnet, J.B., T.K. Wang, and J.C.M. Peng. 1998. *Carbon Fibers*. 3rd ed. Marcel Dekker.

Erman B. and J.E. Mark. 1997. *Structures and Properties of Rubber-Like Networks*. Oxford University Press.

Gent A.N. 1992. *Engineering with Rubber: How to Design Rubber Components*. Hanser Gardner.

Kothandaraman R. 2008. *Rubber Materials*. CRC, Taylor & Francis.

Loadman J.R. 1999. *Analysis of Rubber and Rubber-Like Polymers*. Kluwer Academic Publ.

Mark J.E., B. Erman, and R.E. Eirich. 2005. *Science and Technology of Rubber*, 3rd ed. Academic Press.

Means J. 2006. *Bonding Elastomers: A Review of Adhesives and Processes*. Smithers RAPRA.

Michaeli W. 2003. *Extrusion Dies for Plastics and Rubbers: Design, Engineering, Computation.*, 3rd ed. Hanser Gardner.

Ridley S. 2006. *A Rubber Tire*. Gareth Stevens Publ.

Treloar L.R.G. 2005. *The Physics of Rubber Elasticity*, 3rd ed. Oxford University Press.

White J.L. 1995. *Rubber Processing: Technology, Materials, Principles*. Hanser Gardner.

White J.L. and S.K. De. 2001. *Rubber Technologist's Handbook*. RAPRA.

White J.L. and K.J. Kim. 2007. *Thermoplastics and Rubber Compounds: Technology and Physical Properties*. Hanser Gardner.

Index

MATERIALS SCIENCE

RUBBER CURING and PROPERTIES

In today's world, quality rubber products are defined not only by their strength, durability, and elasticity, but also by their recyclability. During the curing of rubber, an irreversible reaction takes place leading to the creation of a new three-dimensional molecular network where the plastic and viscous material is converted into an elastic one. Ultimately, it is the effectiveness of the curing process that determines the quality of that material.

Rubber Curing and Properties features the work of Professor Jean-Maurice Vergnaud, one of the world's foremost authorities on rubber curing, who teams with chemical engineer Dr. Iosif-Daniel Rosca, to produce the most comprehensive reference available in this field. Including valuable data that will allow researchers and engineers to find solutions to their own problems, this practical work—

- Offers an insightful bird's eye view of the history of the cure process
- Considers the complex problems associated with heat transfer and the methods used for evaluating the kinetics of curing
- Examines the principles and methods involved with the curing of rubber sheets in molds using monodirectional and three-directional heating systems, as well as time-saving injection molding
- Evaluates the mechanical properties of both unvulcanized and vulcanized rubber
- Looks at ways to relate the mechanical properties of rubber under dynamic conditions to the state of cure
- Explains the complex issue of the resistance of rubber to liquids and gas
- Discusses a number of solutions to ongoing problems with recycling scrap rubber, including approaches for using it as raw material

The main findings of this remarkable reference are presented in terms of equations and figures. In all cases, theoretical treatments are offered in a didactic manner, so that readers who are not fully familiar with the terms can, nevertheless, easily understand emerging developments in the field.

85220

ISBN: 978-1-4200-8522-8
90000
9 781420 085228

CRC Press
Taylor & Francis Group
an **informa** business
www.crcpress.com

6000 Broken Sound Parkway, NW
Suite 300, Boca Raton, FL 33487
270 Madison Avenue
New York, NY 10016
2 Park Square, Milton Park
Abingdon, Oxon OX14 4RN, UK

www.crcpress.com